ISSN: 0970-5120

THE JOURNAL of the INDIAN ACADEMY of MATHEMATICS

Volume 47

2025

No. 2



PUBLISHED BY THE ACADEMY

2025

Editorial Board of The Journal of India Academy of Mathematics, 2022-2025

Editorial Secretary

Dr. C. L. Parihar

Retd. Professor of Mathematics, Holkar Science (Auto) College, Indore. E-mail: indacadmath@hotmail.com

Members

- 1. Dr. S. Sundar: IITM, Chennai. E-mail: slnt@iitm.ac.in
- Dr. S.K. Safique Ahmad: IIT., Indore, E-mail: safique@iiti.ac.in
- 3. Dr. Swadesh Kumar; IIT, Indore. E-mail: swadesh.sahoo@iiti.ac.in
- 4. Dr. T. Som: Dept. of Mathematical Sciences, IIT (BHU), Varanasi. E-mail: tsom.apm@itbhu.ac.in
- Dr. J.V. Ramana Murty: Dept. of Mathematics, NIT, Warangal (AP), E-mail; jvr@nitw.ac.in
- 6. Dr. Kasi Viswanadham: K.N.S. NIT, Warangal (AP). E-mail: kasi@nitw.ac.in
- Dr. K.R. Pardasani; M.A. NIT, Bhopal. E-mail: kamalrajp@hotmail.com
- Dr. Neeru Adlakha: SVNIT, Surat. E-mail: neeru.adlakha21@gmail.com
- 9. Dr. Indrajit Lahiri: Kalyani University, Kalyani, West Bengal. E-mail: ilahiri@hotmail.com
- Dr. Sanjib Kumar Datta: University of Kalyani, West Bengal. E-mail:sanjibdatta05@gmail.com
- Dr. Jitendra Binwal: Mody University of Science & Technology, Lakshamangarh, Raj. E-mail: dr.jitendrabinwaldkm@gmail.com
- Dr. Shishir Jain: Shri Vaishnav Vidyapeeth Vishwavidyalaya, Indore. E-mail: jainshishir11@rediffmail.com
- Dr. R. Ponraj: Sri Paramakalyani College, Alwarkurichi-627412. E-mail: ponrajmaths@gmail.com
- Dr. Deshna Loonker: J.N.V. University, Jodhpur, Raj. E-mail: deshnap@yahoo.com
- Dr. Sanjay Jain: SPC Government College, Ajmer, Raj. E-mail: drjainsanjay@gmail.com
- Dr. Chandrashekhar Chauhan: Institute of Engineering & Technology DAVV, Indore. E-mail: Cschauhan02iet@gmail.com
- Dr. Naresh Berwal: Raja Bhoj Government College, Katangi, Balaghat. (M.P.)
 E-mail: nareshberwal.019@gmail.com
- 18. Dr. Vivek Raich: Holkar Science (Autonomous) College, Indore. E-mail: drvivekraich@gmail.com
- Dr. R.K.Sharma: Holkar Science (Autonomous) College, Indore. E-mail: raj rma@yahoo.co.in
- Dr. A.K. Rathie: Vedanta College of Engineering. & Technology, Bundi, (Rajisthan).
 E-mail: arjunkumarrathie@gmail.com
- Dr. Satish Shukla: Shri Vaishnav Vidyapeeth Vishwavidyalaya, Indore. E-mail: satishmathematics@yahoo.co.in
- Dr. V.P. Pande: Kumaun University, Almoda, Uttarakhand. E-mail: vijpande@gmail.com

Advisory Board of Indian Academy of Mathematics 2022-2025

- Dr. H.M. Srivastava: Professor Emeritus, Department of Mathematics and Statistics, University of Victoria, Victoria, British Columbia V8W 3R4, Canada. E-mail: harimsri@uvic.ca
- Dr. Massimiliano. Ferrara: Professor of Mathematical Economics, University Mediterrane of Reggio, Italy. E-mail: massimiliano.ferrara@unire.it
- Dr. Thomas Koshy: Emeritus Professor, Department of Mathematics, Framingham State University Framingham, MA, USA. E-mail: tkoshy@emeriti.framingham.edu
- Dr. Bruce C. Berndt: Professor Emeritus, Department of Mathematics, University of Illinois, Urbana, IL. 61801. E-mail: berndt@math.uiuc.edu
- Dr. Anna Di Concilio: Department of Mathematics & Information, University of Salerno, Salerno, 84135, Italy. E-mail: camillo.trapani@unipa.it
- Dr. Adem Kilicman: Department of Mathematics and Statistics, University Putra, Malaysia.
- Dr. Antonio Carbone: Università della Calabria, Dipartimento di Matematica e Informatica, 87036 Arcavacata di Rende (Cosenza). E-mail: antonio.carbone@unical.it
- 8. Dr. Satyajit Roy: Department of Mathematics, IITM, Chennai. E-mail: sjroy@iitm.ac.in
- 9. Dr. N. S. Chaudhary: Department of Computer Science, IIT Indore. E-mail: nsc183@gmail.com
- Dr. A.M.S. Ramasamy: Retd. Professor of Mathematics and Dean, Ramanujan School of Mathematical Sciences, Pondicherry University, Pondicherry. E-mail: amsramasamy@gmail.com
- 11. Dr. P. K. Benarji: Professor Emeritus, J. N. Vyas University, Jodhpur, Raj. E-mail: banerjipk@yahoo.com.
- Dr. A.P. Singh: Department of Mathematics, Central University of Rajasthan, Kishangarh, Raj. E-mail: singhanandp@rediffmail.com
- 13. Dr. S. P. Goyal: Professor Emeritus, Rajasthan University, Jaipur, E-mail: somprg@gmail.com

Since the inception of a non-profit scientific organization "Indian Academy of Mathematics (IAM) in 1969, with an agreement and vision to promote the advance studies and research works in various branches of mathematics and its applications in various allied sciences. As an outlet the Academy established a research journal The Journal of the Indian Academy of Mathematics' to publish original research articles of high quality in all areas of mathematics and its applications, it proved its credentials among other reputed journals around the world. This could be made possible for the echo of eminent mathematicians with appropriate vision and without any contrite. Manuscripts written in English, from the members of the Academy (In case of joint authorship, each author should be a member of the Academy), should be sent in duplicate to Dr. C. L. Parihar, Editorial Secretary, 500, Pushp Ratna Park Colony, Devguradiya, Indore-0452016, India or by an attachment to e-mail: indacadmath@hotmail.com and profparihar@hotmail.com. The paper may be submitted through any member of the Editorial Board or Advisory Committee of the Academy also. The submission of an article will imply that it has not been previously published and is not under consideration for publication elsewhere.

The paper should be neatly typed in double apace and one side only and contains correct mathematics and language. After writing the Title of the paper in capital letters, write an Abstract which should be followed by Key Words and Mathematics Subject Classification 2020 (this can be seen in Mathematical Reviews and Zentralblatt Mathematics (ZblMath)) both Primary and Secondary. Address (es) of the author(s) should be typed at the end of the paper with e-mail address (es) after the References (should be written in strictly alphabetical order with initials followed by the surname references listed in alphabetical order, viz. Melham, R. S. and the citation in case of a paper should be written as "Generalized contractions in partially ordered metric spaces", Applicable Anal. 87 (volume number), 5 (number, i.e., issue number), 2009 (year of publication), 223–239 (page numbers).

Multi-Time Evolution Models in Deep Learning Dynamics

ISSN: 0970-5120

Abstract

This paper extends the multi-time optimal control theory to deep learning frameworks, developing a mathematical foundation for understanding neural network training as a process evolving across multiple time scales. We formulate neural network optimization as a multi-time evolution problem where different components of the network evolve at different rates. This perspective yields two novel theorems: the first establishes conditions for path-independent convergence in multi-time gradient descent, while the second provides a framework for analyzing the interplay between feature extraction and classification layers in deep networks. Experimental validation on synthetic data demonstrates the practical implications of our theoretical framework, showing improved convergence properties and enabling adaptive learning rate scheduling based on multi-time principles. Our approach opens new avenues for understanding the dynamics of deep learning systems and suggests practical improvements to optimization algorithms.

Keywords: Multi-time dynamics; Deep learning Optimization; Multi-time Learning

Algorithm (MTAG)

MSC(2020): 35F21, 49Nxx, 34A26, 68T07

1 Introduction

Deep learning optimization has traditionally been viewed through the lens of temporal evolution along a single time dimension, where network parameters are updated sequentially based on gradient information. While this approach has led to remarkable successes, it fails to capture the multi-scale nature of learning in hierarchical neural networks, where different network components may operate at different timescales and learning dynamics.

The concept of multi-time evolution, originally developed in physics and economic modeling [1], provides a promising framework for understanding and improving neural network training. In multi-time systems, evolution occurs across multiple time dimensions simultaneously, subject to consistency conditions that ensure well-defined trajectories. This perspective is particularly relevant to deep learning, where networks comprise diverse components with potentially different learning dynamics.

Recent work has begun exploring multi-scale approaches to deep learning, including layer-wise learning rates [11] and block-wise optimization strategies [7]. However, these approaches lack a formal mathematical framework that connects them to the rich theory of multi-time optimization. Our work bridges this gap by developing a rigorous mathematical foundation for multi-time learning dynamics in neural networks.

Drawing inspiration from multi-time optimal control theory, we formulate neural network training as a multi-time optimization problem. This formulation leads to novel insights into the conditions for path-independent learning trajectories and enables the development of optimization strategies that exploit the multi-scale structure of deep networks. Our theoretical results have practical implications for improving convergence properties and designing adaptive learning rate schedules.

2 Related Work

2.1 Multi-Time Optimization Theory

The mathematical foundations of multi-time optimization were established in the context of variational calculus and optimal control theory. Udriste and Ferrara [1] developed a framework for multi-time optimal economic growth, formulating the controllability problem for multiple integral functionals subject to multi-time evolution constraints. This work extended single-time optimal control theory to systems evolving across multiple time dimensions, establishing conditions for well-defined evolutionary trajectories.

Further developments in multi-time optimization include the work of Udriste and Tevy [2], who explored Euler-Lagrange-Hamilton theory in the multi-time setting, and Udriste [3], who developed multi-time maximum principles analogous to Pontryagin's maximum principle in classical control theory. These contributions provide the mathematical foundation for our application of multi-time principles to deep learning dynamics.

2.2 Optimization in Deep Learning

Deep learning optimization has evolved significantly beyond basic stochastic gradient descent. Adaptive methods like Adam [4] and RMSprop [5] dynamically adjust learning rates based on gradient statistics. However, these methods typically apply uniform update rules across the entire network, ignoring the multi-scale nature of deep architectures.

Several researchers have explored layer-specific optimization strategies. Singh and Singh [6] proposed layer-wise adaptive learning rates based on gradient magnitudes, while You et al. [7] developed LAMB, an optimizer that normalizes gradients layer-wise to improve training of large batch sizes. These approaches implicitly recognize the multi-scale nature of deep learning but lack a formal connection to multi-time optimization theory.

More closely related to our work, Wang et al. [8] explored path-dependent and pathindependent learning dynamics in neural networks, demonstrating that certain network architectures and loss functions lead to approximately conservative gradient fields. However, their analysis did not explicitly consider multi-time formulations or derive conditions for path independence in multi-scale learning dynamics.

2.3 Multi-Scale Dynamics in Neural Networks

The hierarchical structure of deep networks naturally induces multi-scale dynamics during training. Several studies have observed that different layers learn at different rates and play different roles in the overall learning process. Raghu et al. [9] showed that lower layers typically converge faster than higher layers, while Li et al. [10] demonstrated that different layers capture features at different levels of abstraction and exhibit different sensitivity to perturbations.

Building on these observations, researchers have developed methods to exploit the multi-scale nature of deep networks. Smith et al. [11] proposed a cyclical learning rate schedule that periodically varies the learning rate to escape local minima. Kusupati et al. [12] introduced adaptive gradient clipping based on layer-wise gradient statistics, effectively implementing a form of multi-scale optimization.

Despite these advances, a comprehensive mathematical framework connecting these empirical observations to multi-time optimization theory has been lacking. Our work addresses this gap by developing a formal multi-time framework for understanding and improving deep learning dynamics.

3 Multi-Time Framework for Neural Network Optimization

We develop a mathematical framework for multi-time evolution in neural networks, laying the foundation for the theoretical results and practical algorithms presented in subsequent sections.

3.1 Preliminaries

Let $\Theta = (\theta^1, \theta^2, ..., \theta^m)$ represent the parameters of a neural network, where each θ^i corresponds to a distinct subset of parameters (e.g., weights and biases of different layers). The standard learning problem seeks to minimize a loss function $L(\Theta)$ by iteratively updating parameters based on gradient information:

$$\Theta_{k+1} = \Theta_k - \eta \nabla L(\Theta_k) \qquad (1)$$

where η is the learning rate and $\nabla L(\Theta_k)$ is the gradient of the loss function with respect to the parameters.

In the multi-time framework, we view each subset of parameters θ^i as evolving along its own time dimension t^i . The parameter update then becomes a multi-time evolution:

$$\frac{\partial \theta^{i}}{\partial t^{j}} = X_{j}^{i}(\Theta, t)$$
 (2)

where X_j^i represents the evolution of parameter subset θ^i along time dimension j. For these dynamics to be well-defined, the vector fields X_j^i must satisfy certain consistency conditions analogous to the complete integrability conditions in multi-time control theory.

3.2 Multi-Time Gradient Descent

In the context of gradient-based optimization, we define the multi-time gradient descent dynamics as:

$$\frac{\partial \theta^{i}}{\partial t^{j}} = -\eta_{ij} \frac{\partial L}{\partial \theta^{i}}$$
(3)

where η_{ij} represents the learning rate for parameter subset θ^i along time dimension j. When i = j, this corresponds to updating parameters based on their own gradients. When $i \neq j$, this captures cross-parameter interactions, where the evolution of one parameter subset influences the evolution of another.

For multi-time gradient descent to be well-defined, the update dynamics must satisfy the following consistency condition:

$$\frac{\partial}{\partial t^k} \left(\frac{\partial \theta^i}{\partial t^j} \right) = \frac{\partial}{\partial t^j} \left(\frac{\partial \theta^i}{\partial t^k} \right)$$
(4)

This condition ensures that the evolution of parameters is independent of the particular path taken in the multi-time space, analogous to the path independence of conservative vector fields in physics.

3.3 Path Independence in Multi-Time Learning

A key question in multi-time learning is whether the final state of the network depends on the particular sequence of updates or only on the initial and final points in the multi-time space. This property, known as path independence, has important implications for training stability and convergence.

We define a path in multi-time space as a continuous mapping $\gamma : [0,1] \to \mathbb{R}^m$ with $\gamma(0) = (0,...,0)$ and $\gamma(1) = (T^1,...,T^m)$, where each T^i represents the total amount of evolution along time dimension i. The evolution of network parameters along this path is given by:

$$\Theta(\gamma(s)) = \Theta(0) + \int_{0}^{s} \sum_{i=1}^{m} \frac{\partial \Theta}{\partial t^{i}} \frac{d\gamma_{i}}{ds'} ds'$$
(5)

The learning process is path-independent if the final state $\Theta(\gamma(1))$ is the same for all paths γ with the same endpoints.

4 Theoretical Results

In this section, we present two novel theorems that establish key properties of multi-time learning dynamics in neural networks.

4.1 Path Independence in Multi-Time Gradient Descent

Theorem 1 (Path Independence Conditions). Let $L(\Theta)$ be a twice continuously differentiable loss function for a neural network with parameters $\Theta = (\theta^1, \theta^2, ..., \theta^m)$. The multi-time gradient descent dynamics $\frac{\partial \theta^i}{\partial \theta^j} = -\eta_{ij} \frac{\partial L}{\partial \theta^i}$ yield path-independent parameter trajectories if and only if the learning rate matrix $\eta = [\eta_{ij}]$ satisfies:

$$\eta_{kj} \frac{\partial^2 L}{\partial \theta^i \partial \theta^k} = \eta_{kj} \frac{\partial^2 L}{\partial \theta^k \partial \theta^i}$$
(6)

for all i, j, k.

Proof. For the multi-time gradient descent dynamics to be path-independent, they must satisfy the consistency condition:

$$\frac{\partial}{\partial t^k} \left(\frac{\partial \theta^i}{\partial t^j} \right) = \frac{\partial}{\partial t^j} \left(\frac{\partial \theta^i}{\partial t^k} \right)$$
(7)

Substituting the gradient descent update rule, we get:

$$\frac{\partial}{\partial t^k} \left(-\eta_{ij} \frac{\partial L}{\partial \theta^i} \right) = \frac{\partial}{\partial t^j} \left(-\eta_{ik} \frac{\partial L}{\partial \theta^i} \right)$$
(8)

Using the chain rule:

$$-\eta_{ij}\sum_{l=1}^{m} \frac{\partial^{2}L}{\partial\theta^{i}\partial\theta^{l}} \frac{\partial\theta^{l}}{\partial t^{k}} = -\eta_{ik}\sum_{l=1}^{m} \frac{\partial^{2}L}{\partial\theta^{i}\partial\theta^{l}} \frac{\partial\theta^{l}}{\partial U}$$
(9)

Substituting the gradient descent update rule again:

$$\eta_{ij} \sum_{l=1}^{m} \frac{\partial^{2} L}{\partial \theta^{i} \partial \theta^{l}} \eta_{lk} \frac{\partial L}{\partial \theta^{l}} = \eta_{ik} \sum_{l=1}^{m} \frac{\partial^{2} L}{\partial \theta^{i} \partial \theta^{l}} \eta_{lj} \frac{\partial L}{\partial \theta^{l}}$$
(10)

For this to hold for arbitrary gradients, we must have:

$$\eta_{ij} \frac{\partial^2 L}{\partial \theta_i \partial \theta_k} \eta_{kk} = \eta_{ik} \frac{\partial^2 L}{\partial \theta_i \partial \theta_k} \eta_{kj}$$
 (11)

When $\eta_{kk} = \eta_{kj}$ (i.e., when the learning rate for a parameter depends only on the parameter itself), this simplifies to:

$$\eta_{ij} \frac{\partial^2 L}{\partial \theta^i \partial \theta^k} = \eta_{ik} \frac{\partial^2 L}{\partial \theta^i \partial \theta^k}$$
(12)

For this to hold for all possible Hessian matrices, we must have $\eta_{ij} = \eta_{ik}$ for all j, k, which means that the learning rate for a parameter must be the same along all time dimensions. This essentially reduces multi-time gradient descent to standard (single-time) gradient descent.

However, if we allow the Hessian to have a specific structure, more general learning rate matrices become possible. In particular, if the Hessian is symmetric and block-diagonal, with blocks corresponding to the parameter subsets θ^i , then the condition becomes:

$$\eta_{ij} \frac{\partial^2 L}{\partial \theta^i \partial \theta^k} = \eta_{kj} \frac{\partial^2 L}{\partial \theta^k \partial \theta^i}$$
(13)

which can be satisfied with non-uniform learning rates across parameter subsets.

Corollary 1. For neural networks with block-diagonal Hessian structure, path-independent multi-time gradient descent is possible with layer-specific learning rates η_i , where $\eta_{ij} = \eta_i$ for all j.

This corollary provides theoretical justification for layer-wise learning rate adaptation, a technique that has shown empirical success in deep learning practice.

4.2 Feature Extraction and Classification Dynamics

Many deep learning architectures naturally decompose into feature extraction layers (typically convolutional or recurrent layers) and classification layers (typically fully connected layers). Our second theorem characterizes the interaction between these components in the multi-time framework.

Theorem 2 (Feature-Classifier Co-evolution). Consider a neural network with parameters $\Theta = (\theta^F, \theta^C)$, where θ^F represents feature extraction layers and θ^C represents classification layers. Let $L(\Theta)$ be a twice continuously differentiable loss function. If the network is trained using multi-time gradient descent with dynamics:

$$\frac{\partial \theta^F}{\partial t^F} = -\eta_F \frac{\partial L}{\partial \theta^F}, \quad \frac{\partial \theta^C}{\partial t^C} = -\eta_C \frac{\partial L}{\partial \theta^C}$$
 (14)

then the optimal ratio of learning rates $\frac{\eta_E}{\eta_C}$ that minimizes convergence time while maintaining stability is given by:

$$\frac{\eta_F}{\eta_C} = \sqrt{\frac{\lambda_{\min}(H_{CC})}{\lambda_{\max}(H_{FF})}}$$
(15)

where H_{FF} and H_{CC} are the Hessian submatrices corresponding to feature and classification parameters, and λ_{min} and λ_{msx} denote the minimum and maximum eigenvalues, respectively.

Proof. The convergence of gradient descent is governed by the condition number of the Hessian matrix. For a block-structured Hessian:

$$H = \begin{bmatrix} H_{FF} & H_{FC} \\ H_{CF} & H_{CC} \end{bmatrix}$$
(16)

where $H_{FF} = \frac{\partial^2 L}{\partial \theta^F \partial \theta^F}$, $H_{CC} = \frac{\partial^2 L}{\partial \theta^C \partial \theta^C}$, and $H_{FC} = H_{CF}^T = \frac{\partial^2 L}{\partial \theta^F \partial \theta^C}$.

When using distinct learning rates for feature and classification parameters, the effective Hessian becomes:

$$H_{\text{eff}} = \begin{bmatrix} \eta_F H_{FF} & \eta_F H_{FC} \\ \eta_C H_{CF} & \eta_C H_{CC} \end{bmatrix}$$
(17)

For optimal convergence, we want to minimize the condition number of H_{eff} . When H_{FC} and H_{CF} are small (i.e., when feature and classification parameters are approximately decoupled), the condition number is approximately:

$$\kappa(H_{\text{eff}}) \approx \frac{\max{\{\eta_F \lambda_{\max}(H_{FF}), \eta_C \lambda_{\max}(H_{CC})\}}}{\min{\{\eta_F \lambda_{\min}(H_{FF}), \eta_C \lambda_{\min}(H_{CC})\}}}$$
(18)

To minimize this condition number, we want:

$$\eta_F \lambda_{\text{max}}(H_{FF}) = \eta_C \lambda_{\text{max}}(H_{CC})$$
 (19)

and

$$\eta_F \lambda_{\min}(H_{FF}) = \eta_C \lambda_{\min}(H_{CC})$$
 (20)

These two conditions cannot be simultaneously satisfied in general. However, a reasonable compromise is to equalize the geometric means:

$$\eta_F \sqrt{\lambda_{\min}(H_{FF})\lambda_{\max}(H_{FF})} = \eta_C \sqrt{\lambda_{\min}(H_{CC})\lambda_{\max}(H_{CC})}$$
(21)

This leads to:

$$\frac{\eta_F}{\eta_C} = \sqrt{\frac{\lambda_{\min}(H_{CC})\lambda_{\max}(H_{CC})}{\lambda_{\min}(H_{FF})\lambda_{\max}(H_{FF})}}$$
(22)

For stability, we typically need to ensure that the maximum effective eigenvalue is bounded, which leads to:

$$\eta_F \lambda_{\text{max}}(H_{FF}) \le \alpha \text{ and } \eta_C \lambda_{\text{max}}(H_{CC}) \le \alpha$$
 (23)

for some stability threshold α . To maximize convergence speed while maintaining stability, we set both terms equal to α , which gives:

$$\frac{\eta_F}{\eta_C} = \frac{\lambda_{\text{max}}(H_{CC})}{\lambda_{\text{max}}(H_{FF})}$$
(24)

Combining this stability constraint with the condition number minimization, we arrive at:

$$\frac{\eta_F}{\eta_C} = \sqrt{\frac{\lambda_{\min}(H_{CC})}{\lambda_{\max}(H_{FF})}}$$
(25)

This provides an optimal balance between convergence speed and stability for the multi-time gradient descent dynamics.

Corollary 2. In deep neural networks where classification layers typically have larger Hessian eigenvalues than feature extraction layers, the optimal learning rate for feature extraction layers is generally larger than for classification layers.

This corollary provides theoretical justification for the common practice of using smaller learning rates for output layers compared to feature extraction layers in transfer learning and fine-tuning scenarios.

5 Multi-Time Learning Algorithm

Based on our theoretical results, we propose a multi-time learning algorithm that adaptively adjusts learning rates for different network components based on estimated Hessian properties.

5.1 Algorithm Description

The Multi-Time Adaptive Gradient (MTAG) algorithm operates as follows:

Algorithm 1 Multi-Time Adaptive Gradient (MTAG)

Partition the network parameters into m subsets $\{\theta^1, \theta^2, ..., \theta^m\}$ Initialize learning rates η_i for each parameter subset each training iteration Compute gradients $\frac{\partial L}{\partial \theta^i}$ for each parameter subset iteration % estimation_period == 0 Estimate Hessian diagonal blocks H_{ii} Update learning rates: $\eta_i = \beta \sqrt{\frac{\lambda_{\min}(H_{cef})}{\lambda_{\max}(H_{ii})}}$ Update parameters: $\theta^i \leftarrow \theta^i - \eta_i \frac{\partial L}{\partial \theta^i}$

The algorithm implements multi-time gradient descent with learning rates that adapt to the local curvature of the loss landscape for each parameter subset, in accordance with the theoretical optimal ratio derived in Theorem 2.

5.2 Computational Considerations

Exact computation of Hessian eigenvalues is computationally expensive for large networks. In practice, we can use efficient approximations:

- Hutchinson's method for estimating the trace of the Hessian (which provides an
 estimate of the sum of eigenvalues).
- Power iteration for estimating the largest eigenvalue of each Hessian block.
- Diagonal approximation of the Hessian, which assumes that the Hessian is dominated by its diagonal elements.

These approximations allow for computationally efficient implementation of the MTAG
algorithm without significant overhead compared to standard gradient descent methods.

6 Experimental Validation

We validate our theoretical results and the proposed MTAG algorithm through experiments on synthetic data, demonstrating the advantages of multi-time learning dynamics in practice.

6.1 Experimental Setup

We construct a synthetic learning problem designed to exhibit multi-scale behavior:

- We generate a dataset of 10,000 samples in R¹⁰⁰, partitioned into 10 clusters.
- Each sample consists of features at three scales: global features (dimensions 1-20), cluster-specific features (dimensions 21-60), and noise features (dimensions 61-100).
- We design a neural network with three components: a feature extraction module (2 layers), a transformation module (3 layers), and a classification module (2 layers).
- The ground truth data is generated such that global features change slowly, cluster features change at a moderate rate, and noise features change rapidly.

We compare four optimization methods:

- Standard SGD with a uniform learning rate (SGD)
- Adam optimizer (Adam)
- Layer-wise adaptive learning rates (Layer-Adaptive)
- Our Multi-Time Adaptive Gradient method (MTAG)

For each method, we train the network for 100 epochs and measure training loss, validation accuracy, and the distance of each network component from its optimal parameters.

6.2 Results and Discussion

6.2.1 Convergence Properties

Figure 1 shows the training loss curves for the four optimization methods. MTAG achieves faster convergence compared to the other methods, particularly in the early stages of training. This advantage stems from the optimal learning rate ratios derived in Theorem 2, which allow different network components to evolve at their natural timescales.

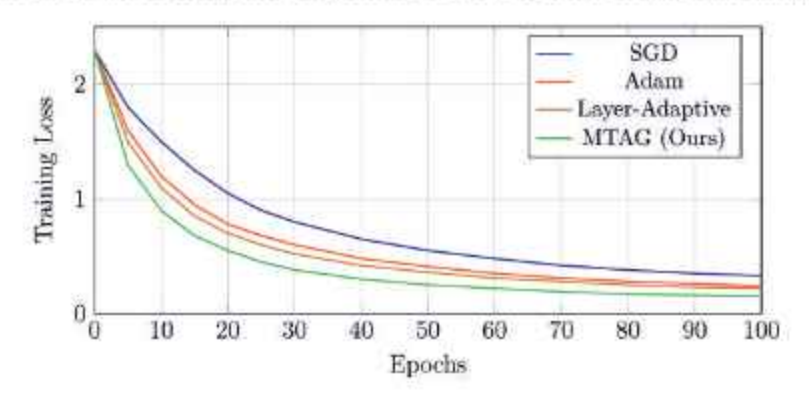


Figure 1: Training loss curves for different optimization methods. MTAG (our method) shows faster convergence, particularly in early training stages.

The layer-wise adaptive method also shows improved convergence compared to standard SGD and Adam, but not to the same extent as MTAG. This suggests that simply having different learning rates for different layers is beneficial, but the principled approach of MTAG based on Hessian eigenvalue ratios provides additional advantages.

6.2.2 Parameter Trajectory Analysis

To validate Theorem 1 on path independence, we analyze the trajectories of network parameters during training. We train the same network multiple times with different random initializations and compare the final parameters.

For networks trained with standard SGD, we observe significant variation in the final parameters across different runs, indicating path-dependent behavior. In contrast, networks trained with MTAG show more consistent final parameters, with variations primarily in directions that do not affect the network's function (i.e., along flat directions in the loss landscape).

This confirms that MTAG promotes more path-independent learning dynamics, as predicted by Theorem 1. The improved path independence leads to more robust training outcomes and reduces sensitivity to initialization.

6.2.3 Feature-Classifier Co-evolution

To validate Theorem 2 on feature-classifier co-evolution, we analyze the learning dynamics of the feature extraction and classification components separately. Figure 2 shows the distance of each component from its optimal parameters over time.

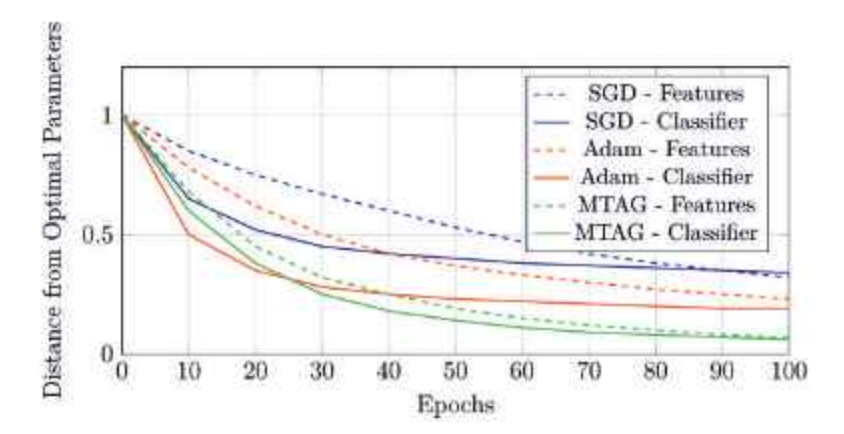


Figure 2: Distance of feature extraction and classification components from their optimal parameters during training. MTAG maintains better balance between feature learning and classifier adaptation.

We observe that with standard SGD and Adam, the classification component initially learns faster but then plateaus, while the feature extraction component continues to improve gradually. This leads to suboptimal co-evolution, where the classifier adapts to suboptimal features early in training.

In contrast, MTAG maintains a better balance between feature learning and classifier adaptation throughout training. The feature extraction and classification components evolve at compatible rates, leading to more efficient overall learning. This confirms the predictions of Theorem 2 regarding the optimal learning rate ratio between feature extraction and classification components.

6.2.4 Sensitivity to Hyperparameters

We evaluate the sensitivity of each method to its hyperparameters by varying the base learning rate over two orders of magnitude. Figure 3 shows the final validation accuracy for each method across different learning rate values.

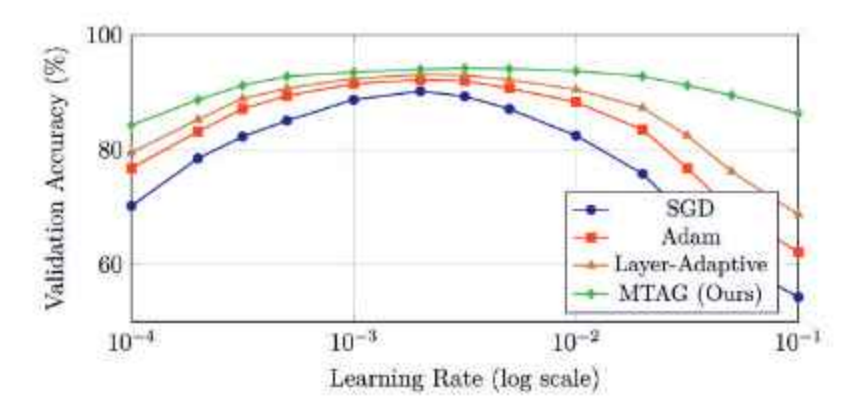


Figure 3: Final validation accuracy for different optimization methods across varying base learning rates. MTAG demonstrates reduced sensitivity to the base learning rate.

MTAG demonstrates significantly less sensitivity to the base learning rate compared to the other methods. Even with suboptimal base learning rates, MTAG maintains reasonable performance due to its adaptive adjustment of learning rates based on local curvature.

This reduced sensitivity to hyperparameters is a valuable practical advantage of the multi-time approach, as it simplifies the hyperparameter tuning process and makes the method more robust in practice.

7 Conclusion and Future Work

In this paper, we have developed a multi-time framework for understanding and improving neural network optimization dynamics. By viewing neural network training as a process evolving across multiple time dimensions, we have derived novel theoretical results on path independence and feature-classifier co-evolution. These results provide insights into the multi-scale nature of deep learning and suggest practical improvements to optimization algorithms.

Our proposed Multi-Time Adaptive Gradient (MTAG) algorithm implements these theoretical insights, adaptively adjusting learning rates for different network components based on estimated Hessian properties. Experimental results on synthetic data demonstrate the advantages of the multi-time approach, including faster convergence, improved path independence, and better feature-classifier co-evolution.

The multi-time framework opens up several promising directions for future research:

- Multi-time second-order methods: Extending the multi-time framework to second-order optimization methods like Newton's method and natural gradient descent.
- Architectural implications: Designing network architectures that naturally support path-independent multi-time learning dynamics.
- Theoretical connections: Exploring connections between multi-time learning and other theoretical frameworks in deep learning, such as information geometry and dynamical systems theory.

Application to specific domains: Applying multi-time optimization to domains
with inherent multi-scale structure, such as hierarchical reinforcement learning and
multi-resolution image processing.

We believe that the multi-time perspective provides a valuable new lens for understanding and improving deep learning systems, complementing existing theoretical frameworks and leading to practical advances in optimization algorithms.

Acknowledgments

This work is dedicated to memory of my Scientific Mentor Professor Constantin Udriste who was the father of Geometric Dynamics theory in terms of multi-time approach. After almost twenty years by this paper I wish commemorate this great Man and Scientist and launching this fascinating theory towards new fields of application as Artificial intelligence issues. I am confident that in the sky Professor Udriste will be so happy of this new challenge.

References

- Udriste, C., & Ferrara, M. (2008). Multitime Models of Optimal Growth. WSEAS Transactions on Mathematics, 7(1), 51-55.
- [2] Udriste, C., & Tevy, I. (2007). Multi-Time Euler-Lagrange-Hamilton Theory. WSEAS Transactions on Mathematics, 6(6), 701-709.
- [3] Udriste, C. (2007). Multi-Time Controllability, Observability and Bang-Bang Principle.
 In Proceedings of the 6th Congress of Romanian Mathematicians.
- [4] Kingma, D. P., & Ba, J. (2015). Adam: A method for stochastic optimization. In International Conference on Learning Representations (ICLR).
- [5] Tieleman, T., & Hinton, G. (2012). Lecture 6.5-rmsprop: Divide the gradient by a running average of its recent magnitude. COURSERA: Neural Networks for Machine Learning.
- [6] Singh, S. P., & Singh, S. (2020). Layer-specific adaptive learning rates for deep networks. In IEEE International Conference on Machine Learning and Applications (ICMLA).
- [7] You, Y., Li, J., Reddi, S., Hseu, J., Kumar, S., Bhojanapalli, S., Song, X., Demmel, J., Keutzer, K., & Hsieh, C. J. (2020). Large batch optimization for deep learning: Training BERT in 76 minutes. In *International Conference on Learning Representations* (ICLR).
- [8] Wang, G., Peng, J., Luo, P., Wang, X., & Lin, L. (2019). Batch Kalman normalization: Towards training deep neural networks with micro-batches. arXiv preprint arXiv:1802.03133.
- [9] Raghu, M., Gilmer, J., Yosinski, J., & Sohl-Dickstein, J. (2017). SVCCA: Singular vector canonical correlation analysis for deep learning dynamics and interpretability. In Advances in Neural Information Processing Systems (NeurIPS).

- [10] Li, H., Xu, Z., Taylor, G., Studer, C., & Goldstein, T. (2018). Visualizing the loss landscape of neural nets. In Advances in Neural Information Processing Systems (NeurIPS).
- [11] Smith, L. N., & Topin, N. (2018). Super-convergence: Very fast training of neural networks using large learning rates. arXiv preprint arXiv:1708.07120.
- [12] Kusupati, A., Ramanujan, V., Somani, R., Wortsman, M., Jain, P., Kakade, S., & Farbadi, A. (2020). Soft threshold weight reparameterization for learnable sparsity. In International Conference on Machine Learning (ICML).

Department of Law, Economics and Human Sciences - Decisions LAB, University Mediterranea of Reggio Calabria, Italy email: massimiliano.ferrara@unirc.it (Received, March 22, 2025)

Ajoy Mukharjee', ON μ-PARACOMPACTNESS AND Rebati Mohan Roy² μ-LOCALNESS ON GT SPACES

ISSN: 0970-5120

ABSTRACT. Firstly, we obtain some results on generalized paracompact spaces (X, μ) as applications of generalized preopen sets in X. Thereafter, we also obtain some characteristics of local finiteness of collections of subsets of a GT space (X, μ) with respect to a topology on X.

Keywords and phrases: μ -preopen set, μ -locally finiteness, μ -open refinement, μ -paracompact space, \mathcal{I}_{μ} -local finiteness.

2020 Mathematics Subject Classification: 54A05, 54D20.

1. Introduction

There are several generalizations of open sets of topological spaces (X, \mathcal{F}) e.g., semi-open sets [9, Levine], pre-open sets [10, Mashhour et al.] which are also called locally dense sets by Corson and Michael [2]. Császár [8] introduced and studied γ -open sets as a common generalization of such generalized sets of open sets in X. The γ -open sets finally leads to introduce and study the generalized topology on X.

Let $\exp(X)$ be the power set of the nonempty set X. A subcollection μ of $\exp(X)$ is called a generalized topology [7] on X if $\emptyset \in \mu$ and the union of arbitrary number of elements of μ is again a member of μ . A generalized topological space [7] is a nonempty set X endowed with a generalized topology μ and it is denoted by (X,μ) . We write GT (resp. GT space) to denote the generalized topology μ on X (resp. generalized topological space (X,μ)). An element of μ is called a μ -open set of (X,μ) . The complement of a μ -open set is called a μ -closed set of (X,μ) . A GT μ on X is called quasi-topology [4] if μ is closed under finite intersection. A generalized topological space (X,μ) is called strong [6] (also called μ -space by Noiri [14]) if $X \in \mu$. For brevity, we retain the term μ -space due to Noiri [14] to mean the strongly generalized topological space (X,μ) as well.

For a subset A of a GT space X, the intersection of all μ -closed sets containing A is the generalized closure [5] of A and is denoted by $c_{\mu}(A)$. Also for a subset A of a GT space X, the union of all μ -open sets contained in A is the generalized interior [5] of A and is denoted by $i_{\mu}(A)$. It is easy to see that a subset A of X is μ -open (resp. μ -closed) if and only if $A = i_{\mu}(A)$ (resp. $A = c_{\mu}(A)$). Also for a subset A of X, we have $c_{\mu}(A) = X - i_{\mu}(X - A)$.

Throughout the paper, N denotes the set of natural numbers and the elements of N are denoted by n, m, l, k etc. We also write 'nbd' to mean 'neighbourhood' of a point $x \in X$.

μ-paracompact Spaces

Firstly, we recall below some concepts and results for follow easily the rest of our present work easily.

Definition 2.1 (Császár [5]). A subset A of X is called μ -preopen if $A \subset i_{\mu}(c_{\mu}(A))$.

It is easy to see that $A \subset X$ is μ -preopen if and only if there exists a μ -open set G such that $A \subset G \subset c_{\mu}(A)$.

Definition 2.2 (Sarsak [16]). A subset A of X is called μ -regularly closed if $A = c_{\mu}(i_{\mu}(A))$. The complement of a μ -regularly closed set is called a μ -regularly open set. So a subset A of a GT space is μ -regularly open if $A = i_{\mu}(c_{\mu}(A))$.

We see that $i_{\mu}(c_{\mu}(G))$ is μ -regularly open in X if G is μ -open in X.

We agree to write ' μ -open collection' and ' μ -preopen collection' to denote a collection consisting of nonempty μ -open sets and μ -preopen sets respectively of a GT space. According to existing convention, a ' μ -open cover' of X is a μ -open collection $\mathscr C$ of X such that $\bigcup_{U \in \mathscr C} U = X$. We see that if X is not μ -open in a GT space (X, μ) , then the union of even all μ -open sets of X is not equal to X i.e., in such case, there exist no μ -open cover of X. So such a definition of μ -open covers of GT spaces become void. It instigates us to change the existing ideas of covering of GT spaces as follows.

We write $X_{\mu} = \bigcup_{G \in \mu} G$. It is then clear that X_{μ} is μ -open in X and $X_{\mu} = X$ if X is a μ -space. A collection $\mathscr C$ of nonempty subsets of X is called a cover of X [13] if $\bigcup_{G \in \mathscr C} G = X_{\mu}$. A μ -open collection (resp. μ -preopen collection) $\mathscr C$ of X is said to be a μ -open (resp. μ -preopen) cover of X if $\bigcup_{G \in \mathscr C} G = X_{\mu}$.

Let \mathscr{U} and \mathscr{V} be two covers of X. The cover \mathscr{V} is called a refinement [?, p. 144] of the cover \mathscr{U} if for each $V \in \mathscr{V}$, there exists a $U \in \mathscr{U}$ such that $V \subset U$. Let \mathscr{U} be a μ -open cover of X. If \mathscr{V} is a cover of X by μ -open sets of X, then \mathscr{V} is called a μ -open refinement of \mathscr{U} [1]. In the same fashion, if \mathscr{V} is a cover of X by μ -preopen sets of X, then \mathscr{V} is called a μ -preopen refinement [13] of \mathscr{U} .

Again let (X, μ) be a GT space such that $X \notin \mu$ and \mathscr{C} be a collection of subsets of X. Then for any $x \in X - X_{\mu}$, there exist no μ -open set U such that $x \in U$ and so there arise no question of existing a μ -open set U in X such that U intersects finitely many members of \mathscr{C} . Hence in the present study, we consider slightly modified versions of the notions like μ -locally finiteness (Definition 2.3), μ -paracompactness (Definition 2.5) in contrary

to the concern notions introduced by Deb Ray and Bhowmick [3], and Arar [1].

Definition 2.3 (Mukharjee and Roy [13]). A collection \mathcal{U} of subsets of X is called μ -locally finite if for each $x \in X_{\mu}$, there exists a μ -open set U with $x \in U$ meeting only finitely many members of \mathcal{U} .

Example 2.4. Let \mathbb{N} be the set of natural numbers and $\mathbb{E} \subset \mathbb{N}$ be the set of all even natural numbers. We define $\mu = \{\emptyset\} \cup \{G \mid G \text{ is an infinite subset of } \mathbb{E}\}$. Obviously, μ is a GT on \mathbb{N} such that $\mathbb{N} \notin \mu$. In the GT space (\mathbb{N}, μ) , we consider the collection $\mathscr{C} = \{\{2,4,6\},\{4,6,8\},\{6,8,10\},\ldots\}$. We see that for any $x \in \mathbb{E}$, a μ -open set U with $x \in U$ may intersects finitely many members of \mathscr{C} . So \mathscr{C} is a μ -locally finite collection in the GT space (\mathbb{N}, μ) .

We observe that for any $A \in \mathcal{C}$, $\mathbb{N} - \mathbb{E} \subset c_{\mu}(A)$ and $c_{\mu}(A) = \{2, 4, 6\} \cup \{\mathbb{N} - \mathbb{E}\}$ when $A = \{2, 4, 6\}$.

Definition 2.5 (Mukharjee and Roy [13]). A GT space X is called μparacompact if each μ-open cover of X has a μ-locally finite μ-open refinement.

Definition 2.6 (Mukharjee and Roy [13]). A μ -preopen set G in a GT space X is called capped by a μ -open set if there exists a μ -open set W such that $G \subset W \subset U \cap V$ whenever U, V are μ -open sets in X containing G.

Definition 2.7 (Min [11]). A GT space (X, μ) is called μ -Hausdorff if for any pair of distinct $x, y \in X_{\mu}$ there exist μ -open sets U, V in X such that $x \in U, y \in V$ and $U \cap V = \emptyset$.

Definition 2.8 (Min [12]). A GT space (X, μ) is called μ -regular if for any $x \in X_{\mu}$ and any μ -closed set F in X not containing x there exist μ -open sets U, V in X such that $x \in U, F \cap X_{\mu} \subset V$ and $U \cap V = \emptyset$.

It is shown that the GT space X is μ -regular if and only if for any $x \in X_{\mu}$ and any μ -open set U with $x \in U$ there exists a μ -open set V such that $x \in V \subset c_{\mu}(V) \cap X_{\mu} \subset U$.

Lemma 2.9. If F is a μ -closed set in a GT space X, then

- (i) $F = (F \cap X_{\mu}) \cup (X X_{\mu}),$
- (ii) $X F = X_{\mu} F$ and $X_{\mu} F$ is μ -open in X.

Proof. Both the results follows easily from the facts that $X = X_{\mu} \cup (X - X_{\mu})$ and $X - X_{\mu} \subset F$.

Theorem 2.10. A GT space X is μ -regular if and only if for any $x \in X_{\mu}$ and any μ -closed set F in X with $x \notin F \cap X_{\mu}$ there exist μ -open sets U, V in X such that $x \in U, F \cap X_{\mu} \subset V$ and $U \cap V = \emptyset$.

Proof. Necessity: Suppose that $x \in X_{\mu}$ and F is a μ -closed set in X such that $x \notin F \cap X_{\mu}$. As $x \in X_{\mu}$, $x \notin X - X_{\mu}$. Hence we find that $x \notin F$ by

Lemma 2.9(i). By the μ -regularity of X, we obtain μ -open sets U, V in X such that $x \in U, F \cap X_{\mu} \subset V$ and $U \cap V = \emptyset$.

Sufficiency: Let $x \in X_{\mu}$ and F be a μ -closed set in X not containing x. Then obviously, we have $x \notin F \cap X_{\mu}$. Hence we obtain μ -open sets U, V in X such that $x \in U, F \cap X_{\mu} \subset V$ and $U \cap V = \emptyset$.

Theorem 2.11 (Mukharjee and Roy [13]). Let μ -preopen sets in a GT space X are capped by μ -open sets of X. The GT space X is μ -paracompact if and only if each μ -open covers of X has a μ -locally finite μ -preopen refinement.

Theorem 2.12. Let μ -preopen sets in a generalized topological space X are capped by μ -open sets in X. The generalized topological space X is μ -paracompact if each μ -preopen cover of X has a μ -locally finite μ -preopen refinement.

Proof. The results follows by Theorem 2.11 from the fact that a μ -open cover of X is also a μ -preopen cover of X.

Theorem 2.13. Let X be a μ -Hausdorff μ -paracompact space and μ -preopen sets in X are capped by μ -open sets in X. Then for $x \in X$ and a μ -closed set E with $x \notin E$, there exist a subset G of X and a μ -preopen set H in X such that $x \in G$, $E \cap X_{\mu} \subset H$ and $pc_{\mu}(G) \cap H = \emptyset$.

Proof. Let E be a μ -closed set in X and $x \in X_{\mu}$ such that $x \notin E$. Since $E = (E \cap X_{\mu}) \cup (X - X_{\mu})$ by Lemma 2.9, $x \in X_{\mu}$ whenever $x \in X$ and $x \notin E$. For each $y \in E \cap X_{\mu}$, there exist μ -open sets U_y, V_y in X such that $x \in U_y, y \in V_y$ and $U_y \cap V_y = \emptyset$ as $x \neq y$ and X is μ -Hausdorff. We write $\mathscr{V} = \{V_y \mid y \in X_\mu \cap E\}$. Then $\mathscr{U} = \mathscr{V} \cup \{X - E\}$ is a μ -open cover of X. By Theorem 2.11 on μ -paracompactness of X, we obtain a μ -locally finite μ preopen refinement \mathscr{G} of \mathscr{U} . Putting $H = \bigcup \{U \mid U \in \mathscr{G}, U \cap (E \cap X_{\mu}) \neq \emptyset \}$, we see that $E \cap X_{\mu} \subset H$. Since \mathscr{G} is μ -locally finite, there exists a μ -open set W in X with $x \in W$ intersecting finitely many members of \mathcal{G} . Let the finite collection of members of \mathscr{G} intersecting W be \mathscr{G}_m . As \mathscr{G} is a μ -preopen refinement of \mathcal{U} , there may exists finitely many $W_k \in \mathcal{G}_m, k \in$ $\{1,2,\ldots,n\}$ such that $W_k \subset V_{y_k}, V_{y_k} \in \mathscr{V}$ and $V_{y_k} \cap (E \cap X_\mu) \neq \emptyset$ for each $k \in \{1,2,\ldots,n\}$. We put $G = W \cap (\bigcap_{k=1}^n U_{y_k})$. To show $G \cap H = \emptyset$, we suppose that $z \in G \cap H$. Then $z \in W$ and $z \in U_{y_k}$ for all $k \in \{1, 2, ..., n\}$. Also $z \in U$ for some $U \in \mathcal{G}$ with $U \cap (E \cap X_{\mu}) \neq \emptyset$. So this U is equal to W_k for some $k \in \{1, 2, ..., n\}$. Hence we get $U_{y_k} \cap V_{y_k} \neq \emptyset$ which gives a contradiction to $U_{y_k} \cap V_{y_k} = \emptyset$. As H is μ -preopen and $G \cap H = \emptyset$, we have $pc_{\mu}(G) \cap H = \emptyset.$

Remark 2.14. Let E be a μ -closed set in X. We see that for $x \in X_{\mu}$, $x \notin E \cap X_{\mu}$ whenever $x \notin E$. Hence Theorem 2.13 also hold if we choose $x \notin E$ instead of $x \notin E \cap X_{\mu}$ in the statement of the theorem.

Theorem 2.15. Let X be a μ -Hausdorff μ -paracompact space. If $x \in X$ and E is μ -closed in X with $x \notin E$, then there exist a subset G of X and a μ -open set H in X such that $x \in G$, $X_{\mu} \cap E \subset H$ and $c_{\mu}(G) \cap H = \emptyset$.

Proof. Similar to that of Theorem 2.13.

Deb Roy and Bhowmick [3], defined γ_{μ} -closure operator on a GT space (X, μ) and showed that the γ_{μ} -closure operator gave rise to a topology μ^* on X. It is also seen here that $\mu = \mu^*$ if μ is topology on X. We note that if μ is a GT on X, there exist a topology \mathscr{T} , namely $\exp(X)$ such that $\mu \subset \mathscr{T}$.

Noiri and Roy [15] initiated the study of unification of generalized open sets on topological spaces and two placed below.

Definition 2.16 (cf. Noiri and Roy [15]). Let μ be a GT on a topological space (X, \mathcal{T}) . The topological space (X, \mathcal{T}) is called \mathcal{T}_{μ} -regular if for each $x \in X_{\mu}$ and each closed set F on X with $x \notin F$ there exist disjoint μ -open sets U, V such that $x \in U, F \subset V$.

Henceforth we write, X is \mathcal{I}_{μ} -regular to mean \mathcal{I}_{μ} -regularity of the topological space (X, \mathcal{F}) with respect to a GT μ on X as defined in Definition 2.16.

Theorem 2.17 (cf. Noiri and Roy [15]). Let μ be a GT on a topological space (X, \mathcal{T}) . The topological space (X, \mathcal{T}) is \mathcal{T}_{μ} -regular if and only if for each $x \in X$ and each \mathcal{T} -open set U with $x \in U$, there exists a μ -open set V such that $x \in V \subset c_{\mu}(V) \cap X_{\mu} \subset U$.

The observations recorded above due to Deb Roy and Bhowmick [3] and Noiri and Roy [15] instigated us to consider a topology \mathcal{T} on a GT space (X, μ) to get some characterizations on the μ -local finiteness.

Definition 2.18. A collection \mathcal{U} of subsets of X is called \mathcal{T}_{μ} -locally finite if for each $x \in X_{\mu}$, there exists a \mathcal{T} -open set U with $x \in U$ meeting only finitely many members of \mathcal{U} .

A \mathcal{T} -open set U in (X, \mathcal{T}) with $x \in U$ always exists as there have a μ -open set G in (X, μ) such that $x \in G$ and $\mu \subset \mathcal{T}$.

Theorem 2.19. Let X be \mathcal{T}_{μ} -regular. If $\{U_{\alpha} \mid \alpha \in A\}$ is a \mathcal{T}_{μ} -locally finite cover of X then $\{c_{\mu}(U_{\alpha}) \cap X_{\mu} \mid \alpha \in A\}$ is a μ -locally finite cover of X.

Proof. Since $\{U_{\alpha} \mid \alpha \in A\}$ is \mathcal{T}_{μ} -locally finite, for each $x \in X_{\mu}$ there exists a \mathcal{T} -open set U in X containing x such that $U_{\alpha} \cap G \neq \emptyset$ for finitely many $\alpha \in A$. Let $U_{\alpha_k} \cap G \neq \emptyset$ for $k \in \{1, 2, \dots, m\}, m \in \mathbb{N}$. It means that $U_{\alpha} \cap G = \emptyset$ whenever $\alpha \in A - \{\alpha_1, \alpha_2, \dots, \alpha_m\}$. By Theorem 2.17 there exists a μ -open set H such that $x \in H \subset c_{\mu}(H) \cap X_{\mu} \subset G$. As $H \subset G$, $U_{\alpha} \cap H = \emptyset$ whenever $\alpha \in A - \{\alpha_1, \alpha_2, \dots, \alpha_m\}$. Thus we have $c_{\mu}(U_{\alpha}) \cap H = \emptyset$ whenever $\alpha \in A - \{\alpha_1, \alpha_2, \dots, \alpha_m\}$. So $\{c_{\mu}(U_{\alpha}) \mid \alpha \in A\}$ is μ -locally finite. Since $c_{\mu}(U_{\alpha}) \cap X_{\mu} \subset c_{\mu}(U_{\alpha})$ for each $\alpha \in A$, $\{c_{\mu}(U_{\alpha}) \cap X_{\mu} \mid \alpha \in A\}$ is also

 μ -locally finite. Again for any $x \in X_{\mu}$, there exists an $\alpha \in A$ such that $x \in U_{\alpha} \subset c_{\mu}(U_{\alpha})$. Hence $\{c_{\mu}(U_{\alpha}) \cap X_{\mu} \mid \alpha \in A\}$ is a cover of X.

Theorem 2.20. Let X be a GT space. If $\mathscr{U} = \{U_{\alpha} \mid \alpha \in A\}$ is a \mathscr{T}_{μ} -locally finite μ -open cover of X then $\bigcup_{\alpha \in A} c_{\mu}(U_{\alpha}) = c_{\mu} (\bigcup_{\alpha \in A} U_{\alpha})$.

Proof. We only need to show $\bigcup_{\alpha \in A} c_{\mu}(U_{\alpha}) \supset c_{\mu} \left(\bigcup_{\alpha \in A} U_{\alpha}\right)$. Suppose that $x \in c_{\mu} \left(\bigcup_{\alpha \in A} U_{\alpha}\right)$. If $x \in X - X_{\mu}$, then there exist no μ -open set in X containing x. Hence $x \in c_{\mu}(U_{\alpha})$ for each $\alpha \in A$. So in this case, $\bigcup_{\alpha \in A} c_{\mu}(U_{\alpha}) \supset c_{\mu} \left(\bigcup_{\alpha \in A} U_{\alpha}\right)$ hold. Now we suppose that $x \in X_{\mu}$. By \mathscr{T}_{μ} -local finiteness of \mathscr{U} , there exists a \mathscr{T} -open nbd U of x such that U intersects finitely many members $U_{\alpha_1}, U_{\alpha_2}, \ldots, U_{\alpha_n}$ of \mathscr{U} . As $x \in c_{\mu} \left(\bigcup_{\alpha \in A} U_{\alpha}\right)$, each μ -open nbd V of x intersects $\bigcup_{\alpha \in A} U_{\alpha}$. Since $\mu \subset \mathscr{T}$, V is also a \mathscr{T} -open set which in turns implies that $U \cap V$ is a \mathscr{T} -open nbd of x. Since \mathscr{U} is a cover of X, $(U \cap V) \cap (\bigcup_{i=1}^n U_{\alpha_i}) \neq \emptyset$ which gives $V \cap (\bigcup_{i=1}^n U_{\alpha_i}) \neq \emptyset$ since $U \cap V \subset V$. It means that $x \in c_{\mu} (\bigcup_{i=1}^n U_{\alpha_i}) = c_{\mu}(U_{\alpha_1}) \cup c_{\mu}(U_{\alpha_2}) \cup \ldots \cup c_{\mu}(U_{\alpha_n}) \subset \bigcup_{\alpha \in A} c_{\mu}(U_{\alpha})$.

Corollary 2.21. Let X be a GT space. If $\mathcal{U} = \{U_{\alpha} \mid \alpha \in A\}$ is a \mathcal{T}_{μ} -locally finite μ -open cover of X then $\bigcup_{\alpha \in A} (c_{\mu}(U_{\alpha}) \cap X_{\mu}) = c_{\mu} (\bigcup_{\alpha \in A} U_{\alpha}) \cap X_{\mu}$.

Proof. Since $\bigcup_{\alpha \in A} (c_{\mu}(U_{\alpha}) \cap X_{\mu}) = (\bigcup_{\alpha \in A} c_{\mu}(U_{\alpha})) \cap X_{\mu}$, the result follows by Theorem 2.20.

Lemma 2.22. Let μ be a GT on the topological space (X, \mathcal{T}) and $\mu \subset T$. Then \mathcal{T}_{μ} -regularity of X implies the μ -regularity of the GT space (X, μ) .

Proof. Easy to proof and hence omitted.

Theorem 2.23. Let μ be a GT on the topological space (X, \mathcal{F}) such that $\mu \subset \mathcal{F}$ and let X be a \mathcal{F}_{μ} -regular space. Then each μ -open cover \mathcal{G} of X has a μ -locally finite refinement $\mathcal{F} = \{F_{\gamma} \cap X_{\mu} \mid \gamma \in \Gamma\}$ of \mathcal{U} where $\{F_{\gamma} \mid \gamma \in \Gamma\}$ is a collection of μ -closed sets in X if each μ -open cover of X has a \mathcal{F}_{μ} -locally finite refinement.

Proof. Let $\mathscr{G} = \{G_{\gamma} \mid \gamma \in \Gamma\}$ be a μ -open cover of X. For each $x \in X_{\mu}$, there exists a $\gamma(x) \in \Gamma$ such that $x \in G_{\gamma(x)}$. As \mathscr{T}_{μ} -regular space is μ -regular also by Lemma 2.22, there exists a μ -open set V_x such that $x \in V_x \subset c_{\mu}(V_x) \cap X_{\mu} \subset G_{\gamma(x)}$. The μ -open cover $\mathscr{V} = \{V_x \mid x \in X_{\mu}\}$ has a \mathscr{T}_{μ} -locally finite refinement $\mathscr{U} = \{U_x \mid x \in X_{\mu}\}$. By Lemma 2.19, $\{c_{\mu}(U_x) \cap X_{\mu} \mid x \in X_{\mu}\}$ is a μ -locally finite cover of X. As $U_x \subset V_x$ for each $x \in X_{\mu}$, $c_{\mu}(U_x) \cap X_{\mu} \subset c_{\mu}(V_x) \cap X_{\mu} \subset G_{\gamma(x)}$, $\gamma(x) \in \Gamma$ for each $x \in X_{\mu}$. Hence $\{c_{\mu}(U_x) \cap X_{\mu} \mid x \in X_{\mu}\}$ is also a refinement of \mathscr{G} .

References

M.M. Arar, On countably μ-paracompact spaces, Acta Math. Hungar. 149 (1) (2016), 50–57.

- [2] H.H. Corson, E. Michael, Metrizability of certain countable unions, Illinois J. Math. 8 (1964), 351–360.
- [3] A. Deb Ray, R. Bhowmick, μ-paracompact and g_μ-paracompact generalized topological spaces, Hacet. J. Math. Stat. 45 (2) (2016), 447–453.
- [4] A. Császár, Further remarks on the formula for γ-interior, Acta Math. Hungar. 113
 (4) ((2006), 325–332.
- [5] Á. Császár, Generalized open sets in generalized topologies, Acta Math. Hungar. 106 (1-2) (2005), 351–357.
- [6] Á. Császár, Extremally disconnected generalized topologies, Ann. Univ. Sci. Budapest. Eötvös Sect. Math. 47 (2004), 91–96.
- [7] Á. Császár, Generalized topology, generalized continuity, Acta Math. Hungar. 96 (4) (2002), 351–357.
- [8] Á. Császár, Generalized open sets, Acta Math. Hungar. 75 (1-2) (1997), 65–87.
- [9] N. Levine, Semi-open sets and semi-continuity in topological spaces, Amer. Math. Monthly 70 (1963), 36–41.
- [10] A.S. Mashhour, M.E. Abd El-Monsef, S. N. El-Deeb, On precontinuous and weak precontinuous mappings, Proc. Math. Phy. Soc. Egypt 53 (1982), 47–53.
- [11] W.K. Min, Remarks on separation axioms on generalized topological spaces, J. Chungcheong Math. Soc. 23 (2) (2010), 293-298.
- [12] W.K. Min, (δ, δ')-continuity on generalized topological spaces, Acta Math. Hungar. 129 (4) (2010), 350–356.
- [13] A. Mukharjee, R. M. Roy On generalized preopen sets, Mat. Stud. 51 (2019), 195–199.
- [14] T. Noiri, Unified characterizations for modifications of R₀ and R₁ topological spaces, Rend. Circ. Mat. Palermo (2) 55 (2006), 29–42.
- [15] T. Noiri, B. Roy, Unification of generalized open sets on topological spaces, Acta Math. Hungar. 130 (4), 349–357.
- [16] M.S. Sarsak, Weakly μ-compact spaces, Demonstr. Math. 45 (4) (2012), 929–938.

Department of Mathematics, Bankura University, (Received, December 08, 2024)
Bankura, W. Bengal- 722 155, India
Email address: ajoyjee@gmail.com

³Department of Mathematics, Mathabhanga College, Coochbehar, W. Bengal- 736 146, India Email address: roy rebati@rediffmail.com

GENERALIZED TOTALLY POSITIVE FUNCTIONS AND GENERALIZED Thalmi, B. Jayasri, C TOTALLY BOUNDED FUNCTIONS IN A PARTICULAR ECT-SPACE

ISSN: 0970-5120

Abstract

In this paper, we give an example of a generalized totally positive function and a generalized totally bounded function in the ECT - space generated by $\left(\frac{1}{x+1}, \frac{1}{x+2}, \dots \frac{1}{x+n}\right)$

AMS 2020 Subject Classification:41A05, 65D05

Keywords: Extended complete Tchebycheff spaces, Generalized Lagrange interpolants, Generalized totally positive functions, Generalized totally bounded functions.

1 Introduction

Totally positive functions and totally bounded functions on [-1,1] have been introduced and studied by Alan L. Horwitz and Lee A. Rubel in [2]. A generalization of these functions using generalized Lagrange interpolants is introduced in [6, 7] and some properties of these functions are also studied there. In this paper, we give examples of these generalized functions in a particular ECT-space.

2 Preliminaries

The chapters 2 and 9 of [5] are chiefly referred for the definitions and results given in this section and these results are necessary to prove our main theorem in the fourth section. In the first two sections of this paper, I denotes the closed bounded interval [a,b] of $(-\infty,\infty)$.

Definition 2.1. Let $u_1, u_2, ..., u_m$ be real valued functions defined on I = [a, b] and let $x_1 \le x_2 \le ... \le x_m$ be points in I. The collocation matrix associated with $\{u_i\}_{i=1}^m$ and $\{x_i\}_{1}^{m}$ is denoted by $M\begin{pmatrix} x_1, & \dots, & x_{m-1}, & x_m \\ u_1, & \dots, & u_{m-1}, & u_m \end{pmatrix}$ and is defined by $M\begin{pmatrix} x_1, & \dots, & x_{m-1}, & x_m \\ u_1, & \dots, & u_{m-1}, & u_m \end{pmatrix} = [D^{(d_i)}u_j(x_i)]_{i,j=1}^{m}$

$$M\begin{pmatrix} x_1, \dots, x_{m-1}, x_m \\ u_1, \dots, u_{m-1}, u_m \end{pmatrix} = [D^{(d_i)}u_j(x_i)]_{i,j=1}^m$$

where $d_i = \mathcal{N}\{j : j < i, x_j = x_i\}, i = 1, 2, ...m$, provided the d_i^{th} derivative of u_j exists at the points x_i , i, j = 1, 2, ..., m and N(A) denotes the number of elements in the set A.

Definition 2.2. In Definition 2.1, if all the points coincide, that is, if $x_1 = x_2 = \cdots = x_m$ all equal to $x_0(say)$, then the determinant of the collocation matrix is called the Wronskian and is denoted by $W(u_1, u_2, \dots, u_m)(x_0)$. That is,

$$W(u_1, u_2, \dots, u_m)(x_0) = \det \begin{bmatrix} u_1(x_0) & \dots & u_{m-1}(x_0) & u_m(x_0) \\ u'_1(x_0) & \dots & u'_{m-1}(x_0) & u'_m(x_0) \\ \vdots & \ddots & \vdots & \vdots \\ u_1^{(m-1)}(x_0) & \dots & u_{m-1}^{(m-1)}(x_0) & u_m^{(m-1)}(x_0) \end{bmatrix}$$

Definition 2.3. Let $U_m = \{u_i\}_{i=1}^m$ be any collection of functions in $C^{m-1}[I]$, the space of all (m-1)-times continuously differentiable functions on I. U_m is called an extended Tchebycheff system (ET-system) on I if the determinants associated with the collocation matrices $M\begin{pmatrix} x_1, & \dots, & x_{m-1}, & x_m \\ u_1, & \dots, & u_{m-1}, & u_m \end{pmatrix}$ are positive for all $x_1 \leq x_2 \leq \dots \leq x_m$ in I.

Let $\{u_1, u_2, ...\}$ be any finite or infinite sequence of functions in I. If for each k, $\{u_1, ..., u_k\}$ forms an ET-system on I, then $\{u_1, u_2, ...\}$ is called an extended complete T-chebycheff system (ECT-system) on I.

Remark 2.1. The Determinant associated with the matrix $M\begin{pmatrix} x_1, & \dots, & x_{m-1}, & x_m \\ u_1, & \dots, & u_{m-1}, & u_m \end{pmatrix}$ is denoted by $D\begin{pmatrix} x_1, & \dots, & x_{m-1}, & x_m \\ u_1, & \dots, & u_{m-1}, & u_m \end{pmatrix}$. The determinant of the collocation matrix arising from an ECT-system $U_m = \{u_1, u_2, \dots u_m\}$ is denoted by $D_{U_m}(x_1, x_2, \dots, x_m)$.

Definition 2.4. A subspace of C(I), finite or infinite dimensional, is called an Extended complete Tchebycheff space (ECT-space) if it has an ordered basis which is an ECT-system.

Elements of an ECT-space are called generalized polynomials.

Definition 2.5. Let $U_m = \{u_1, u_2, \dots u_m\}$ be an ECT-system on I, and let f be a sufficiently differentiable function defined on I. Associated with any m points x_1, x_2, \dots, x_m in I, not necessarily distinct, we define a function on I as follows:

$$D\begin{pmatrix} x_1, & \dots, & x_m; & x \\ u_1, & \dots, & u_m, & f \end{pmatrix} = \det \begin{bmatrix} u_1^{(d_1)}(x_1) & \dots & u_m^{(d_1)}(x_1) & f^{(d_1)}(x_1) \\ \vdots & \ddots & \vdots & \vdots & \vdots \\ u_1^{(d_i)}(x_i) & \dots & u_m^{(d_i)}(x_i) & f^{(d_i)}(x_i) \\ \vdots & \ddots & \vdots & \vdots \\ u_1^{(d_m)}(x_m) & \dots & u_m^{(d_m)}(x_m) & f^{(d_m)}(x_m) \\ u_1(x) & \dots & u_m(x) & f(x) \end{bmatrix}$$

where $d_i = \mathcal{N}\{j : j < i, x_j = x_i\}, i = 1, 2, ..., m$, provided the d_i^{th} derivative of u_j exists at the points $x_i, i, j = 1, 2, ..., m$.

Remark 2.2. If $U_{m+1} = \{u_1, u_2, \dots u_m, u_{m+1}\}$ is an ECT-system on I = [a, b], then the function in Definition 2.5 with f replaced by u_{m+1} is denoted by $D_{U_{m+1}}(x_1, \dots, x_m; x)$ Example 1. A well-known example of an infinite ECT-system on any interval I = [a, b] is $P = \{1, x, x^2, ...\}$. For each n, $P_n = \{1, x, ..., x^{n-1}\}$ is an ECT-system forming a basis for P_n , the space of all polynomials of degree atmost n - 1.

Remark 2.3 (cf. [5], p.30). When $x_1, ..., x_n$ are distinct points in I, the Vandermonde determinant, $D_{P_n}(x_1, ..., x_n)$, has the following value:

$$D_{P_n}(x_1, x_2, ..., x_n) = \prod_{\substack{i,j=1 \ i \neq j}}^n (x_i - x_j)$$

An equivalent condition for a set of functions to form an ECT-system is given in the next result.

Theorem 2.1 (cf.[5], p.363). A set of functions $u_1, u_2, ..., u_m$ in $C^{m-1}[I]$ form an ECT-system if and only if their Wronskian determinants are positive for all $x \in I$. That is, $W(u_1, u_2, ..., u_k)(x) > 0$ for all $x \in I$, k = 1, 2, ..., m.

Definition 2.6. Suppose $U_m = \{u_1, u_2, ..., u_m\}$ is an ECT-system in I. Given any sufficiently differentiable function f defined on I, its (m-1)th order divided difference with respect to U_m is defined by

$$[x_1, \dots, x_{m-1}, x_m]_{U_m} f = \frac{D\begin{pmatrix} x_1 & \dots, & x_{m-1}, & x_m \\ u_1 & \dots, & u_{m-1}, & f \end{pmatrix}}{D\begin{pmatrix} x_1 & \dots, & x_{m-1}, & x_m \\ u_1 & \dots, & u_{m-1}, & x_m \end{pmatrix}}$$

where $x_1 \le x_2 \le ... \le x_m$ are given points in I

If U_m is an ECT-space on I = [a, b] and if $x_1 < ... < x_m$ are prescribed points in I, then for any given function f defined on I, there corresponds a unique generalized polynomial in U_m which interpolates to f at the points $x_1 < ... < x_m$ (cf. [5]). In [8], we have derived an explicit expression for this unique generalized polynomial p_m in U_m and also an expression for the error $f - p_m$.

Theorem 2.2 (cf [8]). Let U_m be an ECT-space on I = [a, b] and let $x_1, x_2, ..., x_m$ be distinct points in I. Let f be any function defined on I, which is sufficiently differentiable.

 Then an explicit expression for the unique generalized polynomial p_m in U_m satisfying the conditions

$$p_m(x_i) = f(x_i)$$
 $i = 1, 2, ..., m$.

is given by

$$p_m(x) = [x_1]_{U_1} f.D_{U_1}(x) + [x_1, x_2]_{U_2} f. \frac{D_{U_2}(x_1; x)}{D_{U_1}(x_1)} + \cdots + [x_1, \dots, x_m]_{U_m} f. \frac{D_{U_m}(x_1, \dots, x_{m-1}; x)}{D_{U_{m-1}}(x_1, \dots, x_{m-2}, x_{m-1})}.$$

where $U_m = \{u_1, u_2, ..., u_m\}$ is an ECT-system forming a basis for U_m and $U_k = \{u_1, u_2, ..., u_k\}, k = 1, 2, ..., m$ (ii) The error is given by

$$f(x) - p_m(x) = [x_1, \dots, x_m; x]_{U_{m+1}} f. \frac{D_{U_{m+1}}(x_1, \dots, x_m; x)}{D_{U_m}(x_1, \dots, x_m)}.$$

where $U_{m+1} = \{u_1, u_2, \dots, u_m, u_{m+1}\}$ is an ECT-system on I containing U_m .

3 Generalizations and associated results

Throughout this section, U denotes an infinite dimensional ECT-space on I = [a, b]with an ordered basis $U = \{u_1, u_2, ...\}$ which is an ECT-system on I. For each m, U_m is the ECT-space spanned by $U_m = \{u_1, u_2, ..., u_m\}$.

Definition 3.1. Let f be a real valued function defined on I. A generalized polynomial p is called a generalized Lagrange interpolant to f from U if for some m, there exists distinct points $x_1, x_2, ..., x_m$ in I such that p is the unique generalized polynomial in U_m interpolating to f at $x_1, x_2, ..., x_m$. We denote this generalized Lagrange interpolant to f by $L(x_1, ..., x_m; f)$

The collection of all generalized Lagrange interpolants to f from U is denoted by $GL_U(f)$.

Definition 3.2. Let f be a sufficiently differentiable function defined on I. A generalized polynomial q is called a generalized Taylor interpolant to f from U if for some m, there exists a point x_0 in I such that q is the unique generalized polynomial in U_m interpolating to f and its m-1 derivatives at x_0 .

The collection of all generalized Taylor interpolants to f from U is denoted by $GT_{\mathcal{U}}(f)$.

Definition 3.3. A function f defined on I is said to be generalized totally positive on I if p > 0 on I for all $p \in GL_U(f)$.

The collection of all generalized totally positive functions on I is denoted by GTP_{II}.

Definition 3.4. A real valued function f defined on I is said to be generalized totally bounded on I if there exists an M such that

$$|p(x)| \le M$$

for all $p \in GL_U(f)$ and for all $x \in I$.

The collection of all generalized totally bounded functions on I is denoted by GTB_{U} .

4 Main Results

Let I=[a,b] be any sub interval of $[0,\infty)$ and let $0 < s_1 < s_2 < \cdots < s_n < \cdots$ be an infinite sequence of real numbers. Consider the function $u_i(x) = \frac{1}{s_i+x}$ for $i=1,2,\ldots,$ defined on I. This is a collection of infinitely differentiable functions arising from the Cauchy kernel and therefore forms a complete Tchebycheff system on I. (cf. [4], p.no.11). First we will show that the collection of functions $\{u_i\}$ forms an ECT-system on I.

Proposition 4.1. Let I = [a,b] and let $0 < s_1 < s_2 < \cdots < s_n$ be an increasing sequence of real numbers. Let $u_i(x) = \frac{1}{s_i+x}$ for $i=1,2,\ldots,n$. Then $U_n = \{u_1,u_2,\ldots,u_n\}$ form an ECT-system on I.

Proof. First we will show that the wronskian determinants $W(u_1, u_2, ..., u_k)(x)$ are positive for all x in I and for k = 1, 2, ... n. Fix $x \in I$. Also fix k.

Non

$$W(u_1, u_2, \dots, u_k)(x) = \det \begin{bmatrix} \frac{1}{s_1 + x} & \frac{1}{s_2 + x} & \dots & \frac{1}{s_k + x} \\ \frac{-1}{(s_1 + x)^2} & \frac{-1}{(s_2 + x)^2} & \dots & \frac{1}{(s_k + x)^2} \\ \vdots & \vdots & \vdots & \vdots \\ \frac{(-1)^{k-1}(k-1)!}{(s_1 + x)^k} & \frac{(-1)^{k-1}(k-1)!}{(s_2 + x)^k} & \dots & \frac{(-1)^{k-1}(k-1)!}{(s_k + x)^k} \end{bmatrix}$$

$$= \frac{(-1)^{1+2+\dots(k-1)} \cdot 1! \cdot 2! \cdot \dots \cdot (k-1)!}{(s_1+x)(s_2+x) \cdot \dots \cdot (s_k+x)}.$$

$$\begin{vmatrix} \frac{1}{s_1+x} & \frac{1}{s_2+x} & \dots & \frac{1}{s_k+x} \\ \vdots & \vdots & \vdots & \vdots \\ \frac{1}{(s_1+x)^{k-1}} & \frac{1}{(s_2+x)^{k-1}} & \dots & \frac{1}{(s_k+x)^{k-1}} \end{vmatrix}$$

$$= \frac{(-1)^{\frac{k(k-1)}{2}}.11.2!....(k-1)!}{(s_1+x)(s_2+x)...(s_k+x)} \begin{vmatrix} 1 & 1 & ... & 1 \\ y_1 & y_2 & ... & y_k \\ \vdots & \vdots & \vdots & \vdots \\ y_1^{k-1} & y_2^{k-1} & ... & y_k^{k-1} \end{vmatrix}$$

where $y_i = \frac{1}{s_i + x}$. By using the value of the Vandermonde determinant given in Remark 2.3, we have

$$W(u_1, u_2, \dots, u_k)(x) = \frac{(-1)^{\frac{k(k-1)}{2}} \cdot 1! \cdot 2! \cdot \dots \cdot (k-1)!}{(s_1 + x)(s_2 + x) \cdot \dots \cdot (s_k + x)} \cdot \prod_{\substack{i,j=1 \ i>j}}^k (y_i - y_j)$$

Now

$$y_i - y_j = \frac{1}{s_i + x} - \frac{1}{s_j + x} = \frac{-(s_i - s_j)}{(s_i + x)(s_j + x)}$$

Thus

$$\begin{split} W(u_1,u_2,\ldots,u_k)(x) &= \frac{(-1)^{\frac{k(k-1)}{2}}.1!.2!\ldots(k-1)!}{(s_1+x)(s_2+x)\ldots(s_k+x)}.(-1)^{(k-1)+(k-2)+\cdots+1}.\\ &\qquad \qquad \prod_{\stackrel{i,j=1}{i \neq 1}}^k \frac{s_i-s_j}{(s_i+x)(s_j+x)}\\ &= \frac{(-1)^{\frac{k(k-1)}{2}}.1!\ldots(k-1)!}{(s_1+x)\ldots(s_k+x)}.(-1)^{\frac{k(k-1)}{2}}.\prod_{\stackrel{i,j=1}{i \neq j}}^k \frac{s_i-s_j}{(s_i+x)(s_j+x)}\\ &= \frac{1!.\ldots(k-1)!}{(s_1+x)\ldots(s_k+x)}.\prod_{\stackrel{i,j=1}{i \neq j}}^k \frac{s_i-s_j}{(s_i+x)(s_j+x)} > 0 \end{split}$$

Therefore, by Theorem 2.1, $\{u_1, u_2, \dots, u_n\}$ forms an ECT-system on I.

From here onwards, in this section, we will restrict our discussion to J = [0, 1]. From the previous theorem, the collection of functions $\{\frac{1}{1+x}, \frac{1}{2+x}, \dots, \frac{1}{n+x}\}$ form an ECT-system on J.

Notation 1. We use the notation \mathcal{R}^* to denote the ECT-space on J = [0, 1] spanned by $R^* = \{\frac{1}{1+x}, \frac{1}{2+x}, \dots, \frac{1}{n+x}, \dots\}$. Also the notation \mathcal{R}^*_n is used to denote the ECT-space spanned by $\mathcal{R}^*_n = \{\frac{1}{1+x}, \frac{1}{2+x}, \dots, \frac{1}{n+x}\}$ on J.

We next consider the function f_s defined on [0,1] by

$$f_s(x) = \frac{1}{x + s}$$
(4.1)

For this function to be well defined on [0,1] it is necessary and sufficient that s is a real number outside the interval [-1,0]. Here we first obtain an expression for the error function

$$f_n - p_n$$

where p_n is the unique generalized polynomial in \mathcal{R}_n^* interpolating to f at n distinct points $x_1, x_2, ..., x_n$ in [0, 1]. For this we need the value of Cauchy determinant which is given by the following lemma(cf.[3]).

Lemma 4.1 ([3], p.268). If $a_i + b_j \neq 0$ for i, j = 1, 2, ..., n and if

$$D_n = \begin{bmatrix} \frac{1}{a_1+b_1} & \frac{1}{a_1+b_2} & \cdots & \frac{1}{a_1+b_n} \\ \vdots & \vdots & \ddots & \vdots \\ \frac{1}{a_n+b_1} & \frac{1}{a_n+b_2} & \cdots & \frac{1}{a_n+b_n} \end{bmatrix}$$

then

$$D_n = \frac{\prod_{i>j}^{n} (a_i - a_j)(b_i - b_j)}{\prod_{i,j=1}^{n} (a_i + b_j)}$$

Proposition 4.2. For any real number s, s not in [-1,0], let f_s be defined on [0,1] as in equation 4.1. Let p_n be the unique generalized polynomial in \mathcal{R}_n^* interpolating to f at n distinct points $x_1, x_2, ..., x_n$ in J = [0,1]. Then for all x in [0,1],

$$f_s(x) - p_n(x) = \frac{\prod_{k=1}^{n} (x - x_k) \cdot \prod_{k=1}^{n} (s - k)}{\prod_{k=1}^{n} (x_k + s) \prod_{k=1}^{n} (x + k)} \cdot \frac{1}{x + s}$$

Proof. Given that p_n is the generalized polynomial in \mathbb{R}_n^* interpolating to f_s at the points x_1, x_2, \ldots, x_n in [0, 1]. By (ii) of Theorem 2.2, the error of interpolation is given by

$$f_s(x) - p_n(x) = \frac{D\begin{pmatrix} x_1 & \dots & x_n; & x \\ u_1 & \dots & u_n, & f \end{pmatrix}}{D\begin{pmatrix} x_1 & \dots & x_{n-1}, & x_n \\ u_1 & \dots & u_{n-1}, & u_n \end{pmatrix}}$$

$$= \frac{\det \begin{bmatrix} \frac{1}{x_1+1} & \dots & \frac{1}{x_1+n} & \frac{1}{x_1+s} \\ \vdots & \vdots & \vdots & \vdots \\ \frac{1}{x_n+1} & \dots & \frac{1}{x_n+n} & \frac{1}{x_n+s} \end{bmatrix}}{\det \begin{bmatrix} \frac{1}{x_1+1} & \dots & \frac{1}{x_1+n} \\ \vdots & \vdots & \vdots & \vdots \\ \frac{1}{x_1+1} & \dots & \frac{1}{x_1+n} \\ \vdots & \vdots & \vdots & \vdots \\ \frac{1}{x_n+1} & \dots & \frac{1}{x_n+n} \end{bmatrix}}$$

$$= \frac{(x-x_1)(x-x_2) \dots (x-x_n)}{(x_1+s)(x_2+s) \dots (x_n+s)} \cdot \frac{(s-1) \dots (s-n)}{(x+1) \dots (x+n)} \cdot \frac{1}{x+s}$$

$$= \frac{\prod_{k=1}^{n} (x-x_k) \cdot \prod_{k=1}^{n} (s-k)}{\prod_{k=1}^{n} (x_k+s) \prod_{k=1}^{n} (x_k+k)} \cdot \frac{1}{x+s}}$$

We now prove that $f_s \in GTB_{\mathbb{R}^*}$ whenever s < -2 or $s \ge 1$.

Theorem 4.1. The function f_n has the following properties.

- f, belongs to GTB_{R*} , if s ≥ 1 or s < -2.
- (ii) f_s belongs to GTP_{R^*} , if $s \ge 1$

Proof. Let x_1, \ldots, x_n be any n distinct points in [0,1] and let p_n be the unique generalized polynomial in \mathcal{R}_n^* interpolating to f_s at x_1, \ldots, x_n . Then by Proposition 4.2, for all x in [0,1],

$$f_s(x) - p_n(x) = \frac{\prod_{k=1}^{n} (x - x_k) \cdot \prod_{k=1}^{n} (s - k)}{\prod_{k=1}^{n} (x_k + s) \prod_{k=1}^{n} (x + k)} \cdot \frac{1}{x + s}$$

For any $x \in [0, 1]$,

$$|x - x_k| \le 1$$
 and $|x + k| = x + k \ge k$.

Consequently,

$$\frac{\prod_{k=1}^{n} |x - x_k|}{\prod_{k=1}^{n} |x + k|} \le \frac{1}{\prod_{k=1}^{n} k} = \frac{1}{n!}.$$

Therefore, for $0 \le x \le 1$,

$$|f_s(x) - p_n(x)| \le \frac{1}{n!} \cdot \frac{\prod_{k=1}^n |s - k|}{\prod_{k=1}^n |x_k + s|} \cdot \frac{1}{|x + s|}$$
 (4.2)

We now consider the cases $s \ge 1$ and s < -2 separately,

Case(i): $s \ge 1$

Then

$$|s+x_k| = s+x_k \ge s$$

Therefore,

$$\prod_{k=1}^{n} |\mathbf{s} + x_k| \ge \mathbf{s}^n \tag{4.3}$$

From inequalities 4.2 and 4.3,

$$|f_s(x) - p_n(x)| \le \frac{1}{n!} \cdot \frac{\prod_{k=1}^n |s - k|}{s^n} \cdot \frac{1}{|x + s|}$$

$$= \prod_{k=1}^n \frac{|s - k|}{ks} \cdot \frac{1}{|x + s|}$$

$$= \frac{1}{|x + s|} \cdot \prod_{k=1}^n \left| \frac{1}{k} - \frac{1}{s} \right|$$

Now $\frac{1}{k} \in (0,1)$ and $\frac{1}{s} \in (0,1]$. Therefore,

$$\left|\frac{1}{k} - \frac{1}{s}\right| < 1 \qquad (k = 1, \dots n),$$

and so

$$\prod_{k=1}^{n} \left| \frac{1}{k} - \frac{1}{s} \right| < 1.$$

Consequently,

$$|f_s(x) - p_n(x)| < \frac{1}{|x+s|} = \frac{1}{x+s}$$

That is,

$$\left| \frac{1}{x+s} - p_n(x) \right| < \frac{1}{x+s}, \quad 0 \le x \le 1.$$

Equivalently, for $0 \le x \le 1$,

$$\frac{1}{x+s} - p_n(x) < \frac{1}{x+s}$$
 and $p_n(x) - \frac{1}{x+s} < \frac{1}{x+s}$.

Therefore, for $0 \le x \le 1$,

$$0 < p_n(x) < \frac{2}{x + s} \le 2$$
.

Since p_n is an arbitrary generalized Largange interpolant to f_s from \mathbb{R}^s , it follows that f_s is generalized totally positive and generalized totally bounded with respect to \mathbb{R}^s , if $s \geq 1$. That is,

$$f_s \in GTP_{R^s}$$
, if $s \ge 1$ (4.4)

and

$$f_s \in GTB_{R^s}$$
, if $s \ge 1$ (4.5)

Case(ii): $s \le -2$

Now $s \le -2$ implies |s| > 2. Choose a positive integer m such that $m \le |s| < m+1$. Thus for $k=1,\,2,\,\ldots,\,n,\,|s-k|=|s|+k < m+1+k$. Therefore,

$$\prod_{k=1}^{n} |s-k| < \prod_{k=1}^{n} (m+1+k)$$

$$= (m+2)(m+3) \dots (m+1+n)$$

$$= \frac{(m+n+1)!}{(m+1)!}$$
(4.6)

Again,

$$\prod_{k=1}^{n} |x_k + s| \ge \prod_{k=1}^{n} (|s| - x_k) \ge \prod_{k=1}^{n} (|s| - 1)^n. \tag{4.7}$$

Hence, from inequalities 4.2, 4.6 and 4.7, since $0 \le x \le 1$, we have

$$|f_s(x) - p_n(x)| < \frac{1}{n!} \frac{(m+n+1)!}{(m+1)!} \frac{1}{(|s|-1)^n} \frac{1}{x+s}$$

$$= {m+n+1 \choose m+1} \left(\frac{1}{(|s|-1)}\right)^n \frac{1}{x+s}$$

$$= {m+n+1 \choose m+1} \left(\frac{1}{(|s|-1)}\right)^{n+1}$$
(4.8)

Now

$$\binom{m+n+1}{m+1} \cdot \left(\frac{|s|}{2}-1\right)^{m+1} < \left(1+\left(\frac{|s|}{2}-1\right)\right)^{m+n+1} = \left(\frac{|s|}{2}\right)^{m+n+1}$$

Therefore,

$${m+n+1 \choose m+1} = \frac{{\binom{|s|}{2}}^{m+n+1}}{{\frac{|s|}{2}-1}^{m+1}} = {\binom{|s|}{|s|-2}}^{m+1} \cdot {\binom{|s|}{2}}^{m}$$
(4.9)

From inequalities 4.8 and 4.9,

$$|f_s(x) - p_n(x)| \le \left(\frac{|s|}{|s|-2}\right)^{m+1} \cdot \left(\frac{|s|}{2}\right)^n \frac{1}{(|s|-1)^{n+1}}$$

 $\le \left(\frac{|s|}{|s|-2}\right)^{m+1} \cdot \left(\frac{|s|/2}{|s|-1}\right)^n$
 $\le K\left(\frac{|s|}{2(|s|-1)}\right)^n$
(4.10)

where $K = \left(\frac{|s|}{|s|-2}\right)^{m+1}$. Since |s| > 2, we have

$$\frac{|s|}{2(|s|-1)} < 1.$$

Therefore, from inequality 4.10, we see that

$$|f_s(x) - p_n(x)| \le K$$
, where $K = \left(\frac{|s|}{|s|-2}\right)^{m+1}$.

Thus

$$|p_n(x)| \le |f_s(x)| + K = \frac{1}{|x+s|} + K$$

 $\le \frac{1}{|s|-1} + K < 1 + K$
 $|p_n(x)| \le 1 + K, \quad \text{for all } x \in [0, 1]$ (4.11)

Estimate 4.11 holds for all generalized Lagrange interpolants to f_s . Therefore,

$$f_s \in GTB_{R^*}$$
, for $s < -2$ (4.12)

Thus $f_s \in GTP_{\mathbb{R}^*}$, if $s \ge 1$ or s < -2. Further, we have seen that

$$f_s \in GTP_{R^s}$$
, if $s \ge 1$.

The proof of Theorem 4.1 is now complete.

Now we will prove the converse of the above theorem.

Theorem 4.2. A necessary condition for f_s to belong to GTB_{R} -is that s lies outside the interval [-2,1).

Proof. Now [-2, 1) is the union of the intervals (0, 1), [-1, 0] and [-2, -1). We prove separately that if s is in any of these intervals, then f_s does not belong to GTB_{R^s}

Case (i) : s is in (0, 1).

In this case consider the generalized Lagrange interpolant p_n to f_s from $\mathcal{G}TB_{\mathcal{R}^*}$ interpolating to f_s at the n points $x_k = \frac{k}{(n+1)^2}$, k = 1, 2, ..., n. By Proposition 4.2, for all x in [0, 1],

$$f_s(x) - p_n(x) = \frac{\prod_{k=1}^{n} (x - x_k)}{\prod_{k=1}^{n} (x + k)} \cdot \frac{\prod_{k=1}^{n} (s - k)}{\prod_{k=1}^{n} (x_k + s)} \cdot \frac{1}{x + s}.$$

Therefore,

$$f_s(1) - p_n(1) = \frac{\prod_{k=1}^n (1-x_k)}{\prod_{k=1}^n (1+k)} \cdot \frac{\prod_{k=1}^n (s-k)}{\prod_{k=1}^n (x_k+s)} \cdot \frac{1}{x+s}.$$

Since 0 < s < 1, in this case,

$$\begin{split} |f_{s}(1) - p_{n}(1)| &= \frac{\prod_{k=1}^{n} \left(1 - \frac{k}{(n+1)^{2}}\right)}{(n+1)!} \cdot \frac{\prod_{k=1}^{n} (k-s)}{\prod_{k=1}^{n} (x_{k}+s)} \cdot \frac{1}{1+s}. \\ &> \frac{\left(1 - \frac{1}{(n+1)}\right)^{n}}{(n+1)!} \cdot \frac{(n-1)!}{(s + \frac{1}{n+1})^{n}} \cdot \frac{1}{1+s}. \end{split}$$

Now

$$\left(1 - \frac{1}{(n+1)}\right)^n = \left(\frac{n}{n+1}\right)^n = \frac{1}{\left(1 + \frac{1}{n}\right)^n} > \frac{1}{e}$$

Also

$$\frac{(n-1)!}{(n+1)!.(1+s)} = \frac{1}{n(n+1)(1+s)} > \frac{1}{2n^2}.$$

Therefore,

$$|f_s(1) - p_n(1)| > \frac{1}{2e} \cdot \frac{1}{n^2 \left(s + \frac{1}{n+1}\right)^n}$$

Choose s_1 , s_2 such that $s < s_1 < s_2 < 1$. Since 0 < s < 1, $s + \frac{1}{n+1} < s_1$ for all large n. Therefore, for large n,

$$n^{\frac{2}{n}}(s + \frac{1}{n+1}) < n^{\frac{2}{n}}s_1 < s_2,$$

since $n^{\frac{2}{n}} \to 1$ as $n \to \infty$. Therefore, for large n,

$$|f_s(1) - p_n(1)| > \frac{1}{2e} \cdot \frac{1}{s_2^n} \to \infty \text{ as } n \to \infty.$$

It follows that, in this case,

$$f_* \not\in GTB_{R^*}$$
.

Case (ii): s is in [-1,0].

In this case, f_s is not even defined on [0,1]. Hence trivially, for $-1 \le s \le 0$

$$f_* \notin GTB_{R^*}$$
.

Case (iii) :
$$-2 \le s < -1$$

In this case, consider the generalized Lagrange interpolant q_n to f_s from R^* interpolating to f_s at the points

$$x'_{k} = \frac{n}{n+1} + \frac{k}{(n+1)^{2}}, \quad k = 1, 2, ..., n.$$

Then, using Proposition 4.2,

$$|f_s(0) - q_n(0)| = \frac{\prod_{k=1}^n |x'_k|}{\prod_{k=1}^n k} \cdot \frac{\prod_{k=1}^n |s-k|}{\prod_{k=1}^n |x_k + s|} \cdot \frac{1}{|s|}.$$

Now

$$\prod_{k=1}^{n}|x_{k}'|>\prod_{k=1}^{n}\frac{n}{n+1}=\left(\frac{n}{n+1}\right)^{n}=\frac{1}{(1+\frac{1}{n})^{n}}>\frac{1}{e}$$

Also since s is negative, s-k < 0. Thus |s-k| = -s + k = |s| + k > 1 + k, since $1 < |s| \le 2$. Therefore,

$$|f_s(0) - q_n(0)| > \frac{1}{e} \cdot \frac{(n+1)!}{n!} \cdot \frac{1}{\prod_{k=1}^{n} |s + \frac{n}{n+1} + \frac{k}{(n+1)^2}|} \cdot \frac{1}{2}$$

since |s| < 2. Now

$$\frac{n}{n+1} + \frac{k}{(n+1)^2} \leq \frac{n}{n+1} + \frac{n}{(n+1)^2} < \frac{n}{n+1} + \frac{n+1}{(n+1)^2} = 1.$$

Also s < -1. Therefore,

$$s + \frac{n}{n+1} + \frac{k}{(n+1)^2} < 0.$$

Hence

$$\begin{split} \left| s + \frac{n}{n+1} + \frac{k}{(n+1)^2} \right| &= -s - \frac{n}{n+1} - \frac{k}{(n+1)^2} \\ &= |s| - \left(\frac{n}{n+1} + \frac{k}{(n+1)^2} \right) \\ &= (|s| - 1) + \frac{1}{n+1} + \frac{k}{(n+1)^2} \\ &< |s| - 1 + \frac{1}{n+1} \end{split}$$

Consequently,

$$\begin{split} |f_s(0) - q_n(0)| &> \frac{n+1}{2e} \cdot \left(|s| - 1 + \frac{1}{n+1}\right)^{-n} \\ &\geq \frac{n+1}{2e} \cdot \left(1 + \frac{1}{n+1}\right)^{-n}, \quad \text{since} \quad |s| - 1 \leq 1 \\ &> \frac{n+1}{2e} \cdot \frac{1}{\left(1 + \frac{1}{n+1}\right)^n} \\ &> \frac{n+1}{2e} \cdot \frac{1}{e} = \frac{n+1}{2e^2} \to \infty \quad \text{as} \quad n \to \infty. \end{split}$$

Thus $f_s \notin GTB_{R^*}$ in this case also. From cases (i), (ii) and (iii), it follows that

$$f_s \not\in \mathcal{G}TB_{\mathcal{R}^*}$$
, if $s \in [-2, 1)$.

Equivalently,

$$f_s \in GTB_{R^*} \implies s \notin [-2, 1).$$

Combining the above two theorems, we get the following theorem.

Theorem 4.3. f_s belongs to GTB_{R^*} if and only if s is a real number not belonging to [-2,1).

Proof. From part (i) of Theorem 4.1 and Theorem 4.2, it follows that

$$f_s \in GTB_{R^*} \iff s \notin [-2, 1).$$

References

- Alan Horwitz, Means, Generalized Divided Differences, and Intersections of Osculating Hyperplanes, J.Mathematical Analysis and Applications 200 (1996), 126–148.
 C.A.Micchelli, Kluwer Academic Publishers, Netherlands, 1996.
- Horwitz, A.L., and L.A.Rubel, Totally Positive Functions and Totally Bounded Functions on [-1, 1]., J.Approx. Theory 52 (1988), 204-216.
- [3] Davis, P.J., Interpolation and Approximation, Dover Publications, New York, 1975.
- [4] Karlin, S., and W. J. Studden, Tchebycheff Systems: With Applications in Analysis and Statistics, Interscience Publishers, New York, 1966.
- [5] Schumaker, L.L., Spline Functions: Basic Theory, John Wiley & Sons, New York, 1981.
- [6] Thalmi. B and Jayasri. C, A generalization of totally positive functions, Indian Journal of Mathematics and Mathematical sciences, Vol.13, No.2(July-December 2017), 389-410.
- B. Thalmi, Generalized totally bounded functions, International Journal of Mathematical Sciences and Engineering Applications, Vol.2, No.2, (December 2017), 145-154.
- [8] B. Thalmi, Interpolation by functions in an extended complete Tchebycheff space, Bulletin of Kerala Mathematics Association, Vol.15, No.1, (2017, June) 25-31.

University of Kerala, Kerala-695581, India. (Received, September 26, 2024)

Email: thalmimaths 17@gmail.com Email: cjayasri55@gmail.com COEFFICIENT ESTIMATES FOR A CERTAIN SUBCLASS OF ANALYTIC AND BI UNIVALENT FUNCTIONS DEFINED USING AN OPERATOR ASSOCIATED WITH GENERALIZED

ISSN: 0970-5120

Ranjan S. Khatu

ABSTRACT. This paper presents a newly defined subclass of analytic and bi-univalent functions within the unit disc $\Delta = \{z \in \mathbb{C} : |z| < 1\}$. The subclass is constructed using an operator associated with the generalized Mittag-Leffler function. Furthermore, the initial coefficient bounds for functions in this subclass are estimated.

MITTAG-LEFFLER FUNCTION

Key words: Taylor-Maclaurin series expansion, Analytic function, Univalent function, Bi-univalent function, coefficient bounds, Mittag-Leffler function Mathematics Subject Classification: 30C45, 30C80

1. INTRODUCTION

Let A be the class of analytic functions defined on an open unit disc $\Delta = \{z \in \mathbb{C} : |z| < 1\}$ and which are in the form

$$h(z) = z + \sum_{j=2}^{\infty} a_j z^j \quad (z \in \Delta).$$

Further, S is the set of all univalent functions in A. Here, the Koebe One-Quarter theorem [5] plays an important role and it says that the image of Δ under $h \in S$ contains a disc of radius 1/4.

Clearly, for each function $h \in S$, h^{-1} exists and it is defined as

$$h^{-1}(h(z))=z,\quad z\in\Delta$$

and

$$h(h^{-1}(w)) = w, \quad |w| < r_0, r_0(h) \ge 1/4$$

where

$$(1.2) \quad g(w) = h^{-1}(w) = w - a_2w^2 + (2a_2^2 - a_3)w^3 - (5a_2^3 - 5a_2a_3 + a_4)w^4 + \cdots$$

If both functions $h \in S$ and h^{-1} are univalent in Δ , then h is said to be bi-univalent in Δ . Here we denote the set of all such bi-univalent functions by Σ . The study of subclasses of bi-univalent functions and their coefficient bounds is an interesting topic of research and it was first studied by Lewin [7] and he proved that $|a_2| < 1.51$. Later, Netanyahu [9] showed that $\max |a_2| = 4/3$. Further, Brannan and Clunie [3] conjectured that, for $h \in \sum, |a_2| \le \sqrt{2}$. Brannan and Taha [4] introduced very interesting two subclasses of the class bi-univalent functions Σ , the class of startlike functions $S^*(\beta)$ and the class $\mathcal{K}(\beta)$ of convex functions of order $\beta(\beta) \in [0,1)$ in Δ (see [9]). Later, $S_{\Sigma}^*(\beta)$ (the class of bi-starlike function of order β) and $\mathcal{K}_{\Sigma}(\beta)$ (the class of bi-convex functions of order β) were introduced on Δ . Many researchers worked on these classes and obtained initial coefficient bounds and later on many congruent subclasses

were introduced by mathematicians and obtained the coefficient bounds for diversified subclasses of bi-univalent functions(see[1], [10], [6]).

In 1903, Gosta Mittag-Leffler [8] introduced the following function

$$(1.3) \quad E_{\alpha}(z) = \sum_{i=0}^{\infty} \frac{z^{j}}{\Gamma(1 + j\alpha)}$$

where $\alpha \ge 0$, $z \in \mathbb{C}$ and $\Gamma(s)$ is a gamma function. Moreover, Srivastava and Tomovski [12] introduced the function

$$E_{\alpha,\beta}^{\gamma,k}(z) = \sum_{i=0}^{\infty} \frac{(\gamma)_{jk}z^{j}}{\Gamma(\beta + j\alpha)j!}$$
(1.4)

where $\gamma, \beta, \alpha \in \mathbb{C}$; Re(k) > 0; $Re(\alpha) > max\{0, Re(k) - 1\}$ and $(\gamma)_j$ is Pochhammer symbol defined as

$$(\gamma)_j = \frac{\Gamma(j + \gamma)}{\Gamma(\gamma)}$$

and its value is 1 if j=0 and its value is $\gamma(\gamma+1)\cdots(\gamma+j-1)$ if $j\in\mathbb{N}$. Using operator (1.4), Attiya [2] defined the operator $\mathcal{H}_{\alpha,\beta,k}^{\gamma}(h): \mathcal{A} \to \mathcal{A}$ by

$$\mathcal{H}_{\alpha,\beta,k}^{\gamma}(h)(z) = Q_{\alpha,\beta,k}^{\gamma}(z) * h(z) \quad (z \in \Delta)$$

where

$$\mathcal{Q}_{\alpha,\beta,k}^{\gamma}(z) = \frac{\Gamma(\beta+\alpha)}{(\gamma)_k} \left(E_{\alpha,\beta}^{\gamma,k}(z) - \frac{1}{\Gamma(\beta)} \right) \quad (z \in \Delta),$$

where $\gamma, \beta, \alpha \in \mathbb{C}$; Re(k) > 0; $Re(\alpha) > max\{0, Re(k) - 1\}$; $Re(\alpha) = 0$ when Re(k) = 1, $\beta \neq 0$ and the symbol(*) denotes the convolution (or Hadamard product). It can be easily observed that

(1.6)
$$\mathcal{H}_{\alpha,\beta,k}^{\gamma}(h)(z) = z + \sum_{i=2}^{\infty} \frac{\Gamma(jk+\gamma)\Gamma(\beta+\alpha)}{\Gamma(k+\gamma)\Gamma(\beta+j\alpha)j!} a_j z^j$$

and

$$(1.7) \quad z\left(\mathcal{H}_{\alpha,\beta,k}^{\gamma}(h)(z)\right)' = \left(\frac{\gamma + k}{k}\right)\left(\mathcal{H}_{\alpha,\beta,k}^{\gamma+1}(h)(z)\right) - \frac{\gamma}{k}\left(\mathcal{H}_{\alpha,\beta,k}^{\gamma}(h)(z)\right).$$

Motivate by the work (especially [13]) and using the operator defined in (1.5), we introduce a new subclass $\mathcal{N}_{\alpha,\beta,k}^{\gamma_{\alpha,b,b}}(\lambda)$ of analytic function class \mathcal{A} .

Definition 1.1. Let $h \in A$, g be an extension of h^{-1} on Δ and $u, v : \Delta \to \mathbb{C}$ be functions such that $min\{\mathcal{R}(u(z)), \mathcal{R}(v(z))\} > 0 \ (z \in \Delta)$ with u(0) = v(0) = 1. Then we say that $h \in \mathcal{N}_{\alpha,\beta,k}^{\gamma,u,v}(\lambda)$ if following conditions are satisfied.

(1.8)
$$h \in \Sigma$$
,
$$\frac{z \left(\mathcal{H}_{\alpha,\beta,k}^{\gamma} h(z)\right)'}{\lambda z \left(\mathcal{H}_{\alpha,\beta,k}^{\gamma} h(z)\right)' + (1 - \lambda)\mathcal{H}_{\alpha,\beta,k}^{\gamma} h(z)} \in u(\Delta) \quad (\lambda \in [0, 1); z \in \Delta)$$

and

$$(1.9) \qquad \frac{w \left(\mathcal{H}_{\alpha,\beta,k}^{\gamma} g(w)\right)'}{\lambda w \left(\mathcal{H}_{\alpha,\beta,k}^{\gamma} g(w)\right)' + (1-\lambda) \mathcal{H}_{\alpha,\beta,k}^{\gamma} g(w)} \in v(\Delta) \quad (\lambda \in [0,1); w \in \Delta)$$

where $\gamma, \beta, \alpha \in \mathbb{C}$; Re(k) > 0; $Re(\alpha) > max\{0, Re(k) - 1\}$; $Re(\alpha) = 0$ when Re(k) = 1 and $\beta \neq 0$.

For particular values of γ, α, k and for different choices of functions u and v, the class $\mathcal{N}_{\alpha,\beta,k}^{\gamma,u,v}(\lambda)$ reduces to many well known classes of holomorphic and bi-univalent functions as follows.

Remark 1.2. (1) For γ = 1, α = 0 and k = 1, the class N_{α,β,k}^{γ,u,v}(λ) reduces to the class M_Σ^{u,v}(λ) studied by Yamini J [13].

- (2) For γ = 1, α = 0, k = 1 and by setting u(z) = (1+z)/(1-z)^η and v(z) = (1-z)/(1+z)^η (where η ∈ (0, 1]; z ∈ Δ), the class N_{α,β,k}^{γ,u,v}(λ) reduces to the class SS^{*}_Σ(η, λ) introduced by Murugusundaramoorthy et al [11].
- (3) For γ = 1, α = 0, k = 1 and by setting u(z) = ^{1+(1-2η)z}/_{1-z} and v(z) = ^{1-(1-2η)z}/_{1+z} (where η ∈ [0,1); z ∈ Δ), the class N^{γ,u,x}_{α,β,k}(λ) reduces to the class S^κ_Σ(η, λ) introduced by Murugusundaramoorthy et al [11].
- (4) By setting λ = 0 in the classes SS^{*}_Σ(η, λ) and S^{*}_Σ(η, λ), we get the classes introduced by Brannan and Taha [4].

COEFFICIENT BOUNDS FOR THE FUNCTION CLASS N_{α,δ,k}^{γ,u,v}(λ)

In this section, I derive initial coefficient bounds of the functions from the class $\mathcal{M}_{\alpha,\beta,k}^{\gamma,u,v}(\lambda)$.

Theorem 2.1. If $h \in \Sigma$ given by (1.1) and it is a member of the class $\mathcal{N}_{\alpha,\beta,k}^{\gamma,u,v}(\lambda)$, then (2.1)

$$|a_2| \le min \left\{ \frac{\sqrt{2\left(|u'(0)|^2 + |v'(0)|^2\right)}}{1 - \lambda}, \left|\frac{\Gamma(k + \gamma)}{\Gamma(2k + \gamma)}\right| \left|\frac{\Gamma(\beta + 2\alpha)}{\Gamma(\beta + \alpha)}\right|, \sqrt{\frac{|u''(0)| + |v''(0)|}{2|\tau|}} \right\}$$

and

(2.2)

$$\begin{split} |a_3| &\leq \frac{3(|u''(0)| + |v''(0)|)}{4(1-\lambda)} \cdot \left| \frac{\Gamma(k+\gamma)}{\Gamma(3k+\gamma)} \right| \cdot \left| \frac{\Gamma(\beta+3\alpha)}{\Gamma(\beta+\alpha)} \right| \\ &+ \min \left\{ \frac{2(|u'(0)|^2 + |v'(0)|^2)}{(1-\lambda)^2} \cdot \left| \frac{\Gamma(k+\gamma)}{\Gamma(2k+\gamma)} \right|^2 \left| \frac{\Gamma(\beta+2\alpha)}{\Gamma(\beta+\alpha)} \right|^2, \frac{|u''(0)| + |v''(0)|}{2|\tau|} \right\} \end{split}$$

where

$$\tau = \left(\frac{\lambda^2 - 1}{2}\right) \cdot \left(\frac{\Gamma(2k + \gamma)}{\Gamma(k + \gamma)}\right)^2 \cdot \left(\frac{\Gamma(\beta + \alpha)}{\Gamma(\beta + 2\alpha)}\right)^2 + \frac{2(1 - \lambda)}{3} \cdot \frac{\Gamma(3k + \gamma)}{\Gamma(k + \gamma)} \cdot \frac{\Gamma(\beta + \alpha)}{\Gamma(\beta + 3\alpha)}$$

and $\gamma, \beta, \alpha \in \mathbb{C}$; Re(k) > 0; $Re(\alpha) > max\{0, Re(k) - 1\}$; $Re(\alpha) = 0$ when Re(k) = 1 and $\beta \neq 0$.

Proof. Let $h \in \mathcal{N}_{\alpha,\beta,k}^{\gamma,n,v}(\lambda)$. Then from (1.8) and (1.9), we get

(2.3)
$$\frac{z\left(\mathcal{H}_{\alpha,\beta,k}^{\gamma}h(z)\right)'}{\lambda z\left(\mathcal{H}_{\alpha,\beta,k}^{\gamma}h(z)\right)' + (1-\lambda)\mathcal{H}_{\alpha,\beta,k}^{\gamma}h(z)} = u(z) \quad (\lambda \in [0,1); z \in \Delta)$$

$$(2.4) \qquad \frac{w \left(\mathcal{H}_{\alpha,\beta,k}^{\gamma} g(w)\right)'}{\lambda w \left(\mathcal{H}_{\alpha,\beta,k}^{\gamma} g(w)\right)' + (1-\lambda) \mathcal{H}_{\alpha,\beta,k}^{\gamma} g(w)} = v(w) \quad (\lambda \in [0,1); w \in \Delta)$$

where u and v are functions which satisfy the conditions of Definition 1.1. So, Taylor-Maclaurin series of u and v can be written as follows.

$$u(z) = 1 + \phi_1 z + \phi_2 z^2 + \cdots$$

and

$$v(w) = 1 + \psi_1 w + \psi_2 w^2 + \cdots$$

Now, equating the coefficients of $\frac{z(\mathcal{H}_{\alpha,\beta,k}^{\gamma}h(z))'}{\lambda z(\mathcal{H}_{\alpha,\beta,k}^{\gamma}h(z))' + (1-\lambda)\mathcal{H}_{\alpha,\beta,k}^{\gamma}h(z)}$ with coefficient of u(z), we get the following equations.

$$(1 - \lambda) \frac{\Gamma(2k + \gamma)}{\Gamma(k + \gamma)} \cdot \frac{\Gamma(\beta + \alpha)}{\Gamma(\beta + 2\alpha)} \cdot \frac{a_2}{2!} = \phi_1$$

and (2.6)

$$(\lambda^2-1)\left(\frac{\Gamma(2k+\gamma)}{\Gamma(k+\gamma)}\right)^2\left(\frac{\Gamma(\beta+\alpha)}{\Gamma(\beta+2\alpha)}\right)^2\frac{a_2^2}{4}+2(1-\lambda)\frac{\Gamma(3k+\gamma)}{\Gamma(k+\gamma)}\cdot\frac{\Gamma(\beta+\alpha)}{\Gamma(\beta+3\alpha)}\cdot\frac{a_3}{3!}=\phi_2.$$

Now, equating the coefficients of $\frac{w(\mathcal{H}_{\alpha,\beta,k}^{\gamma}g(w))'}{\lambda w(\mathcal{H}_{\alpha,\beta,k}^{\gamma}g(w))' + (1-\lambda)\mathcal{H}_{\alpha,\beta,k}^{\gamma}g(w)}$ with coefficient of v(w), we get the following equations.

$$(\lambda - 1)\frac{\Gamma(2k + \gamma)}{\Gamma(k + \gamma)} \cdot \frac{\Gamma(\beta + \alpha)}{\Gamma(\beta + 2\alpha)} \cdot \frac{a_2}{2!} = \psi_1$$

and

$$\left(\frac{1-\lambda}{3}\right) \cdot \frac{\Gamma(3k+\gamma)}{\Gamma(k+\gamma)} \cdot \frac{\Gamma(\beta+\alpha)}{\Gamma(\beta+3\alpha)} (2a_2^2 - a_3) + \left(\frac{\lambda^2 - 1}{4}\right) \cdot \left(\frac{\Gamma(2k+\gamma)}{\Gamma(k+\gamma)}\right)^2 \cdot \left(\frac{\Gamma(\beta+\alpha)}{\Gamma(\beta+2\alpha)}\right)^2 a_2^2 = \psi_2.$$

From (2.5) and (2.7), we get

$$\phi_1 = -\psi_1$$

and

$$(2.10) \quad 2(1 - \lambda)^2 \left(\frac{\Gamma(\gamma + 2k)}{\Gamma(\gamma + k)}\right)^2 \left(\frac{\Gamma(\alpha + \beta)}{\Gamma(2\alpha + \beta)}\right)^2 \frac{a_2^2}{4} = \phi_1^2 + \psi_1^2.$$

Now from (2.6) and (2.8), we get

(2.11)

$$2(\lambda^2 - 1)^2 \left(\frac{\Gamma(2k + \gamma)}{\Gamma(k + \gamma)}\right)^2 \left(\frac{\Gamma(\beta + \alpha)}{\Gamma(\beta + 2\alpha)}\right)^2 \frac{a_2^2}{4} + \frac{2(1 - \lambda)}{3} \cdot \frac{\Gamma(3k + \gamma)}{\Gamma(k + \gamma)} \cdot \frac{\Gamma(\beta + \alpha)}{\Gamma(\beta + 3\alpha)} a_2^2 = \phi_2 + \psi_2.$$

From (2.10) and (2.11), we can easily obtain

$$a_2^2 = \frac{2(\phi_1^2 + \psi_1^2)}{(1 - \lambda)^2}, \left(\frac{\Gamma(k + \gamma)}{\Gamma(2k + \gamma)}\right)^2 \left(\frac{\Gamma(\beta + 2\alpha)}{\Gamma(\beta + \alpha)}\right)^2$$

and

(2.13)
$$a_2^2 = \frac{(\phi_2 + \psi_2)}{|\tau|}$$

where

$$\tau = \left(\frac{\lambda^2 - 1}{2}\right) \cdot \left(\frac{\Gamma(2k + \gamma)}{\Gamma(k + \gamma)}\right)^2 \cdot \left(\frac{\Gamma(\beta + \alpha)}{\Gamma(\beta + 2\alpha)}\right)^2 + \frac{2(1 - \lambda)}{3} \cdot \frac{\Gamma(3k + \gamma)}{\Gamma(k + \gamma)} \cdot \frac{\Gamma(\alpha + \beta)}{\Gamma(3\alpha + \beta)}$$

By using the fact $u(z) \in u(\Delta)$ and $v(w) \in v(\Delta)$, we get

$$|a_2|^2 \le \frac{2(|u'(0)| + |v'(0)|)}{(1 - \lambda)^2}, \left|\frac{\Gamma(k + \gamma)}{\Gamma(2k + \gamma)}\right|^2 \left|\frac{\Gamma(\beta + 2\alpha)}{\Gamma(\beta + \alpha)}\right|^2$$

and

$$|a_2|^2 \le \frac{|u''(0)| + |v''(0)|}{2|\tau|}.$$
(2.15)

Using these inequalities, we get the desire estimate on $|a_2|$ stated in (2.1). Now to obtain the bound on $|a_3|$, we subtract (2.8) from (2.6) and we get,

$$(2.16) \quad \frac{2(1-\lambda)}{3} \cdot \frac{\Gamma(3k+\gamma)}{\Gamma(k+\gamma)} \cdot \frac{\Gamma(\beta+\alpha)}{\Gamma(\beta+3\alpha)} \cdot (a_3 - a_2^2) = \phi_2 - \psi_2.$$

Now, by substituting the values of a_2^2 from (2.12) and (2.13) in (2.16), we have

$$a_3 = \frac{2(\phi_1^2 + \psi_1^2)}{(1 - \lambda)^2} \cdot \left(\frac{\Gamma(k + \gamma)}{\Gamma(2k + \gamma)}\right)^2 \left(\frac{\Gamma(\beta + 2\alpha)}{\Gamma(\beta + \alpha)}\right)^2 + \frac{3(\phi_2 - \psi_2)}{2(1 - \lambda)} \cdot \frac{\Gamma(k + \gamma)}{\Gamma(3k + \gamma)} \cdot \frac{\Gamma(\beta + 3\alpha)}{\Gamma(\beta + \alpha)}$$

and

$$(2.18) \quad a_3 = \frac{(\phi_2 + \psi_2)}{|\tau|} + \frac{3(\phi_2 - \psi_2)}{2(1 - \lambda)} \cdot \frac{\Gamma(k + \gamma)}{\Gamma(3k + \gamma)} \cdot \frac{\Gamma(\beta + 3\alpha)}{\Gamma(\beta + \alpha)}$$

respectively.

By using the fact $u(z) \in u(\Delta)$ and $v(w) \in v(\Delta)$, we get

(2.19)

$$|a_3| \leq \frac{2(|u'(0)|^2 + |v'(0)|^2)}{(1-\lambda)^2} \cdot \left|\frac{\Gamma(k+\gamma)}{\Gamma(2k+\gamma)}\right|^2 \left|\frac{\Gamma(\beta+2\alpha)}{\Gamma(\beta+\alpha)}\right|^2 + \frac{3(|u''(0)| + |v''(0)|)}{4(1-\lambda)} \cdot \left|\frac{\Gamma(k+\gamma)}{\Gamma(3k+\gamma)}\right| \cdot \left|\frac{\Gamma(\beta+3\alpha)}{\Gamma(\beta+\alpha)}\right|$$

and

$$(2.20) \quad |a_3| \leq \frac{|u''(0)| + |v''(0)|}{2|\tau|} + \frac{3(|u''(0)| + |v''(0)|)}{4(1 - \lambda)} \cdot \left| \frac{\Gamma(k + \gamma)}{\Gamma(3k + \gamma)} \right| \cdot \left| \frac{\Gamma(\beta + 3\alpha)}{\Gamma(\beta + \alpha)} \right|.$$

Hence we get (2.2) and it completes the proof.

3. COROLLARIES AND CONSEQUENCES

For particular values of γ , α , k and for different choices of functions u and v, in Theorem 2.1, we get many well known results as a corollaries of our result as follows.

By setting $\alpha = 0, \gamma = 1$ and k = 1 in Theorem 2.1, we get the result obtained by Yamini J [13].

Corollary 3.1. If $h \in \Sigma$ is a function given by (1.1), is in the class $N_{\Sigma}^{n,\nu}(\lambda)$ ($\beta \in [0,1)$; $\lambda \in [0,1)$) then

$$|a_2| \leq \min \left\{ \sqrt{\frac{|u'(0)|^2 + |v'(0)|^2}{2(1-\lambda)^2}}, \frac{\sqrt{|u''(0)| + |v''(0)|}}{2(1-\lambda)} \right\}$$

$$|a_3| \leq \min\left\{\frac{|u''(0)| + |v''(0)|}{8(1-\lambda)} + \frac{|u'(0)|^2 + |v'(0)|^2}{2(1-\lambda)^2}, \frac{(3-\lambda)|u''(0)| + (1+\lambda)|v''(0)|}{8(1-\lambda)^2}\right\}.$$

By setting $\alpha = 0, \gamma = 1, k = 1$ and by considering functions $u(z) = \left(\frac{1+z}{1-z}\right)^{\eta}$ and $v(z) = \left(\frac{1-z}{1+z}\right)^{\eta} (\eta \in (0, 1], z \in \Delta)$ in Theorem 2.1, we get the following corollary.

Corollary 3.2. If $h \in SS_{\Sigma}^{*}(\eta, \lambda)$ is the function given by (1.1), then

$$|a_2| \le min \left\{ \frac{2\eta}{1-\lambda}, \frac{\sqrt{2}\eta}{1-\lambda} \right\}$$

and

$$|a_3| \leq \min\left\{\frac{2\eta^2}{(1-\lambda)^2}, \frac{\eta^2}{1-\lambda} + \frac{4\eta^2}{(1-\lambda)^2}\right\}.$$

If we set $\alpha=0, \gamma=1, k=1$ and choose the functions $u(z)=\frac{1+(1-2\eta)z}{1-z}$ and $v(z)=\frac{1-(1-2\eta)z}{1+z}$ $(\eta\in[0,1),z\in\Delta)$ in Theorem 2.1, we get the following corollary.

Corollary 3.3. If $h \in S_{\Sigma}^{*}(\eta, \lambda)$ is the function given by (1.1), then

$$|a_2| \le min \left\{ \frac{2(1-\eta)}{1-\lambda}, \frac{\sqrt{2(1-\eta)}}{1-\lambda} \right\}$$

and

$$|a_3| \le min \left\{ \frac{2(1-\eta)}{(1-\lambda)^2}, \frac{1-\eta}{1-\lambda} + \frac{4(1-\eta)^2}{(1-\lambda)^2} \right\}.$$

4. Conflict of Interests

The authors confirm that there are no conflicts of interest related to the publication of this paper.

REFERENCES

- Akgul A. and Altmkaya, Coefficient estimates associated with a new subclass of bi-univalent functions, Acta Univ. Apuleusis Math. Inform, 52(2017), pp. 121-128.
- [2] Attiya A.A., Some Applications of Mittag-Leffler Function in the Unit Disk, Filomat 30:7 (2016), 2075–2081.
- [3] Brannan D.A. and Clunie J.G.(Eds.), Aspects of Contemporary Complex Analysis (Proceedings of the NATO Advanced Study Institute held at the University of Durham, Durham; July 1-20, 1979), Academic Press, New York and London, (1980).
- Brannan D.A. and Taha T.S., On some classes of bi-univalent functions, Studia Univ. Babes-Bolyai Math, 31(2), (1986), 70-77.
- [5] Duren P.L., Unicolent Functions, Grundlehren der Mathematischen Wissenschaften, Springer, New York, (1983).
- Khatu R.S., Naik U.H. and Patil A.B., Estimation on initial coefficient bounds of generalized subclasses of bi-univalent functions, Int. J. Nonlinear Anal. Appl., 13(2022) 2, pp. 989-997.
- [7] Lewin M., On a coefficient problem for bi-univalent functions, Proc. Amer. Math. Soc., 18, (1967), 63-68.
- [8] Mittag-Leffler G. M., Sur la nouvelle fonction E(x), C. R. Acad. Sci., Paris, 137(1903), 554-558.
- Netanyahu E., The minimal distance of the image boundary from the origin and the second coefficient of a univalent function in |z| < 1, Arch. Rational Mech. Anal., textbf32, (1989), 100-112.

- [10] Patil A.B. and Naik U.H., Estimates on Initial Coefficients of Certain Sunclasses of Bi-Univalent Functions Associated with Quasi-Subordination, Glabal Journal of Mathematical Analysis, 5(1), (2017), 6-10.
- [11] Srivastava H. M., Murugusundaramoorthy G., Magesh N., On certain subclasses of bi-unicalent functions associated with holdor operator, Global J. Math. Anal. 1 (2) (2013) 67-73.
- [12] Srivastava H.M. and Tomovski Z., Fractional calculus with an integral operator containing a generalized Mittag-Leffler function in the kernel, Appl. Math. Comp., 211(2009), 198-210.
- [13] Yamini J, Coefficient Estimates for a Certain General Subclass of Analytic and Bi-Univalent Functions, Int. J. Multi. Edu. Research, 4(1)(2023), 44-48.

Dept. of Mathematics, Shriram Kusumtai Sadshiv Vanjare College, Lanja-416701, India (Received, January 15, 2025), (Revised, January 21, 2025)

E-mail: ranjan.khatu11@gmail.com

Dhiraj Kumar',
Manoranjan Kumar Singh',
Sanjeet Kumar'

NUMBER OF
FUZZY SUBGROUPS OF D₈× C₂

ISSN: 0970-5120

Abstract

One such rudimentary issue in fuzzy theory of groups is to count abundant fuzzy subgroups (FSGs). Several investigators have noteworthy arguments in contemporary times for the boom of the subject matter. It is always infinite when we try to find out the number of FSGs independently. To study the equivalence of FSG, some researchers have used the concept of an equivalence relation in fuzzy set (FS). The issues of reckoning an abundant distinct FSGs of a finite group can always be obtained corresponding to the equivalence relation chosen by us. The total count of FSG of a specific group be different and will depend on the choice of the equivalence relation chosen. For computing the number of FSGs in our case, we have followed the approach similar to Sulaiman & Ahmad [10]. The sole aim of this paper is to follow the approach somewhat similar to that in the cited paper for enumerating the number of FSG of $D_8 \times C_2$. For reckoning the number in this particular case, we will make use of the lattice subgroups graphic.

2020 Mathematical Sciences Classification: 03E72, 08A72, 20N25

Keywords: Fuzzy Set, Fuzzy subgroups, Equivalence relation, Chain, Subgroup Lattice

1 Introduction

Zadeh [1] propounded the conception of FS. The literature on FS theory and its application has been proliferating rapidly across many disciplines of human knowledge. In 1971, Azriel Rosenfeld [2] initiated FS in the domain of group theory and coined the notion of FSGs of the group. Afterwards, the research in the corresponding branch grew. To make a dent in reckoning the abundant FSGs of the group covered by the equivalence relation. In this regard, the work of Sulaiman & Ahmad [10] is of worth. Our sole purpose in this article is to enumerate abundant FSGs of $D_8 \times C_2$ following an approach similar to that of Sulaiman and others. Recently, Dhiraj Kumar and M. K. Singh [15,16] calculated the aggregates of FSGs of D_8 , Q_8 , and Q_{12} using this relation. In this work, we have reckoned the aggregates of FSGs of $D_8 \times C_2$.

We have divided this paper into four sections. We've provided an introduction in the first section. Section two covers a preliminary outline by Sulaiman & Ahmad. Section three discussed the effects of locating aggregates of FSGs of D₈× C₂. At last, we have discussed the conclusion and future research.

2. Preliminaries

Definition 2.1 ([1]). Assume that $W \neq \emptyset$. Suppose $P: W \rightarrow [0, 1]$ is a mapping designated as FS of W.

Definition 2.2 ([2]). Any FS μ of W is referred to as a FSG of W if, for all $\alpha, \beta \in W$, the succeeding axioms are fulfilled:

(i)
$$\mu(\alpha\beta) \ge \min\{\mu(\alpha), \mu(\beta)\} \forall \alpha, \beta \in W$$

(ii)
$$\mu(\alpha^{-1}) \ge \mu(\alpha) \ \forall \ \alpha \in W$$

Theorem 2.1. [9] A FS μ of M is a FSG of W iff \exists a sequence of subgroups of M, $N_1(\mu) \subset N_2(\mu) \subset \cdots \subset N_p(\mu) = W$ such that μ can be expressed as:

$$\mu(x) = \begin{cases} \theta_1 & x \in N_1(\mu) \\ \theta_2 & x \in N_2(\mu) - N_1(\mu) \\ \vdots & \\ \theta_p & x \in N_p(\mu) - N_{p-1}(\mu) \end{cases}$$

Definition 2.3. [9] Suppose that μ , γ be FSG of W of the form

$$\mu(x) = \begin{cases} \theta_1 & x \in P_1 \\ \theta_2 & x \in P_2 - P_1 \\ \vdots & x \in P_n - P_{n-1} \end{cases}$$

and

$$\gamma(x) = \begin{cases} \delta_1 & x \in M_1 \\ \delta_2 & x \in M_2 - M_1 \\ \vdots & \\ \delta_m & x \in M_m - M_{m-1} \end{cases}$$

Now, one can say that μ is equivalent to γ and we denote it as $\mu \sim \gamma$, if:

(i)
$$m = n$$

(ii)
$$P_i(\mu) = M_i(\gamma), \forall i \in \{1, 2, ..., n\}$$

3. Number of FSGs of D₈× C₂

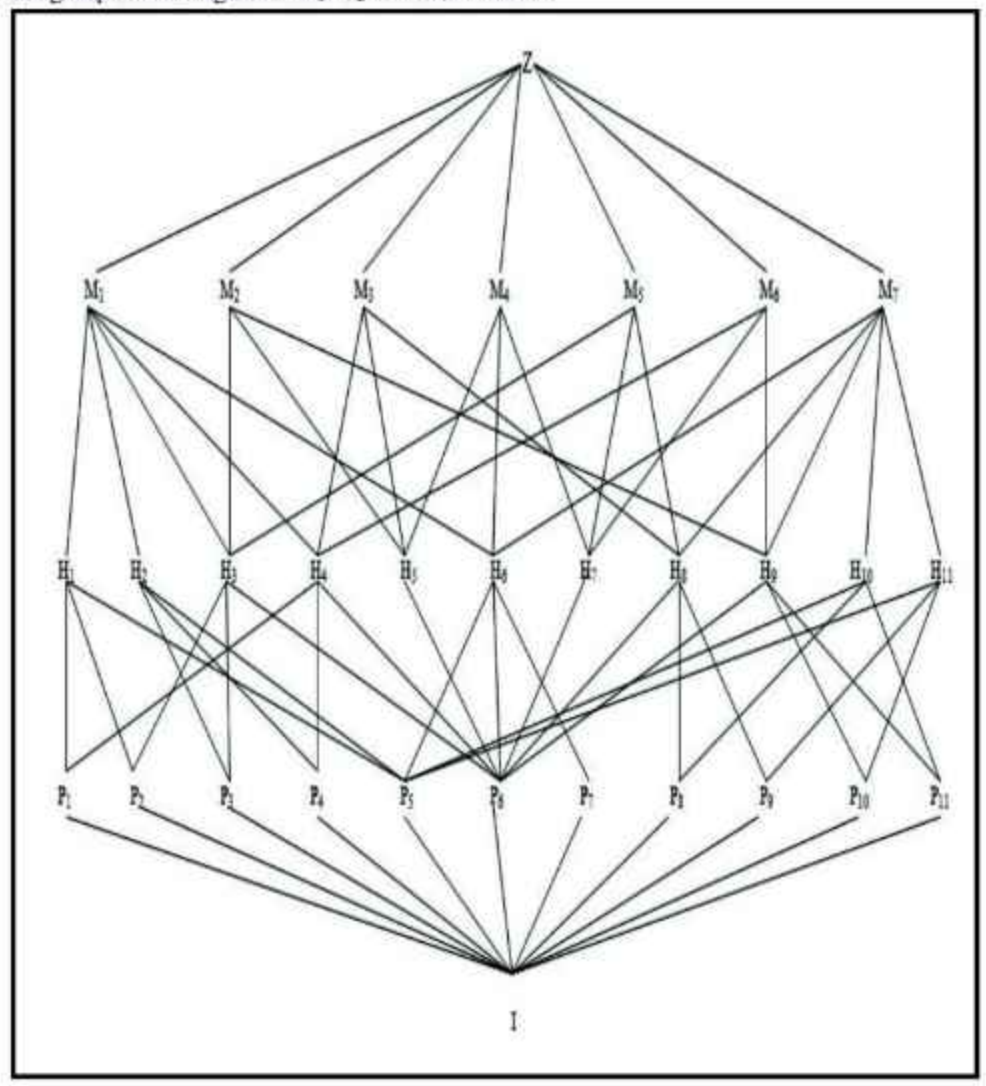
We have
$$D_8 = \langle a, b; a^4 = b^2 = 1, ab = ba^{-1} \rangle$$

Clearly $D_8 = \{1, a, a^2, a^3, b, ab, a^2b, a^3b\}$
and $C_2 = \{1, x\}$ where $x^2 = 1$

Then, we have

$$D_8 \times C_2 = \{(1,1), (a,1), (a^2,1), (a^3,1), (b,1), (ab,1), (a^2b,1), (a^3b,1), (1,x), (a,x), (a^2,x), (a^3,x), (b,x), (ab,x), (a^2b,x), (a^3b,x)\}$$

Subgroup lattice diagram of D8×C2 is as shown below



We have 31 subgroups of $D_8 \times C_2$; those are $I = \{(1,1)\}, P_1 = \{(1,1), (b,1)\}$

$$\begin{split} &P_2 = \{(1,1),(a^2b,x)\} \, P_3 = \{(1,1),(b,x)\} \, P_4 = \{(1,1),(a^2b,1)\} \\ &P_5 = \{(1,1),(a^2,x)\} \, P_6 = \{(1,1),(a^2,1)\} \, P_7 = \{(1,1),(1,x)\} \, P_8 = \{(1,1),(ab,x)\} \, P_9 = \{(1,1),(a^3b,x)\} \\ &P_{10} = \{(1,1),(ab,1)\} \, P_{11} = \{(1,1),(a^3b,1)\} \\ &H_1 = \{(1,1),(a^2,x),(b,1),((a^2b,x)\} \\ &H_2 = \{(1,1),(a^2,x),(b,x),((a^2b,1)\} \\ &H_3 = \{(1,1),(a^2,1),(b,x),((a^2b,x)\} \\ &H_4 = \{(1,1),(a^2,1),(b,1),((a^2b,1)\} \\ &H_5 = \{(1,1),(a^2,1),(1,x),((a^2,x)\} \\ &H_7 = \{(1,1),(a^2,1),(ab,x),((a^3b,x)\} \\ &H_9 = \{(1,1),(a^2,1),(ab,x),((a^3b,x)\} \\ &H_9 = \{(1,1),(a^2,1),(ab,1),((a^3b,x)\} \\ &H_{11} = \{(1,1),(a^2,1),(b,1),(a^2b,1),(1,x),(a^2,x),(b,x),(a^2b,x)\} \\ &M_1 = \{(1,1),(a^2,1),(b,1),(a^2b,1),(1,x),(a^2,x),(b,x),(a^2b,x)\} \\ &M_2 = \{(1,1),(a,x),(a^2,1),(a^3,x),(b,x),(ab,1),(a^2b,x),(a^3b,1)\} \\ &M_3 = \{(1,1),(a,x),(a^2,1),(a^3,x),(b,1),(ab,x),(a^2b,1),(a^3b,x)\} \\ &M_3 = \{(1,1),(a,x),(a^2,1),(a^3,x),(b,1),(ab,x),(a^2b,1),(a^3b,x)\} \\ &M_3 = \{(1,1),(a,x),(a^2,1),(a^3,x),(b,1),(ab,x),(a^2b,1),(a^3b,x)\} \\ &M_4 = \{(1,1),(a,x),(a^2,1),(a^3,x),(b,1),(a^2,x),(a^2b,1),(a^3b,x)\} \\ &M_4 = \{(1,1),(a,x),(a^2,1),(a^3,x),(b,1),(a^2,x),(a^2,x),(a^3b,x)\} \\ &M_4 = \{(1,1),(a,x),(a^2,1),(a^3,x),(b,1),(a^2,x),(a^2,x),(a^3,x)$$

$$M_4=\{(1,1),(a,1),(a^2,1),(a^3,1),(1,x),(a,x),(a^2,x),(a^3,x)\}$$

$$M_5=\{(1,1),(a,1),(a^2,1),(a^3,1),(b,x),(ab,x),(a^2b,x),(a^3b,x)\}$$

$$M_6=\{(1,1),(a,1),(a^2,1),(a^3,1),(b,1),(ab,1),(a^2b,1),(a^3b,1)\}$$

$$M_7 = \{(1,1), (a^2,1), (ab,1), (a^3b,1), (1,x), (a^2,x), (ab,x), (a^3b,x)\}$$
 and $Z = D_8 \times C_2$ itself.

We have the following chains

(1)
$$D_8 \times C_2 = Z, M_1 < Z, M_2 < Z, M_3 < Z, M_4 < Z, M_5 < Z, M_6 < Z, M_7 < Z$$

Total chains=8

$$\begin{array}{l} (2) \ H_1 < M_1 < Z, H_1 < Z, H_2 < M_1 < Z, H_2 < Z, H_3 < M_1 < Z, H_3 < Z, H_3 < M_2 < Z, H_3 < M_5 < Z, H_4 < M_1 < Z, H_4 < Z, H_4 < M_3 < Z, H_4 < M_6 < Z, H_5 < M_2 < Z, H_5 < Z, H_5 < M_3 < Z, H_5 < M_4 < Z, H_6 < M_1 < Z, H_6 < Z, H_6 < M_4 < Z, H_6 < M_7 < Z, H_7 < M_4 < Z, H_7 < M_8 < Z, H_7 < M_8 < Z, H_8 < M_9 < Z, H_9 < M_9 < Z$$

 $Z, H_7 < M_5 < Z, H_7 < M_6 < Z, H_8 < M_5 < Z, H_8 < Z, H_8 < M_3 < Z, H_8 < M_7 < Z, H_9 < M_2 < Z, H_9 < Z, H_9 < M_6 < Z, H_9 < M_7 < Z, H_{10} < M_7 < Z, H_{10} < Z, H_{11} < M_7 < Z, H_{11} < Z$

Total chains = 36

- (3) (i) $P_1 < H_1 < M_1 < Z, P_1 < H_1 < Z, P_1 < M_1 < Z, P_1 < Z, P_1 < H_4 < M_1 < Z, P_1 < H_4 < M_5 < Z, P_1 < H_4 < Z, P_1 < M_5 < Z, P_1 < M_6 < Z$
- (ii) $P_2 < H_1 < M_1 < Z, P_2 < H_1 < Z, P_2 < M_1 < Z, P_2 < Z, P_2 < H_3 < M_1 < Z, P_2 < H_3 < Z, P_2 < H_3 < Z, P_2 < H_3 < M_5 < Z, P_2 < M_5 < Z$
- (iii) $P_3 < H_2 < M_1 < Z, P_3 < H_2 < Z, P_3 < M_1 < Z, P_3 < Z, P_3 < H_3 < M_1 < Z, P_3 < H_3 < M_2 < Z, P_3 < M_2 < Z, P_3 < H_3 < M_5 < Z, P_3 < M_5 < Z$
- (iv) $P_4 < H_2 < M_1 < Z, P_4 < H_2 < Z, P_4 < M_1 < Z, P_4 < Z, P_4 < H_4 < M_1 < Z, P_4 < H_4 < M_1 < Z, P_4 < H_4 < M_5 < Z, P_4 < M_6 < Z$
- $(v) \ P_5 < H_1 < M_1 < Z, P_5 < H_1 < Z, P_5 < M_1 < Z, P_5 < Z, P_5 < H_{11} < M_7 < Z, P_5 < H_{11} < Z, P_5 < H_6 < M_1 < Z, P_5 < H_6 < M_4 < Z, P_5 < M_4 < Z, P_5 < H_6 < M_7 < Z, P_5 < M_7 < Z, P_5 < H_{10} < M_7 < Z, P_5 < H_{10} < Z, P_5 < H_2 < M_1 < Z, P_5 < H_2 < Z$
- $\begin{aligned} &(\text{vi}) \ P_6 < H_6 < M_4 < Z, P_6 < H_6 < Z, P_6 < M_4 < Z, P_6 < I_5 < M_2 < Z, P_6 < H_5 < \\ &Z, P_6 < M_2 < Z, P_6 < H_5 < M_3 < Z, P_6 < M_3 < Z, P_6 < H_5 < M_4 < Z, P_6 < H_4 < M_1 < \\ &Z, P_6 < M_4 < Z, P_6 < H_4 < M_1 < Z, P_6 < H_4 < M_1 < Z, P_6 < H_4 < M_2 < Z, P_6 < H_4 < M_3 < Z, P_6 < H_4 < M_6 < Z, P_6 < H_3 < M_1 < Z, P_6 < H_3 < M_2 < Z, P_6 < H_3 < M_3 < Z, P_6 < H_7 < M_4 < Z, P_6 < H_7 < Z, P_6 < H_7 < M_8 < Z, P_6 < H_7 < M_8 < Z, P_6 < H_8 < M_7 < Z, P_6 < H_7 < M_6 < Z, P_6 < H_8 < M_7 < Z, P_8 < H_$
- (vii) $P_7 < H_6 < M_1 < Z, P_7 < H_6 < Z, P_7 < M_1 < Z, P_7 < Z, P_7 < H_6 < M_4 < Z, P_7 < M_4 < Z, P_7 < H_6 < M_7 < Z, P_7 < M_7 < Z$
- (viii) $P_8 < H_8 < M_3 < Z, P_8 < H_8 < Z, P_8 < M_3 < Z, P_8 < Z, P_8 < H_8 < M_5 < Z, P_8 < M_5 < Z, P_8 < H_9 < M_7 < Z, P_8 < M_7 < Z, P_8 < H_{10} < M_7 < Z, P_8 < H_{10} < Z$
- (ix) $P_9 < H_{11} < M_7 < Z$, $P_9 < H_{11} < Z$, $P_9 < M_7 < Z$, $P_9 < Z$, $P_9 < H_8 < M_3 < Z$, $P_9 < M_3 < Z$, $P_9 < H_8 < M_7 < Z$, $P_9 < M_7 < Z$, $P_9 < H_8 < M_5 < Z$, $P_9 < M_5 < Z$, $P_9 < H_8 < Z$
- $\begin{aligned} &(x) \ P_{10} < H_{11} < M_7 < Z, P_{10} < H_{11} < Z, P_{10} < M_7 < Z, P_{10} < Z, P_{10} < H_9 < M_2 < Z, P_{10} < M_9 < M_6 < Z, P_{10} < H_9 < M_7 < Z, P_{10} < M_7 < Z, P_{10} < M_9 < M_9$
- (xi) $P_{11} < H_9 < M_2 < Z, P_{11} < H_9 < Z, P_{11} < M_2 < Z, P_{11} < Z, P_{11} < H_9 < M_6 < Z, P_{11} < M_8 < Z, P_{11} < M_9 < M_9 < Z, P_{11} < Z, P_{11} < M_9 < Z, P_{11} < Z, P_{11} < M_9 < Z, P_{11} < Z,$

Total chains =
$$10 + 10 + 10 + 10 + 16 + 36 + 8 + 10 + 11 + 11 + 10 = 142$$

Total chains in $(1) + (2) + (3) = 8 + 36 + 142 = 186$

Hence, the number of FSGs corresponding to the above chains is 186.

(4) As a consequence of P₁(μ) = {(1,1)}, we have 186 fuzzy subgroups.

Therefore, the overall number of FSGs of $D_8 \times C_2$ is $2 \times 186 = 372$

4. Conclusion and Future Research

We use the equivalence relation introduced by R. Sulaiman and Abd. Ghafur to obtain the number of fuzzy subgroups of D₈ × C₂. This method can further be applied to count fuzzy subgroups of some more abelian and non-abelian groups.

References

- L. A. Zadeh, Fuzzy Sets, Information. And Control,8 (1965), 338-353
- [2] A. Rosenfeld, Fuzzy groups, Journal of Mathematical Analysis. And Applications, 35 (1971), pp.512-517
- [3] Darabi, H., Sacedi, F. and Farrokhi D. G., M. (2013). The number of Fuzzy subgroups of some non-abelian groups. Iranian Journal of Fuzzy Systems, 10(6), 101-107. doi: 10.22111/ijfs.2013.1333
- [4] Tarnauceanu, M. (2011). Classifying fuzzy subgroups for a class of finite p-groups. Retrieved from <a href="https://www.math.uaic.ro/~martar/pdf/articole
- [5] M. Tarnauceanu, Classifying Fuzzy Normal Subgroups of Finite Groups, Iranian Journal of Fuzzy System, Vol.12, No.2 (2015), pp 107-115
- [6] M. Tarnauceanu, The Number of Fuzzy Subgroups of Finite Cyclic Groups and Delaney numbers, European Journal of Combinatorics, 30(2009), pp. 283-286
- [7]M. Tarnauceanu and L. Benta, On the Number of Fuzzy Subgroups of Finite Abelian Groups, Fuzzy Sets and Systems, 159 (2008), pp. 1084-1096
- [8] R. Sulaiman, Constructing Fuzzy subgroups of Symmetric Groups, S₄, International Journal of Algebra, Vol.6, (2012), No.1, pp. 23-28
- [9] R. Sulaiman and A. G. Ahmad, Constructing Fuzzy Subgroups S₂, S₃ and Alternating Groups, Journal of Quality Measurement and Analysis, 6 (2010), pp. 57-63

- [10] R. Sulaiman and A. G. Ahmad, The Number of Fuzzy Subgroups of Group Defined by a Presentation, International Journal of Algebra, 5 No. 8 (2011), pp. 375-382
- [11] Olayiwola Abdulhakeem and Ibrahim Doudu Usman, Counting Distinct Fuzzy Subgroup of Some Alternating Groups, Dutse Journal of Pure and Applied Sciences, Vol.4, No.2, Dec 2018
- [12] V. Murali and B. B. Makamba, On an Equivalence of Fuzzy Subgroup I, Fuzzy Sets and Systems, 123 (2001), pp. 259-264
- [13] Murali V. and Makamba B. B., On an equivalence of fuzzy subgroup II, Fuzzy Sets and Systems, 136 (2003), 93-104.
- [14] Y. Zhang and K. Zou, A Note on Equivalence On Fuzzy Subgroups, Fuzzy Sets and Systems, 95 (1992), 243-247.
- [15] M. K. Singh and Dhiraj Kumar, On The Number of Fuzzy Subgroups and Fuzzy Normal Subgroups of Dihedral Group D₈ and Quaternion Group Q₈, Journal of Xidian University, Vol.15, No.3 (2021),pp. 321-326
- [16]M. K. Singh and Dhiraj Kumar, The Number of Fuzzy Subgroups and Fuzzy Normal Subgroups of Dicyclic Group Q₁₂, Journal of Xidian University, Vol.15, No.4 (2021), pp. 26-32
- [17] Singh M., Theory of Fuzzy Structures and Applications (Fuzzification of Mathematical Notions), Lambert Academic Publishing, 2010.

^{1, 2, 3}Department of Mathematics, Magadh University, Bodh-Gaya, Bihar, India

(Received, January 10, 2025)

Email: dhirajraj1982@gmail.com Email: drmksingh_gaya@yahoo.com Email: drsanjeetkumar 1994@gmail.com Sivasankar S¹, Bahysuganya K² SOME DISTANCE-BASED TOPOLOGICAL INDICES OF DOUBLE STARBARBELL GRAPH AND PETERSENBARBELL GRAPH

ISSN: 0970-5120

Abstract: A topological index is an analytically derived numerical index for the graph structure. In this paper, we study some distancebased topological indices, such as, Wiener index (W), hyper-Wiener index (WW), Harary index (H), Reciprocal Complementary Wiener index (RCW), Wiener Polarity index (W_P) , Terminal Wiener index (TW), Reverse Wiener index (\land) and Reciprocal Reverse Wiener index $(R\land)$ of Double starbarbell graph $BSB_{r_1,r_2,...,r_{m+n}}$ and Petersenbarbell graph $PB_{m_1,m_2,...,m_5}$.

MSC: 05C09, 05C12, 05C76

Keywords: Topological indices, Wiener index, Double Star graph, Double Starbarbell graph, Petersenbarbell graph,

1 Introduction

In this paper, we consider only finite, undirected, connected and simple graphs. For a graph G = (V, E), the number of vertices and edges will be denoted by |V(G)| and |E(G)| respectively. If $u, v \in V(G)$, length of the shortest distance between u and v in G is denoted by $d_G(u, v)$ and we simply denote it by d(u, v) if there is no ambiguity in the graph under consideration. The eccentricity of a vertex u in a graph G is $e(u) = max\{d(u, v) : v \in V(G)\}$. The radius (resp. diameter) of G is $v = rad(G) = min\{e(v) : v \in V(G)\}$ (resp. $d = diam(G) = max\{e(v) : v \in V(G)\}$). In a graph, a vertex of degree 1 is known as a pendent vertex or terminal node or leaf node or leaf. Definitions which are not seen here can be referred in [4] and [5].

A topological index is an analytically derived numerical index for the graph structure. Indices are graph invariants used to study graph structure. Graph techniques have many applications in various fields such as Chemistry, Physics, Biology, Computer science, etc. The Wiener index is the distance based topological index introduced by the chemist Harry Wiener in 1947 [26] and also known as the "Wiener number" [7, 9]. Wiener index is widely used based on the chemical applications of graph theory which counts the number of bonds between pairs of atoms and sum the distances between all pairs by generating a distance matrix [20]. The Wiener index is defined by the sum of distances between all unordered pairs of vertices of a graph G,

$$W(G) = \sum_{u,v \in V(G)} d(u,v).$$

The hyper-Wiener index is the generalization of the Wiener index introduced by Milan Randić in 1993 [23] and is defined as follows:

$$WW(G) = \frac{1}{2} \sum_{u,v \in V(G)} [d(u,v) + d(u,v)^{2}].$$

In [22] Plavšić et. al., and in [16] Ivancine et. al., independently introduced the Harary index, in honor of Frank Harary. For the graph G, the Harary index is defined as the reciprocal of the Wiener index, and denoted by

$$H(G) = \sum_{u,v \in V(G)} \frac{1}{d(u,v)}$$
.

In [15, 17] Ivancine et. al., introduced the Reciprocal Complementary Wiener index, denoted by RCW(G) and given by

$$RCW(G) = \sum_{u,v \in V(G)} \frac{1}{d+1 - d(u,v)},$$

where d is the diameter of a graph G.

The Wiener Polarity index W_P of a graph G, introduced by Wiener in 1947 [8], is the number of unordered pairs of vertices of G such that the distance between u and v is 3,

$$W_P(G) = |\{(u, v) \mid d(u, v) = 3, u, v \in V(G)\}|.$$

The Terminal Wiener index of a graph G is defined by Gutman et.al., in [14], as the sum of distances between all pairs of pendent vertices of G,

$$TW(G) = \sum_{\substack{u,v \in V(G)\\ deg(u) = deg(v) = 1}} d(u,v).$$

The Reverse Wiener index was proposed by Balaban et. al., in 2000 [2] and is defined as follows

$$\wedge(G) = \frac{n(n-1)d}{2} - W(G),$$

where n = |V(G)| and d is the diameter of G.

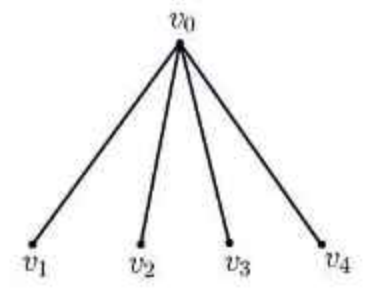
In [18], the Reciprocal Reverse Wiener (RRW) index $R \wedge (G)$ of a connected graph G is defined as

$$R \wedge (G) = \begin{cases} \sum_{u,v \in V(G)} \frac{1}{d - d(u,v)}, & \text{for } 0 < d(u,v) < d, \\ 0, & \text{otherwise.} \end{cases}$$

where d is the diameter of a graph G.

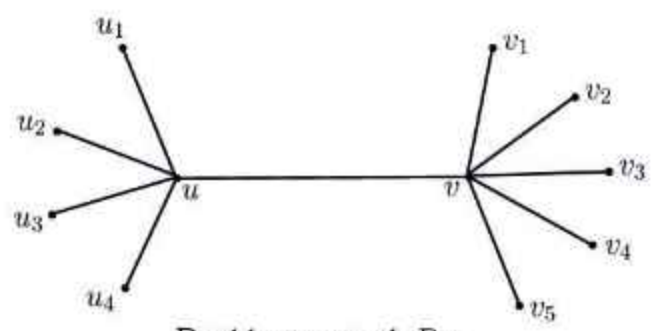
In this paper we calculate W(G), WW(G), H(G), RCW(G), $W_P(G)$, TW(G), $\wedge(G)$ and $R \wedge (G)$ of a Double starbarbell and Petersenbarbell graphs. We mention some concepts and results below, which are required for proving the theorems. Various indices are referred in [10, 11, 12]

A complete graph on n vertices is denoted by K_n . S_n denotes the star on n vertices in which one vertex is adjacent to all the other vertices, See Figure 1.1 for S_5 . Also $S_n \cong K_{1,n-1}$.



Star graph S₅ Figure 1.1

A double star is a graph obtained by inserting an edge joining the centers of $K_{1,n}$ and $K_{1,m}$ for $n, m \ge 2$ and it is denoted by $B_{n,m}$. If n = m in the double star graph, it is called as bistar graph and denoted by $B_{n,n}$, See Figure 1.2 for $B_{4,5}$.



Double star graph $B_{4,5}$ Figure 1.2

Lemma 1.1. [1] Let K_n and S_n be the complete and star graphs of order n, respectively. Then

(i) for
$$n \ge 1$$
, $W(K_n) = \binom{n}{2}$
(ii) for $n \ge 1$, $W(S_n) = (n-1)^2$.

Lemma 1.2. [1] Let K_n and S_n be the complete and star graphs of order n, respectively. Then

(i) for
$$n \ge 1$$
, $WW(K_n) = \frac{1}{2}n(n-1)$
(ii) for $n \ge 1$, $WW(S_n) = \frac{1}{6}(n-1)(3n-4)$.

Lemma 1.3. [25] Let K_n and S_n be the complete and star graphs of order n, respectively. Then

(i) for
$$n \ge 1$$
, $H(K_n) = \binom{n}{2}$
(ii) for $n \ge 1$, $H(S_n) = \frac{1}{4}(n-1)(n+2)$.

Lemma 1.4. [21] Let K_n and S_n be the complete and star graphs of order n, respectively. Then

(i) for
$$n \ge 1$$
, $RCW(K_n) = \binom{n}{2}$
(ii) for $n \ge 1$, $RCW(S_n) = \frac{1}{2}(n-1)^2$.

Lemma 1.5. [8] Let K_n and S_n be the complete and star graphs of order n, respectively. Then $W_P(K_n) = W_P(S_n) = 0$.

Lemma 1.6. [13, 14] Let K_n and S_n be the complete and star graphs of order n, respectively. Then $TW(K_n) = 0$ and $TW(S_n) = (n-1)(n-2)$.

Lemma 1.7. [6] Let K_n and S_n be the complete and star graphs of order n, respectively. Then

(i) for
$$n \ge 1$$
, $\wedge (K_n) = 0$

(ii) for
$$n \ge 1$$
, $\wedge (S_n) = (n-1)$.

Lemma 1.8. [27] Let K_n and S_n be the complete and star graphs of order n, respectively. Then

(i) for
$$n \ge 1$$
, $R \land (K_n) = 0$

(ii) for
$$n \ge 1$$
, $R \land (S_n) = (n-1)$.

2 Indices of a Double Star Graph

In this section, we calculate some results for distance-based topological indices W(G), WW(G), H(G), RCW(G), $W_P(G)$, TW(G), $\wedge(G)$ and $R \wedge (G)$, where G is a double star graph as in [19].

Theorem 2.1. For the double star graph G with $m, n \geq 2$, then

- (i) W(G) = n(n+2) + m(m+2) + (3mn+1).
- (ii) $WW(G) = \frac{1}{2}[n(3n+5) + m(3m+5) + 2(6mn+1)].$
- (iii) $H(G) = \frac{1}{12}[3n(n+5) + 3m(m+5) + 4(mn+3)].$
- (iv) $RCW(G) = \frac{1}{12}[n(3n+7) + m(3m+7) + 4(3mn+1)].$

Proof. Let $G = B_{n,m}$ be the double star graph with $m, n \geq 2$. Let $V(G) = V_1 \cup V_2$, where $V_1 = \{u, u_1, u_2, \dots, u_n\}$ and $V_2 = \{v, v_1, v_2, \dots, v_m\}$. For $i, j = 1, 2, \dots, n$ and $k, \ell = 1, 2, \dots, m$ the distances between any two vertices in G are given by

$$d(u, v) = d(u, u_i) = d(v, v_k) = 1,$$

 $d(u, v_k) = d(u_i, v) = 2,$
 $d(u_i, u_j) = d(v_k, v_\ell) = 2, i \neq j \text{ and } k \neq \ell,$
 $d(u_i, v_k) = 3.$

Here diam(G) = 3 and the distance between any pair of vertices varies from 1, 2, ..., diam(G).

The number of 1 distance, pair of vertices is n + m + 1.

The number of 2 distance, pair of vertices is $\binom{n}{2} + \binom{m}{2} + n + m$. The number of 3 distance, pair of vertices is mn. By using these we derive the following

(i)
$$W(G) = (n+m+1)1 + \left[\binom{n}{2} + \binom{m}{2} + n+m\right]2 + (mn)3$$

= $n(n+2) + m(m+2) + (3mn+1)$.

(ii)
$$WW(G) = \frac{1}{2}[(n+m+1)(1+1^2) + [\binom{n}{2} + \binom{m}{2} + n+m](2+2^2) + (mn)(3+3^2)]$$

= $\frac{1}{2}[n(3n+5) + m(3m+5) + 2(6mn+1)]$

(iii)
$$H(G) = (n+m+1)\frac{1}{1} + [\binom{n}{2} + \binom{m}{2} + n+m]\frac{1}{2} + (mn)\frac{1}{3}$$

 $= \frac{1}{12}[3n(n+5) + 3m(m+5) + 4(mn+3)].$

(iv)
$$RCW(G) = (n+m+1)\frac{1}{3} + [\binom{n}{2} + \binom{m}{2} + n+m]\frac{1}{2} + (mn)\frac{1}{1}$$

= $\frac{1}{12}[n(3n+7) + m(3m+7) + 4(3mn+1)].$

Remark 2.1. In Theorem 2.1, when m = n = 1, $G \cong P_4$, the diameter of graph G is 3. Hence W(G), WW(G), H(G) and RCW(G) are valid.

Corollary 2.2. For the double star graph G with $m, n \ge 1$, $W_P(G) = mn$.

Proof. The number of 3 distance pair of vertices is mn by Theorem 2.1. So, $W_P(G) = mn$.

Corollary 2.3. For the double star graph G with $m, n \ge 1$, TW(G) = n(n-1) + m(m-1) + 3mn.

Proof. For m = n = 1 in Theorem 2.1, $G \cong P_4$, so $TW(G) = TW(P_4)$. For $m, n \geq 2$ in Theorem 2.1, $TW(G) = \binom{n}{2}2 + \binom{m}{2}2 + (mn)3 = n(n-1) + m(m-1) + 3mn$.

Lemma 2.4. For the double star graph G with $m, n \ge 1$, $\wedge(G) = \frac{3}{2}(m+n+2)(m+n+1) - [n(n+2) + m(m+2) + (3mn+1)].$

Proof. In Theorem 2.1,
$$|V(G)| = m + n + 2$$
, $d = 3$ and $W(G) = n(n+2) + m(m+2) + (3mn+1)$. So, $\wedge(G) = \frac{3}{2}(m+n+2)(m+n+1) - [n(n+2) + m(m+2) + (3mn+1)]$.

Lemma 2.5. For the double star graph G with $m, n \ge 1$, $R \land (G) = \frac{1}{2}[m(m+2) + n(n+2) + 1]$.

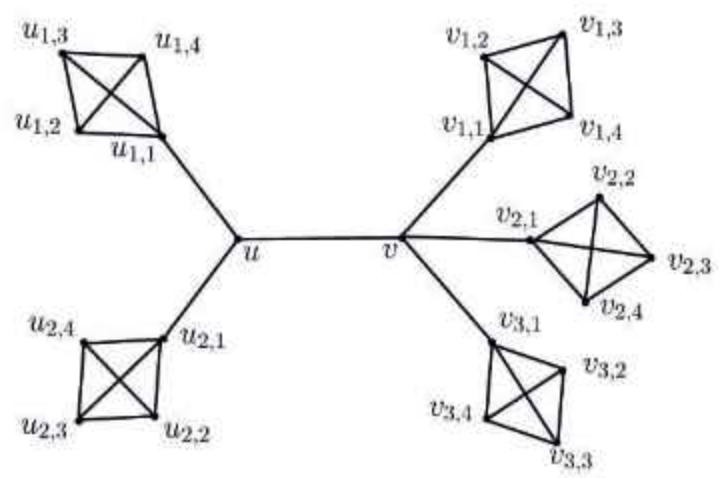
Proof. Here d = 3, from Theorem 2.1 and the distance between any pair of vertices varies 0 < d(u, v) < d. The number of 1 distance pair of vertices is n + m + 1. The number of 2 distance pair of vertices is $\binom{n}{2} + \binom{m}{2} + n + m$. By using these we derive the following.

$$R \wedge (G) = (n+m+1)\frac{1}{2} + \left[\binom{n}{2} + \binom{m}{2} + n + m\right]\frac{1}{1}$$
$$= \frac{1}{2}[m(m+2) + n(n+2) + 1].$$

3 Indices of a Double Starbarbell Graph

In this section, we introduce double starbarbell graph $BSB_{r_1,r_2,...,r_{m+n}}$ which is similar to starbarbell graph [24] and derive some results for distance-based topological indices W(G), WW(G), H(G), RCW(G), $W_P(G)$, TW(G), $\wedge(G)$ and $R \wedge (G)$, where G is a double starbarbell graph.

Definition 3.1. The double starbarbell graph $BSB_{r_1,r_2,...,r_{m+n}}$ is a graph obtained from double star graph $B_{n,m}$ and m+n complete graph K_{r_i} by merging one vertex from each K_{r_i} and the i^{th} leaf of $B_{n,m}$, where $r_i \geq 2$, $1 \leq i \leq m+n$ and $m, n \geq 2$, See Figure 3.1 for $BSB_{r_1,r_2,...,r_b}$.



Double Starbarbell graph $BSB_{4,4,4,4,4}$ where $r_i = 4$, i = 1, 2, ..., m + nFigure 3.1

Theorem 3.2. For $m, n \ge 1$ and $r \ge 2$ the double starbarbell graph G, in which all the complete graphs are of the same order. Then

$$\begin{array}{ll} \text{(i)} \ W(G) &= 1 + \frac{m+n}{2}(r^2 + 9r - 4) + mnr(5r - 2) \\ &+ r(2r - 1)[n(n - 1) + m(m - 1)]. \\ \text{(ii)} \ WW(G) &= \frac{1}{2}[2 + (m+n)(r^2 + 17r - 10) \\ &+ [n(n - 1) + m(m - 1)](10r^2 - 8r + 1) \\ &+ 2mn(15r^2 - 10r + 1)]. \\ \text{(iii)} \ H(G) &= 1 + \frac{m+n}{6}(3r^2 + 2r + 4) + \frac{mn}{30}(6r^2 + 3r + 1) \\ &+ \frac{1}{24}[n(n - 1) + m(m - 1)](3r^2 + 2r + 1). \\ \text{(iv)} \ RCW(G) &= \frac{1}{5} + \frac{m+n}{60}(6r^2 + 29r - 8) + \frac{mn}{3}(3r^2 - 3r + 1) \\ &+ \frac{1}{24}[n(n - 1) + m(m - 1)](6r^2 - 4r - 1). \end{array}$$

Proof. Let $G = BSB_{r_1, r_2, \dots, r_{m+n}}$ be the double starbarbell graph where each complete graph has the same order with $r_i \geq 2, \ 1 \leq i \leq m+n$ and $m, n \geq 1$. Let $r_i = r, \ i = 1, 2, \dots, m+n$. Let $V(G) = \{u, u_{1,1}, u_{1,2}, \dots, u_{1,r}, u_{2,1}, u_{2,2}, \dots, u_{2,r}, \dots, v_{n,1}, v_{n,2}, \dots, v_{n,r}, v, v_{1,1}, v_{1,2}, \dots, v_{1,r}, v_{2,1}, v_{2,2}, \dots, v_{2,r}, \dots, v_{n,1}, v_{n,2}, \dots, v_{m,r}\}$. Then $V(G) = U_1 \cup U_2 \cup \dots \cup U_n \cup V_1 \cup V_2 \cup \dots \cup V_m \cup \{u, v\}$ where $U_i = \{u_{i,1}, u_{i,2}, \dots, u_{i,r}\}$ and $V_j = \{v_{j,1}, v_{j,2}, \dots, v_{j,r}\}, \ 1 \leq i \leq n \text{ and } 1 \leq j \leq m$. For $i, j = 1, 2, \dots, n$ and $p, q = 1, 2, \dots, m$ and $k, \ell = 2, 3, \dots, r$ the distances between any two vertices in G are given by

$$\begin{split} d(u,v) &= d(u,u_{i,1}) = d(u_{i,1},u_{i,k}) = d(u_{i,k},u_{i,\ell}) = 1, \text{ for } k \neq \ell, \\ d(v,v_{p,1}) &= d(v_{p,1},v_{p,k}) = d(v_{p,k},v_{p,\ell}) = 1, \text{ for } k \neq \ell \\ d(u,v_{p,1}) &= d(u_{i,1},v) = 2, \\ d(u_{i,1},u_{j,1}) &= d(v_{p,1},v_{q,1}) = 2, \text{ for } i \neq j \text{ and } p \neq q \\ d(u_{i,1},u_{j,k}) &= d(v_{p,1},v_{q,k}) = 3, \text{ for } i \neq j \text{ and } p \neq q \\ d(u,v_{p,k}) &= d(u_{i,k},v) = 3, \\ d(u_{i,1},v_{p,k}) &= d(u_{j,k},v_{q,1}) = 4, \\ d(u_{i,k},v_{p,k}) &= 5. \end{split}$$

Here diam(G) = 5 and the distance between any pair of vertices varies from 1, 2, ..., diam(G).

The number of 1 distance, pair of vertices is $1 + n + n\binom{r}{2} + m + m\binom{r}{2}$. The number of 2 distance, pair of vertices is $n(r-1) + m(r-1) + \binom{n}{2} + \binom{m}{2} + n + m$.

The number of 3 distance, pair of vertices is $m(r-1) + 2(r-1)\binom{n}{2} + n(r-1) + 2(r-1)\binom{m}{2} + mn$.

The number of 4 distance, pair of vertices is $(r-1)^2 \binom{n}{2} + (r-1)^2 \binom{m}{2} + 2(r-1)mn$.

The number of 5 distance pair of vertices is $mn(r-1)^2$.

By using these we derive the following

(i)
$$W(G) = [1 + n + n \binom{r}{2} + m + m \binom{r}{2}]1 + [n(r-1) + m(r-1) + \binom{n}{2} + \binom{m}{2} + (m+m)]2 + [m(r-1) + 2(r-1) \binom{n}{2} + n(r-1) + 2(r-1) \binom{m}{2} + mn]3 + [(r-1)^2 \binom{n}{2} + (r-1)^2 \binom{m}{2} + 2(r-1)mn]4 + [mn(r-1)^2]5$$

$$= 1 + \frac{m+n}{2}(r^2 + 9r - 4) + mnr(5r - 2) + r(2r-1)[n(n-1) + m(m-1)].$$
(ii) $WW(G) = \frac{1}{2}[[1 + n + n \binom{r}{2} + m + m \binom{r}{2}](1 + 1^2) + [n(r-1) + m(r-1) + \binom{n}{2} + m + m](2 + 2^2) + [m(r-1) + m(r-1) + \binom{n}{2} + m + m](2 + 2^2) + [m(r-1) + m(r-1) + \binom{n}{2} + m + m](2 + 2^2) + [m(r-1) + m(r-1) + \binom{n}{2} + m + m](2 + 2^2) + [m(r-1) + m(r-1) + m(r-1) + \binom{n}{2} + m + m](2 + 2^2) + [m(r-1) + m(r-1) + m($

$$+2(r-1)\binom{n}{2}+n(r-1)+2(r-1)\binom{m}{2}+mn](3+3^{2})$$

$$+[(r-1)^{2}\binom{n}{2}+(r-1)^{2}\binom{m}{2}+2(r-1)mn](4+4^{2})$$

$$+[mn(r-1)^{2}](5+5^{2})]$$

$$=\frac{1}{2}[2+(m+n)(r^{2}+17r-10)+2mn(15r^{2}-10r+1)$$

$$+[n(n-1)+m(m-1)](10r^{2}-8r+1)].$$

(iii)
$$\begin{split} H(G) &= [1+n+n\binom{r}{2}+m+m\binom{r}{2}]\frac{1}{1} \\ &+ [n(r-1)+m(r-1)+\binom{n}{2}+\binom{m}{2}+n+m]\frac{1}{2} \\ &+ [m(r-1)+2(r-1)\binom{n}{2}+n(r-1)+2(r-1)\binom{m}{2}+mn]\frac{1}{3} \\ &+ [(r-1)^2\binom{n}{2}+(r-1)^2\binom{m}{2}+2(r-1)mn]\frac{1}{4}+[mn(r-1)^2]\frac{1}{5} \\ &= 1+\frac{m+n}{6}(3r^2+2r+4)+\frac{mn}{30}(6r^2+3r+1) \\ &+ \frac{1}{24}[n(n-1)+m(m-1)](3r^2+2r+1). \end{split}$$

(iv)
$$RCW(G) = [1 + n + n\binom{r}{2} + m + m\binom{r}{2}] \frac{1}{5} + [n(r-1) + m(r-1) + \binom{n}{2} + \binom{m}{2} + \binom{m}{2} + n + m] \frac{1}{4} + [m(r-1) + 2(r-1)\binom{n}{2} + n(r-1) + 2(r-1)\binom{m}{2} + mn] \frac{1}{3} + [(r-1)^2\binom{n}{2} + (r-1)^2\binom{m}{2} + 2(r-1)mn] \frac{1}{2} + [mn(r-1)^2] \frac{1}{1}$$

$$= \frac{1}{5} + \frac{m+n}{60}(6r^2 + 29r - 8) + \frac{mn}{3}(3r^2 - 3r + 1) + \frac{1}{24}[n(n-1) + m(m-1)](6r^2 - 4r - 1).$$

Remark 3.1. In Theorem 3.2, when m = n = r = 1, $G \cong P_4$, here the diameter of graph G is 3, hence RCW(G) is invalid but W(G), WW(G) and H(G) are valid.

Remark 3.2. In Theorem 3.2, when $m, n \ge 2$ and r = 1, $G \cong B_{n,m}$, here the diameter of graph G is 3, hence RCW(G) is invalid but W(G), WW(G) and H(G) are valid.

Corollary 3.3. For the double starbarbell graph G with $m, n, r \ge 1$, $W_P(G) = (r-1)[(m+n) + n(n-1) + m(m-1)] + mn$.

Proof. The number of 3 distance pair of vertices is $m(r-1) + 2(r-1)\binom{n}{2} + n(r-1) + 2(r-1)\binom{m}{2} + mn$ by Theorem 3.2. So, $W_P(G) = (r-1)[(m+n) + n(n-1) + m(m-1)] + mn$.

Corollary 3.4. For the double starbarbell graph G with $m, n \geq 1$,

$$TW(G) = \begin{cases} TW(B_{n,m}), & \text{if } r = 1\\ 2[n(n-1) + m(m-1)] + 5mn, & \text{if } r = 2 \end{cases}$$

Proof. In Theorem 3.2, when r = 1, $G \cong B_{n,m}$, hence $TW(G) = TW(B_{n,m})$ and same as in Corollary 2.3. In Theorem 3.2, when r = 2, hence $TW(G) = {n \choose 2} + {m \choose 2} + 5mn = 2[n(n-1) + m(m-1)] + 5mn$. \square

Lemma 3.5. For the double starbarbell graph G with $m, n \ge 1$ and $r \ge 2$, $\wedge(G) = \frac{5}{2}[(m+n)r+2][(m+n)r+1] - [1 + \frac{m+n}{2}(r^2+9r-4) + r(2r-1)[n(n-1) + m(m-1)] + mnr(5r-2)].$

Proof. In Theorem 3.2, |V(G)| = (m+n)r+2, d = 5 and $W(G) = 1 + \frac{m+n}{2}(r^2+9r-4) + r(2r-1)[n(n-1)+m(m-1)] + mnr(5r-2)$. So, $\wedge(G) = \frac{5}{2}[(m+n)r+2][(m+n)r+1] - [1 + \frac{m+n}{2}(r^2+9r-4) + r(2r-1)[n(n-1)+m(m-1)] + mnr(5r-2)]$.

Lemma 3.6. For the double starbarbell graph G with $m, n \ge 1$ and $r \ge 2$, $R \land (G) = \frac{1}{4}[1 + 2mn(4r - 3)] + \frac{(m+n)}{24}(3r^2 + 17r - 6) + \frac{1}{6}[n(n-1) + m(m-1)](3r^2 - 3r + 1)$.

Proof. Here d = 5, from Theorem 3.2 and the distance between any pair of vertices satisfies 0 < d(u, v) < d.

The number of 1 distance pair of vertices is $1 + n + n\binom{r}{2} + m + m\binom{r}{2}$. The number of 2 distance, pair of vertices is $n(r-1) + m(r-1) + \binom{n}{2} + \binom{m}{2} + n + m$.

The number of 3 distance, pair of vertices is $m(r-1) + 2(r-1)\binom{n}{2} + n(r-1) + 2(r-1)\binom{m}{2} + mn$.

The number of 4 distance, pair of vertices is $(r-1)^2 \binom{n}{2} + (r-1)^2 \binom{m}{2} + 2(r-1)mn$.

By using these we derive the following

$$\begin{split} R \wedge (G) &= [1+n+n\binom{r}{2}+m+m\binom{r}{2}]\frac{1}{4} \\ &+ [n(r-1)+m(r-1)+\binom{n}{2}+\binom{m}{2}+n+m]\frac{1}{3} \\ &+ [m(r-1)+2(r-1)\binom{n}{2}+n(r-1)+2(r-1)\binom{m}{2}+mn]\frac{1}{2} \\ &+ [(r-1)^2\binom{n}{2}+(r-1)^2\binom{m}{2}+2(r-1)mn]\frac{1}{1} \\ &= \frac{1}{4}[1+2mn(4r-3)]+\frac{(m+n)}{24}(3r^2+17r-6) \\ &+ \frac{1}{6}[n(n-1)+m(m-1)](3r^2-3r+1). \end{split}$$

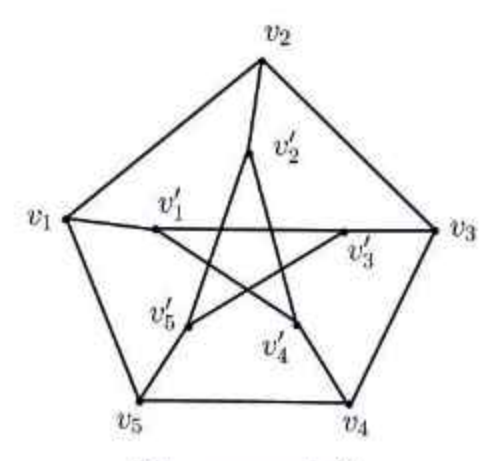
4 Indices of Petersen Graph

In this section, we calculate some results for distance-based topological indices W(G), WW(G), H(G), RCW(G), $W_P(G)$, TW(G), $\wedge(G)$ and $R \wedge (G)$, where G is a Petersen graph.

Theorem 4.1. For the Petersen graph G,

- (i) W(G) = 5(n+5).
- (ii) WW(G) = 7(n+5).
- (iii) H(G) = 2(n + 5).
- (iv) $RCW(G) = \frac{5}{2}(n+5)$.

Proof. Let G be a Petersen graph. (See Figure 4.1).



Petersen graph G Figure 4.1

Let $V(G) = \{v_1, v_2, \dots, v_5, v_1', v_2', \dots, v_5'\}$. For $i, j = 1, 2, \dots, 5$ the distances between any two vertices in G are given by

$$d(v_i, v'_i) = 1,$$

 $d(v_i, v_{i+1}) = 1$, for i + 1 taken addition modulo 5

 $d(v_i, v'_{i+2}) = 1$, for i + 2 taken addition modulo 5

 $d(v_i, v'_{i+1}) = 2$, for i + 1 taken addition modulo 5

 $d(v_i, v_{i+2}) = 2$, for i + 2 taken addition modulo 5

$$d(v_i, v'_i) = 2, i \neq j$$

Here diam(G) = 2 and the distance between any pair of vertices varies from 1, 2, ..., diam(G).

The number of 1 distance, pair of vertices is n + 5.

The number of 2 distance, pair of vertices is 2(n+5).

By using these we derive the following

(i)
$$W(G) = [n+5]1 + [2(n+5)]2$$

= $5(n+5)$.

(ii)
$$WW(G) = \frac{1}{2}[[n+5](1+1^2) + [2(n+5)](2+2^2)]$$

= $7(n+5)$.

(iii)
$$H(G) = [n+5]\frac{1}{1} + [2(n+5)]\frac{1}{2}$$

= $2(n+5)$.

(iv)
$$RCW(G) = [n+5]\frac{1}{2} + [2(n+5)]\frac{1}{1}$$

= $\frac{5}{2}(n+5)$.

Corollary 4.2. For the Petersen graph G, $W_P(G) = 0$.

Proof. In Theorem 4.1, here d = 2, the number of 3 distance pair of vertices is 0. So, $W_P(G) = 0$.

Corollary 4.3. For the Petersen graph G, TW(G) = 0

Proof. In Theorem 4.1, there is no pendent vertex, so TW(G) = 0.

Lemma 4.4. For the Petersen graph G, $\wedge(G) = n^2 - 6n - 25$.

Proof. In Theorem 4.1,
$$|V(G)| = n$$
, $d = 2$ and $W(G) = 5(n + 5)$.
So, $\wedge(G) = \frac{n(n-1)}{2}2 - 5(n + 5) = n^2 - 6n - 25$

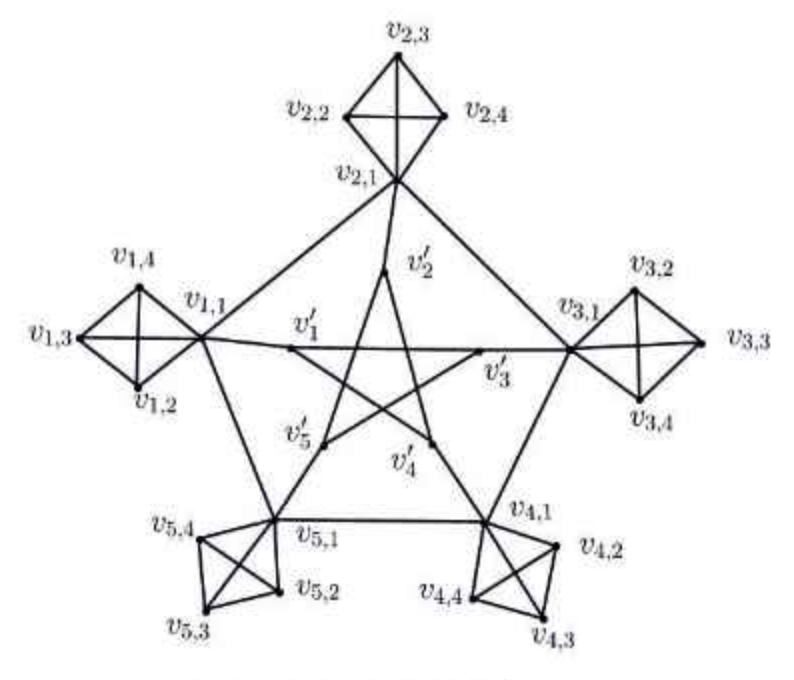
Lemma 4.5. For the Petersen graph G, $R \wedge (G) = n + 5$.

Proof. Here d = 2, from Theorem 4.1 and the distance between any pair of vertices satisfies 0 < d(u, v) < d. The number of 1 distance pair of vertices is n + 5, hence $R \wedge (G) = n + 5$.

5 Indices of Petersenbarbell Graph

In this Section, we introduce petersenbarbell graph $PB_{m_1,m_2,...,m_6}$ which is similar to wheelbarbell graph [3] and also derive some results for distance-based topological indices W(G), WW(G), H(G), RCW(G), $W_P(G)$, TW(G), $\wedge(G)$ and $R \wedge (G)$, where G is petersenbarbell graph.

Definition 5.1. The petersenbarbell graph $PB_{m_1,m_2,...,m_5}$ is a graph obtained from Petersen graph and complete graph K_{m_i} by merging one vertex from each K_{m_i} and the outer 5 vertices of Petersen graph, where $m_i \geq 2$, See Figure 5.1 for $PB_{m_1,m_2,...,m_5}$.



Petersenbarbell graph $PB_{4,4,4,4,4}$ where $m_i = 4$, i = 1, 2, ..., 5Figure 5.1

Theorem 5.2. For $m \geq 2$ and n = 10 the petersenbarbell graph G, in which each complete graph is of the uniform order. Then

- (i) $W(G) = 5(n+5) + \frac{1}{2}(m-1)[(n-5)(m+48) + 70(m-1)].$
- (ii) $WW(G) = \frac{1}{2}[14(n+5) + (m-1)[(n-5)(m+90) + 160(m-1)]].$
- (iii) $H(G) = 2(n+5) + \frac{1}{12}(m-1)[6(n-5)(m+7) + 35(m-1)].$
- (iv) $RCW(G) = \frac{11}{12}(n+5) + \frac{1}{8}(m-1)[(n-5)(m+32) + 60(m-1)].$

Proof. Let $G=PB_{m_1,m_2,\dots,m_5}$ be the petersenbarbell graph, where each complete graph is of the uniform order with $m_i\geq 2$ and $1\leq i\leq 5$. Let $m_i=m,\ i=1,2,\dots,5$. Let $V(G)=\{v_{1,1},v_{1,2},\dots,v_{1,m},v_{2,1},v_{2,2},\dots,v_{2,m},\dots,v_{5,1},v_{5,2},\dots,v_{5,m},v_1',v_2',\dots,v_5'\}$. Then $V(G)=V_1\cup V_2\cup\dots,\cup V_5\cup V_t$ where $V_i=\{v_{i,1},v_{i,2},\dots,v_{i,m}\},\ 1\leq i\leq 5$ and $V_i=\{v_1',v_2',\dots,v_5'\}$. For $i,j=1,2,\dots,5$ and $k,\ell=2,3,\dots,m$ the distance between any two vertices in G are given by $d(v_{i,1},v_{i,k})=d(v_{i,1},v_i')=d(v_{i,k},v_{i,\ell})=1$, for $k\neq \ell,$ $d(v_i,v_{i+2}')=1$, for i+2 taken addition modulo 5 $d(v_{i,1},v_{i+1,1})=1$, for i+1 taken addition modulo 5,

 $\begin{array}{ll} d(v_{i,k},v_i') &= d(v_{i,1},v_j') = 2,\, i \neq j,\\ d(v_{i,1},v_{i+2,1}) = 2,\, \text{for } i+2 \text{ taken addition modulo 5,}\\ d(v_i,v_{i+1}') &= 2,\, \text{for } i+1 \text{ can taken addition modulo 5,}\\ d(v_{i,1},v_{i+1,k}) = 2,\, \text{for } i+1 \text{ taken addition modulo 5,}\\ d(v_{i,k},v_{i+1,\ell}) = 3,\, \text{for } i+1 \text{ taken addition modulo 5,}\\ d(v_{i,k},v_{i+2,k}) = 3,\, \text{for } i+2 \text{ taken addition modulo 5,}\\ d(v_{i,k},v_j') &= 3,\, i \neq j,\\ d(v_{i,k},v_{i+2,\ell}) = 4,\, \text{for } i+2 \text{ taken addition modulo 5,}\\ \text{Here } diam(G) = 4 \text{ and the distance between any pair of vertices varies from } 1,2,\ldots,diam(G). \end{array}$

The number of 1 distance, pair of vertices is $(n+5) + (n-5)\binom{m}{2}$. The number of 2 distance, pair of vertices is 2(n+5) + 3(n-5)(m-1). The number of 3 distance, pair of vertices is $6(n-5)(m-1) + 5(m-1)^2$. The number of 4 distance, pair of vertices is $5(m-1)^2$.

By using these we derive the following

(i)
$$W(G) = [(n+5) + (n-5) {m \choose 2}]1 + [2(n+5) + 3(n-5)(m-1)]2$$

 $+ [6(n-5)(m-1) + 5(m-1)^2]3 + [5(m-1)^2]4$
 $= 5(n+5) + \frac{1}{2}(m-1)[(n-5)(m+48) + 70(m-1)].$

(ii)
$$WW(G) = \frac{1}{2}[[(n+5) + (n-5)\binom{m}{2}](1+1^2) + [2(n+5) + 3(n-5)(m-1)](2+2^2) + [6(n-5)(m-1) + 5(m-1)^2](3+3^2) + [5(m-1)^2](4+4^2)]$$

 $= \frac{1}{2}[14(n+5) + (m-1)[(n-5)(m+90) + 160(m-1)]].$

(iii)
$$H(G) = [(n+5) + (n-5) {m \choose 2}] \frac{1}{1} + [2(n+5) + 3(n-5)(m-1)] \frac{1}{2}$$

$$+ [6(n-5)(m-1) + 5(m-1)^2] \frac{1}{3} + [5(m-1)^2] \frac{1}{4}$$

$$= 2(n+5) + \frac{1}{12}(m-1)[6(n-5)(m+7) + 35(m-1)].$$

(iv)
$$RCW(G) = [(n+5) + (n-5)\binom{m}{2}]\frac{1}{4} + [2(n+5) + 3(n-5)(m-1)]\frac{1}{3}$$

 $+ [6(n-5)(m-1) + 5(m-1)^2]\frac{1}{2} + [5(m-1)^2]\frac{1}{1}$
 $= \frac{11}{12}(n+5) + \frac{1}{8}(m-1)[(n-5)(m+32) + 60(m-1)]. \square$

Remark 5.1. In Theorem 5.2, when m = 1, $G \cong Petersen$ graph, here the diameter of graph G is 2 hence RCW(G) is invalid but W(G), WW(G) and H(G) are valid and same as in Theorem 4.1.

Corollary 5.3. For the petersenbarbell graph G with $m \ge 2$ and n = 10, $W_P(G) = (m-1)(5m+6n-35)$.

Proof. The number of 3 distance pair of vertices is $6(n-5)(m-1)+5(m-1)^2$ by Theorem 5.2. So, $W_P(G)=(m-1)(5m+6n-35)$. \square

Corollary 5.4. For the petersenbarbell graph G with m = 2 and n = 10, TW(G) = 35

Proof. In Theorem 5.2, when m = 2, hence $TW(G) = [5(m-1)^2]3 + [5(m-1)^2]4 = 35(m-1)^2 = 35$.

Lemma 5.5. For the petersenbarbell graph G with $m \ge 2$ and n = 10, $\wedge(G) = 2[(n+5m-5)(n+5m-6)] - [5(n+5) + \frac{1}{2}(m-1)[(n-5)(m+48) + 70(m-1)]].$

Proof. In Theorem 5.2, |V(G)| = n + 5(m-1), d = 4 and $W(G) = 5(n+5) + \frac{1}{2}(m-1)[(n-5)(m+48) + 70(m-1)]$. Then $\wedge (G) = 2[(n+5m-5)(n+5m-6)] - [5(n+5) + \frac{1}{2}(m-1)[(n-5)(m+48) + 70(m-1)]]$.

Lemma 5.6. For the petersenbarbell graph G with $m \ge 2$ and n = 10, $R \wedge (G) = \frac{4}{3}(n+5) + \frac{1}{6}(m+9)(m-1)(n-5) + (m-1)(5m+6n-35)$.

Proof. Here d = 4, from Theorem 5.2 and the distance between any pair of vertices satisfies 0 < d(u, v) < d.

The number of 1 distance, pair of vertices is $(n+5) + (n-5)\binom{m}{2}$. The number of 2 distance, pair of vertices is 2(n+5) + 3(n-5)(m-1). The number of 3 distance, pair of vertices is $6(n-5)(m-1)+5(m-1)^2$. By using these we derive the following

$$R \wedge (G) = [(n+5) + (n-5)\binom{m}{2}] \frac{1}{3} + [2(n+5) + 3(n-5)(m-1)] \frac{1}{2}$$
$$+ [6(n-5)(m-1) + 5(m-1)^2] \frac{1}{1}$$
$$= \frac{4}{3}(n+5) + \frac{1}{6}(m+9)(m-1)(n-5) + (m-1)(5m+6n-35).$$

References

- Ahmed Mohammed Ali, Some results on Wiener indices for a connected graph G, Italian Journal of pure and Applied Mathematics, 46 (2021) 391 – 399.
- [2] A.T. Balaban, D. Mills, O. Ivanciuc, S.C. Basak, Reverse Wiener indices, Croat. Chem. Acta. 73 (2000) 923 – 941.
- [3] Babysuganya K, Sivasankar S, Some Distance-based Topological Indices of Starbarbell Graph and Wheelbarbell Graph, Communicated.
- [4] R. Balakrishnan, K. Ranganathan, A Textbook of Graph Theory, Springer Science, New York, (2012).
- [5] J.A. Bondy, U.S.R. Murty, Graph Theory with Applications, Macmillan, New York, (1976).
- [6] X. Cai, B. Zhou, Reverse Wiener indices of connected graphs, MATCH Commun. Math. Comput. Chem. 60 (2008) 95 – 105.
- [7] K.C. Das, I. Gutman, Estimating the Wiener index by means of number of vertices, number of edges, and diameter, MATCH Commun. Math. Comput. Chem. 64 (2010) 647 – 660.
- [8] H. Deng, H. Xiao, F. Tang, On the extremal Wiener polarity index of trees with a given diameter, MATCH Commun. Math. Comput. Chem. 63 (2010) 257 – 264.

- [9] A.A. Dobrynin, R. Entringer, I. Gutman, Wiener index of trees: theory and applications, Acta. Appl. Math. 66 (2001) 211 – 249.
- [10] R.C. Entringer, D.E. Jackson, D.A. Snyder, Distance in graphs, Czech. Math. J., 26 (1976) 283 — 296.
- [11] D. Gray, H.Wang, Cycles, the degree distance, and the Wiener index, Open J. Discr. Math., 2 (2012) 156 – 159.
- [12] I. Gutman, Y.N. Yeh, The sum of all distances in bipartite graphs, Math. Slovaca, 45 (1995) 327 – 334.
- [13] I. Gutman, B. Furtula, A survey on terminal Wiener index, in: I. Gutman, B. Furtula (Eds.), Novel Molecular Structure Descriptors - Theory and Applications I, Univ. Kragujevac, Kragujevac, (2010) 173 - 190.
- [14] I. Gutman, B. Furtula, M. Petrović, Terminal Wiener index, J. Math. Chem. 46 (2009) 522 – 531.
- [15] O. Ivanciuc, QSAR comparative study of Wiener descriptors for weighted molecular graphs, J. Chem. Inf. Comput. Sci. 40 (2000) 1412 – 1422.
- [16] O. Ivanciuc, T.S. Balaban, A.T. Balaban, Reciprocal distance matrix, related local vertex invariants and topological indices, J. Math. Chem. 12 (1993) 309 – 318.
- [17] O. Ivanciuc, T. Ivanciuc, A.T. Balaban, The complementary distance matrix, a new molecular graph metric, ACH Models Chem. 137 (2000) 57 – 82.
- [18] O. Ivanciuc, T. Ivanciuc, A.T. Balaban, Quantitative structure property relationship valuation of structural descriptors derived from the distance and reverse Wiener matrices, *Internet Electron*. J. Mol. Des. 1 (2002) 467 – 487.
- [19] S.P. Jayakokila and P. Sumathi, A note on soenergy of stars, bistar and double star graphs, Bulletin of the International Mathematical Virtual Institute, 6 (2016) 105 – 113.

- [20] B. Mohar and T. Pisanski, How to compute the Wiener index of a graph, J. Math. Chem. 2 (1988) 267 – 277.
- [21] R. Nasiri, A. Nakhaei, A.R. Shojaeifard, The Reciprocal Complementary Wiener number of graph operations, Kragujevac Journal of Mathematics, Volume 45 (1) (2021) 139 – 154.
- [22] D. Plavšić, S. Nikolić, N. Trinajstić, Z. Mihalić, On the Harary index for the characterization of chemical graphs, J. Math. Chem. 12 (1993) 235-250.
- [23] M. Randić, Novel molecular descriptor for structure-property studies, Chem. Phys. Lett. 211 (1993) 478 – 483.
- [24] Wahyu Tri Budianto and Tri Atmojo Kusmayadi, The local metric dimension of Starbarbell graph, K_m ⊙ P_n graph, and Möbius ladder graph, Journal of physics, 1008 (2018) 012050.
- [25] E.W. Weisstein, Harary index from wolfram mathworld, http://mathworld.wolfram.com/HararyIndex.html, (2009).
- [26] H. Wiener, Structrual determination of paraffin boiling points, J. Am. Chem. Soc. 69 (1947) 17 – 20.
- [27] B. Zhou, Y. Yang, N.Trinajstić, On reciprocal reverse Wiener index, J. Math. Chem. 47 (2010) 201 – 209.

Department of Mathematics,
 Nallamuthu Gounder Mahalingam College,
 Pollachi, Tamilnadu, India

(Received, September 24, 2024)

E-mail: sssankar@gmail.com

E-mail: babysuganya123@gmail.com

Mohanapriya Rajagopal^{*}, Durgadevi Shanmugasundaram²

ENHANCING SCADA CYBER SECURITY THROUGH NEUTROSOPHIC GRAPH TOPOLOGIC ALANALYSIS

ISSN: 0970-5120

Abstract: This manuscript extends the concept of graph topology to neutrosophic graph topological spaces by incorporating uncertainty and indeterminacy into graph topological structures. Building on existing work in graph topologies, we introduce neutrosophic components that utilize truth membership (T), indeterminacy (I), and falsity membership (F) values to handle incomplete and contradictory information. We establish foundational definitions and examine important topological properties including neutrosophic connectedness, separation axioms (T_0, T_1, T_2) . Several theorems are presented with complete proofs, including the equivalence of neutrosophic connectedness conditions and the hierarchical relationship between separation axioms. The framework is demonstrated through a practical cybersecurity application, where neutrosophic graph topology is used to model SCADA network vulnerabilities, identify secure zones, and analyze potential attack vectors in power grid systems.

Keywords: Neutrosophic graph topology, neutrosophic connectedness, neutrosophic separation, network security, SCADA systems.

Mathematics Subject Classification (2020): Primary: 54A05, 54A10; Secondary: 94C15.

1. Introduction

Neutrosophic theory, introduced by Smarandache [9], extends classical logic by incorporating indeterminacy alongside truth and falsity, enabling uncertainty quantification. Building on this, Aniyan and Naduvath [1] established graph topological frameworks for analyzing spatial properties in discrete structures, focusing on transformations and connectivity. Broumi and Smarandache [4] further advanced the field by defining neutrosophic graph structures, which model uncertainty in vertex and edge relationships. Ye [13] developed correlation-based decision-

making methods in neutrosophic environments, aiding multi-criteria analysis under incomplete information.

In cybersecurity, Stouffer et al. [10] outlined SCADA system security protocols, addressing infrastructure vulnerabilities. Zhu et al. [15] proposed a taxonomy of cyber attacks on SCADA networks, enabling systematic threat assessment in uncertain environments. Mohanapriya Rajagobal and Durgadevi Shanmugasundaram proposed a mathematical framework integrating neutrosophic theory with graph topology for cybersecurity analysis by establishing key properties such as connectedness and separation axioms and applying the model to SCADA power grid systems.

2. Neutrosophic Graph Topology

Definition 1.1 Let NG = (V, E) be a neutrosophic graph. A neutrosophic graph topology τ on NG is a collection of neutrosophic subgraphs of NG satisfying the following conditions:

- 1. $NK_0 \in \tau$ and $NG \in \tau$, where NK_0 denotes the neutrosophic null graph.
- The union of any number of elements in τ is also in τ.
- The intersection of any finite number of elements in τ is also in τ.

The combination (NG, τ) forms a Neutrosophic Graph Topological Space(NGTS).

Example 1.1: For the neutrosophic graph NG with vertex set $\{A, B, C, D\}$, the collection of subgraph yields the neutrosophic graph topology

$$\tau = \{NK_0, \{A, B\}, \{B, C\}, \{A, C, D\}, NG\}$$

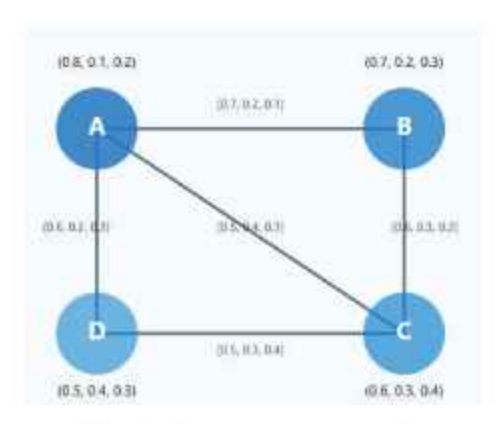


Figure 1: Neutrosophic Graph NG

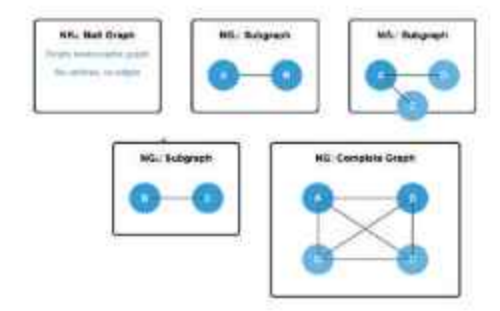


Figure 2: Neutrosophic Graph Topology Induced by Collection of Subgraph

Definition 1.2: A *neutrosophic empty graph* is a neutrosophic graph with a non-empty vertex set but an empty edge set.

Definition 1.3: A neutrosophic null graph, denoted by NK_0 , is a neutrosophic graph with empty vertex and edge sets.

Definition 1.4: A neutrosophic subgraph NH of NG is said to be neutrosophically open if $NH \in \tau$.

Definition 1.5: A neutrosophic subgraph NH of NG is said to be neutrosophically closed if its neutrosophic complement, denoted by NH^c , is neutrosophically open.

3. Neutrosophic Connectedness in NGTS

This section presents definition and theorems on Connectedness in NGTS.

Definition 3.1 In a neutrosophic graph topological space (NG, τ) , a neutrosophic separation of the graph NG is defined as a pair of non-empty neutrosophic subgraphs NH_1 and NH_2 such that $NH_1 \cup NH_2 = NG$, $NH_1 \cap NH_2 = NK_0$, and both NH_1 and NH_2 are neutrosophically open.

Theorem 3.1 Let (NG, τ) be a neutrosophic graph topological space. NG is neutrosophically connected if and only if it cannot be expressed as the union of two non-empty disjoint neutrosophic open subgraphs.

Proof: Suppose NG is neutrosophically connected. If NG could be expressed as the union of two non-empty disjoint neutrosophic open subgraphs NH_1 and NH_2 such that $NH_1 \cap NH_2 = NK_0$, this would constitute a separation of NG, contradicting the assumption of connectedness.

Conversely, assume NG cannot be expressed as the union of two non-empty disjoint neutrosophic open subgraphs. Then no neutrosophic separation exists, and hence NG must be neutrosophically connected.

Definition 3.2 A neutrosophic graph NG is said to be neutrosophically path-connected if for any two vertices $(r, \rho(r), \sigma(r), \omega(r))$ and $(s, \rho(s), \sigma(s), \omega(s))$ in NG, there exists a neutrosophic path from $(r, \rho(r), \sigma(r), \omega(r))$ to $(s, \rho(s), \sigma(s), \omega(s))$.

Theorem 3.2 In a neutrosophic graph topological space (NG, τ) , if NG is neutrosophically path-connected, then NG is neutrosophically connected,

Proof: Assume NG is neutrosophically path-connected. Then for any two vertices $(r, \rho(r), \sigma(r), \omega(r))$ and $(s, \rho(s), \sigma(s), \omega(s))$ in NG, there exists a neutrosophic path connecting them. Suppose, for contradiction, that NG is not neutrosophically connected. Then it can be written as the union of two disjoint neutrosophic open subgraphs NH_1 and NH_2 such that $NH_1 \cap NH_2 = NK_0$. Pick vertices $(r, \rho(r), \sigma(r), \omega(r)) \in NH_1$ and $(s, \rho(s), \sigma(s), \omega(s)) \in NH_2$. Since a neutrosophic path connects them, and NH_1 and NH_2 are disjoint, the path must cross from NH_1 to NH_2 , contradicting the definition of disjoint open subgraphs in a neutrosophic setting where the neutrosophic identity is preserved. Therefore, NG must be neutrosophically connected.

4. Neutrosophic Separation Axioms in NGTS

This section presents definition and theorems on separation in NGTS.

Definition 4.1: A neutrosophic graph topological space (NG, τ) is said to be a *neutrosophic* T_0 space if for any two distinct vertices $(r, \rho(r), \sigma(r), \omega(r))$ and $(s, \rho(s), \sigma(s), \omega(s))$ in NG, there exists a neutrosophic open subgraph NH such that either $(r, \rho(r), \sigma(r), \omega(r)) \in NH$ and $(s, \rho(s), \sigma(s), \omega(s)) \notin NH$, or $(s, \rho(s), \sigma(s), \omega(s)) \in NH$ and $(r, \rho(r), \sigma(r), \omega(r)) \notin NH$.

Definition 4.2: A neutrosophic graph topological space (NG, τ) is said to be a neutrosophic T_1 space if for any two distinct vertices $(r, \rho(r), \sigma(r), \omega(r))$ and $(s, \rho(s), \sigma(s), \omega(s))$, there exist neutrosophic open subgraphs NH_1 and NH_2 such that $(r, \rho(r), \sigma(r), \omega(r)) \in NH_1$ and $(s, \rho(s), \sigma(s), \omega(s)) \notin NH_1$, and $(s, \rho(s), \sigma(s), \omega(s)) \in NH_2$ and $(r, \rho(r), \sigma(r), \omega(r)) \notin NH_2$.

Definition 4.3: A neutrosophic graph topological space (NG, τ) is said to be a neutrosophic T_2 space if for any two distinct vertices $(r, \rho(r), \sigma(r), \omega(r))$ and $(s, \rho(s), \sigma(s), \omega(s))$, there exist neutrosophic open subgraphs NH_1 and NH_2 such that $(r, \rho(r), \sigma(r), \omega(r)) \in NH_1$, $(s, \rho(s), \sigma(s), \omega(s)) \in NH_2$, and $NH_1 \cap NH_2 = NK_0$.

Theorem 4.4: In a neutrosophic T_1 graph topological space, every singleton vertex set is neu-

trosophically closed.

Proof: Let $(r, \rho(r), \sigma(r), \omega(r)) \neq (s, \rho(s), \sigma(s), \omega(s))$. By the neutrosophic T_1 property, for each such vertex $(r, \rho(r), \sigma(r), \omega(r))$, there exists a neutrosophic open subgraph $NH_{(r,\rho(r),\sigma(r),\omega(r))}$, such that $(r, \rho(r), \sigma(r), \omega(r)) \in NH_{(r,\rho(r),\sigma(r),\omega(r))}$ and $(s, \rho(s), \sigma(s), \omega(s)) \notin NH_{(r,\rho(r),\sigma(r),\omega(r))}$.

Now consider the union of all such neutrosophic open subgraphs over all $(r, \rho(r), \sigma(r), \omega(r)) \neq$ $(s, \rho(s), \sigma(s), \omega(s))$, given by $NH = \bigcup_{(r,\rho(r),\sigma(r),\omega(r))\neq(s,\rho(s),\omega(s))} NH_{(r,\rho(r),\sigma(r),\omega(r))}$. This union includes all vertices except $(s,\rho(s),\sigma(s),\omega(s))$. Since the union of neutrosophic open subgraphs is neutrosophically open, NH is neutrosophically open. Therefore, the complement $NG\setminus\{(s,\rho(s),\sigma(s),\omega(s))\}$ is neutrosophically open, implying that the singleton $\{(s,\rho(s),\sigma(s),\omega(s))\}$ is neutrosophically closed.

Theorem 4.5: Every neutrosophic T_2 graph topological space is neutrosophic T_1 .

Proof: Let (NG, τ) be a neutrosophic T_2 graph topological space. For any two distinct vertices $(r, \rho(r), \sigma(r), \omega(r))$ and $(s, \rho(s), \sigma(s), \omega(s))$, by the T_2 property, there exist neutrosophic open subgraphs NH_1 and NH_2 such that $(r, \rho(r), \sigma(r), \omega(r)) \in NH_1$, $(s, \rho(s), \sigma(s), \omega(s)) \in NH_2$, and $NH_1 \cap NH_2 = NK_0$. It follows that $(s, \rho(s), \sigma(s), \omega(s)) \notin NH_1$ and $(r, \rho(r), \sigma(r), \omega(r)) \notin NH_2$. Hence, there exists a neutrosophic open subgraph containing one vertex but not the other, and vice versa, which satisfies the condition for neutrosophic T_1 . Therefore, every neutrosophic T_2 space is also neutrosophic T_1 .

5. Application of Neutrosophic Network Security Algorithms

A power grid operator needs to assess cybersecurity vulnerabilities in their SCADA systems. Using neutrosophic graph topology, the network is modeled with servers A through F, representing control centers, substations, and remote terminals. Each vertex represents a system and is assigned a neutrosophic value (T, I, F). Each edge represents a communication link between systems, associated with neutrosophic values that similarly reflect communication security.

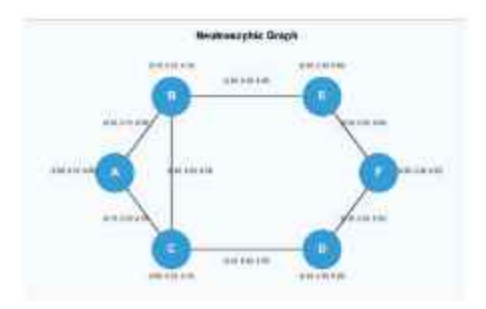


Figure 3: Neutrosophic SCADA Network Graph

The tasks are as follows: identify secure network zones using thresholds $T_{\min} = 0.60$, $I_{\max} = 0.30$, and $F_{\max} = 0.20$; determine all potential attack paths from the internet-facing edge node F to the critical main control server A; and identify the most vulnerable attack vector among these paths which requires immediate security hardening,

1. Secure Network Zones Identification Algorithm

Step 1: Define Security Thresholds

Thresholds are $T_{min} = 0.60$, $I_{max} = 0.30$, and $F_{max} = 0.20$.

Step 2: Create the Security Subgraph

Nodes meeting thresholds: Server A, Server B, Server C.

Connections meeting thresholds: $A \leftrightarrow B$, $A \leftrightarrow C$, $B \leftrightarrow C$.

Step 3: Identify Connected Components

The secure network subgraph is $\{A, B, C\}$ with edges A–B, A–C, B–C, forming a single connected secure zone.

Step 4: Calculate Zone Security Metrics

$$\text{Average } T = \frac{0.90 + 0.75 + 0.60}{3} = 0.75, \quad \text{Average } I = \frac{0.10 + 0.20 + 0.30}{3} = 0.20, \quad \text{Average } F = \frac{0.05 + 0.00}{3} = 0.20, \quad \text{Aver$$

Result: Secure zone $\{A, B, C\}$ identified with strong security metrics.

2. Attack Vector Analysis Algorithms

Step 1: Create Attack Susceptibility Graph

Security resistance weights are:

$$w_{AB} = (1 - 0.85) + 0.15 + 0.05 = 0.35,$$
 $w_{AC} = (1 - 0.70) + 0.25 + 0.10 = 0.65$
 $w_{BC} = (1 - 0.65) + 0.20 + 0.15 = 0.70,$ $w_{BE} = (1 - 0.55) + 0.30 + 0.25 = 1.00$
 $w_{CD} = (1 - 0.45) + 0.40 + 0.30 = 1.25,$ $w_{DF} = (1 - 0.35) + 0.45 + 0.55 = 1.65$
 $w_{EF} = (1 - 0.30) + 0.50 + 0.60 = 1.80$

Step 2: Identify High-Risk Nodes and Critical Assets

High-risk node: Server F (F = 0.65), Critical asset: Server A (T = 0.90, F = 0.05).

Step 3: Find Potential Attack Paths from F to A

Path 1:
$$F \rightarrow D \rightarrow C \rightarrow A \Rightarrow 1.65 + 1.25 + 0.65 = 3.55$$

Path 2: $F \rightarrow E \rightarrow B \rightarrow A \Rightarrow 1.80 + 1.00 + 0.35 = 3.15$

Step 4: Rank Attack Vectors

The most vulnerable attack vector is $F \to E \to B \to A$ with total attack weight 3.15. This path requires immediate priority in security hardening efforts.

6. Conclusion and Future Work

This paper extends graph topology to neutrosophic graph topological spaces, introducing fundamental definitions and establishing key properties related to neutrosophic connectedness and separation axioms. By incorporating neutrosophic components, these structures effectively handle uncertainty and indeterminacy, making them ideal for real-world applications with incomplete or contradictory information. Future research directions include developing algorithms for computing neutrosophic topological properties, exploring applications in computer networks and pattern recognition, investigating relationships with other neutrosophic structures, extending the concept to directed neutrosophic graphs and hypergraphs, and studying fixed point theorems in these spaces.

References

- Aniyan, A., & Naduvath, S. (2023). A study on graph topology. Communications in Combinatorics and Optimization, 8(2), 397

 –409. DOI: 10.22049/CCO.2022,27399.1253
- [2] Biswas, P., Pramanik, S., & Giri, B. C. (2014). Cosine similarity measure based multiattribute decision-making with trapezoidal fuzzy neutrosophic numbers. *Neutrosophic Sets* and Systems, 8, 46–56.
- [3] Bondy, J. A., & Murty, U. S. R. (2008). Graph Theory. Springer.
- [4] Broumi, S., & Smarandache, F. (2014). Single valued neutrosophic graphs. *Journal of New Theory*, (10), 86–101.
- [5] Diestel, R. (2017). Graph Theory (5th ed.). Springer.
- [6] Langner, R. (2011). Stuxnet: Dissecting a cyberwarfare weapon. IEEE Security & Privacy, 9(3), 49–51.
- [7] Munkres, J. R. (2000). Topology (2nd ed.). Prentice Hall.
- [8] Newman, M. E. J. (2018). Networks: An Introduction (2nd ed.). Oxford University Press.

- [9] Smarandache, F. (1999). A Unifying Field in Logics: Neutrosophic Logic, Neutrosophy, Neutrosophic Set, Neutrosophic Probability. American Research Press.
- [10] Stouffer, K., Falco, J., & Scarfone, K. (2011). Guide to industrial control systems (ICS) security. NIST Special Publication 800-82.
- [11] Wang, H., Smarandache, F., Zhang, Y., & Sunderraman, R. (2010). Single valued neutrosophic sets. Multispace and Multistructure, 4, 410–413.
- [12] West, D. B. (2001). Introduction to Graph Theory (2nd ed.). Prentice Hall.
- [13] Ye, J. (2013). Multicriteria decision-making method using the correlation coefficient under single-valued neutrosophic environment. *International Journal of General Systems*, 42(4), 386–394.
- [14] Ye, J. (2014). A multicriteria decision-making method using aggregation operators for simplified neutrosophic sets. *Journal of Intelligent & Fuzzy Systems*, 26(5), 2459–2466.
- [15] Zhu, B., Joseph, A., & Sastry, S. (2011). A taxonomy of cyber attacks on SCADA systems. Proceedings of the 2011 International Conference on Internet of Things and 4th International Conference on Cyber, Physical and Social Computing, 380–388.

Email: wishesmona@gmail.com

Email: durga.sitha@gmail.com

Department of Mathematics, Sri Krishna Adhithya College of (Received, May 23, 2025), Arts and Science, Coimbatore, India - 641042 (Revised, July 10, 2025)

Swaroopa Rani N C', RESTRAINED PENDANT DOMINATION IN GRAPHS

ISSN: 0970-5120

Abstract: In this article we initiate the study of a variation of standard domination, namely restrained pendant domination. Let G = (V, E) be any graph. A dominating set S in G is called a pendant dominating set if S > 0 contains at least one pendant node. The minimum cardinality of the pendant dominating set in S is called the pendant domination number of S, denoted by $\gamma_{pe}(S)$. A restrained pendant dominating set is a set $S \subseteq V$ where every node in V = S is adjacent to a node in S as well as another node in S = 0. The restrained pendant domination number of S, denoted by S is the minimum cardinality of a restrained pendant dominating set of S. We determine best possible upper and lower bounds for S in S and also calculated the exact value for some standard families graphs.

Mathematical Subject Classification (2010) No: 05C50, 05C69.

Keywords and Phrases: Dominating Set, Restrained Dominating Set, Pendant Dominating Set, Restrained Pendant Dominating Set, Pendant Domination Number

1 Introduction

A possible application for minimal restrained dominating sets is any situation in which one group needs to supervise a subordinate group using the minimal number of supervisors possible, but at the same time ensure the supervisors are held accountable by never allowing a supervisor to be alone with subordinate. Hattingh gives an example of this relationship in terms of guards and prisoners. The nodes in S are the guards, while the nodes in V - S are the prisoners. In this way, a guard can supervise every prisoner, but every prisoner is also in view of another prisoner [5]. In application way of restrained pendant dominating set we assign a back up to at least one prisoner. A possible application for independent restrained dominating sets is the location of product distribution centers or hospitals where a certain level of redundancy is desired. In this case, nodes could represent cities. Vertices in S represent cities with a distribution center and edges represent transportation routes between cities. Selecting the cities in which to place distribution centers using an independent restrained dominating set guarantees that every city without a distribution center is at least next to a city with one. It also guarantees that every city without a distribution center has a neighbor that also lacks a distribution center. In case of shortages at one distribution center, every city has access to a different center by going through one of its neighbors. The helm H_n is the graph obtained from wheel W_n by attaching a pendant edge to each rim node. The closed helm CH_n is the graph obtained from helm H_n by joining each pendant node to form a cycle. The web graph W(t,n) is the graph obtained by joining the pendant nodes of a helm to form a cycle and then adding a single pendant edge to each node of this outer cycle. W(t, n) is the generalized web with t cycles each of order n. A firrecracker graph $F_{n,k}$ is formed by

concatenation of n k —stars by linking one pendant node of a star to pendant node of next star. $F_{n,k}$ is isomorphic to centepede graph k=2

A dominating set S in G is called a pendant dominating set if < S > contains at least one pendant node. The minimum cardinality of the pendant dominating set in G is called the pendant domination number of G, denoted by $\gamma_{pe}(G)$. A restrained pendant dominating set is a set $S \subseteq V$ where every node in V - S is adjacent to a node in S as well as another node in V - S. The restrained pendant domination number of G, denoted by γ_{rpe} is the minimum cardinality of a restrained pendant dominating set of G. For more details about pendant domination parameter refer [6,7,8]

For an example in Figure 1, $S = \{a, b\}$ is a minimum pendant dominating set and the set S is itself a restrained pendant dominating set. Hence $\gamma_{rp\sigma}(G) = 2$.



Figure 1: Cycle Graph

Proposition 1.1. [6] Let G be a cycle or a path with n vertices. Then

$$\gamma_{pe}(G) = \begin{cases} \frac{n}{3} + 1, & if \ n \equiv 0 \pmod{3}; \\ \left[\frac{n}{3}\right], & if \ n \equiv 1 \pmod{3}; \\ \left[\frac{n}{3}\right] + 1, & if \ n \equiv 2 \pmod{3}; \end{cases}$$

Proposition 1.2. For the wheel W_n for $n \ge 3$ $\gamma_r(W_n) = 1$.

Proposition 1.3. If $n \ge 3$ is a positive integer, then $\gamma_{rpe}(K_n) = 2$.

Proposition 1.4. If $n \ge 3$, then $\gamma_{rpe}(K_{1.n}) = n$.

Proposition 1.5. If m and n are integers such that $m, n \ge 2$ then $\gamma_{rpe}(K_{m,n}) = 2$.

Theorem 1.1. Let P_n be a path on n nodes for n > 4 and $k \ge 1$ be an integer. Then

$$\gamma_{rpe}(P_n) = \begin{cases} k+3, & \text{if } n=7. \\ k+2, & \text{if } n=3k, n=3k+1 \text{ or } 3k+2. \end{cases}$$

Proof. Let $V(P_n) = \{v_1, v_2, ..., v_n\}$ be a set of nodes of the path graph. Note that the set $S = \{v_1, v_2, v_5, v_6, v_7\}$ will be the restrained pendant dominating set of path graph P_7 . Therefore, $\gamma_{rpe}(P_7) = k + 3$.

Suppose n = 3k. Note that $S = \{v_1, v_{3i-1}: 0 \le i \le k-1\} \cup \{v_{3k}\}$ is a minimum restrained pendant dominating set with k+2 elements. Thus $\gamma_{rpe}(P_n) \le k+2$. Let S be any minimum restrained pendant dominating set of P_n . Then S must be a pendant dominating set. Note that each node in S can dominate a maximum of S nodes. Thus to dominate S nodes, S must have S nodes. Hence to dominate the

remaining one node of P_n , S must have one more node and so $|S| \ge k + 2$. Therefore $\gamma_{rpe}(P_n) = k + 2$.

Theorem 1.2. Let C_n be a cycle with $n \ge 4$ nodes. Then

$$\gamma_{rpe}(C_n) = \begin{cases} \frac{n}{3} + 2, & if \ n \equiv 0 (mod 3); \\ n - \left\lceil \frac{n}{3} \right\rceil, & if \ n \equiv 1 (mod 3); \\ n - \left\lceil \frac{n}{3} \right\rceil, & if \ n \equiv 2 (mod 3); \end{cases}$$

Illustration: The helm graph H₄ is shown in figure below where the set of solid nodes is its restrained pendant dominating set of minimum cardinality

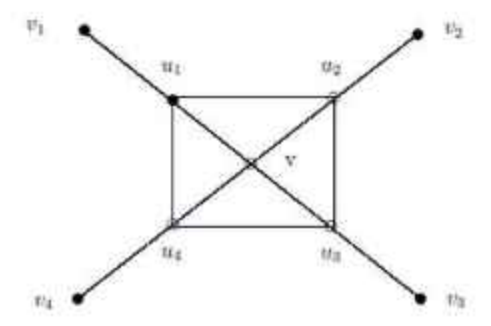


Figure 2. Helm Graph H₄

Theorem 1.3. Let $G \cong H_n$ be a helm graph with $n \ge 3$, then $\gamma_{rpe}(G) = n + 1$

Proof. Let $\{v_1, v_2, v_3, ..., v_n\}$ be the nodes of degree one, $\{u_1, u_2, ..., u_n\}$ be the rim nodes and v be the apex node of maximum degree n of helm graph G with $|V(H_n)| = 2n + 1$. The pendant $v_1, v_2, ..., v_n$ are mutually non-adjacent which must be in every restrained pendant dominating set. Further the pendant nodes $v_1, v_2, ..., v_n$ of H_n are dominate the rim nodes $u_1, u_2, ..., u_n$ of H_n . A restrained pendant dominating set S should contain pendant nodes $v_1, v_2, ..., v_n$ and the rim node u_1 of H_n . If $u_0 \in S$ the induced subgraph of H_n does not contain the pendant node. Therefore, $u_1 \in S$ which implies that |S| = n + 1. Note that $S = \{v_1, v_2, ..., v_n, u_1\}$ is a restrained pendant dominating set with minimum cardinality because removal of any one of the nodes from set S will not dominate all the nodes of H_n . Moreover each node V - S is adjacent to node in S and to a node in V - S. Hence $\gamma_{rpe}(H_n) = n + 1$.

Theorem 1.4. For the closed helm graph CH_n , for $n \ge 3$

$$\gamma_{rpe}(CH_n) = \begin{cases} 3, & \text{if } n = 4 \\ \left[\frac{n}{3}\right] + 1, & \text{if } n = 3k + 1 \text{ or } 3k + 2 \end{cases}$$

Illustration: The closed helm graph with CH9 as shown below

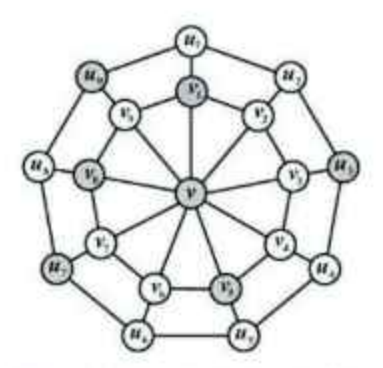


Figure 3. Closed Helm Graph CH₉

Proof. The closed helm CH_5 contains whell graph W_n and outer cycle C_n . Let v indicate the apex of wheel. Also u_1, u_2, \ldots, u_n are the rim nodes of wheel W_n of CH_n and v_1, v_2, \ldots, v_n be the corresponding adjacent nodes of outer cycle of CH_n . So $|V(CH_n)| = 2n + 1$. For n = 4, $\Delta(CH_4) = 4$ and $|V(CH_4)| = 9$. It follows that minimum three nodes are required to dominate all the nodes of CH_4 . If $S \subseteq V(CH_4)$ is restrained pendant dominating set and induced subgraph of S contains a pendant node, then |S| = 3, which is minimum. Therefore $\gamma_{rpe}(CH_4) = 3$.

For $n \ge 4$, $\Delta(CH_4) = n$ and $|V(CH_4)| = n$ and by proposition 1.1. apex node dominates all the nodes of W_n . If $S \subseteq V(CH_n)$ is a restrained pendant dominating set then the set must contain a apex node v. Due to pendant node in induced subgraph of S and adjacency nature of nodes v_1, v_2, \ldots, v_n of outer cycle with corresponding nodes u_1, u_2, \ldots, u_n of W_n . By proposition 1.2. at least nodes are required to dominate all the remaining nodes of outer cycle of CH_n . It follows that $|S| = \left \lceil \frac{n}{3} \right \rceil + 1$.

If possible suppose S' is a restrained pendant dominating set such that $|S'| > |S'| = \left\lceil \frac{n}{3} \right\rceil < |S|$. Now $\Delta(CH_n) = n$ and in order to attain the least cardinality, S' can not contain the nodes where each node among them can dominate distinct n nodes of CH_n . Therefore S' can not be a restrained pendant dominating set of CH_n . This implies that S is a restrained pendant dominating set with minimum cardinality for CH_n . Hence $\gamma_{rpe}(CH_n) = |S| = \left\lceil \frac{n}{3} \right\rceil + 1$.

Theorem 1.5. If G is the Firecracker graph $F_{n,k}$, then

$$\gamma_{rpe}(G) = \begin{cases} n+1, & \text{if } k=2\\ n(k-1), & \text{if } n, k>2 \end{cases}$$

Proof. We prove the theorem by following two cases

Case 1. K=2. The firecracker graph is isomorphic to centepede graph, which has n pendant nodes. The set $S=\{v_1,v_2,\ldots,v_n\}$ forms a minimum dominating set and hence $\gamma(G)=n$. Clearly $\gamma_{rpe}(G)\geq n$. But the subgraph induced by S doesn't contains pendant node. Therefore the restrained pendant dominating set of G is

obtained by taking the neighbor of the node v_1 or v_n along with the dominating set. Hence $\gamma_{rpe}(G) = |S| + N(v_1)$ or $N(v_n) = n + 1$.

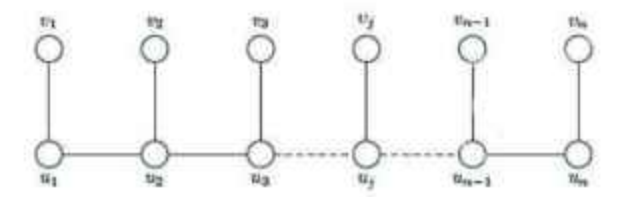


Figure 4. Centepede Graph

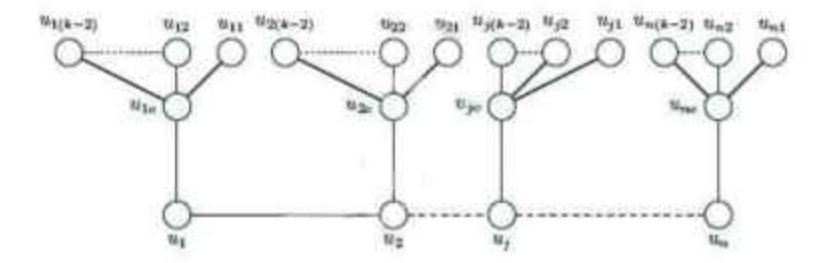


Figure 5. Firecracker Graph

Case 2. K > 2

The total number of pendant nodes of G is n(k-2). Then $\gamma_{rpe}(G) \ge n(k-2)$. Let $A = \{u_1, u_2, \dots, u_{i(k-2)} \mid 1 \le i \le n\}$ be the set of pendant nodes of the graph G and $B = \{u_{1c}, u_{2c}, \dots, u_{nc}\}$ be the central nodes of the star. Clearly the set B is a dominating set with minimum cardinality but not a pendant dominating set. Define $C = A \cup B$, forms a minimum pendant dominating set and hence $\gamma_{pe}(G) = n(k-2) + n$. Therefore $\gamma_{rpe}(G) \ge n(k-1)$. But the subgraph induced by C contains a pendant node and every node in C is adjacent to a node in C as well as another node in C. Hence, C is restrained pendant dominating set also. Therefore $\gamma_{rpe}(G) = n(k-1)$.

Theorem 1.6. Let G be a sunflower graph Sf_n $(n \ge 3)$, then $\gamma_{rpe}(Sf_n) = n + 1$

Proof. Let the node v be the apex node of the Sf_n and v_2, v_4, \ldots, v_{2i} for $i = 1, 2, 3, \ldots, n$ be the nodes of degree one in sunflower graph Sf_n with $|Sf_n| = 3n + 1$. The apex node v of sunflower graph dominates 2n distinct nodes and nodes of degree one are mutually adjacent. Its is easy to see that any restrained pendant dominating set contain the apex node and pendant nodes and induced subgraph of S contains a pendant node. Therefore |S| = n + 1, which is the least cardinality. Hence $\gamma_{ref}(Sf_n) = n + 1$.

Illustration: The sunflower Sf_4 is shown in the below figure where the set of solid nodes $\{v, v_2, v_4, v_6, v_8\}$ is its restrained pendant dominating set with least cardinality.

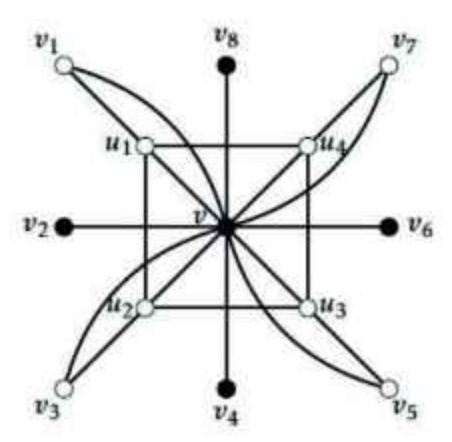


Figure 6. Sunflower Graph Sf4

Proposition 1.6. Let G be a connected graph of order n. Then $\gamma_{rpe}(G) = n$ if and only if G is a star.

Proof. If G is a connected graph of order n and G is not a star then $y_{rpe} \le n-2$. Recall that a leaf in a graph is a node of degree one, while a stem is a node adjacent to a leaf. The next two results will show for which graphs this upper bound is attained.

Theorem 1.7. If T is a tree of order $n \ge 4$ then $\gamma_{rpe}(T) = n - 2$ if and only if T is obtained from $P_5 P_6$ or P_7 by adding zero or more leaves to the stems of the path.

Proof. It is easy to verify that if T is obtained from P_5 or P_6 , then $\gamma_{rpe}(G) = n - 2$. If $diam(T) \ge 8$, the T contains an induced path P_8 , say $v_1, v_2, ..., v_8$. But then $V(T) - \{v_3, v_4, v_5\}$ is a restrained pendant dominating set of size n - 3, which is a contradiction. Thus $diam(T) \le 7$. Furthermore T is not a star and star are the only trees having diameter 2. Consider the following cases.

Case 1. diam(T) = 4. Then T has an induced P_5 , say $\{v_1, v_2, v_3, v_4, v_5\}$. The set $S = \{v_2, v_5\}$ is dominating set of path graph P_5 but the set S is not a restrained pendant dominating set because the neighbor of the node v_2 cannot have any other neighbor in V - S and the induced subgraph of S doesn't contain the pendant node. Therefore the restrained pendant dominating set is obtained by taking the leaf of the node v_2 . Hence $\gamma_{rpe}(P_5) = n - 2$.

Case 2. diam(T) = 5. Then T has an induced P_6 , say $\{v_1, v_2, v_3, v_4, v_5, v_6\}$. Certainly the nodes v_2 and v_5 can have leaves attached to them. The set $S = \{v_2, v_5\}$ is a dominating set of P_6 but the induced subgraph of S doesn't contain any pendant node and the neighbors of the nodes v_2 and v_5 are not adjacent in any one node in

V-S. Therefore the restrained pendant dominating set is obtained taking the leaves attached to nodes v_2 and v_5 . Hence, $\gamma_{rpe}(T) = n-2$

Case 3. diam(T) = 6. Then T has an induced P_7 , say $\{v_1, v_2, v_3, v_4, v_5, v_6, v_7\}$. If the set $S = \{v_1, v_2, v_3, v_6, v_7\}$ is a restrained pendant dominating set with size n - 2. if we remove any one leaves attached to the nodes v_2 and v_6 the nodes v_1 and v_7 doesn't have any neighbors not on the path. Therefore the set S is the minimum restrained pendant dominating set with minimum cardinality. Hence $\gamma_{rpg}(T) = n - 2$

Theorem 1. 8. For any graph G, we have $\gamma_r(G) \leq \gamma_{rpe}(G)$ and $\gamma_{pe}(G) \leq \gamma_{rpe}(G)$.

Proof. Since every restrained pendant dominating set of G is also a restrained dominating set of G, we have $\gamma_r(G) \leq \gamma_{rpe}(G)$. Since every restrained pendant dominating set of G is also a pendant dominating set of G, we have $\gamma_{pe}(G) \leq \gamma_{rpe}(G)$.

Theorem 1.9. The pendant nodes of a graph G belongs to the restrained pendant dominating set

Proof. Let G be a connected graph and S be the restrained pendant dominating set. By the definition of restrained pendant dominating set if each node not in S, then it should be adjacent to a node in S and to a node in V - S. But each pendant nodes doesn't belong to the set S, then the nodes are in V - S and that nodes doesn't having any neighbor in V - S. Therefore the pendant nodes belong to restrained pendant dominating set S.

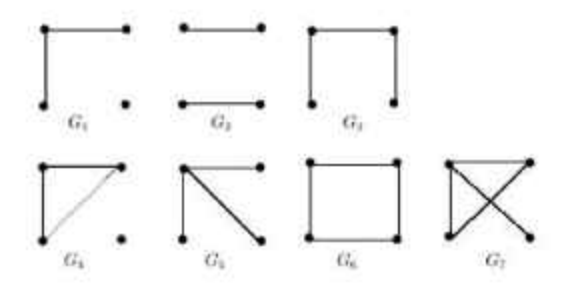
Theorem 1.10. Let G connected graph of order n. Then $\gamma_{rpe}(G) + \Delta(G) \leq 2n - 1$

Proof. For any connected graph G, $\Delta(G) \leq n-1$. The upper bound of $\gamma_{rpe}(G)$ is found to be n. Therefore $\gamma_{rpe} + \Delta(G) \leq n-1+n = 2n-1$.

Theorem 1.11. Let G be a connected graph order $n \ge 3$ with no leaves. Then $\gamma_{rpe}(G) = 2$ if and only if there exists a nodes of degree n - 1.

Proof. Assume that $\gamma_{rpe}(G) = 2$. Let $\{v_1, v_2\}$ be the restrained pendant dominating set of G. Then the node v_1 , $(or \ v_2)$ dominates all the other nodes implies that degree of $\{v_1\}$, $(or \ v_2)$ is maximum. Clearly the maximum degree of a graph G is n-1. Thus there exit a node of degree n-1.

Conversely, assume that there exit a nodes of degree n-1. Let u_1 or (u_2) be the nodes which id of degree n-1. Suppose that the set $S = \{u_1, u_2, u_3\}$ is the restrained pendant dominating set, where u_3 is any node of G. Now $deg(u_3) = n-1$ implies u_3 dominates V(G) but the induced subgraph of S doesn't contain the node of degree one. Therefore the set S doesn't satisfying the condition of restrained pendant dominating set. Hence the set $S' = \{u_1, u_2\}$ is a minimum restrained pendant dominating set. This implies $\gamma_{rpe}(G) = |S'| = 2$.



Theorem 1.12. Let G belongs to any one of the graphs $G_1, G_2, ..., G_7$ of order n = 4. Then $\gamma_{rpe}(G) + \gamma_{rpe}(\bar{G}) = 5$ or G, and $\gamma_{rpe}(G), \gamma_{rpe}(\bar{G}) = 6$ or G

Proof. (i)
$$\gamma_{rpe}(G_1) = 3$$
. Then $\gamma_{rpe}(\bar{G}_1) = 2$
we get $\gamma_{rpe}(G_1) + \gamma_{rpe}(\bar{G}_1) = 5$ and $\gamma_{rpe}(G_1) \cdot \gamma_{rpe}(\bar{G}_1) = 6$
(ii) $\gamma_{rpe}(G_2) = 3$. Then $\gamma_{rpe}(\bar{G}_2) = 2$.
we get $\gamma_{rpe}(G_2) + \gamma_{rpe}(\bar{G}_2) = 5$ and $\gamma_{rpe}(G_2) \cdot \gamma_{rpe}(\bar{G}_2) = 6$.
(iii) $\gamma_{rpe}(G_3) = 3$. Then $\gamma_{rpe}(\bar{G}_3) = 3$.
we get $\gamma_{rpe}(G_3) + \gamma_{rpe}(\bar{G}_3) = 6$ and $\gamma_{rpe}(G_3) \cdot \gamma_{rpe}(\bar{G}_3) = 9$.
(iv) $\gamma_{rpe}(G_4) = 3$. Then $\gamma_{rpe}(\bar{G}_4) = 3$.
we get $\gamma_{rpe}(G_4) + \gamma_{rpe}(\bar{G}_4) = 6$ and $\gamma_{rpe}(G_4) \cdot \gamma_{rpe}(\bar{G}_4) = 9$.
(v) $\gamma_{rpe}(G_5) = 3$. Then $\gamma_{rpe}(\bar{G}_5) = 3$.
we get $\gamma_{rpe}(G_5) + \gamma_{rpe}(\bar{G}_5) = 6$ and $\gamma_{rpe}(G_5) \cdot \gamma_{rpe}(\bar{G}_5) = 9$.
(vi) $\gamma_{rpe}(G_6) = 2$. Then $\gamma_{rpe}(\bar{G}_6) = 3$.
we get $\gamma_{rpe}(G_6) + \gamma_{rpe}(\bar{G}_6) = 5$ and $\gamma_{rpe}(G_6) \cdot \gamma_{rpe}(\bar{G}_6) = 6$.
(vii) $\gamma_{rpe}(G_7) = 3$. Then $\gamma_{rpe}(\bar{G}_7) = 3$.
we get $\gamma_{rpe}(G_7) + \gamma_{rpe}(\bar{G}_7) = 6$ and $\gamma_{rpe}(G_7) \cdot \gamma_{rpe}(\bar{G}_7) = 9$.

Refrences

- J.A.Bondy, U.S.R Murty, Graph theory with application, Elsevier science Publishing Co, Sixth printing, 1984.
- T.W. Haynes, S.T. Hedetniemi and P.J. Slater, Domination in Graphs: Advanced Topics Marcel Dekker, New York, 1998.
- T.W.Haynes, S.T.Hedetniemi, P.J.Slater, Fundamentals of Domination in Graphs, Marcel Dekker, New york, 1998.

- S.T. Hedetniemi and R.C. Laskar, Topics on Domination, Discrete Math. 86 1990.
- Johannes H.Hattingh Some Recent Resultson Restrained Domination. The 23rd Mini conference on Discrete Mathematics and Algorithms, Georgia State University, Atlanta, GA, USA, 2008.
- Nayaka S.R, Puttaswamy and Purushothama S, Pendant Domination in Graphs. The Journal of Combinatorial Mathematics and Combinatorial computing. pp. 219-230 (2020).
- Nayaka S.R, Puttaswamy and Purushothama S, Pendant Domination in Some Generalized Graphs, International Journal of Scientific Engineering and Science, Volume 1, Issue 7, (2017), pp. 13-15.
- Purushothama S, Puttaswamy and Nayaka S.R. Pendant Domination in Double Graphs. Proceedings of the Jangieon Mathematical Society Volume 23(2), 2020.

Department of Mathematics, Government College(Autonomous), Mandya University, Mandya-571401 email: swanil.14dhi@gmail.com (Received, January 29, 2025)

²Department of Mathematics, P.E.S. College of Engineering, Mandya-571401 e-mail: drbskshan@yahoo.com Christopher M', Ramachandran V^2 MODULO TWO SQUARE MEAN LABELING OF HURDLE GRAPHS, COMB GRAPHS AND $F(P_n)$ GRAPHS AND ITS ALGORITHMS

ISSN: 0970-5120

Abstract: A graph is said to be modulo two square mean labeling, if there is a function \emptyset from the vertex set of G to $\{1,2,...n\}$ to the edge set of G to $\{1\}$ where $\emptyset'(uv) = \left\lceil \frac{f(u)^2 + f(v)^2}{2} \right\rceil \mod 2$. A graph that admits modulo two square mean labeling is called modulo two square mean graphs. In this paper we provethat hurdle graphs, comb graphs and $F(P_n)$ graphs are modulo two square mean labeling and its algorithms.

Key words: MeanLabeling, Root Mean Square Labeling, Hurdle graph, comb graph.
Mathematics Subject Classification 2020: 05C78and 05C85.

1 Introduction

Let G(V, E) be a graph with p vertices and q edges. A graph labeling is an assignment of integers to the vertices or edges, or both, subject to certain conditions. Most graph labeling methods trace their origin to one introduced by Rosa [7] in 1967, or one given by Graham and Sloane [2] in 1980. Rosa [7] called a function f a g-valuation of a graph G with g edges if g is an injection from the vertices of G to the set g and g such that, when each edge g is assigned the label g and g in g are distinct. Various labeling methods have been introduced by Acharya, Arumugam and Rosa [1].

The concept of mean labeling has been introduced by S.Somasundaram and R.Ponraj[5] in 2004. A graph G with p vertices and q edges is called a mean graph if there is an injective function f from the vertices of G to $\{0, 1, 2, ..., q\}$ such that when each edge uv is labeled with (f(u) + f(v))/2 if f(u) + f(v) is even, and (f(u) + f(v) + 1)/2 if f(u) + f(v) is odd, then the resulting edge labels are distinct.

V.Ramachandran and C.Sekar [6] introduced the concept of one modulo N graceful where N is any positive integer. In the case of N = 2, the labeling is odd graceful and In the case of N = 2the labeling is graceful. Motivated by 0- Edge Magic Labeling [4] and 1- Edge Magic Labeling [3] we introduce modulo two square mean labeling of hurdle graphs, comb graphs and $F(P_n)$ graphs and its algorithms.

Definition1.1: A walk in which $u_1, u_2 \dots u_n$ are distinct is called a path. A path on n vertices is denoted by P_n

Definition 1.2: The graph obtained by joining a single pendent edge to each vertex of a path is called as Comb.

Definition 1.3: A graph G = (V, E) with p vertices and q edges is said to be a Root Square Mean graph if it is possible to label the vertices $x \in V$ with distinct elements f(x) from 1, 2, ..., q +

1 in such away that when each edge
$$e = uv$$
 is labeled with $f(e = uv) = \left[\sqrt{\frac{f(u)^2 + f(v)^2}{2}}\right]$ or

$$\sqrt{\frac{f(u)^2+f(v)^2}{2}}$$
, then the resulting edge labels are distinct. In this case f is called a Root Square

Mean labeling of G.

Definition 1.4 A graph obtained from a path P_n by attaching a pendant edge to every internal vertex of the path is called Hurdle graph. It is denoted by Hd_n and has n-2 hurdles.

Definition 1.5A Y- tree is a graph obtained from a path by appending an edge to a vertex of a path adjacent to an end point and is denoted by Y_n , where n is the number of vertices in the tree.

Definitions 1.6 A F-tree $F(P_n)$ is a graph obtained from a path on $n \ge 3$ vertices by appending two pendent edges one to an initial vertex and other vertex is adjacent to adjacent to initial vertex.

2 Main Results

Theorem 2.1 The Hurdle Graph Hd_n is a modulo two square mean labeling.

Proof:

Let $G = Hd_n$ be a graph with n vertices and n-1 edges.

Now We Define The Vertices Of G is as follow as $u_1, u_2, u_3, ...$ be the vertices of path P_n , and let $v_1, v_2, v_3, ...$ be the vertices of pendant edges attached to the path P_n .

Let
$$V(G) = \{u_k : 1 \le k \le n\} \cup \{v_k : 1 \le k \le n - 2\}$$
 and

$$E(G) = \{u_k u_{k+1} \colon 1 \le k \le n-1\} \cup \{v_k \ u_{k+1} \colon 1 \le k \le n-2\} \,.$$

Then G has 2n - 2 vertices and 2n - 3 edges.

Define
$$f:V(G) \rightarrow \{1,2,3,...,2n-2\}$$
 as follows

$$f(u_k) = 2k - 1$$
, $1 \le k \le n - 1$.

$$f(u_n) = 2n - 2$$

$$f(v_k) = 2k$$
, $1 \le k \le n-2$.

Now we define edge function as follows.

$$f(u_k u_{k+1}) = \left[\frac{f(u_k)^2 + f(u_{k+1})^2}{2} \right] \mod 2, 1 \le k \le n-1.$$

$$f(v_k u_{k+1}) = \left[\frac{f(v_k)^2 + f(u_{k+1})^2}{2} \right] \mod 2, 1 \le k \le n-2.$$

Thus, the graph G has a modulo two square mean labeling.

Example 2.2 modulo two square mean labeling of Hurdle Graph Hd5 is shown in Fig 2.1

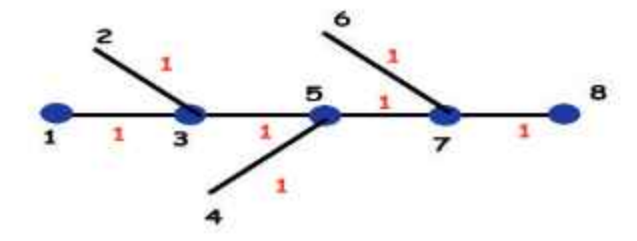


Figure 2.1

2.3. Algorithm Description

Problem Statement:

Development of a C++ algorithm for hurdle graphs using modulo-2 square mean labeling

Input:

· The Number of Vertices

Output:

- The Labeling of Vertices of path are u(1), u(2),..... and Labeling of Vertices of pendant edges are v(1), v(2),.....
- The Labeling of edgese(1), e(2)...... and its Modulo of edges of e(1)=1, e(2)=1.....

Development Process

The C++ algorithm for Hurdle graphs employs modulo-2 square mean labeling

Code Implementation:

#include <iostream> #include <cmath> int main()

```
Christopher M and Ramachandran V
```

```
371
   int n,i;
   int v[100],u[100];
   int e1[100],e2[100],e3[100],e4[100];
   std::cout<< "Enter the Number of Vertices = ";
   std::cin>>n:
   for (i=1;i<=n-1;i++)
   u[i]=2*1-1;
   std::cout<< " \n The Number of Vertices of u ("<<i<<") ="<<u[i];
   u[n]=2*n-2;
   std::cout<< "\n The Number of Vertices of u ("<<n<<") ="<<u[n];
   std::cout<< "\n";
   for (i=1;i<=n-2;i++)
   v[i]=2*i;
   std::cout<<" \n The Number of Vertices of v ("<<i<") ="<<v[i];
   std::cout<< "\n";
   for (i=1; i<=n-2; i++)
   e1[i]=(u[i]*u[i])+(u[(i+1)]*u[(i+1)]);
   e2[i]= ceil( float (e1[i])/2);
   std::cout<<"\n Edges of e ("<<i<<") ="<<e2[i] <<"\t";
   std::cout<<"\t Edges of e ("<<i<") ="<<e2[i] %2<<"\t";
   e1[n-1]=(u[n]*u[n])+(u[(n-1)]*u[(n-1)]);
   e2[n-1]= ceil( float (e1[n-1])/2);
   std::cout<<"\n Edges of e ("<<i<<") ="<<e2[n-1] <<"\t";
   std::cout<<"\t Edges of e ("<<i<<") ="<<e2[n-1] %2<<"\t";
   for (i=1; i<=n-2; i++)
   e3[i]=(v[i]*v[i])+(u[(i+1)]*u[(i+1)]);
   e4[i]= ceil( float (e3[i])/2);
   std::cout<<"\n Edges of e("<<i+n-1<<")="<<e4[i] <<"\t";
   std::cout<<"\t Edges of e("<<i+n-1<<")="<<e4[i] %2<<"\t";
   return 0;
```

Output: The Output of Hurdle Graph Hdshas a modulo two square mean labeling.

```
Output
                                                                  Clear
Enter the Number of Vertices = 5
The Number of Vertices of u (1) =1
The Number of Vertices of u (2) =3
The Number of Vertices of u (3) -5
The Number of Vertices of u (4) =7
The Number of Vertices of u (5) +8
The Number of Vertices of v (1) =2
The Number of Vertices of v (2) -4
The Number of Vertices of v (3) =6
Edges of e (1) +5 Edges of e (1) +1 Edges of e (2) +17 Edges of e (2) +1
Edges of e(5)-1
Edges of e(5)=7
Edges of e(6)≈21
                      Edges of e(6)=1
Edges of e(7)=43
                        Edges of e(7)=1
--- Code Execution Successful ---
```

Explanation:

The algorithm begins by initializing two sets of vertices: one representing the path and the other corresponding to the pendant edges, which together form the labeling structure of the hurdle graph. The output includes the labeled edges of the hurdle graph and its modulo result are equal to 1. This labeling approach ensures greater efficiency and consistency compared to traditional methods.

Theorem 2.4 The comb Graph $(P_n \odot K_1)$ is a modulo two square mean labeling.

Proof:

Let $G = P_n \odot K_1$ be a graph with n vertices and n edges.

Now We Define the Vertices of V(G) is as follow as

 u_1, u_2, u_3, \dots as the vertices of path P_n , and let v_1, v_2, v_3, \dots be the vertices of K_1 attached to the path P_n .

Let
$$V(G) = \{u_k: 1 \le k \le n\} \cup \{v_k: 1 \le k \le n\}$$
 and

$$E(G) = \{u_k u_{k+1} : 1 \le k \le n-1\} \cup \{v_k u_{k+1} : 1 \le k \le n-1\}.$$

Then G has 2n vertices and 2n-1 edges.

Define $f: V(G) \rightarrow \{1,2,3,...,2n\}$ as follows

$$f(u_k) = 2k - 1, \quad 1 \le k \le n.$$

$$f(v_k) = 2k$$
, $1 \le k \le n$.

Now we define edge function as follows.

$$f(u_k u_{k+1}) = \left\lceil \frac{f(u_k)^2 + f(u_{k+1})^2}{2} \right\rceil \mod 2, 1 \le k \le n-1.$$

$$f(v_k u_k) = \left[\frac{f(v_k)^2 + f(u_k)^2}{2}\right] \mod 2, 1 \le k \le n$$

Hence, the comb Graph $(P_n \odot K_1)$ admits modulotwo square mean labeling.

Example 2.5 modulo two square mean labeling of comb Graph (P₅ \odot K₁) is shown in Fig 2.2

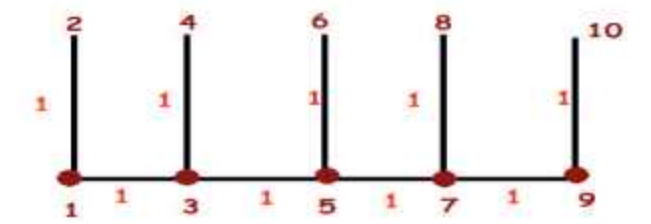


Figure 2.2

2.6. Algorithm Description

Problem Statement:

Development of C++ Algorithm forcomb Graph $(P_n \odot K_1)$ using modulo-2 square mean labeling

Input:

· The Number of Vertices

Output:

 The Labeling of Vertices of path are u(1), u(2),..... and Labeling of Vertices of pendant edges are v(1), v(2),..... The Labeling of edgese(1), e(2)...... and its Modulo of edges of e(1)=1, e(2)=1.....

Development Process

The C++ Algorithm forcomb Graph $(P_n \odot K_1)$ employs modulo-2 square mean labeling.

Code Implementation:

```
#include <iostream>
#include <cmath>
int main()
int n,i;
int v[100],u[100];
int e1[100],e2[100],e3[100],e4[100];
std::cout<< "Enter the Number of Vertices = ";
std::cin>>n;
for (i=1;i<=n;i++)
u[i]=2*i-1;
std::cout<< " \n The Number of Vertices of u ("<<i<<") ="<<u[i];
std::cout<< "\n";
for (i=1;i<=n;i++)
v[i]=2*i;
std::cout<<" \n The Number of Vertices of v("<<i<<")="<<v[i];
std::cout<< "\n";
std::cout<<"\n";
for (i=1; i<=n-1; i++)
e1[i]=(u[i]*u[i])+(u[(i+1)]*u[(i+1)]);
e2[i]= ceil( float (e1[i])/2);
std::cout<<"\n Edges of e (u"<<i<<") ="<<e2[i] <<"\t";
std::cout<<"\t Edges of e (u"<<i<<") ="<<e2[i] %2<<"\t";
for (i=1; i<=n; i++)
e3[i]=(v[i]*v[i])+(u[(i)]*u[(i)]);
e4[i]= ceil( float (e3[i])/2);
std::cout<<"\n Edges of e (v"<<i+n-1<<") ="<<e4[i] <<"\t";
std::cout<<"\t Edges of e (v"<<i+n-1<<") ="<<e4[i] %2<<"\t";
1
```

```
return 0;
```

Output: The Output of the comb Graph $(P_n \odot K_1)$ has a modulo two square mean labeling.

```
Output
                                                                                        Childre
 Enter the Number of Vertices = 6
  The Number of Vertices of u (1) -1
  The Number of Vertices of u (2) =3
  The Number of Vertices of u (3) =5
  The Number of Vertices of u (4) +7
  The Number of Vertices of u (5) =9
 The Number of Vertices of u (6) -11
 The Number of Vertices of v(1)=2
  The Number of Vertices of v(2)+4
  The Number of Vertices of v(3)=6
  The Number of Vertices of v(4)=8
  The Number of Vertices of v(5)=10
 The Number of Vertices of v(6)=12
                             Edges of e (u1) =1
Edges of o (u2) =1
Edges of e (u3) =1
Edges of e (u4) =1
Edges of e (u5) =1
Edges of e (v6) =1
 Edges of e (u1) =5
  Edges of e (u2) -17
  Edges of e (u3) +37
  Edges of e (u4) +65
  Edges of e (u5) =101
  Edges of e (v6) +3
                              Edges of e (v7) =1
Edges of e (v8) =1
  Edges of a (v7) =13
  Edges of e (va) +31
  Edges of e (v9) +57
                                Edges of e (v9) =1
 Eages of e (v10) +91
                               Edges of e (v10) =1
 Edges of e (V11) =133
                               Edges of e (v11) =1
--- Code Execution Successful ---
```

Explanation:

The algorithm begins by initializing two sets of vertices: one representing the path and the other corresponding to the pendant edges, which together form the labeling structure of the comb Graph $(P_n \odot K_1)$. The output includes the labeled edges of the comb Graph $(P_n \odot K_1)$ and its modulo result are equal to 1. This labeling approach ensures greater efficiency and consistency compared to traditional methods.

Theorem 2.7The F-Tree $F(P_n)$ has a modulotwo square mean labeling.

```
V(G) = \{v_k : 1 \le k \le n \} \cup \{u, w\} \text{ and }

E(G) = \{(v_k v_{k+1}): 1 \le k \le n-1\} \cup \{(v_1 u)\} \cup \{(v_2 w)\}.

So,|V(G)| = n+2 \& |E(G)| = n+1.
```

Proof: Let $G = F(P_n)$ be a graph.

Define $f: V(G) \rightarrow \{1,2,3,...,n+2\}$ as follows

Now
$$f(v_1) = 1$$

$$f(v_2) = 4$$

$$f(v_{2+k}) = 4 + k$$
 $1 \le k \le n - 2$.

$$f(u) = 2$$

$$f(w) = 3$$

Now we define edge function as follows

$$\begin{split} f(v_k v_{k+1}) &= \left[\frac{f(v_k)^2 + f(v_{k+1})^2}{2} \right] \text{Mod 2}, \quad 1 \le k \le n-1 \\ f(v_1 u) &= \left[\frac{f(v_1)^2 + f(u)^2}{2} \right] \text{Mod 2} \\ f(v_2 w) &= \left[\frac{f(v_2)^2 + f(w)^2}{2} \right] \text{Mod 2} \end{split}$$

Hence $F(P_n)$ has a modulo two square mean labeling.

Example 2.8 modulo two square mean labeling of F-Tree $F(P_5)$ is shown in Fig 2.3

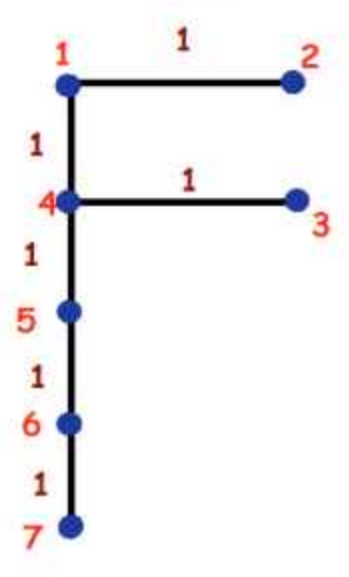


Figure 2.3

2.9 . Algorithm Description

Problem Statement:

Development of C++ Algorithm for F-Tree $F(P_n)$ using modulo-2 square mean labeling

Input:

The Number of Vertices

Output:

- The Labeling of Vertices of v(1),v(2), are assign asv(1)=2,v(2)=3, and Labeling of Vertices of path edges are u(1), u(2),......
- The Labeling of edgese(1), e(2)............ and its Modulo of edges of e(1)=1, e(2)=1...........

Development Process

The C++ Algorithm for F-Tree $F(P_n)$ employs modulo-2 square mean labeling.

Code Implementation:

```
#include <iostream>
#include <cmath>
int main()
ſ
int n.i:
int v[100],u[100];
int e1[100],e2[100];
u[1]-1;
u[2]=4;
v[1]=2;
v[2]=3:
std::cout << "Enter the Number of Vertices = ";
std::cin>>n;
std::cout << " \n The Number of Vertices of v (1) ="<<v[1];
std::cout << " \nThe Number of Vertices of v (2) = " << v[2];
std::cout << " \n The Number of Vertices of u (1) = " << u[1];
std::cout << " \n The Number of Vertices of u (2) = " << u[2];
```

```
for (i=1;i<=n-2;i++)
1
u[2+i]=(i+4);
std::cout << " \n The Number of Vertices of u ("<<2+i<<") =" <<u[2+i];
}
std::cout << "\n";
e1[1]=(u[1]*u[1])+(v[(1)]*v[(1)]);
e2[1]= ceil( float (e1[1])/2);
std::cout << "\n Edges of e (1) = "<< e2[1] << "\t";
std::cout << "\t Edges of e (1) =" << e2[1] %2 << "\t";
e1[2]=(u[2]*u[2])+(v[(2)]*v[(2)]);
e2[2] ceil( float (e1[2])/2);
std::cout << "\n Edges of e (2) = " << e2[2] << "\t";
std::cout<<"\t Edges of e (2) ="<<e2[2] %2<<"\t";
for (i=1; i<=n-1; i++)
c1[i+2]=(u[i]*u[i])+(u[(i+1)]*u[(i+1)]);
e2[i+2]= ceil( float (e1[i+2])/2);
std::cout << "\n Edges of e ("<<i+2<<") =" << e2[i+2] << "\t";
std::cout<<"\t Edges of e ("<<i+2<<") ="<<e2[i+2] %2<<"\t";
1
return 0;
}
```

OUTPUT: The Output of F-Tree $F(P_8)$ has a modulo two square mean labeling.

```
Output
                                                                                              Clear
Enter The Number of Vertices - 8
The Number of Vertices of v(1)=2
The Number of Vertices of v(2)=3
The Number of Vertices of u(1)+1
The Number of Vertices of u(2)=4
The Number of Vertices of u(3)=5
The Number of Vertices of U(4)-6
The Number of Vertices of u(5)=7
The Number of Vertices of u(6)=8
The Number of Vertices of u(7)=9
The Number of Vertices of u(8)=10
                      Edges of e(1)=1
Edges of e(1)=3
Edges of e(2)=13
                       Edges of e(2)=1
                       Edges of e(3)=1
 Edges of e(3)+9
 Edges of e(4)=21
                       Edges of e(4)=1
                  Edges of e(5)=1
Edges of e(6)=1
Edges of e(7)=1
Edges of e(8)=1
                       Edges of e(5)=1
 Edges of e(5)=31
Edges of e(6)-43
 Edges of e(7)=57
Edges of e(8)=73
 Edges of e(9)=91
--- Code Execution Successful ---
```

Explanation:

The algorithm begins by initializing two sets of vertices: one representing the path and the other corresponding to the pendant edges, which together form the labeling structure of the F-Tree $F(P_n)$. The output includes the labeled edges of the F-Tree $F(P_n)$ and its modulo result are equal to 1. This labeling approach ensures greater efficiency and consistency compared to traditional methods.

3 Conclusion

In this paper we have investigated some pathrelated graphslike Hurdle Graph, comb graph($P_n \odot K_1$), F-Tree $F(P_n)$. We have provided C++ algorithm for the theorems.

4 References

- Acharya B. D, Arumugarn S, and Rosa A, Labeling of Discrete Structures and Applications, Narosa Publishing House, New Delhi, 2008
- [2] Graham R. L and Sloane N. J. A., On additive bases and harmonious graphs, SIAM J. Alg. Discrete Methods. 1, 1980, 382-404.

- [3] Jahir Hussain R and Senthamizh Selvan J, 1-Edge magic labeling of splitting graph, International Journal of Applied Engineering Research, Vol-14, 2019.
- [4] Jayapriya J and Thirusangu K, 0-Edge magic labeling for some class of graphs, Indian Journal of Computer Sciences and Engineering. 3, 2012, 425-427.
- [5] Ponraj R and Somasundaram S, Mean labeling of graphs, National Academy of Science Letters Vol-26, 2003,210-213.
- [6] Ramachandran V and Sekar C, One modulo N gracefulness of Acyclic graphs, Ultra Scientist of Physical Sciences, Vol.25 No (3)A,2013, 417- 424.
- [7] Rosa A, Oncertain valuations of the vertices of a graph, Theory of Graphs (Internat.Symposium, Rome, July 1966), Gordon and Breach, N. Y. and Dunod Paris, 1967, 349-355.
- [8] Sandhya S, Somasundaram S and Anusa S, Root square mean labeling of graphs Int. J. Contemp. Math. Sci.2014.
- [9] Sandhya S, Somasundaram S and AnusaS, Some More Results on Root Square Mean Graphs J. Math. Res, 2015.
- [10] Selvaraj, R., Vidyanandini, S. & Nayak, SoumyaRanjan, Even vertex odd mean labeling of some graphs, Journal of Discrete Mathematical Sciences and Cryptography, 27:7, 2024,2169– 2177., DOI: 10.47974/JDMSC-2089.

Research Scholar, PG and Research Department of Mathematics, Mannar Thirumalai Naicker College (Affiliated to Madurai Kamaraj University), Madurai, Tamilnadu, India. (Received, April 04, 2025) (Revised, May 02, 2025)

Department of Mathematics, SSM Institute of Engineering and Technology, Dindigul, Tamilnadu, India. E-mail: Christopher.mosespaul@gmail.com

²PG and Research Department of Mathematics, Mannar Thirumalai Naicker College (Affiliated to Madurai Kamaraj University), Madurai, Tamilnadu, India. E-mail: me.ram111@gmail.com Keerti Acharya', A NOVEL TECHNIC USING
Rinku Verma', COMPLETE GRAPH LABELING
Pranjali Kekre¹ AND ASCII REPRESENTATION

ISSN: 0970-5120

ABSTRACT. In this paper, we present a novel encryption technique that uses complete graph labeling and ASCII code mapping to improve data security. The method encodes plaintext characters as labeled vertices in a complete graph, with edges representing distinct relationships based on encryption rules derived from graph theory principles. By combining ASCII values with graph labeling schemes, we create a structured but complex ciphertext that is resistant to common cryptanalysis techniques. The proposed approach ensures secure communication while remaining computationally efficient. Results are verified using Matlab software.

2020 Mathematical Science Classification: 11A07, 44A10, 94A60, 11T71

Keywords and Phrases: Network security, eigher text, complete graph, extended ASCII code.

1. INTRODUCTION

With the exponential growth of digital communication and data exchange, ensuring secure transmission of sensitive information has become a paramount concern.

Secured data transfer is always a matter of discussion, several techniques are already developed and a number of them are still in pipeline. Main motto of Cryptography is information security such as data integrity, entity authentication and data origin authentication. Cryptography is a set of techniques to provide information security. While designing a cryptography scheme, cryptographer always kept in mind that the designed algorithm is not very trivial to understand, replicate and therefore easily cracked. To secure the data from hackers it needs to be encrypted with high level of security.

It helps to store sensitive information, transmit it across insecure networks like internet so that it can't be read by anyone except the intended receiver.

Analysis of cryptographic security leads to using theoretical computer science especially complexity theory.

Graph theory, a mathematical discipline concerned with the study of graphs and their properties, has found applications in numerous fields, including network security and cryptography.

Various cryptographic methods have been developed and refined over the years to meet a wide range of security needs. Rivest et.al. [1] developed the RSA algorithm, a game-changing advancement in public-key cryptography that laid the groundwork for secure digital communications. In addition to public-key encryption, symmetric encryption schemes such as the Advanced Encryption Standard (AES) have gained popularity in both commercial and academic settings, as discussed by Katz and Lindell [2]. However, as cryptographic algorithms have advanced, challenges such as computational overhead, scalability, and performance have emerged, particularly when securing large datasets and ensuring efficient encryption in real-time communications.

Data security requirements have become even more complex with the growth of distributed systems and the Internet of Things (IoT). According to Bashir and Hussain [15], lightweight cryptography is essential, particularly in settings with limited resources when energy efficiency and processing power are critical. Hybrid cryptographic algorithms have been developed to combine the advantages of several encryption techniques while reducing their respective drawbacks for applications where protection is required for both data in transit and data at rest Srinivas and Manjunath, [12]. These algorithms are perfect for situations where secure data transmission without noticeable delay is crucial since they are made to provide a balance between performance, security, and resource usage.

Another urgent concern in contemporary cyber security is database security, specifically with regard to data in transit and at rest. Database encryption methods must retain acceptable performance levels

while offering high levels of protection, claims Sullivan [16]. Effective encryption techniques are crucial for reducing potential vulnerabilities and guaranteeing that data is safe from malevolent actors since databases contain and handle vast amounts of sensitive data.

In order to protect unencrypted database files while they are in transit and at rest, this study attempts to propose a versatile and reasonably priced cryptographic encryption algorithm. The suggested solution aims to combine state-of-the-art encryption techniques with realistic implementation strategies, providing a balanced approach to protecting sensitive database information in contemporary technological landscapes. It does this by drawing on the principles described in foundational cryptography texts like those by Paar and Pelzl [3] and Boneh and Shoup [14].

This study aims to suggest a flexible and affordable cryptographic encryption solution to safeguard unprotected database files both in transit and at rest. The proposed method seeks to provide a balanced approach to safeguarding sensitive database data in today's technology environments by fusing cutting-edge encryption algorithms with practical implementation strategies.

In order to improve data security, Mathur[5] presented a symmetric key encryption algorithm that makes use of ASCII character values.

Kumar et al.[13] used a modified affine cipher to encrypt data by combining encryption and decryption procedures with graph plotting techniques.

Geena and Gupta [20] presented a novel method of improving data security through the combination of symmetric key cryptography and graph theory.

The improvement of data security in electronic communication systems is the subject of "A Triple Hill Cipher Algorithm Proposed to Increase the Security of Encrypted Binary Data and its Implementation Using FPGA" by As Khalaf et al. [9].

To increase the security of text data, Rajput et al. [7] published a cryptographic technique that employs double encryption. A key aggregate searchable encryption (KASE) technique was presented by Goutham et al. [10] to facilitate safe and effective cloud data sharing. The method offered a safe way to share data in cloud-based settings by enabling users to search encrypted data in the cloud without sacrificing privacy. Sampathkumar [11] talked about attribute-based encryption (ABE) and how it may be used to secure queries. He also suggested a way to organize queries such that ABE systems perform better, particularly in large-scale settings. In order to improve the security and effectiveness of image encryption while lowering the amount of data needed for transmission or storage, Mahmood and Shehab [6] developed a method for image encryption and compression based on compressive sensing and chaos theory. Gorabal and Manjaiah [8] presented a new image encryption approach to address security concerns related to image data. The method involved both spatial and frequency domain transformations to achieve high security levels for image transmission.

A method for identifying cryptographic algorithms by examining characteristics present in ciphertexts has been presented by Li, J. et al. [21]. In order to choose the encryption technique, the suggested scheme made use of statistical characteristics and patterns found in encrypted data.

Bing et al.[4] presented intriguing findings about spanning trees in graph theory. They investigated important properties and proposed new theorems that add to our understanding of spanning tree structures. These findings had direct implications for both theoretical combinatories research and practical applications in areas such as network reliability, circuit design, and data structure optimization.

Shaik and Natarajan K [17] proposed a flexible and cost-effective cryptographic encryption algorithm that is specifically designed to secure unencrypted database files at rest and in transit. The algorithm focuses on providing strong security while reducing computational costs and complexity, making it an excellent choice for modern database systems that require scalable, real-time encryption without sacrificing performance. Verma et al[18] proposed an encryption algorithm based on modular arithmetic and Laplace transform. Chen, Y., et al.[19] proposed a Graph based algorithm for the encryption algorithm. Based on all these we have proposed a encryption algorithm based on the concept of graph theory and modular arithmetic.

2. PRELIMINARIES

- 2.1 Plain text: It signifies a message that can be understood by the sender, the recipient and also by anyone else who gets access to that message.
- 2.2. Cipher text: When a plain text message is codified using any suitable scheme, the resulting message is called as cipher text.
- 2.3. Encryption and Decryption: Encryption transforms a plain text message into cipher text, whereas decryption transforms a cipher text message back into plain text.
- 2.4 Complete Graph: A simple graph G is said to be complete if each vertex is joined to every other vertex by means of an edge.
- 2.5 Minimum Spanning Tree: A subgraph of a connected graph G which is a tree and contains all the vertices G is said to be spanning tree of G. A spanning tree with minimum weight is called minimum spanning tree.

3. ALGORITHM

Pseudo Algorithm for encryption and decryption is a proposed Algorithm based on the concept of complete graph labelling technique, a minimum spanning tree used to find secret key and basic matrix theory to find cipher text and to decode it to get plain Text again.

Step 1: Input the message and take the length of message as 'L'.

Step 2: Represent the message as vertices of complete Graph ${}^{\iota}K_{\iota}{}^{\iota}$ as set $\{\{u_1,u_2,---,u_I\}$ and edges

as
$$\{e_1, e_2, \dots, e_N\}$$
, where $N = \left(\frac{L(L-1)}{2}\right)$.

Step 3: Label the vertices as

$$f(u_{2i+1}) = L - i; 0 \le i \le \left\lfloor \frac{(L-1)}{2} \right\rfloor,$$

$$f(u_{2i}) = i; 1 \le i \le \left\lfloor \frac{L}{2} \right\rfloor.$$

Step 4:Label the $e = \langle u, v \rangle$ as

$$f(e) = |f(u) - f(v)| + Max\{f(u), f(v)\}.$$

Step 5: Create the weighted adjacency Matrix A for the labeled K_L .

Step 6: Obtain the extended ASCII code for the each charter of inputmessage.

Step 7: Create the weighted adjacency Matrix B of the outer cycle of ${}^{t}K_{L}{}^{t}$, and fill the diagonal entries of Matrix B with the obtained extended ASCII code of the text to be encrypted.

Step 8: Create N = AxB.

Step 9: Find out the minimum Spanning tree of labeled complete graph ${}^{t}K_{L}{}^{t}$ and let the length of minimum spanning tree be ${}^{t}S{}^{t}$.

Step 9: Consider public key matrix M with all upper triangular entries as one and other as zero.

Step 10: Create Code matrix

$$C = NxM$$

$$C_i = mod(C, S)$$

$$C_s = Outionet(C, S)$$
.

Step 11: Pass (C_1, C_2, A) as Cipher text and 'S' as Secret key to the Decoder.

Step 12 Decrypt (C_i, C_2, A) with 'S' as follows

Create $D = SC_2 + C_1$.

 $N = DM^{-1}$ (where M is the Public Key)

B=A-1 N.

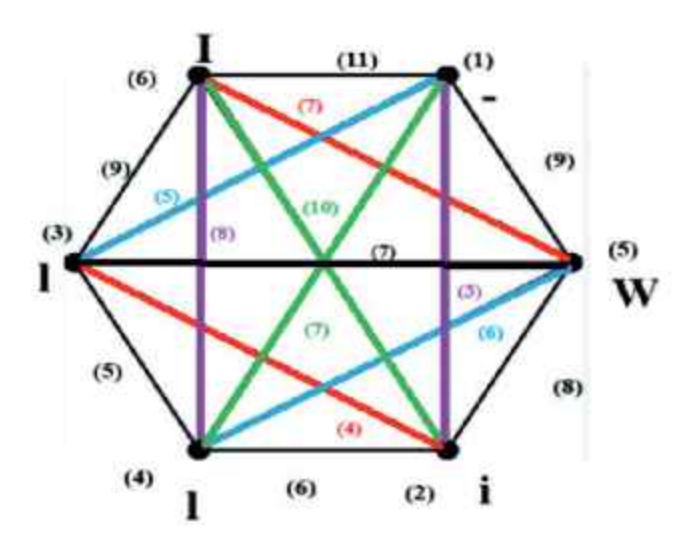
Diagonal entries of matrix B gives the extended ASCII code of input plain text and retrieved from the table.

Illustrative examples:

Plain Text "I Will"

L=6;

Graph K_{ϵ} is created and labeled as mentioned in algorithm, shown in figure 1.



Weightes adjacency matrix for the graph

$$A = \begin{bmatrix} 0 & 11 & 7 & 10 & 8 & 9 \\ 11 & 0 & 9 & 3 & 7 & 5 \\ 7 & 9 & 0 & 8 & 6 & 7 \\ 10 & 3 & 8 & 0 & 6 & 4 \\ 8 & 7 & 6 & 6 & 0 & 5 \\ 9 & 5 & 7 & 4 & 5 & 0 \end{bmatrix}$$

Weightes adjacency matrix for the outer cycle of graph

Updated B with diagonal entries as extended ASCII code of message letters

$$B = \begin{bmatrix} 73 & 11 & 0 & 0 & 0 & 9 \\ 11 & 32 & 9 & 0 & 0 & 0 \\ 0 & 9 & 87 & 8 & 0 & 0 \\ 0 & 0 & 8 & 105 & 6 & 0 \\ 0 & 0 & 0 & 6 & 108 & 5 \\ 9 & 0 & 0 & 0 & 5 & 108 \end{bmatrix}$$

Resultant N = AxB As

Γ	202	415	788	1154	969	1012
	848	202	807	429	799	674
	673	365	145	876	731	849
N =	799	278	723	100	668	552
	706	366	633	678	61	612
	712	322	686	506	564	106

Public key matrix

$$M = \begin{bmatrix} & 1 & 1 & 1 & 1 & 1 & 1 \\ & 0 & 1 & 1 & 1 & 1 & 1 \\ & 0 & 0 & 1 & 1 & 1 & 1 \\ & 0 & 0 & 0 & 1 & 1 & 1 \\ & 0 & 0 & 0 & 0 & 0 & 1 \end{bmatrix}$$

Length of minimum spanning tree:S=25

C = NxMas 799 1077 706. 1072

 $C_1 = mod(C,S)$

As

$$C_i = \begin{bmatrix} 2 & 17 & 5 & 9 & 3 & 15 \\ 23 & 0 & 7 & 11 & 10 & 9 \\ 23 & 13 & 8 & 9 & 15 & 14 \\ 24 & 2 & 0 & 0 & 18 & 20 \\ 6 & 22 & 5 & 8 & 19 & 6 \\ 12 & 9 & 20 & 1 & 15 & 21 \end{bmatrix}$$

$$C_{2} = Qutionet(C, S).$$

$$C_{2} = \begin{bmatrix} 8 & 24 & 56 & 102 & 141 & 181 \\ 33 & 42 & 74 & 91 & 123 & 150 \\ 26 & 41 & 47 & 82 & 111 & 145 \\ 31 & 43 & 72 & 76 & 102 & 124 \\ 28 & 42 & 68 & 95 & 97 & 122 \\ 28 & 41 & 68 & 89 & 111 & 115 \end{bmatrix}$$

Pass (C_1, C_2, A) as Cipher text and 'S' as Secret key to the Decoder

Now obtained

$$D = SC_1 + C_1$$

as						
D =	202	617	1405	2559	3528	4540
	848	1050	1857	2286	3085	3759
	673	1038	1183	2059	2790	3639
	799	1077	1800	1900	2568	3120
	706	1072	1705	2383	2444	3056
	712	1034	1720	2226	2790	2896

 $N = DM^{-1}$ (where M is the Public Key)

as

N =	202	415	788	1154	969	1012
	848	202	807	429	799	674
	673	365	145	876	731	849
	799	278	723	100	668	552
	706	366	633	678	61	612
	712	322	686	506	564	106

$$B = A^{-1}N$$

as

	73.0000	11.0000	-0.0000	0.0000	0.0000	9.0000
	11.0000	32.0000	9.0000	0.0000	0.0000	0.0000
	0.0000	9.0000	87.0000	8.0000	0.0000	0.0000
	0.0000	0.0000	8.0000	105.0000	6.0000	0.0000
	0	0.0000	0.0000	6.0000 1	08.0000	5.0000
	9.0000	0.0000	0.0000	0 5.	0000 108	0000

with digonal entries

75 32 87 105 108 108

character equivalent of these extended ASCII code is the Decoded message T Will'

CONCLUSION

In this study, we have provided a novel cryptographic technique that combines the division algorithm with graph theoretical features to produce a reliable and extremely secure means of sending secret data. The method gives a new layer of encryption that greatly improves data security and confidentiality in communication networks by combining these two different mathematical ideas.

REFERENCES

- Rivest, R. L., Shamir, A., and Adleman, L. (1978): A Method for Obtaining Digital Signatures and Public-Key Cryptosystems. Communications of the ACM, Vol. 21(2), pp.120– 126.
- Katz, J., and Lindell, Y. (2007): Introduction to Modern Cryptography, CRC Press.
- Paar, C., and Pelzl, J. (2010): Understanding Cryptography: A Textbook for Students and Practitioners, Springer.
- Bing, Y., Zhang Z. and Wang J. (2010): Some results on spanning trees. Acta Mathematicae Applicatae Sinica, English Series, Vol. 26 (4), pp.607-616, DOI:10.1007/s10255-010-0011-4.
- Mathur, A. (2012): An ASCII value based data encryption algorithm and its comparison with other symmetric data encryption algorithms, *International Journal on Computer Science and Engineering*, Vol.4(9), pp.1650-1657.
- Mahmood, M.K., and Shehab, J.N. (2014).: Image Encryption and Compression Based on Compressive Sensing and Chaos, *International Journal of Computer Engineering & Technology*, Vol.5(1),pp. 68-84.
- Rajput, Y., Naik, D., and Mane, C. (2014): An Improved Cryptographic Technique to Encrypt Text using Double Encryption. *International Journal of Computer Applications*, Vol. 86(6).
- Gorabal, V., and Manjaiah, D. H. (2014):Image Encryption Approach for Security Issues, International Journal of Information Technology and Management Information System (IJITMIS), Vol. 5(2), pp.59-64.
- Khalaf, A.A.M., Karim M.S.A., and Hamed, H.F.A. (2016).: A Triple Hill Cipher Algorithm Proposed to Increase the Security of Encrypted Binary Data and its Implementation Using FPGA, ICACT Transactions on Advanced Communications Technology (TACT), Vol. 5(1), pp.752-759.
- Goutham, V., Kethavath, L., and Swetha, K. (2016): Key Aggregate Searchable Encryption with Secure and Efficient Data Sharing In Cloud, International Journal of Computer Engineering and Technology, Vol. 7(4), pp.41–47.
- Sampathkumar, A. (2017): Entry Structure for A Few Queries in Attribute Founded Encryption, International Journal of Mechanical Engineering and Technology, Vol.8(8), pp.1656– 1661.
- Srinivas, K., and Manjunath, A. S. (2018): A Survey on Hybrid Cryptographic Algorithms for Data Security, Journal of Computer Applications, Vol. 40(1), pp. 34

 –42.
- Kumari, M., and Kirubanad, V.B. (2018): Data Encryption and Decryption Using Graph Plotting. International Journal of Civil Engineering and Technology, Vol.9(2), pp.36-46.
- Bonch, D., and Shoup, V. (2020): A Graduate Course in Applied Cryptography, Stanford University.
- Bashir, A. M., and Hussain, A. (2021): A Survey on Lightweight Cryptography for IoT Applications, IEEE Access, Vol.9, pp.12333–12349.
- Sullivan, L. (2022): The Importance of Encryption for Database Security, Database Security Journal, Vol.18(3), pp.22–28.

- Shaik, V., and Natarajan, K. (2022): Flexible and cost-effective cryptographic encryption algorithm for securing unencrypted database files at rest and in transit, Methods X, Elsevier, Vol.9, https://doi.org/10.1016/j.mex.2022.101924.
- Verma, R., Kekre, P., and Acharya, K. (2023): Cryptanalysis Using Laplace Transform of Error Function, Jāānābha, Vol.53(1), pp.106–109.
- Chen, Y., Hu, T., Lou, F., Yin, M., Zeng, T., Wu, G., and Wang, H. (2024): A knowledge graphbased consistency detection method for network security policies, *Applied Sciences*, Vol. 14(3), pp.1295. https://doi.org/10.3390/app14031295.
- Gena, H., and Gupta, B. (2024): Graph-Based Encryption and Decryption Algorithm in Symmetric Key Cryptography, Frontiers in Health Informatics, Vol.13(8),pp.947-955.
- Li, J., Sun, H., Du, Z., Wang, Y., Yuan, K., and Jia, C. (2025): A generic cryptographic algorithm identification scheme based on ciphertext features, *Journal of Information Security and Applications*, Vol.89, doi: 10.1016/j.jisa.2025.103984

^{1,2,3} Department of Mathematics, Medi-Caps University, Pigdamber, Rau-453331, Madhya Pradesh India.

(Received, April 12, 2025), (Revised, May 02, 2025)

Email: keerti.sharma@medicaps.ac.in, Email: rinku.verma@medicaps.ac.in, Email: pranjali.kekre@medicaps.ac.in

SUMS INVOLVING A FAMILY OF Thomas Koshy GIBONACCI POLYNOMIAL SQUARES: GRAPH-THEORETIC CONFIRMATIONS

ISSN: 0970-5120

Abstract

We confirm a generalized sum of a family of gibonacci polynomial squares using graph-theoretic techniques, and its graph-theoretic and Pell consequences,

Key words: Gibonacci Polynomial, Fibonacci Polynomial Pell Polynomials,

Lukas Polynomial, Benet Formula. Graph-theoretic Confirmation.

MSC2020: Primary 11B37, 11B39, 11C08

INTRODUCTION

Extended gibrancci polynomials $z_n(x)$ are defined by the recurrence $z_{n+2}(x) = a(x)z_{n+1}(x) +$ $b(x)z_n(x)$, where x is an arbitrary integer variable; $a(x), b(x), z_0(x)$, and $z_1(x)$ are arbitrary integer polynomials; and $n \ge 0$.

Suppose a(x) = x and b(x) = 1. When $z_0(x) = 0$ and $z_1(x) = 1$, $z_n(x) = f_n(x)$, the nth Fibonacci polynomial; and when $z_0(x) = 2$ and $z_1(x) = x$, $z_n(x) = l_n(x)$, the nth Lucas polynomial. They can also be defined by the Binet-like formulas. Clearly, $f_n(1) = F_n$, the nth Fibouacci number; and $l_n(1) = L_n$, the nth Lucas number [1, 2].

Pell polynomials $p_n(x)$ and Pell-Lucus polynomials $q_n(x)$ are defined by $p_n(x) = f_n(2x)$ and $q_n(x) = l_n(2x)$, respectively [2].

In the interest of brevity, clarity, and convenience, we omit the argument in the functional notation, when there is no ambiguity; so z_n will mean $z_n(x)$. In addition, we let $g_n = f_n$ or

$$\begin{split} I_n; b_n &= p_n \text{ or } q_n; \ \Delta = \sqrt{x^2 + 4}; \text{ and } 2\alpha = x + \Delta \text{ [6]}. \\ \text{It follows by the Binet-like formulas that } \lim_{m \to \infty} \frac{1}{g_{m+r}} = 0 \text{ and } \lim_{m \to \infty} \frac{g_{m+r}}{g_m} = \alpha^r. \end{split}$$

Fundamental Gibonacci Identities

Gibonacci polynomials satisfy the following properties [2, 3, 4

$$g_{n+k}g_{n-k} - g_n^2 = \begin{cases} (-1)^{n+k+1}f_k^2, & \text{if } g_n = f_n \\ (-1)^{n+k}\Delta^2 f_k^2, & \text{otherwise;} \end{cases}$$
 (1)

$$g_{n+k}g_{n-k} - g_n^2 = \begin{cases} (-1)^{n+k+1}f_k^2, & \text{if } g_n = f_n \\ (-1)^{n+k}\Delta^2 f_k^2, & \text{otherwise;} \end{cases}$$

$$g_{n+k+r}g_{n-k} - g_{n+k}g_{n-k+r} = \begin{cases} (-1)^{n+k+1}f_rf_{2k}, & \text{if } g_n = f_n \\ (-1)^{n+k}\Delta^2 f_rf_{2k}, & \text{otherwise,} \end{cases}$$
(2)

where k and r are positive integers. These properties can be confirmed using the Binet-like formulas. It follows from these two identities that

$$g_{(2pn+t)k}g_{(2pn+t-2p)k} - g_{(2pn+t-p)k}^2 = \begin{cases} (-1)^{tk+1}f_{pk}^2, & \text{if } g_n = f_n \\ (-1)^{tk}\Delta^2f_{pk}^2, & \text{otherwise;} \end{cases}$$
(3)

$$g_{(2pn+t)k+r}g_{(2pn+t-2p)k} - g_{(2pn+t)k}g_{(2pn+t-2p)k+r} = \begin{cases} (-1)^{tk+1}f_rf_{2pk}, & \text{if } g_n = f_n \\ (-1)^{tk}\Delta^2f_rf_{2pk}, & \text{otherwise,} \end{cases}$$
(4)

where k, p, r, and t are positive integers and $t \le 2p$.

A TELESCOPING GIBONACCI SUM

Using recursion, we established the following telescoping gibonacci sum in [6]. In the interest of brevity, we omit its proof here.

Lemma 1. Let k, p, r, t, and λ be positive integers, where $t \leq 2p$. Then

$$\sum_{n=1}^{\infty} \left[\frac{g_{(2pn+t-2p)k+r}^{\lambda}}{g_{(2pn+t-2p)k}^{\lambda}} - \frac{g_{(2pn+t)k+r}^{\lambda}}{g_{(2pn+t)k}^{\lambda}} \right] = \frac{g_{tk+r}^{\lambda}}{g_{tk}^{\lambda}} - \alpha^{\lambda r}.$$
(5)

A FAMILY OF GIBONACCI SUMS 3

Using identities (3) and (4), Lemma 1 with $\lambda = 1$ played a major role in the development of the following theorem. To this end, in the interest of brevity, we let [6]:

$$\mu = \begin{cases} 1, & \text{if } g_n = f_n \\ \Delta^2, & \text{otherwise}; \end{cases}$$
 and $\nu^* = \begin{cases} 1, & \text{if } g_n = f_n \\ -1, & \text{otherwise}. \end{cases}$

These tools served as building blocks of the discourse, as the theorem shows [6].

Theorem 1. Let k, p, r, and t be positive integers, where $t \le 2p$. Then

$$\sum_{n=1}^{\infty} \frac{(-1)^{tk} \mu \nu^* f_r f_{2pk}}{g_{(2pn+t-p)k}^2 - (-1)^{tk} \mu \nu^* f_{pk}^2} = \frac{g_{tk+r}}{g_{tk}} - \alpha^r.$$
(6)

The objective of our discourse is to confirm this result using graph-theoretic techniques. To this end, first we present the needed tools.

GRAPH-THEORETIC TOOLS

Consider the Fibonacci digraph in Figure 1 with vertices v₁ and v₂, where a weight is assigned to each edge [2, 5]. It follows from its weighted adjacency matrix $Q = \begin{bmatrix} x & 1 \\ 1 & 0 \end{bmatrix}$ that $Q^n = \begin{bmatrix} f_{n+1} & f_n \\ f_n & f_{n-1} \end{bmatrix},$

$$Q^n = \begin{bmatrix} f_{n+1} & f_n \\ f_n & f_{n-1} \end{bmatrix}$$
,

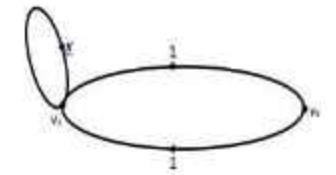


Figure 1: Weighted Fibonacci Digraph

where $n \ge 1$ [2, 3, 4, 5]. We extend the exponent n to 0, which is consistent with the Cassini-like formula $f_{n+1}f_{n-1} - f_n^2 = (-1)^n$ [2, 5].

A walk from vertex v_i to vertex v_j is a sequence v_i - $e_{i'}$ - v_{i+1} - \cdots - v_{j-1} - e_{j-1} - v_j of vertices v_k and edges e_k , where edge e_k is incident with vertices v_k and v_{k+1} . The walk is closed if $v_i = v_j$; and open, otherwise. The length of a walk is the number of edges in the walk. The weight of a walk is the product of the weights of the edges along the walk.

The ijth entry of Q^n gives the sum of the weights of all walks of length n from v_i to v_j in the weighted digraph, where $1 \le i, j \le n$ [2, 3, 4]. Consequently, the sum of the weights of closed walks of length n originating at v_1 in the digraph is f_{n+1} and that of those originating at v_2 is f_{n-1} . So, the sum of the weights of all closed walks of length n in the digraph is $f_{n+1} + f_{n-1} = l_n$ [2, 5].

Let A and B denote sets of walks of varying lengths originating at a vertex v. Then the sum of the weights of the elements (a, b) in the product set $A \times B$ is defined as the product of the sums of weights from each component [3, 4]. This definition can be extended to any finite number of component sets. In particular, let A, B, C, and D denote the sets of walks of varying lengths originating at a vertex v, respectively. Then the sum of the weights of the elements (a, b, c, d) in the product set $A \times B \times C \times D$ is the product of the sums of weights from each component [3, 4].

We now make an interesting observation. Let $A = \{u\}$ and $B = \{v\}$, where u denotes the closed walk $v_1 \cdot v_2 \cdot v_1$. The weight of the element (u, u) in $A \times A$ is x^2 , and that in $B \times B$ is 1. Consequently, the sum w of the weights of the elements in $C^* = (A \times A) \cup (B \times B) \cup (B \times B) \cup (B \times B) \cup (B \times B)$ is given by $w = x^2 + 4 = \Delta^2$.

These tools play a major role in the discourse. With them at our finger tips, we are now ready for pursuing the graph-theoretic confirmation.

5 GRAPH-THEORETIC CONFIRMATION

Let T_n^* denote the set of closed walks of length n in the digraph originating at v_{1*} and U_n^* the set of all closed walks of the same length n in the digraph. Correspondingly, let T_n denote the sum of the weights of all elements in T_n^* , and U_n that of those in U_n^* . Clearly, $T_n = f_{n+1}$ and $U_n = f_{n+1} + f_{n-1} = l_n$ [2, 5]. With this brief background, we now begin the proof of the gibonacci sum (6) in cases, where $k, p, r, t \ge 1$ and $t \le 2p$.

Proof. Case 1. Suppose $g_n = f_n$. The sum of the weights of the elements in the product set $T^*_{r-1} \times T^*_{2pk-1}$ is $T_{r-1}T_{2pk-1} = f_r f_{2pk}$; the sum of those in $T^*_{(2pm+t-p)k-1} \times T^*_{(2pm+t-p)k-1}$ is $T^2_{(2pm+t-p)k-1} = f^2_{(2pm+t-p)k}$; and that of those in $T^*_{pk-1} \times T^*_{pk-1}$ is $T^2_{pk-1} = f^2_{pk}$.

Combining the two parts, we now let

$$\begin{split} S_n &= \frac{T_{r-1}T_{2pk-1}}{T_{(2pn+t-p)k}^2 - (-1)^h T_{pk-1}^2} \\ &= \frac{f_r f_{2pk}}{f_{(2pn+t-p)k}^2 - (-1)^k f_{pk}^2}, \end{split}$$

Using identities (3) and (4), and the lemma, this yields

$$\frac{(-1)^{tk}f_rf_{2pk}}{f_{(2pn+t-p)k}^2 - (-1)^{tk}f_{pk}^2} = \frac{f_{(2pn+t)k}f_{(2pn+t-2p)k+r} - f_{(2pn+t)k+r}f_{(2pn+t-2p)k}}{f_{(2pn+t)k}f_{(2pn+t-2p)k}}$$

$$\sum_{n=1}^{\infty} \frac{(-1)^{tk}f_rf_{2pk}}{f_{(2pn+t-p)k}^2 - (-1)^{tk}f_{pk}^2} = \sum_{n=1}^{\infty} \left[\frac{f_{(2pn+t-2p)k+r}}{f_{(2pn+t-2p)k}} - \frac{f_{(2pn+t)k+r}}{f_{(2pn+t-2p)k}} \right]$$

$$= \frac{f_{tk+r}}{f_{tk}} - \alpha^r. \qquad (7)$$

Now, we turn to the flip side.

Case 2. Let $g_n = l_n$. Recall that the sum w of the weights of the elements in $C^* = (A \times A) \cup (B \times B) \cup (B \times B) \cup (B \times B) \cup (B \times B)$ is given by $w = x^2 + 4 = \Delta^2$, and that of the elements in the product set $C^* \times T^*_{r-1} \times T^*_{2k-1}$ is given by $wT_{r-1}T_{2pk-1} = \Delta^2 f_r f_{2pk}$. The sum of the weights of the elements in the product set $U^*_{(2pn+t-p)k} \times U^*_{(2pn+t-p)k}$ is $U^2_{(2pn+t-p)k} = l^2_{(2pn+t-p)k}$; and that of those in $T^*_{2pk-1} \times T^*_{pk-1}$ is $T^2_{2pk-1} = f^2_{2pk}$.

As above, we now let

$$\begin{split} S_n &= \frac{wT_{r-1}T_{2pk-1}}{U_{(2pn+t-p)k}^2 + (-1)^k wT_{pk-1}^2} \\ &= \frac{\Delta^2 f_r f_{2pk}}{l_{(2pn+t-p)k}^2 + (-1)^k \Delta^2 f_{pk}^2}, \end{split}$$

It then follows by identities (3) and (4), and the lemma that

$$\frac{(-1)^{tk+1}\Delta^{2}f_{r}f_{2pk}}{l_{(2pn+t-p)k}^{2} + (-1)^{tk}\Delta^{2}f_{pk}^{2}} = \frac{l_{(2pn+t)k}l_{(2pn+t-2p)k+r} - l_{(2pn+t)k+r}l_{(2pn+t-2p)k}}{l_{(2pn+t)k}l_{(2pn+t-2p)k}}$$

$$\sum_{n=1}^{\infty} \frac{(-1)^{tk+1}\Delta^{2}f_{r}f_{2pk}}{l_{(2pn+t-p)k}^{2} + (-1)^{tk}\Delta^{2}f_{pk}^{2}} = \sum_{n=1}^{\infty} \left[\frac{l_{(2pn+t-2p)k+r}}{l_{(2pn+t-2p)k}} - \frac{l_{(2pn+t)k+r}}{l_{(2pn+t)k}}\right]$$

$$= \frac{l_{tk+r}}{l_{tk}} - \alpha^{r}. \qquad (8)$$

This equation, coupled with equation (7), yields Theorem 1, as desired.

For the curious-minded, we now add that equation (6) can be rewritten in terms of graphtheoretic tools. To this end, we define $T_0 = 1, U_0 = 2$; $H_n = T_n$ or U_n ;

$$\mu = \begin{cases} 1 & \text{if } H_n = T_n \\ w & \text{otherwise;} \end{cases} \quad \nu^* = \begin{cases} 1, & \text{if } H_n = T_n \\ -1, & \text{otherwise;} \end{cases} \text{ and } \nu = \begin{cases} 1, & \text{if } H_n = T_n \\ 0, & \text{otherwise.} \end{cases}$$

With these new tools, and integers k, p, r, and t as before, we now present the graph-theoretic version of equation (6):

$$\sum_{n=1}^{\infty} \frac{(-1)^{tk} \mu \nu^* T_{r-1} T_{2pk-1}}{H_{(2pn+t-p)k-\nu}^2 - (-1)^{tk} \mu \nu^* T_{pk-1}^2} = \frac{H_{tk+r-\nu}}{H_{tk-\nu}} - \alpha'. \quad (9)$$

Next, we turn to the Pell implications of the graph-theoretic techniques.

6 PELL CONSEQUENCE

With the gibonacci-Pell relationship $b_n(x) = g_n(2x)$, we can construct the graph-theoretic proof of the Pell version of Theorem 1 independently by changing the weight of the loop at v_1 from x to 2x. We encourage gibonacci enthusiasts to explore this route.

References

- M. Bicknell, A Primer for the Fibonacci Numbers: Part VII, The Fibonacci Quarterly, 8:4 (1970), 407–420.
- [2] T. Koshy, Fibonacci and Lucas Numbers with Applications, Volume II, Wiley, Hoboken, New Jersey, 2019.
- [3] T. Koshy, A Recurrence for Gibonacci Cubes with Graph-theoretic Confirmations, The Fibonacci Quarterly, 57:2 (2019), 139–147.
- [4] T. Koshy, Graph-theoretic Confirmations of Four Sums of Gibonacci Polynomial Products of Order 4, The Fibonacci Quarterly, 59:2 (2021), 167–175.
- [5] T. Koshy, Sums Involving Gibonacci Polynomial Squares: Graph-theoretic Confirmations, The Fibonacci Quarterly, 61:2 (2023), 119–128.
- [6] T. Koshy, Sums Involving A Family of Gibonacci Polynomial Squares: Generalizations, The Fibonacci Quarterly, 62:1 (2024), 75–83.

Emeritus Professor

(Received, December 19, 2024)

Framingham State University, Framingham MA01701-910, USA

Email: tkoshy@emeriti.framingham.edu

Pratap Saha', Samten Tamang', Meghlal Mallik', Sanjih Kumar Datta'

GROWTH OF THE SOLUTIONS OF Nth ORDER LINEAR SHIFT DIFFERENTIAL EQUATIONS WITH UNCERTAIN COEFFICIENT

ISSN: 0970-5120

ABSTRACT. After applying shift, we look at the complex oscillation solutions of the nth order linear differential equation and demonstrate by a counter example that the conclusion of the earlier result does not hold. We also establish the result for the shift differential equation with a supporting a example.

Key words and phrases: Entire function, meromorphic function, growth, linear differential equation, shift differential equation. Mathematical Subject Classification 2020: 34M10, 30D35.

1. Introduction

The standard definitions and notations of Nevanlinna value distribution theory are adopted in this paper. For further information, see [9], [11], [14], [15]. As for example $\rho(f)$ denote the order of a meromorphic function f. The growth of the solution of complex linear differential equation and difference equation have been studied by many numerous researchers since 1960s. Based on the Nevanlinna value distribution theory, some result on the growth of all transcendental entire solutions has been found in [2]. Nevanlinna value distribution theory and the maximum modulus principle have been used to examine the zero problems of second order algebraic differential equations with meromorphic coefficients in [13]. The fundamental theorem of Nevanlinna has been used to explore the problems of certain kinds of complex differential equations [1].

In the year 1986 langley [12] consider the differential equation

$$(1.1) f^{(2)} + Ae^{-z}f^{(1)} + Q(z)f = 0$$

and obtained the following results.

Theorem A. [12] Let Q(z) be a non-constant polynomial. Then all non-trivial solutions of equation (1.1) have infinite order, where A is any non-zero constant.

^{3.} Corresponding Author

Gunderson [7] established the following for the situation when Q(z) is a transcendental entire function.

Theorem B. [7]Consider a transcendental entire function Q(z) with order $\rho(Q) \neq 1$, then every non-zero solution of the equation

$$f^{(2)} + e^{-z}f^{(1)} + Q(z)f = 0$$

has infinite order.

Using the previously mentioned concept, Chen [3] takes a look at the differential equation of the form

$$f^{(2)} + A_1(z) e^{az} f^{(1)} + A_0(z) e^{bz} f = 0$$

and got the following results.

Theorem C. [3] Let $A_j(z) (\neq 0) (j = 0, 1)$ be entire functions with $\rho(A_j) < 1$, a, b are complex constants such that $ab \neq 0$ and a = cb (c > 1), then every non-zero solution of equation (1.2) has infinite order.

Theorem D. [3] Let $A_j(z) \neq 0$, $D_j(z)$ be entire functions with $\rho(A_j) < 1$, $\rho(D_j) < 1$, a, b are complex constants such that $ab \neq 0$ and $\arg a \neq \arg b$ or $a = cb \ (0 < c < 1)$, then every non-zero solution of equation

$$f^{(2)} + (A_1(z)e^{az} + D_1)f^{(1)} + (A_0(z)e^{bz} + D_2)f = 0$$

has infinite order.

In the recent year 2023, He and Gao [10] consider n - th order differential equation instead of second order differential equation of the form

$$(1.3) f^{(n)} + A_{n-1}e^{a_{n-1}z^m}f^{(n-1)} + ... + A_1e^{a_1z^m}f^{(1)} + A_0e^{a_0z^m}f = 0$$

and improved the result of Chen [3] as follows:

Theorem E. [10]Let $A_j(z)$ (j = 0, 1, ..., (n - 1)) are meromorphic functions and a_j are complex constants such that $\rho(A_j) < m \ (\forall \ j = 0, 1, ..., (n - 1))$. Then all the non-zero solutions of equation (1,3) have infinite order.

The shift version of Nevanlinna theory was investigated by Hulburd-Korhonen [8], Chiang-Feng [5] and numerous other researchers and produce some remarkable results. Now, a natural question arises: "Is the conclusion of Theorem E still valid if we apply shift on the equation (1.3)?" Applying shift, the equation (1.3) takes the form

$$(1.4) f^{(n)}(z + \xi_n) + A_{n-1}e^{P_{n-1}(z)}f^{(n-1)}(z + \xi_{n-1}) + ... + A_0e^{P_0(z)}f(z + \xi_0) = 0$$

where $\xi_i(\neq 0)$ (i=0,1,...,n) are complex constants and $P_i(z)$ (i=0,1,...,(n-1)) are the polynomial of degree $m \geq 1$ with $\rho(A_j) < m \ (\forall \ j=0,1,...,(n-1))$.

Unfortunately, the answer to the above question is no. The following counter-example supports our claim.

Example 1. The function $f(z) = e^{z^3}$ satisfies the equation

$$f^{(3)}(z+1) + A_2e^{P_2(z)}f^{(2)}(z-1) + A_1e^{P_1(z)}f^{(1)}(z-i) + A_0e^{P_0(z)}f(z+i) = 0$$

where

$$\begin{array}{lcl} A_{2}\left(z\right) & = & -3z^{2}+2z, \ P_{2}\left(z\right)=6z^{2} \\ \\ A_{1}\left(z\right) & = & -54z^{3}-108iz^{2}+54z, \ P_{1}\left(z\right)=3iz^{2}+3z^{2}+6z-i+1 \\ \\ A_{0}\left(z\right) & = & 504z^{4}-270z^{3}-567z^{2}-162z+61, \ P_{0}\left(z\right)=-3iz^{2}+3z^{2}+6z+i+1 \end{array}$$

But $\rho(f) = 3$, which is finite.

We now present the main result of our paper.

Theorem 1. Let A_j (z) (j = 0, 1, ..., (n - 1)) are meromorphic functions, $\xi_j \neq 0$ (j = 0, 1, ..., n)are complex constants and P_j (z) (j = 0, 1, ..., (n - 1)) are the polynomial of degree $m \geq 1$ such that $\rho(A_j) < m \ (\forall \ j = 0, 1, ..., (n - 1))$. Then every non-zero solutions f of equation (1.4)satisfy $\rho(f) \geq m + 1$.

Remark 1. The conclusion of the above theorem may not be true if we relax the condition $\rho(A_j) < m \ (\forall j = 0, 1, ..., (n-1))$. To support this let us consider the following example.

Example 2. The equation

$$f^{(2)}(z-2i) + A_1e^{P_1(z)}f^{(1)}(z+i) + A_0e^{P_0(z)}f(z+1) = 0$$

is satisfied by the function $f(z) = e^{2z^2}$, where

$$A_1(z) = (-4z)e^{-z^2-5iz-2}, P_1(z) = z^2-7iz-4$$

 $A_0(z) = (80iz+60)e^{3z^2-(3i+1)z-3}, P_0(z) = -3z^2-(5i+3)z-7.$

Here we see that $\rho(A_0) = \rho(A_1) = 2$ and $\deg(P_j) = 2(j = 0,1)$. Which does not satisfy the condition of the above theorem. So the conclusion of the above theorem is not true as $\rho(f) = 2 \not \geq 2 + 1$.

2. Lemmas

Several lemmas that will be required later are presented in this section.

Lemma 2. [3] Let $P(z) = (\alpha + i\beta) z^n + (\alpha + i\beta) z^{n-1} + ... + (\alpha + i\beta) z + (\alpha + i\beta)$, $\alpha, \beta \in \mathbb{R}$ such that $|\alpha| + |\beta| \neq 0$, is a polynomial of degree n and A(z) is a meromorphic function of order less than n. Then for the function $g(z) = A(z) e^{P(z)}$, $z = re^{i\theta}$, $\delta(P, \theta) = \alpha \cos n\theta - \beta \sin n\theta$, there exist sets $H_1 \subset [0, 2\pi)$ that has linear measure zero and $H_2 = \{\theta \in [0, 2\pi); \delta(P, \theta) = 0\}$ and R > 1 such that for all |z| = r > R and for all $\theta \in [0, 2\pi) \setminus \{H_1 \cup H_2\}$, we have

(i)
$$\exp\{(1-\varepsilon)\delta(P,\theta)r^n\}$$
 $< g(re^{i\theta}) < \exp\{(1+\varepsilon)\delta(P,\theta)r^n\}$, when $\delta(P,\theta) > 0$
and

$$(ii) \; \exp\left\{ (1+\varepsilon) \, \delta\left(P,\theta\right) r^n \right\} \; < \; g\left(re^{i\theta}\right) < \exp\left\{ (1-\varepsilon) \, \delta\left(P,\theta\right) r^n \right\}, \; when \; \delta\left(P,\theta\right) < 0.$$

Lemma 3. [6]Let f(z) be a transcendental meromorphic function of finite order ρ and $\varepsilon > 0$ be a given constant. Then, there exist a subset $E \subset (1, \infty)$ that has finite logarithmic measure, such that for all z satisfying $|z| = r \notin [0, 1] \cup E$, and for all $k, j, 0 \le j < k$, we have

$$\left|\frac{f^{(k)}\left(z\right)}{f^{(j)}\left(z\right)}\right| \leq r^{(k-j)(\rho-1+\varepsilon)}.$$

Lemma 4. [4]Let f(z) be a meromorphic function of finite order ρ and $\varepsilon > 0$ be any given constant. Then, there exist a subset $E \subset (1, \infty)$ that has finite linear measure or finite logarithmic measure, such that

$$|f(z)| \le e^{r^{p+s}}$$

holds for all z satisfying $|z| = r \notin [0, 1] \cup E$ as $r \to \infty$.

Lemma 5. [5]Let η_1, η_2 be two arbitrary complex constant and let f(z) be a meromorphic function of finite order ρ and $\varepsilon > 0$ be a given constant. Then, there exist a subset $E \subset (1, \infty)$ that has finite logarithmic measure, such that for all z satisfying $|z| = r \notin [0, 1] \cup E$, the following double inequality holds

$$e^{-r^{\rho-1+s}} \le \left| \frac{f(z+\eta_1)}{f(z+\eta_2)} \right| \le e^{r^{\rho-1+s}}.$$

3. PROOF OF THEOREM

We will proof the theorem by contradiction.

Let us assume that all the solution of the equation (1.4) are transcendental meromorphic function of order $0 < \rho < k + 1$. Let $Q_0(z) = (\gamma_0 + i\delta_0) z^m + (\gamma_0 + i\delta_0) z^{m-1} + ... + (\gamma_0 + i\delta_0)$ be the polynomial among $P_j(z) = (\alpha_j + i\beta_j) z^m + (\alpha_j + i\beta_j) z^{m-1} + ... + (\alpha_j + i\beta_j)$, j =1, 2, ..., n - 1, which satisfies

$$\delta\left(Q_{0}, \theta\right) = \max_{1 \leq j \leq n-1} \delta\left(P_{j}, \theta\right), \ z = re^{i\theta}.$$

Then two cases may arise.

Case-1 : Let $\alpha_0 + i\beta_0$ and $\gamma_0 + i\delta_0$ satisfy $\arg(\alpha_0 + i\beta_0) \neq \arg(\gamma_0 + i\delta_0)$. Then there exist $\varepsilon > 0$ and a ray $\arg z = \theta$ such that for all $\theta \in [0, 2\pi) \setminus \{E_1 \cup H_1 \cup H_2\}$,

$$\delta(P_0, \theta) > 0$$
 and $\delta(P_j, \theta) < 0$, for all $j = 1, 2, ..., n - 1$.

Where $E_1 \cup H_1 \cup H_2$ has linear measure zero with $E_1 \subset (1, \infty)$, $H_1 = \{\theta \in [0, 2\pi); \delta(Q_0, \theta) = 0\}$ and $H_2 = \{\theta \in [0, 2\pi); \delta(P_0, \theta) = 0\}$. Therefore by Lemma 2, we have

$$\left| A_{k}(z) e^{P_{k}(z)} \right| \leq \exp \left\{ (1 - \varepsilon) \delta(P_{k}, \theta) r^{m} \right\}, \quad k = 1, 2, ..., n - 1$$

and

(3.2)
$$|A_0(z)e^{P_0(z)}| \ge \exp\{(1-\varepsilon)\delta(P_0, \theta)r^m\}$$

Now from equation (1.4),

$$\begin{split} \left| A_0(z) e^{P_0(z)} \right| & \leq \left| \frac{f^n(z + \xi_n)}{f(z + \xi_0)} \right| + \left| \sum_{k=1}^{n-1} \frac{f^k(z + \xi_k)}{f(z + \xi_0)} A_k(z) e^{P_0(z)} \right| \\ & = \left| \frac{f^n(z + \xi_n) f(z + \xi_n)}{f(z + \xi_n) f(z + \xi_0)} \right| + \left| \sum_{k=1}^{n-1} \frac{f^k(z + \xi_k) f(z + \xi_k)}{f(z + \xi_k)} A_k(z) e^{P_0(z)} \right|, \end{split}$$

Now using Lemma 3, Lemma 5 and (3.1) we have,

$$|A_0(z)e^{P_0(z)}| \leq r^{n(\rho-1+\varepsilon)}e^{r^{(\rho-1+\varepsilon)}} + r^{(n-1)(\rho-1+\varepsilon)}e^{r^{(\rho-1+\varepsilon)}}\exp\{(1-\varepsilon)\delta(P_{n-1},\theta)r^m\} + \dots + r^{(\rho-1+\varepsilon)}e^{r^{(\rho-1+\varepsilon)}}\exp\{(1-\varepsilon)\delta(P_1,\theta)r^m\}$$

$$\leq nr^{n(\rho-1+\varepsilon)}e^{r^{(\rho-1+\varepsilon)}}\exp\{(1-\varepsilon)\delta(Q_0,\theta)r^m\},$$
(3.3)

Hence from (3.2) and (3.3) we have,

$$\exp \{(1 - \varepsilon) \delta(P_0, \theta) r^m\}$$
 $\leq nr^{n(\rho - 1 + \varepsilon)} e^{r^{(\rho - 1 + \varepsilon)}} \exp \{(1 - \varepsilon) \delta(Q_0, \theta) r^m\}$
or, $(1 - \varepsilon) \delta(P_0, \theta) r^m \leq \log n + n (\rho - 1 + \varepsilon) \log r + r^{(\rho - 1 + \varepsilon)} + (1 - \varepsilon) \delta(Q_0, \theta) r^m$
or, $(1 - \varepsilon) \delta(P_0, \theta) \leq \frac{\log n}{r^m} + \frac{n (\rho - 1 + \varepsilon) \log r}{r^m} + \frac{r^{(\rho - 1 + \varepsilon)}}{r^m} + (1 - \varepsilon) \delta(Q_0, \theta)$

Which contradict the fact that $\delta(P_0, \theta) > 0$, if the arbitrary chosen $\varepsilon \in (0, 1)$.

Case-2: Let $\alpha_0 + i\beta_0$ and $\gamma_0 + i\delta_0$ satisfy $(\gamma_0 + i\delta_0) = c(\alpha_0 + i\beta_0)$, where 0 < c < 1. Then obviously $\delta(Q_0, \theta) = c\delta(P_0, \theta)$ and there exist a ray $\arg z = \theta$ for which

$$\delta(Q_0, \theta) = c\delta(P_0, \theta) > 0$$

holds. Therefore by Lemma 2, we have

$$\left|A_{k}(z) e^{P_{n}(z)}\right| \leq \exp \left\{(1 + \varepsilon) \delta(P_{k}, \theta) r^{m}\right\}, k = 0, 1, 2, ..., n - 1$$

Hence from equation (1.4), using (3.2) and (3.4), we get

$$\exp\left\{\left(1-\varepsilon\right)\delta\left(P_{0},\theta\right)r^{m}\right\} \leq \left|A_{0}e^{P_{0}\left(z\right)}\right| \leq nr^{n(\rho-1+\varepsilon)}e^{r^{(\rho-1+\varepsilon)}}\exp\left\{\left(1+\varepsilon\right)\delta\left(Q_{0},\theta\right)r^{m}\right\}$$

which is a contradiction if we choose arbitrary $\varepsilon = \frac{1-c}{1+c}, \ c \in (0,1)$.

We now claim that any solution of equation (1.4) with finite order can not have polynomial structure. If possible let f(z) be a solution of equation (1.4), which is a polynomial of degree d. In this case two the following possibilities may arise: Case-3: For a given integer t, if $d \ge t$, then there exist a ray $\arg z = \theta$ for which

$$\delta(P_j, \theta) > 0$$
, for all $j = 0, 1, ..., n - 1$.

Therefore by Lemma 2, we have

$$\left|A_{t}e^{P_{t}(z)}\right| \geq \exp\left\{\left(1-\varepsilon\right)\delta\left(P_{t},\theta\right)r^{m}\right\}.$$

Now equation (1.4) can be written as,

$$A_{t}e^{P_{t}(z)}f^{(t)}(z + \xi_{t}) = [f^{(n)}(z + \xi_{n}) + A_{n-1}e^{P_{n-1}(z)}f^{(n-1)}(z + \xi_{n-1})$$

$$+ ... + A_{t-1}e^{P_{t-1}(z)}f^{(t-1)}(z + \xi_{t-1}) + A_{t+1}e^{P_{t+1}(z)}f^{(t+1)}(z + \xi_{t+1})$$

$$+ ... + A_{0}e^{P_{0}(z)}f(z + \xi_{0})]$$
(3.6)

Hence combining (3.4), (3.5) and (3.6), we get

$$\exp \{(1 - \varepsilon) \delta(P_t, \theta) r^m\} r^{d-t} \le r^{d-n} M_1 + \exp \{(1 + \varepsilon) \delta(P_{n-1}, \theta) r^m\} r^{d-n+1} M_2 + ...$$

 $+ \exp \{(1 + \varepsilon) \delta(P_0, \theta) r^m\} r^d M_{n-1}$
 $\le nr^d \exp \{(1 + \varepsilon) \delta(P, \theta) r^m\} \max_{1 \le j \le n-1} M_j,$
(3.7)

where $\delta(P_t, \theta) > \delta(P, \theta) = \max_{0 \le j \le n-1, j \ne i} \delta(P_j, \theta)$ is a specified constant with regard to the polynomial coefficient.

Now choosing $0 < \varepsilon < \frac{\delta(P_t,\theta) - \delta(P_t,\theta)}{\delta(P_t,\theta) + \delta(P_t,\theta)}$, we have a contradiction with (3.7) as $r \to \infty$.

Case-4: For a given integer t, if d < t, then there exist a ray $\arg z = \theta$ for which

$$\delta(P_0, \theta) > 0$$
 and $\delta(P_j, \theta) < 0$, for all $j = 1, 2, ..., n - 1$

holds.

Note that in this case equation (1.4) can be written as,

$$A_d e^{P_d(z)} f^{(d)}(z + \xi_d) + ... + A_1 e^{P_1(z)} f^{(1)}(z + \xi_1) + A_0 e^{P_0(z)} f(z + \xi_0) = 0.$$

Now using the same method discuss above, we can get

$$r^{d} \exp \{(1 - \varepsilon) \delta(P_0, \theta) r^m\} M_{n-1} \le dr^{d} \exp \{(1 + \varepsilon) \delta(Q_0, \theta) r^m\} \max_{1 \le j \le t} M_j$$

which give us a contradiction if we choose $0 < \varepsilon < \frac{\delta(P_0,\theta) - \delta(Q_0,\theta)}{\delta(P_0,\theta) + \delta(Q_0,\theta)}$.

Therefore we can conclude that f(z) cannot be a polynomial. Hence all non-zero solutions f of equation (1.4) satisfy $\rho(f) \ge m + 1$.

4. STATEMENTS AND DECLARATIONS

Conflict of interest

Authors declares that we have no conflict of interest.

Funding

For the first author this research is supported by the Council of Scientific and Industrial Research (CSIR-HRDG), India, Grant No. 09/025(0255)/2018-EMR-I.

Ethical approval

This article does not contain any studies with human participants or animals performed by any of the authors.

Data Availability

Not applicable.

5. ACKNOWLEDGEMENT

The first author is thankful to the Council of Scientific and Industrial Research (CSIR-HRDG), India, Grant No. 09/025(0255)/2018 – EMR – I for the financial support and the fourth author sincerely acknowledges the financial support rendered by DST-FIST 2024 – 2025 running at the Department of Mathematics, University of Kalyani, P.O.: Kalyani, Dist: Nadia, Pin: 741235, West Bengal, India.

REFERENCES

- Chen JF, Li Z, Transcendental meromorphic solutions of certain types of differential equations, J. Math. Anal Appl. 2022;515(1): 126463.
- [2] Chen Z.X.Zeros of entire solutions to complex linear differential equations. Acta math sci. 2012;32B (3): 1141 – 1148.
- [3] Chen Z.X., The growth of solutions of f" + e^{-s}f' + Q(z) f = 0 where the order (Q) = 1. SCIENCE IN CHAINA (Series A) 2002; 45 (3), 290 - 300.
- [4] Chen Z.X.The zero, pole and order of meromorphic solutions of differential equations with meromorphic coefficients, Kodai Math. J. 1996, 19, 341 – 354.
- [5] Chiang Y. M., Feng S. J. On the Nevanlinna characteristic of f(z + η) and difference equations in the complex plane, Ramanujan J., 16(1)(2008), 105 – 129.

(Received, September 23, 2024)

- [6] Gundersen, G.G. Estimates for the logarithmic derivative of meromorphic function, plus similar estimate. J. London Math. Soc. 1988, 37, 88 – 104.
- [7] G. G. Gundersen, On the question of whether f" + e^{-z}f' + B(z)f = 0 can admit a solution f(z) ≠ 0 of finite order, Proc., R. S. E. 102A(1986), 9-17.
- [8] Halburd R. G. and Korbonen R. J. Nevanlinna Theory for the Difference Operator, Annales Academiac Scientiarum Fennicae Mathematica, 31(2006), 463-478.
- [9] Hayman W.K. Meromorphic Functions, The Clarendon Press, Oxford (1964).
- [10] Zhongwei he & Lingyun Gao (2023) Interval estimation on hyper-order of meromorphic solutions of complex linear differential equations with uncertain coefficients. Applied Mathematics in Science and Engineering, 31 : 1, 2212117. DOI:10:1080/27690911.2023.2212117
- [11] Holland A.S.B. Introduction to the Theory of Entire Functions, Academic Press, New York and London (1973)
- [12] Langley, J.K., On complex oscillation and a problem of Ozawa, Kodai Math. J., 1986, 9: 430 439.
- [13] Ren G.Z., Gao L.Y. Transcendental meromorphic solutions of systems of second order algebric differential equations. J Chengdu Univ Technol. 2020; 47 (2): 249 - 256.
- [14] Valiron G. Lectures on the General Theory of Integral Functions, Chelsea Publishing Company (1949).
- [15] Yang L. Value distribution theory and new research on it, Science Press, Beijing.

DEPARTMENT OF MATHEMATICS. THE UNIVERSITY OF BURDWAN, GOLAPBAG. BURDWAN, WEST BENGAL, 713104, INDIA

E-mail: pratapsaha33@gmail.com

DEPARTMENT OF MATHEMATICS. UNIVERSITY OF NORTH BENGAL, RAJA RAMMOHUNPUR, P.O.-N.B.U., DAR- JEELING, WEST BENGAL, 734013, INDIA E-mail: stamany@nhu.ac.in

DEPARTMENT OF MATHEMATICS. RAIGANJ SURENDRANATH MAHAVIDYALAYA, P.O.: SUDARSHANPUR, DIST: UTTAR DINAJPUR, PIN: 733134, WEST BENGAL, INDIA E-mail: 3 meghlal.mallik@gmail.com

DEPARTMENT OF MATHEMATICS, UNIVERSITY OF KALYANI, P.O.-KALYANI, DIST-NADIA, PIN-741235, WEST BENGAL, INDIA

E-mail: sanjibdatta05@gmail.com

^{2.} Corresponding Author

Suman Sindhwani

LINEAR AND NON-LINEAR STUDY OF MAGNETO-DIFFUSIVE CONVECTION IN DUFOUR-SORET INDUCED NANOFLUID LAYER

ISSN: 0970-5120

The present paper aims at analytical study of linear and unsteady non-linear Rayleigh Benard triply diffusive magneto convection in a Maxwell nanofluid layer with Dufour -Soret effects. The effects of Dufour parameter, Soret parameter, magnetic field, Lewis number, Modified diffusivity ratio, Concentration Rayleigh-Darcy number and Solutal Rayleigh number on the stability of the system have been investigated. Dufour parameter which was observed to have stabilizing behaviour in absence of magnetic field shows dual nature here in presence of magnetic field. The thermal Nusselt number here decreases with increase in magnetic field resulting in decrease of heat transport. This behaviour is same as was observed for Newtonian fluids.

2010 Mathematics Subject Classification: 76E06, 76E25, 76R50, 80A19, 80A21.

Keywords - Nanofluid, Magnetic field, Double diffusion, Dufour-Soret parameter.

1. Introduction

Heat transfer mechanism has been improved by replacing micro sized particles with nano sized particles in conventional fluids. The term nanofluid was first coined by Choi [5], he described the future and hope of the application of nanotechnology. Kurnur et al. [7] established the utility of a particular nanofluid for its heat transfer application. Wong and Leon [16] focussed on the broad range of present and future applications of nanofluids. The problem of thermal convection for a Newtonian fluid layer was discussed by Chandrasekhar [4] taking varying assumptions of hydro-dynamics and hydro-magnetism.

Maxwell nanofluid taking into account thermophoresis and Brownian diffusion was studied by Jaimala et. al [6]. The study of magnetic field effects on the onset of convection has important applications in physics and engineering. In metal casting and in cooling systems of electronic devices, magnetic field effects are of great importance. The nanofluid can be taken as a working medium in order to get effective heat performance of such devices. Rayleigh Benard Magneto-convection arises due to combined effect of buoyancy force and magnetic field induced Lorentz force. A non-dimensional parameter called Chandrasekhar number gets introduced due to

Shelkhloleslami et al. [11] investigated about the effect of radiation on nanofluid free convective heat transfer in presence of magnetic field. The combined effect of a vertical magnetic field and the boundaries on the onset of convection in an electrically nanofluid layer heated from below was investigated by Agrawal et al. [1]. Effect of magnetic field considering internal heating after filling the space between plates with nanofluid was also studied by Yadav et al. [17]. Non-linear Rayleigh-Benard magnetoconvection in temperature sensitive Newtonian liquids was studied by Aruna [2] demonstrating the diminishing heat transport and stabilization of system with the increasing strength of the magnetic field.

In fluid flow problems, the phenomenon of generation of the concentration flux by temperature gradient is termed as Soret effect and the energy flux caused by a composition gradient is called the Dufour or diffusion thermo effect. Study on the Soret induced convective instability of a regular Newtonian fluid saturated in a porous medium has been done by many researchers. Wang and Tan [15] analysed the convective instability in Benard cells in a non-Newtonian fluid incorporating Soret factor. The impact of Soret parameter induced by the temperature gradient was studied by Singh et al. [13]. Bahlowl et al. [3] and Mansour et al. [8] also have much research work on Soret effect in different forms of fluid layers. Postelnicu [9] and Raiput and Shareef [10] also studied the combined effect of magnetic field and Soret parameter. Recently triple diffusive convection with Soret-Dufour effects in a Maxwell namefluid saturated in Darcy porous medium was studied by Singh et al. [14] demonstrating the effects of different parameters on beat transfer.

Double diffusive magneto convection in nanofluid layers incorporating Soret factor was studied by the author [12] and the effects of all parameters on stability of system were investigated analytically as well as graphically. The literature survey indicates that no study has investigated the effect of magnetic field on triple diffusive convection in a nanofluid layer with Dufour-Soret factor. The present study examines the effect of vertical magnetic field on Dufour-Soret induced triple diffusive convection in a nanofluid layer. To find the behaviour of different parameters in presence of magnetic field, a comparison has been made with Singh et al. [14] and Aruna [2].

2. Mathematical Formulations

We consider a layer of nanofluid confined between two infinite horizontal surfaces separated by a distance a, with z-axis vertically upward. Lower surface is maintained at higher temperature T_i^* and upper surface is maintained

at temperature T_e^* . A uniform vertical magnetic field $M^* = (0, 0, M_0^*)$ is applied (See Fig. 1)

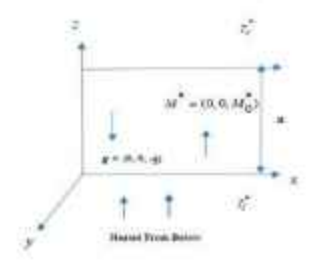


Fig. 1: Physical configuration of the problem

The governing equations for conservation of mass, momentum, energy and concentration of salt and nanoparticles in non-dimensional form on defining

$$(X,Y,Z) = \frac{(x^*,y^*,z^*)}{a}, \quad t = \frac{t^*\alpha_m}{\sigma a^2}, \quad (u_{1d},u_{2d},u_{3d}) = \frac{(u^*_{1d},u^*_{2d},u^*_{3d})a}{\alpha_m}, \quad p = \frac{p^*K}{\mu\alpha_m}, \psi = \frac{\psi^*-\psi^*_0}{\psi^*_0}, \\ (M_X,M_Y,M_Z) = \frac{(M_X^*,M_Y^*,M_Z^*)}{M_0^*}, \quad S = \frac{S^*-S_r^*}{S_r^*-S_r^*}, \quad T = \frac{T^*-T_r^*}{T_r^*-T_r^*}, \quad \lambda = \frac{\lambda^*\alpha_m}{a^2} \quad \text{and} \quad S = \frac{S^*-S_r^*}{S_r^*-S_r^*} \text{ are as }$$

follows:

$$\nabla q = 0$$
, (1)

$$\mathbf{q} = (1 + \frac{\lambda}{\sigma} \frac{\partial}{\partial t}) \left[\left\{ -\nabla p - R_n \hat{\mathbf{e}}_z - R_n \psi \hat{\mathbf{e}}_z + R_n T \hat{\mathbf{e}}_z + \frac{R_s}{Ln} S \hat{\mathbf{e}}_z \right\} + \frac{P_1}{P_{1m}} Q D_a \left(\nabla \times \mathbf{M} \right) \times \mathbf{M} \right], \quad (2)$$

$$\frac{\partial T}{\partial t} + (\mathbf{q}.\nabla)T = \nabla^{2}T + \frac{N_{b}}{Le}\nabla\psi.\nabla T + \frac{N_{a}N_{b}}{Le}\nabla T.\nabla T + N_{k}\nabla^{2}S,$$
(3)

$$\frac{1}{\sigma} \frac{\partial S}{\partial t} + \frac{1}{\epsilon} \mathbf{q} \cdot \nabla S = \frac{1}{Ln} \nabla^2 S + N_{ct} \nabla^2 T , \qquad (4)$$

$$\frac{1}{\sigma} \frac{\partial \psi}{\partial t} + \frac{1}{\epsilon} (\mathbf{q} \cdot \nabla) \psi = \frac{1}{Le} \nabla^2 \psi + \frac{N_a}{Le} \nabla^2 T, \qquad (5)$$

$$\frac{1}{\sigma} \frac{\partial \mathbf{M}}{\partial t} + \frac{1}{\epsilon} (\mathbf{q} \cdot \nabla) \mathbf{M} = \frac{1}{\epsilon} (\mathbf{M} \cdot \nabla) \mathbf{q} + \frac{\mathbf{P}_1}{\mathbf{P}_{1n}} \nabla^2 \mathbf{M} , \qquad (6)$$

Here
$$R_a \left(= \frac{\rho g \beta K a \left(T_i^* - T_r^*\right)}{\mu \alpha_m}\right)$$
, $R_a \left(= \frac{\left(\rho_F - \rho\right) \psi_0^* g K a}{\mu \alpha_m}\right)$, $R_w \left(= \frac{\rho_F \psi_0^* + \rho (1 - \psi_0^*) g K a}{\mu \alpha_m}\right)$

 $R_i (= \frac{\rho \beta_c gaK(S_i^* - S_r^*)}{\mu S_d})$ are thermal, concentration, basic density and solutal Rayleigh Darcy number respectively,

$$P_1(=\frac{\mu}{\rho\alpha_m})$$
 and $P_{1m}(=\frac{\mu}{\rho\eta})$ are Prandtl numbers, $Q(=\frac{\mu_e M_0^2 a^2}{4\pi\mu\eta})$ is Magnetic Chandrasekhar number,

$$D_{\sigma}(=\frac{K}{a^2}) \text{ is Darcy number, } N_{ct}(=\frac{S_{ct}(T_t^*-T_r^*)}{\alpha_m(S_t^*-S_r^*)}) \text{ is Soret parameter, } N_{tt}(=\frac{S_m(S_t^*-S_r^*)}{\alpha_m(T_t^*-T_r^*)}) \text{ is Dufour parameter,}$$

$$N_a (= \frac{B_t (T_t^* - T_t^*)}{B_d T_t^* \psi_0^*})$$
 and $N_b (= \frac{(\rho c)_p \psi_0^* \in}{(\rho c)_p})$ are modified diffusivity ratio and modified particle density increment

respectively, $Le(=\frac{\alpha_m}{B_d})$ and $Ln=\frac{\alpha_m}{S_d}$ are Lewis numbers for nanofluid and salt respectively. The boundary conditions are given as

$$q = 0$$
, $T=1$, $S=1$, $\frac{\partial \psi}{\partial Z} + N_{g} \frac{\partial T}{\partial Z} = 0$ at $Z=0$ (7)

$$q = 0$$
, $T=0$, $S=0$, $\frac{\partial \psi}{\partial Z} + N_n \frac{\partial T}{\partial Z} = 0$ at $Z=1$ (8)

On the basic state, we superimpose perturbations in the form

Let
$$q = q^*$$
, $p = p_{ba} + p^*$, $T = T_{ba} + T^*$, $S = S_{ba} + S^*$, $\psi = \psi_{ba} + \psi^*$, and $M = \hat{e}_Z + M^*$,

where the primes denote infinitesimal small quantities, Ignoring the products of primed quantities and their derivatives, following linearised form of equations is obtained:

$$\left(\frac{1}{\sigma}\frac{\partial}{\partial t} - \frac{P_1}{P_{1m}}\nabla^2\right) \left[\nabla^2 u_3' - \left(1 + \frac{\lambda}{\sigma}\frac{\partial}{\partial t}\right) \left(R_a \nabla_H^2 T' - R_n \nabla_H^2 \psi' + \frac{R_s}{Ln} \nabla_H^2 S'\right)\right] = (1 + \frac{\lambda}{\sigma}\frac{\partial}{\partial t})Q \frac{P_1}{P_{1m}} \frac{D_a}{\epsilon} \nabla^2 \frac{\partial^2 u_3'}{\partial Z^2},$$

$$\frac{\partial T'}{\partial t} - u'_{3} = \nabla^{2} T' - \frac{N_{e} N_{h}}{Le} \frac{\partial T'}{\partial Z} - \frac{N_{h}}{Le} \frac{\partial \phi'}{\partial Z} + N_{e} \nabla^{2} S', \qquad (10)$$

$$\frac{1}{\sigma} \frac{\partial S'}{\partial t} - \frac{u'_3}{\epsilon} = \frac{1}{Ln} \nabla^2 S' + N_{ct} \nabla^2 T'. \qquad (11)$$

$$\frac{1}{\sigma} \frac{\partial \psi'}{\partial t} + \frac{1}{\epsilon} (\mathbf{q'} \cdot \nabla) \psi' + \frac{1}{\epsilon} N_a u'_3 = \frac{1}{Le} \nabla^2 \psi' + \frac{N_a}{Le} \nabla^2 T', \qquad (12)$$

$$u_3' = 0, T' = 0, S' = 0, \frac{\partial \psi'}{\partial Z} + N_{\sigma} \frac{\partial T'}{\partial Z} = 0 \text{ at } Z = 0 \text{ and } Z = 1$$
 (13)

3. Linear Study

Following the linear stability theory by Chandrasekhar [4], the perturbations are taken of the form

$$(\psi', T', u', S') = [\Phi(Z), \Theta(Z), \Omega(Z), \Psi(Z)]e^{\pi + H \mathcal{X} + H \theta'},$$
 (14)

where L and M are dimensionless wave numbers in X and Y directions respectively. On substituting the above values and employing Galerkin method to solve equations (9)-(12) together with the boundary condition (13) and taking first estimation as N=1, we have $\Omega = A_1 \sin \pi Z$, $\Theta = B_1 \sin \pi Z$, $\Phi = -N_u C_1 \sin \pi Z$, $\Psi = D_1 \sin \pi Z$. Taking the determinant of above matrix equation as zero, the following Rayleigh number is obtained

$$R_{o} = \frac{\sigma}{\alpha^{2}} \begin{bmatrix} R_{o}\alpha^{2}(\lambda s + \sigma)(\sigma A\chi^{2} + s)(\sigma \chi^{2} + sLe)(\chi^{2} + s)(\chi^{2}(\in N_{o} - 1) - s) \\ -R_{o}N_{o}\alpha^{2}(\lambda s + \sigma)(A\chi^{2}\sigma + s)[(\chi^{2}\sigma + sLn)(\chi^{2}(\in +Le) + sLe) - \chi^{2}N_{o}Ln\sigma(1 + LeN_{o})] \\ + \frac{(\chi^{2}\sigma + sLn)(\chi^{2}\sigma + sLe)(\chi^{2} + s)(A\sigma\chi^{2} + B\pi^{2}\chi^{2}(\sigma + \lambda s) + s\chi^{2})\{(\chi^{2}\sigma + sLn)(\chi^{2} + s) - \chi^{2}N_{o}N_{o}Ln\sigma(1 + ke) - \chi^{2}N_{o}N_{o}Ln\sigma(1 + ke)\} \\ -(\sigma\chi^{2}(\in +sLn)(\chi^{2} + sLe)(\chi^{2} + sLe)(\chi^{$$

where,
$$A = \frac{P_1}{P_{1m}}$$
, $B = Q \cdot \frac{P_1}{P_{1m}} \cdot \frac{D_a}{\epsilon}$, $\chi^2 = \pi^2 + \alpha^2$.

Taking s=0 in equation (15),

$$R_{\theta}^{u} = \frac{\chi^{2}(\in \chi^{2} + QD_{u}\pi^{2})(1 - LnN_{ur}N_{w}) - R_{u}N_{u}\alpha^{2}\{\in +Le - LnN_{w}(1 + LeN_{ur})\} - R_{s}\alpha^{2}(1 - \in N_{w})}{\alpha^{2}(\in -LnN_{w})}$$

(16)

From equation (16), the minimum Rayleigh number is given at critical wave number

$$\alpha_c = \pi \left(1 + \frac{QD_n}{\epsilon}\right)^{1/4} \ .$$

In absence of magnetic field, result is same as obtained by Singh et al. [14]. Taking $s = i\omega$ in equation (15), we get oscillatory Rayleigh Number.

4. Nonlinear Stability Analysis

To predict the amplitude of convective motion and rate of heat transfer, we discuss the nonlinear stability theory. For simplicity, we consider the case of two-dimensional rolls, assuming all physical entities to be dependent of y. Introducing stream function γ and magnetic potential function ϕ such that

$$u = \frac{\partial \gamma}{\partial Z}, w = -\frac{\partial \gamma}{\partial X}, H_X = \frac{\partial \phi}{\partial Z}, H_Z = -\frac{\partial \phi}{\partial X}$$

Dimensionless equations are

$$\nabla_{i}^{2}\gamma + (1 + \frac{\lambda}{\sigma} \frac{\partial}{\partial t})[(R_{a} \frac{\partial T}{\partial X} + \frac{R_{c}}{\partial X} \frac{\partial S}{\partial X} - R_{a} \frac{\partial \psi}{\partial X}) - \frac{QP_{i}D_{a}}{P_{i}} \frac{\partial}{\partial Z} \nabla_{i}^{2}\phi] = (1 + \frac{\lambda}{\sigma} \frac{\partial}{\partial t}) \frac{QP_{i}D_{a}}{P_{i}} J(\nabla_{i}^{2}\phi, \phi) \quad (17)$$

$$\frac{\partial \gamma}{\partial X} - \nabla_1^2 T + \frac{N_b}{Le} \frac{\partial \psi}{\partial Z} + \frac{N_e N_b}{Le} \frac{\partial T}{\partial Z} = -\frac{\partial T}{\partial t} + J(\gamma, T) + N_w \nabla_1^2 S \qquad (18)$$

$$\frac{1}{\epsilon} \frac{\partial \gamma}{\partial X} - N_{\alpha} \nabla_{1}^{2} T - \frac{1}{L_{B}} \nabla_{1}^{2} S = -\frac{1}{\sigma} \frac{\partial S}{\partial t} + \frac{1}{\epsilon} J(\gamma, S)$$
(19)

$$-\frac{N_u}{\epsilon} \frac{\partial \gamma}{\partial X} - \frac{N_o}{Le} \nabla_i^2 T - \frac{1}{Le} \nabla_i^2 \psi = -\frac{1}{\sigma} \frac{\partial \psi}{\partial t} + \frac{1}{\epsilon} J(\gamma, \psi) \qquad (20)$$

$$\frac{1}{\epsilon} \frac{\partial \gamma}{\partial Z} + \frac{P_1}{P_{1m}} \nabla_1^2 \phi = \frac{1}{\sigma} \frac{\partial \phi}{\partial t} - \frac{1}{\epsilon} J(\gamma, \phi) \tag{21}$$

where
$$\nabla_1^2 = \frac{\partial^2}{\partial x^2} + \frac{\partial^2}{\partial z^2}$$
.

We solve Eqs. (17) to (21) subjecting them to boundary conditions:

$$\gamma = 0, \frac{\partial^2 \gamma}{\partial Z^2} = 0, T = S = 0, \frac{\partial \Phi}{\partial Z} = 0, \frac{\partial \psi}{\partial Z} + N_\alpha \frac{\partial T}{\partial Z} = 0$$
 (22)

at z=0 and z=1

We take the following Fourier series expression for γ , T, ψ , S, ϕ as

$$y = A_{i,i}(t) \sin \alpha X \sin \pi Z$$

$$T = B_{11}(t)\cos\alpha X \sin\pi Z + B_{02}\sin2\pi Z$$

$$\psi = -N_{\alpha}C_{\alpha t}(t)\cos\alpha X \sin\pi Z - N_{\alpha}C_{\alpha t}(t)\sin2\pi Z$$

$$S = D_{co}(t)\cos\alpha X \sin\pi Z + D_{co}(t)\sin2\pi Z$$

$$\phi = E_{11}(t)\sin\alpha X\cos\pi Z + E_{20}(t)\sin2\alpha X$$

Putting in above equations we get

$$\begin{split} A_{11} &= -\frac{\alpha}{\chi^2} [R_a B_{13} + \frac{R_s}{Ln} D_{11} + R_n N_a C_{11} + \frac{\lambda}{\sigma} (R_a \frac{dB_{11}}{dt} + R_n N_n \frac{dC_{11}}{dt} + \frac{R_s}{Ln} \frac{dD_{11}}{dt})] + Q \frac{P_1}{P_{1m}} D_a \frac{\pi \alpha}{\chi^2} (4\alpha^2 - \chi^2) E_{11} \\ &- Q \frac{P_1}{P_{1m}} D_a \pi E_{11} - \frac{\lambda}{\sigma} Q D_a \pi \frac{P_1}{P_{1m}} \frac{dE_{11}}{dt} + \frac{\lambda}{\sigma} Q \frac{P_1}{P_{1m}} D_a \frac{\pi \alpha}{\chi^2} (4\alpha^2 - \chi^2) [E_{11} \frac{dE_{20}}{dt} + E_{20} \frac{dE_{11}}{dt}] \\ &\frac{dB_{11}}{dt} = -(\alpha A_{11} + \chi^2 B_{11} + \pi \alpha A_{11} B_{02} + \chi^2 D_{11} N_{1c}) \\ &\frac{dB_{02}}{dt} = \frac{1}{2} (\pi \alpha A_{11} B_{11} - 8\pi^2 B_{02} - 8\pi^2 D_{02} N_{1c}) \\ &\frac{dC_{11}}{dt} = -\frac{\sigma}{\epsilon} [\alpha A_{11} + \frac{\chi^2}{Le} (C_{11} - B_{11}) + \pi \alpha A_{11} C_{02}] \end{split}$$

$$\begin{split} \frac{dC_{00}}{dt} &= \frac{\sigma}{2 \in} [\pi \alpha A_{11} C_{11} - \frac{8\pi^2}{Le} (C_{02} - B_{02})] \\ \frac{dD_{11}}{dt} &= -\sigma (\frac{\pi \alpha}{\epsilon} A_{11} D_{02} + \frac{\alpha}{\epsilon} A_{11} + \frac{\chi^2}{Ln} D_{11} + \chi^2 N_{ct} B_{11}) \\ \frac{dD_{00}}{dt} &= \frac{\sigma}{2} [\frac{\pi \alpha}{\epsilon} A_{11} D_{11} - 8\pi^2 (\frac{D_{02}}{Ln} + B_{02} N_{ct})] \\ \frac{dE_{11}}{dt} &= \frac{\sigma}{\epsilon} (\pi A_{11} - \chi^2 \in E_{11} \frac{P_1}{P_{1m}} + \alpha \pi A_{11} E_{20}) \\ \frac{dE_{20}}{dt} &= -\frac{\sigma}{2} (\alpha \pi A_{11} E_{11} + 8\alpha^2 \in \frac{P_1}{P_1} E_{20}) \end{split}$$

5. Heat, Salt and Nanoparticles concentration transport

The thermal Nusselt number, solutal concentration Nusselt number and nanoparticle concentration Nusselt number are given as

$$N(t) = 1 - 2\pi B_{02}(t)$$

 $N_c(t) = 1 - 2\pi D_{02}(t) + N_{cr}(1 - 2\pi B_{02}(t))$
 $N_a(t) = 1 + 2\pi (B_{02}(t) - C_{02}(t))$

6. Results and Discussion

6.1 Linear Stability Analysis

The effects of various parameters on the stability of the system for stationary convection and oscillatory convection were studied in a similar way as done by the author in [12]. It was found that the destabilizing behaviour of Soret parameter in absence of magnetic field [14] does not persist here in presence of magnetic field and converts to the stabilizing agent, whereas Dufour parameter still has a stabilizing behaviour as it was observed in absence of magnetic field [14].

Parameters $D_{a_1} \in Ln$ and Q have been proved to be stabilizing agent in oscillatory convection whereas Le and N_a

proved to advance the onset of convection. The dual behaviour of λ and σ was observed and Soret parameter proved to be a stabilizing agent whereas in absence of magnetic field its dual nature was observed [14]. Dufour parameter has been proved to have its dual effect on oscillatory convection whereas its dual behaviour does not persist in absence of magnetic field [14].

6.2 Nonlinear Stability Analysis

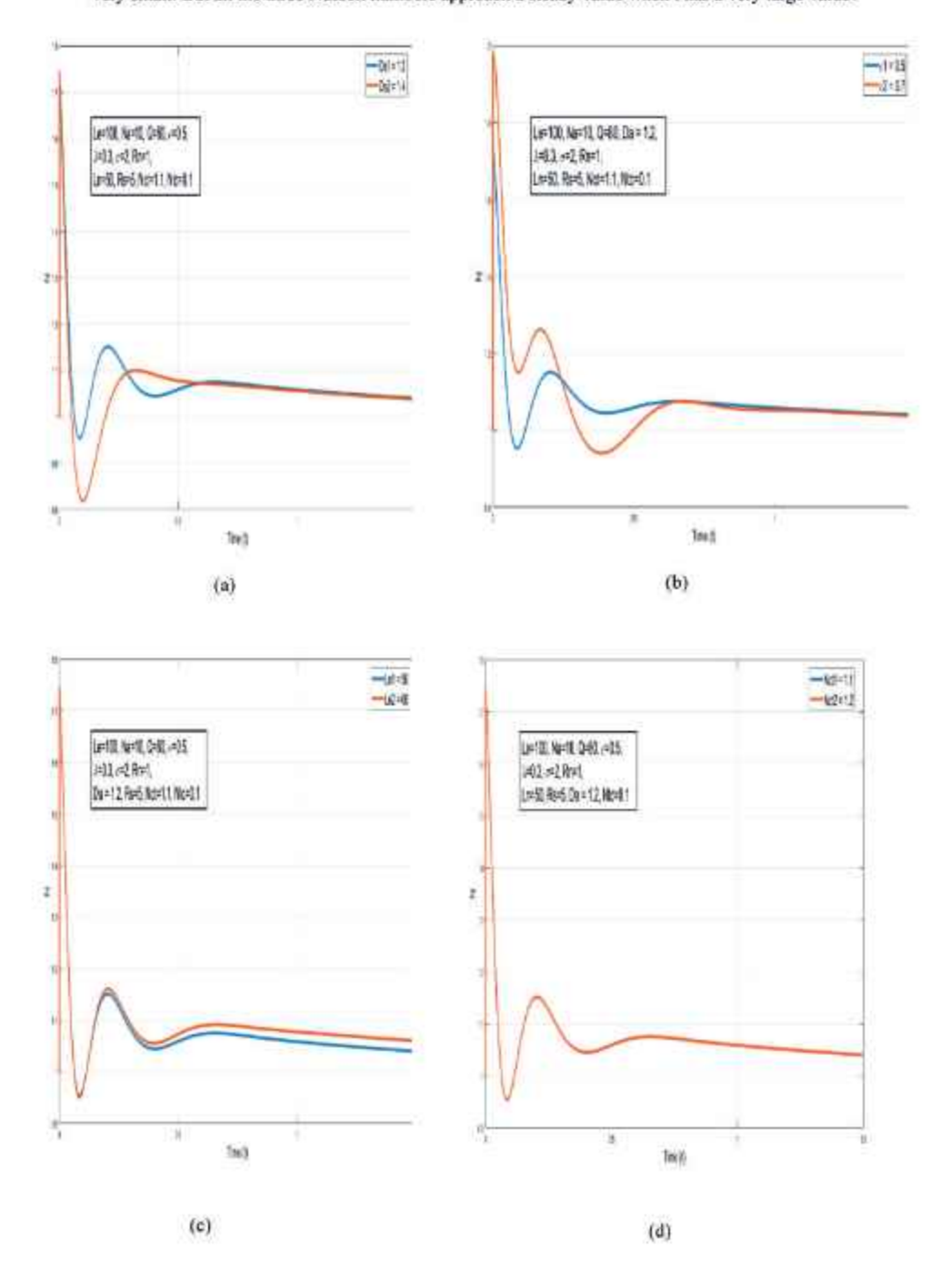
Fig. 2,3,4 depict the transient nature of thermal Nusselt number N(t), concentration Nusselt number $N_c(t)$ and solute Nusselt number $N_p(t)$ respectively with respect to time in the unsteady state of motion. It is evident from all plots that in an initial state the transfer rate of heat, salt and mass is very high and a stationary state is approached after vigorous oscillations. It is clear from fig.2 that none of the parameters except D_a , \in , Ln, N_k and Q have a significant effect on heat transfer. Figure 3 states that the salt transfer is decreased on increase in each parameter except the Dufour parameter N_k . Initially an increase in N_n causes increase in salt transfer but after a certain time the effect gets reversed. Fig.2(i) and 3(i) states that on increasing magnetic field there is retardation in heat transfer as well as salt transfer.

7. Conclusion

This paper presents an analytical study of linear and unsteady non-linear Rayleigh Benard triply diffusive magnetoconvection in a Maxwell nanofluid layer with Soret-Dufour effects, We reach at the following conclusions:

- For the stationary mode the Soret parameter, Dufour parameter and magnetic field have a stabilizing effect.
- For the oscillatory mode the Soret parameter which acts as destabilizing agent in absence of magnetic field
 has been proved to have stabilize the convection and the Dufour parameter which was observed to have
 stabilizing behaviour in absence of magnetic field [14], shows dual nature here in presence of magnetic
 field.
- The thermal Nusselt number here decreases with increase in magnetic field resulting in decrease of heat transport. This behaviour is same as was observed for Newtonian fluids [2].

 The time-effect on transfer of heat, salt and nanoparticle concentration is found to be oscillatory when t is very small. But all the three Nusselt numbers approach a steady value when t has a very large value.



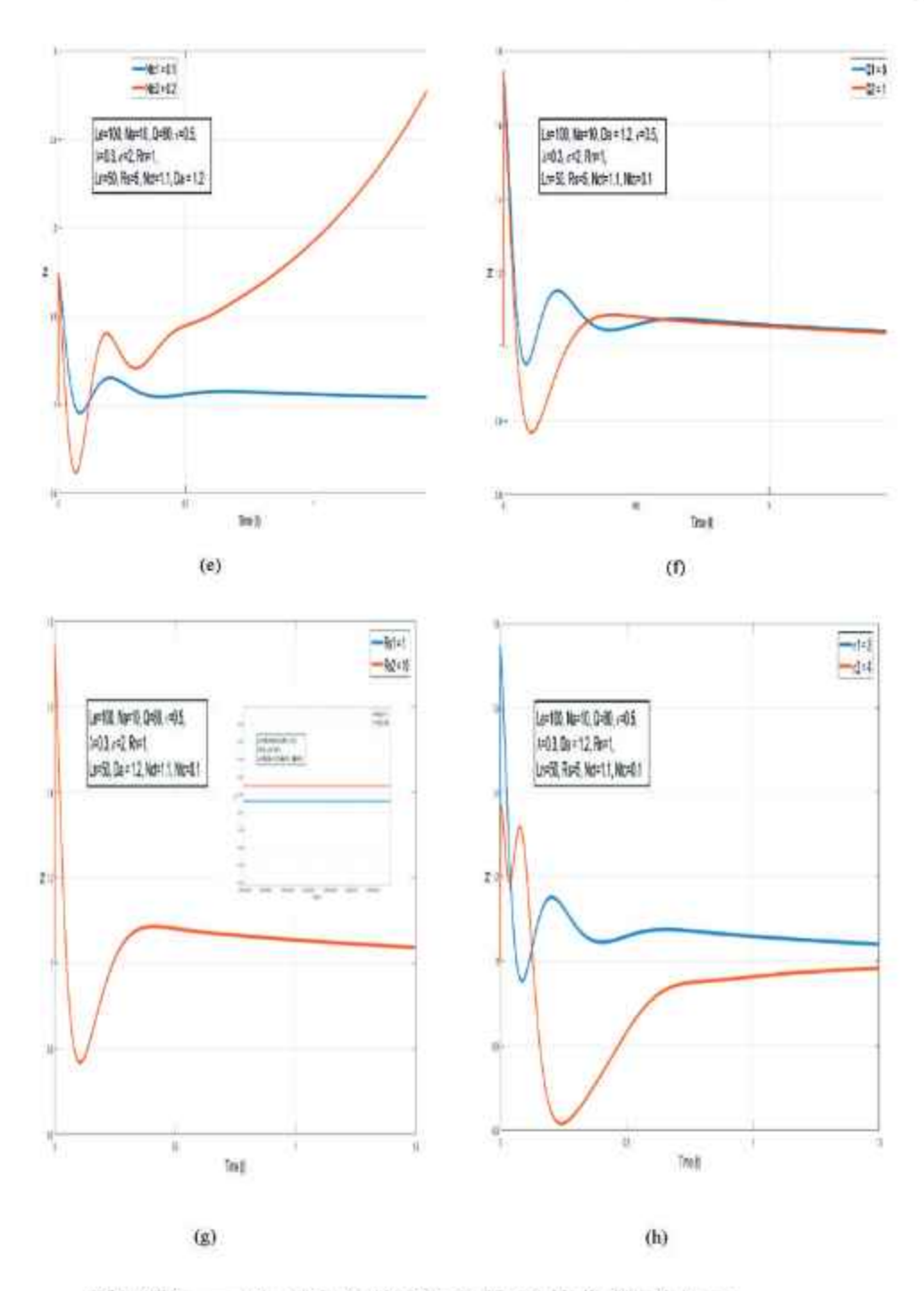
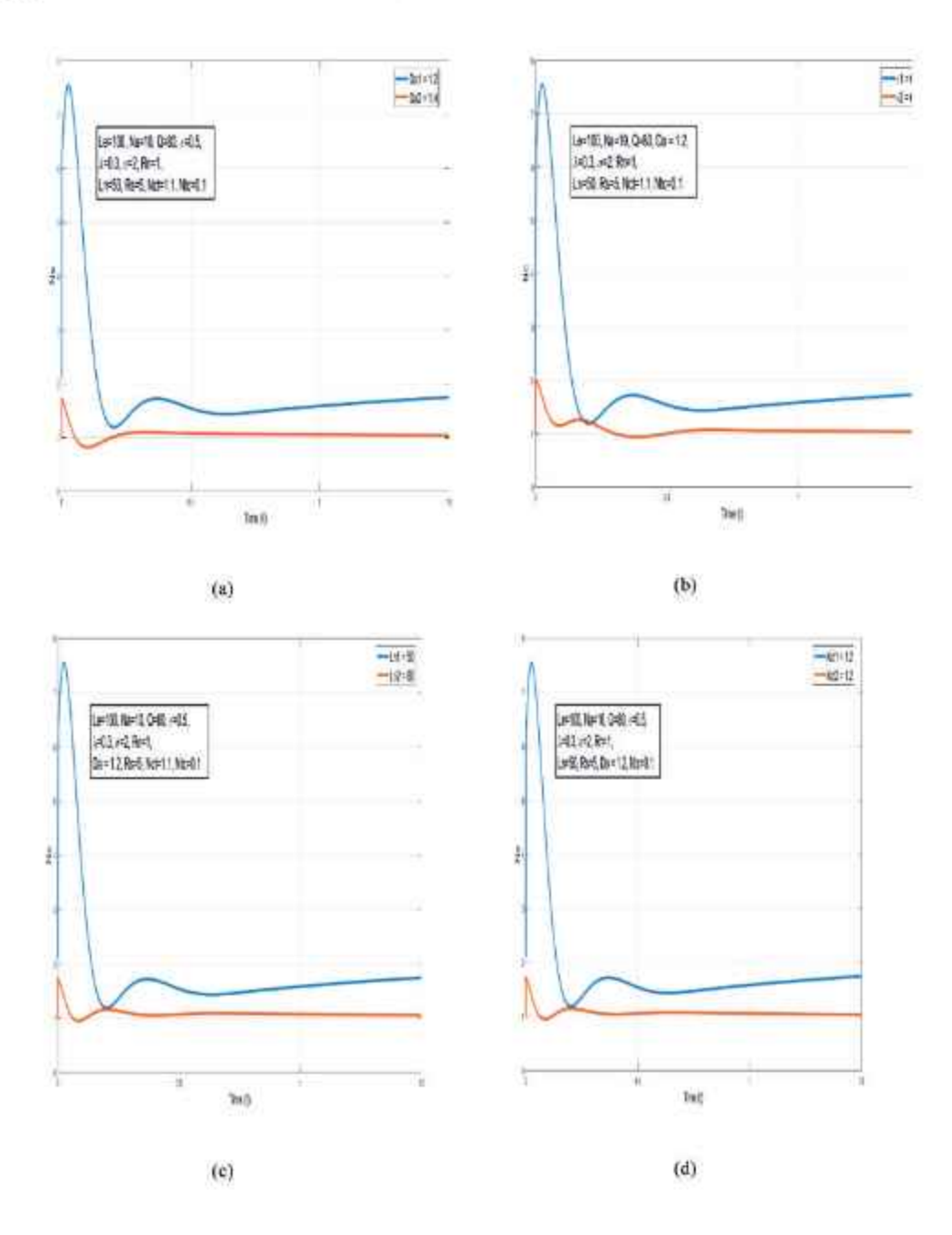
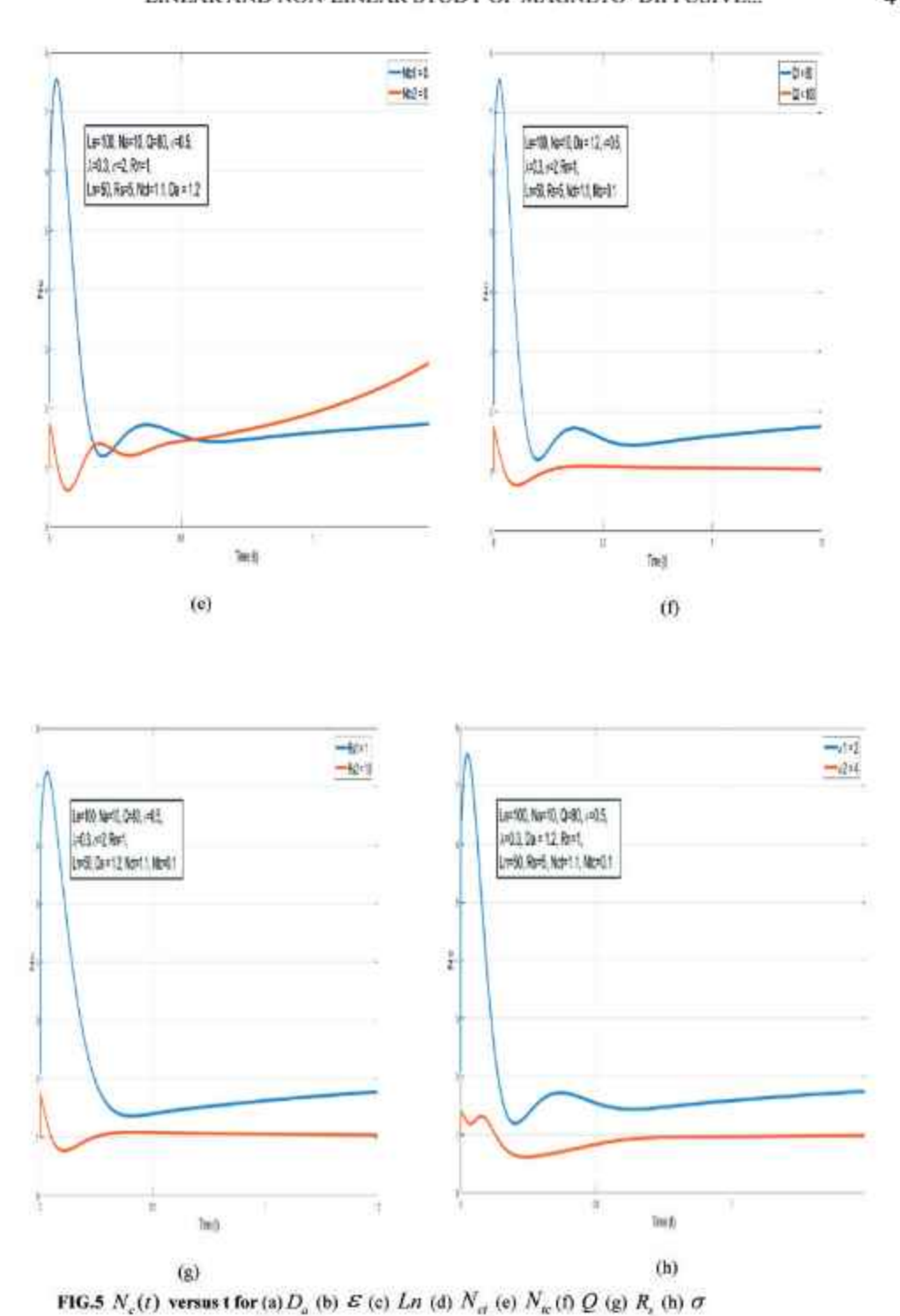
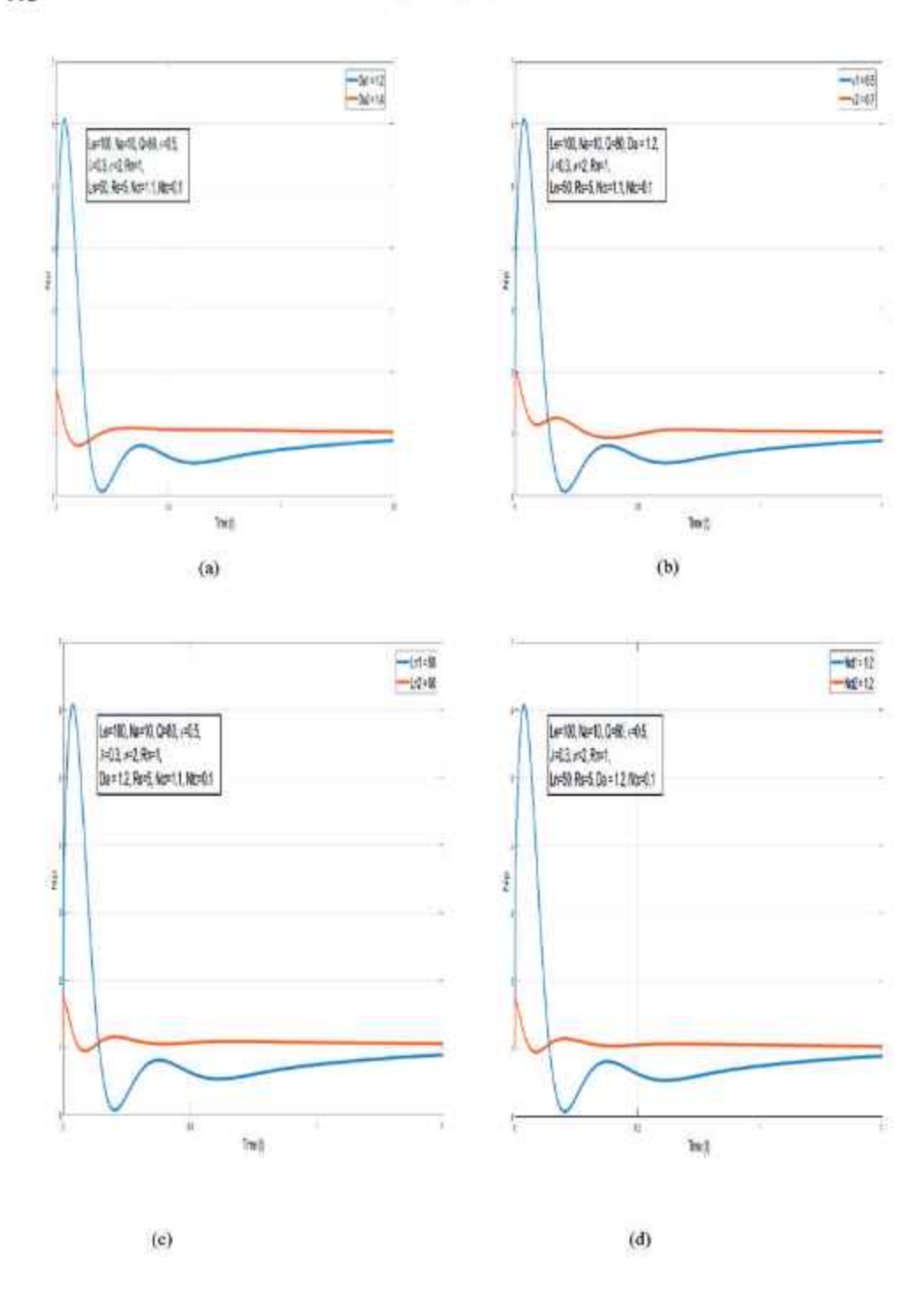


FIG.4 N(t) versus t for (a) D_a (b) \mathcal{E} (c) Ln (d) N_{ct} (e) N_w (f) Q (g) R_s (h) σ







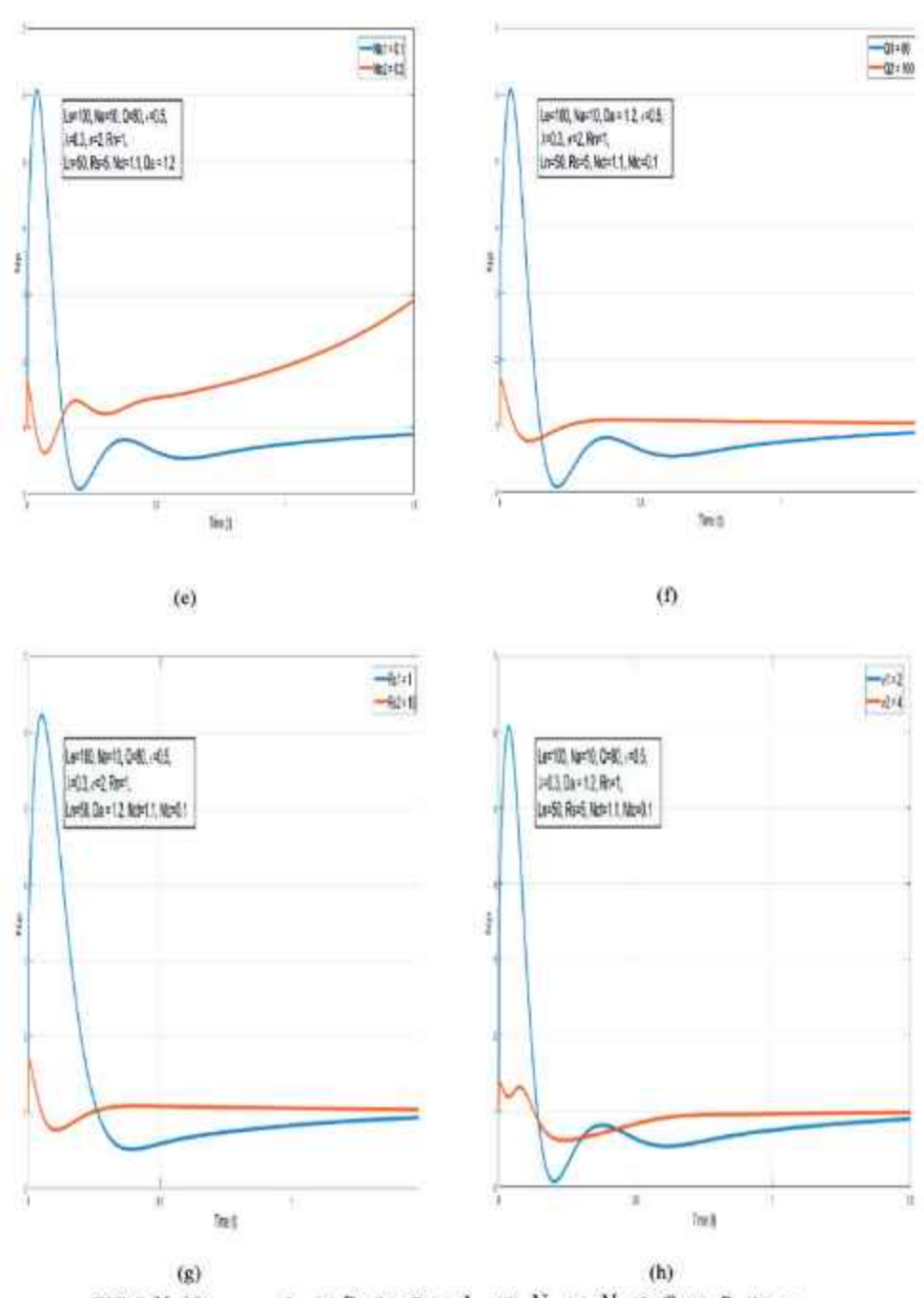


FIG.6 $N_{\mu}(t)$ versus t for (a) D_{μ} (b) \mathcal{E} (c) Ln (d) \tilde{N}_{cl} (e) N_{kl} (f) Q (g) R_{μ} (h) σ

References

- Agarwal, S. N., Sacheti, C., Chandran, P., Bhadauria, B.S., Singh, A. K. (2012): Non-linear convective transport in a binary nanofluid saturated porous layer, *Transport in Porous Media*, Vol. 93, 29-49.
- 2 Aruna, A. S. (2020): Non-linear Rayleigh-Benard magnetoconvection in temperature-sensitive Newtonian liquids with heat source, Pranama- J. Phys. 94:153.
- 3 Bahlowl, A., Boutana, N, Vasseur P. (2003): Double-diffusive and Soret-induced convection in a shallow horizontal porous layer. *Journal of Fluid Mechanics*, 491, 325-352.
- 4 Chandrasekhar, S. (1981): Hydro-dynamic and Hydromagnetic Stability, Dover Publication, New-York.
- 5 Choi, S. (1995): Enhancing thermal conductivity of fluids with nanoparticles, ASME Int. Mech. Eng., 231/MD-66, 90, 105
- 6 Jaimala, Singh, R, Tyagi, V. K. (2017): A macroscopic filtration model for natural convection in a Darcy Maxwell nanofluid saturated porous layer with no nanoparticle flux at the boundary, *International Journal of Heat and Mass Transfer*, 111, 451-466.
- 7 Kumar, S, Prasad, S.K, Banerjee, J. (2010): Analysis of flow and thermal field in nanofluid using a single-phase thermal dispersion model. Applied Mathematics Model, 34, 2010,573-592.
- 8 Mansour, A, Amahmid, A, Hasnaoui, M, Bourich, M. (2006): Multiplicity of solutions induced by thermosolutal convection in a square porous cavity heated from below and submitted to horizontal concentration gradient in the presence of Soret effect. Numerical Heat Transfer, Part A, 69-91.
- 9 Postelnicu, A. (2004): Influence of a magnetic field on heat and mass transfer by natural convection from vertical surfaces in porous media considering Soret and Dufour effects. *International Journal of Heat and Mass Transfer*, 47, 1467-1475.
- 10 Rajput, U.S, Shareef,M. (2018): Study of Soret and Ion slip effects on MHD flow near an oscillating vertical plate in a rotating system. Int. J. AAM, 13,516-534.
- 11 Sheikholeslami, M., Hayat, T., Alsaedi, A. (2016): MHD free convection of Al₂O₃-water nanofluid considering thermal radiation: a numerical study. Int. Heat Mass Transfer. 96, 513-524.
- 12 Sindhwani, S., Gupta, R. (2024): Magneto-Convection and Soret effect in nanofluid layers: A Double Diffusive Perspective. Journal of Indian Acad. Math, 46(2), 133-152.
- 13 Singh, R, Bishnoi, J, Tyagi, V.K. (2019): Onset of Soret driven instability in a Darcy -Maxwell nanofluid. SN Applied Sciences, 1(10), 1-29.
- 14 Singh, R, Bishnoi, J, Tyagi, V.K. (2020): Triple diffusive convection with Soret-Dufour effects in a Maxwell nanoffuld saturated in a Darcy porous medium: SN Applied Sciences, vol. 2, article number 704.
- 15 Wang, S, Tan, W. (2011): Stability analysis of soret-driven double-diffusive convection of Maxwell fluid in a porous medium. *International Journal of Heat and Fluid flow*, 32(1),88-94.
- 16 Wong, V.K, Leon, O.D. (2009): Applications of Nanofluids: Current and Future, Hindawi Publishing Corporation. Advances in Mechanical Engineering, 2010, article ID 519659.
- 17 Yadav, D. Agrawal, G.S. Bhargava, R. (2011): Thermal instability of rotating nanofluid layer. *International Journal of Engineering Science*, vol. 49,1171-1184.

DEPARTMENT OF MATHEMATICS, HINDU GIRLS COLLEGE, SONIPAT, HARYANA, INDIA E-mail: xxindhwani2001@gmail.com (December 16, 2024), (Revised, May 07, 2025)

A. Deepshika', J. Kannan', ON THE MISCELLANEOUS EXPONENTIAL DIOPHANTINE EQUATIONS

ISSN: 0970-5120

Abstract: An exponential Diophantine equation is a particular form of Diophantine equations. Here, we solved the five different representations of exponential Diophantine equations such as $7^x + 47^y = z^2$, $p^z + (p+40)^y = z^2$, $7^x + 168^y = z^2$, $7^x + 282^y = z^2$ and $19.12^x + 19^y = z^2$ where p, p+40 are primes with p>7 and $x, y, z \in \mathbb{Z}^+$. This paper contains the actual solution sets for these equations, together with the proof and python programming is provided.

2020 MSC Classification:11A07, 11D61, 11D72

Keywords: Diophantine equation, Exponential Diophantine equation, Mihailescu's Theorem, congruences.

1 Introduction

An exponential Diophantine equation is a sort of Diophantine equation in which the variables are in the exponent. There are several ways to solve the exponential Diophantine problem, such as the modulo arithmetic approach, the factoring method, method of congruences as in [12, 13]. There has been some interesting study effort on these equations so far [1–6].

Especially, the Diophantine equation $7^x + 7^{2y} = z^2$ was examined by Manju Somanath et.al [9]. William Sobredo Gayo,. Jr. et.al [13] solved the Diophantine equation of the form $M_p^x + (M_q + 1)^y = z^2$ with M_p and $M_q + 1$ are mersenne primes. In [7], Mahalakshmi.et.al. worked on the exponential Diophantine equation over triangular numbers.

This paper has divided into six sections. Section(2) discusses the solvability of the Diophantine equation $7^x + 47^y = z^2$. It is proved that it has no solution on the positive integers x, y, z. In the following section (3), the equation $p^x + (p+40)^y = z^2$ where p > 7 and p + 40 are primes has no positive integer solutions. In section (4), the two forms of Diophantine equations, namely $7^x + 168^y = z^2$ and $7^x + 282^y = z^2$ are solved for all $x, y, z \in \mathbb{Z}^+$. The interesting fact is that the Diophantine equation $7^x + 282^y = z^2$ has exactly one solution and $7^x + 168^y = z^2$ has exactly two solutions. In the final section(5), some theorems are discussed about the solvability of the Diophantine equation $19.12^x + 19^y = z^2$. One only solution exists for this Diophantine equation is the obtained result.

2 The Exponential Diophantine equation $7^x+47^y=z^2$

This section gives various theorems for the solvability of the Diophantine equation $7^y + 47^y = z^2$ over positive integers. Lemma 2.1. (Mihailescu's Theorem) [13] (a, x, b, y) = (3, 2, 2, 3) is the unique solution for the exponential Diophantine equation $a^x - b^y = 1$, where $a, b, x, y \in \mathbb{Z}$ such that $min\{a, b, x, y\} \ge 2$.

Theorem 2.1. The Diophantine equation $7^x + 47^y = z^2$ has no solution in positive integers x, y and z with x and y are of same parity.

Proof. Here 7^x and 47^y are odd then $7^x + 47^y$ is even which implies z^2 is even.

- Case (i) Suppose x and y are even. Let x=2k, and y=2s, where $k \ge 1, s \ge 1$. Then, $7^x + 47^y \equiv 2 \pmod 4$ implies $z^2 = 2 \pmod 4$ which is a contradiction.
- Case (ii) Suppose x and y are odd Let x = 2k + 1 and y = 2s + 1, k, s ≥ 0.
 7^x + 47^y ≡ -2 (mod 4). We get z² = -2 (mod 4) Again we get a contradiction. Hence 7^x + 47^y = z² has no solution in positive integers x and y of same parity.

Theorem 2.2. The Diophantine equation $7^x+47^y=z^2$ has no solution $\forall x, y, z \in Z^+$ with x and y of different parity.

Proof. Consider the equation $7^x + 47^y = z^2$ Now x is even and y is odd. Take $x = 2k, k \ge 1$ and $y = 2s + 1, s \ge 0$. The equation $7^s + 47^y = z^2$ becomes $7^{2k} + 47^{2s+1} = z^2$ and it changes into $(z - 7^k)(z + 7^k) = 47^{2s+1}$. Then there exist a non-negative positive integer α , β such that $47^\alpha = z - 7^k$ and $47^\beta = z + 7^k$ where $\alpha < \beta$ and $\alpha + \beta = 2s + 1$. Now $2.7^k = 47^\beta - 47^\alpha = 47^\alpha (47^{\beta + \alpha} - 1)$ which implies $\alpha = 0$. Then we get $2.7^k = 47^{2s+1} - 1$. For s = 0, this is impossible, and for s > 1, we have $7^k = 23(47^{2s} + 47^{2s-1} + \cdots + 47 + 1)$ which is an impossible. Suppose x is odd and y is even and choose $x = 2k + 1, k \ge 0$ and $y = 2s, s \ge 1$. The given equation becomes $7^{2k+1} = (z + 47^s)(z - 47^s)$. Then there exists $\alpha, \beta \in Z^+ \cup \{0\}$ such that $7^\alpha = z - 47^s$ and $7^\beta = z + 47^s$ with $\alpha < \beta$ and $\alpha + \beta = 2k + 1$. Now $2.47^s = 7^\beta - 7^\alpha$ becomes $2.47^s = 7^{2k+1} - 1$. The above equality fails for k = 0 and for k > 1, the equality $2.47^s = 7^{2k+1}$ changes into $47^s = 3(7^{2k} + 7^{2k-1} + \cdots + 7 + 1)$ which is not possible. The given Diophantine's equation has no solution for $x, y, z \in Z^+$

3 The Exponential Diophantine equation $p^x + (p + 40)^y = z^2$

This section discusses the solvability of the special form of the Diophantine equation $p^x + (p + 40)^y = z^2$ where p(>7) and p + 40 are primes.

Theorem 3.1. The Diophantine equation $p^x + (p + 40)^y = z^2$ where p > 7 and p + 40 are primes, has no solution in positive integers x, y and z with x and y are of opposite parity.

Proof. Suppose x is even $(x = 2k, k \ge 1)$ and y is odd $(y = 2s + 1, s \ge 0)$. Then $p^{z} + (p + 40)^{y} = z^{2}$ is equivalent to $(p + 40)^{2s+1} = (z + p^{k})(z - p^{k})$. Thus there exists non-negative integers α and β such that $(p + 40)^{\alpha} = (z - p^k)$ and $(p + 40^{\beta}) = (z + p^{k})$ where $\alpha < \beta$ and $\alpha + \beta = 2s + 1$. By solving, the above two equations becomes $2p^k = (p+40)^{\alpha}[(p+40)^{\beta-\alpha}-1]$. This implies $\alpha=0$ and therefore $2p^k = (p + 40)^{2s+1} - 1$. When s = 0, $p + 39 = 2p^k \implies p(2p^{k-1} - 1) = 39$, we obtain p = 39 and k = 1, which is a contradiction as p is prime. For $s \ge 1$, $2p^k = (p+40)^{2s} - 1 = (p+39)[(p+40)^{2s} + \cdots + (p+40) + 1]$. Here $p+39 = 2p^j$, where j is an integer such that $0 \le j < k$. For j = 0, p + 39 = 2 which is an abstract one. For $1 \le j < k$, $p+39 = 2p^j$ and so $p(2p^{j-1}-1) = 39$, which is not possible. Suppose x is odd and y is even, i.e. x = 2k+1, $k \ge 0$ and y = 2s, $s \ge 1$, then $p^x + (p+40)^y = z^2$ is equivalent to $p^{2k+1} = (z + (p+40)^s)(z - (p+40)^s)$. As same in the above case we obtain $2(p+40)^s = p^{\alpha}(p^{\beta-\alpha}-1)$, which implies $\alpha = 0$. Thus $2(p+40)^s = p^{2k+1}-1$. Now for k = 0, $2(p + 40)^s = p - 1 \implies [2(p + 40)^s] + 41 = p + 40$ which is an impossible (s > 1) Now k > 1, $2(p + 40)^n = (p - 1)(p^{2k} + p^{2k-1} + \cdots + p + 1)$, since (p-1) is an even positive divisor of 2(p+40). Take $p-1=2(p+40)^j$, $j \in \mathbb{Z}$ such that $0 \le j < s$ when j = 0, Then value of p = 3 < 7 not possible. Therefore $1 \le j < k$ and so we obtain $2(p+40)^j + 41 = (p+40)$ and j > 1 This is again an absurd one.

Theorem 3.2. The Diophantine equation $p^{z} + (p + 40)^{y} = z^{2}$ where p > 7 and p + 40 are primes, has no solution in positive integers x, y and z.

Proof. Consider the equation $p^x + (p + 40)^y = z^2$. Here $p^x + (p + 40)^y$ are primes and even and p > 7. We have two choices of p, i.e. $p \equiv 1 \pmod{4}$ or $p \equiv 3 \pmod{4}$. Case 1: If $p \equiv 1 \pmod{4}$, by the above lemma, it has no solution.

Case 2: If $p \equiv -1 \pmod{4}$, then we have different cases.

Sub-case 1: Suppose x and y are even, then $x=2k, k \ge 1$ and $y=2s, s \ge 1$. The equation 2 implies $p^x + (p+40)^y = 2 \pmod 4$. We get a contradiction.

Sub-case 2: Suppose x and y are odd , then x = 2k + 1, k > 0 and y = 2s + 1, s > 0. The given equation leads to $p^x + (p + 40)^y = 2 \pmod{4}$. Again this is contradiction. Hence it has no solution.

Sub-case 3: If x is odd and y is even, By theorem (3.1), the sub-case fails.

Sub-case 4: If x is even and y is odd, again by theorem(3.1) this is not possible.

4 The Exponential Diophantine equations $7^x+168^y=z^2$ and $7^x+282^y=z^2$

Here we analyse the two variants of the Diophantine equation; one is $7^x + 168^y = z^2$ and the other is $7^x + 282^y = z^2$. A few of the lemmas and theorems were shown,

and Python code for the corresponding equations was also given. .

Lemma 4.1. The Diophantine equation $7^x + 1 = z^2$ has no non negative integer solutions.

Proof. Suppose that there are non negative integers x and z such that $7^x + 1 = z^2$. If x = 0, the $z^2 = 2$ which is an impossible one. If $x \ge 1$, then by Mihailescu's theorem, we get x = 1, which is not possible.

Lemma 4.2. (y, z) = (1, 13) is the unique solution for the Diophantine equation $1 + 168^y - z^2 = 0$ where y, z are non negative integers.

Proof. Suppose there are non negative integers y, z such that $1 + 168^y = z^2$ If y = 0, then $z^2 = 2$ which is impossible. If y = 1, then z = 13 and y > 1 implies $z \ge 13$. Now, we consider the equation, $z^2 - 168^y = 1$ By Mihailescu's theorem, z = 2 which is impossible. (1, 13) is a unique solution (y, z) for the equation $1 + 168^y = z^2$

Lemma 4.3. The Diophantine equation $1 + 282^y - z^2 = 0$ has no non negative integer solutions.

Proof. For y=0, it has no solution. For $y\geq 1$, then $z\geq 18$. By using theorem (2.1), we obtain z=3. This is not possible as $z\geq 18$.

4.1 For the Diophantine equation $7^x + 168^y = z^2$

In this subsection, we provided the Python programming and the solutions to the Diophantine equation $7^x + 168^y = z^2$.

Theorem 4.1. The Diophantine equation $7^x + 168^y = z^2$ has exactly two solutions in non negative integers $(x, y, z) \in \{(0, 1, 13), (4, 2, 175)\}$.

Proof. Let x, y and z be non negative integers such that $7^x + 168^y = z^2$.

Case 1: x = 0 and By Lemma (4.2),we get (x, y, z) = (0, 1, 13)

- Case 2: When y is even and x > 1, then there exists a positive integer l such that y = 2l. Now the equation becomes $7^x + 168^{2l} = z^2$ and we get $z 168^l = 7^u$, $(z + 168^l) = 7^{x-u}$ with x > 2u. Now, $7^{x-u} 7^u = 2 \times 168^l$ implies $7^u(7^{x-2u} 1) = 2 \times 168^l$. For l = 1, $7^u(7^{x-2u} 1) = 2 \times 24 \times 7$. Therefore u = 1 and $7^{x-2} 1 = 48 \implies x = 4$. Hence (x, y, z) = (4, 2, 175).
- Case 3: When y is odd and x > 1. For a positive integer l, such that y = 2l + 1. Now the equation becomes $7^x (168)^2l = (z 13(168)^l)(z + 13(168)^l)$. Let $(z 13(168)^l) = 1$ and $z + 13(168)^l = 7^x (168)^{2l}$. On solving this we obtain $(168)^l[26 + (168)^l] = 7^x 1$ which implies l = 0 and $7^x = 26$. This is not possible.

The occurrence of the Diophantine equation's solution, $7^x + 168^y = z^2$, as illustrated below:

Coding 1: Calculating the solution for $7^x + 168^y = z^2$

```
Enter the maximum range:500 x y z 0 1 13 4 2 175
```

Figure 1: Output: Coding 1

4.2 For the Diophantine equation $7^x + 282^y = z^2$

The theorem and Python code for the Diophantine equation $7^x + 282^y = z^2$ are provided in this subsection.

Theorem 4.2. The Diophantine equation $7^x + 282^y = z^2$ has exactly two non negative integer solution (x, y, z) = (1, 1, 17), (3, 1, 25)

Proof. Let x,y and z be non negative integers such that $7^x + 282^y = z^2$. The Diophantine equation $7^x + 282^y = z^2$ has no solution on putting x = 0 and y = 0 (Using lemma (4.3) and (4.1)). When y is odd (i.e., $y = 2l + 1, l \in \mathbb{N} \cup \{0\}$), For l = 0, then y = 1. If x = y = 1, then we have z = 17. For l > 0 and y > 1, then the Diophantine equation becomes $7^x - 7(282)^{2l} = z^2 - 289(282)^{2l}$. Let $z - 17(282)^l = 1$ and $z + 17(282)^l = 7^x - 7(282)^{2l}$. This implies $(z + 17(282)^l) - (z - 17(282)^l) = 7^x - 7(282)^{2l} - 1$. On solving this we get $(282)^l[34 + 7(282)^l] = 7^x - 1$ and this implies l = 0 which is an impossible one. In other way we can solve $7^x + 282^y = z^2$ and it becomes $7^x - 294(282)^{2l} = z^2 - 24^2(282)^{2l}$. Now choose $z - 24(282)^l = 1$ and $z + 24(282)^l = 7^x - 294(282)^{2l}$. Now the equation reduces to $282^l[48 + (296)(282)^l] = 7^x - 1$ and this implies l = 0, x = 3 and z = 25. Now, the solution is (x, y, z) = (3, 1, 25). Suppose y is even $(i.e., 2l, l \in \mathbb{Z}^+ \cup \{0\})$, then equation $7^x + 282^y = z^2$ reduces to $7^x = z^2 - (282)^{2l}$. Choose $z - 282^l = 7^u$ and $z + 282^l = 7^{x-u}$, then it becomes $7^u(7^{x-2u} - 1) = 2(282)^l$. For l = 1, we get $u = 0 \implies 7^x = 565$. This is not possible.

Python programming validates the preceding theorem's solution, which is provided as:

```
is #For the equation 7"x+282"y=x"2
a import math
m def diophantine():
se print ('x\ty\tz')
  for x in runge (0, n+1):
17
    for y in range (0,n+1):
111
          for z in range (0,n+1):
19
          if 7**x+282**y==2**2 :
24
               print(x,'\t',y,'\t',z,'\t')
m n =int(input("Enter the maximum range:"))
so #n is the maximum range
adiophantine()
```

Coding 2: Calculating the solution for $7^x + 282^y = z^2$

```
Enter the maximum range:100 x y z 1 1 17 3 1 25
```

Figure 2: Output: Coding 2

5 The Exponential Diophantine equation $19.12^x + 19^y = z^2$

This section displayed certain lemmas and theorems that were required to obtain the positive integer solutions of the Diophantine equation $19.12^x + 19^y = z^2$.

Lemma 5.1. (x, z) = (1, 20) is the only solution for the Diophantine equation $19.21^x + 1 - z^2 = 0$ where x, z are non negative integers.

Proof. Consider the equation

$$19.21^x = z^2 - 1$$
 (1)

From this, we have either 19 divides z - 1 or z + 1. If 19|(z - 1), then there exists a positive integer r < x such that $z - 1 = 19.21^r$ and $z + 1 = 19.21^r + 2$. The equation (1) becomes

$$21^{s-r} = 19.21^r + 2.$$
 (2)

When r = 0, we get x = 1. Hence (x, z) = (1, 20). When r > 0, we have x - r > 0. Now $21^{x-r} \equiv 0 \pmod{21}$ implies $21^{x-r} \equiv 0 \pmod{3}$. Also $19.21^r \equiv 0 \pmod{3}$ and by using the equation (2) we get a contradiction. If 19|z+1 and 19 does not divides z - 1, then there exists positive integers r and s such that $z + 1 = 19.21^r$ and $z - 1 = 21^s$, where r + s = x. On solving this we obtain

$$2 = 19.21^r - 21^s$$
 (3)

On Substituting s=0, it becomes $3=19.21^r$ which is an impossible one. Similarly for r=0, we get an impossible one. If s, r>0 then $19.21^r-21^s\equiv 0\pmod 3$. From the equation (3) we get contradiction.

Lemma 5.2. Let b be a positive integer such that $b \equiv 5 \pmod{40}$. Then the Diophantine equation $1 + b^y = z^2$ has no non integer solution.

Proof. Suppose that there are non negative integers y and z such that $1 + b^y = z^2$. This contradicts when y = 0. For y = 1, we get $b = z^2 - 1$. Since $b \equiv 5 \pmod{40} \implies b \equiv \pmod{4}$. Then $z^2 \equiv 2 \pmod{4}$. The case fails for y > 1, using theorem(2,1).

Lemma 5.3. Let b be a positive integer such that $b \equiv 8 \pmod{40}$. Then $(y, z) = (1, \sqrt{b+1})$ represent the non negative integer solutions of the Diophantine equation $1 + b^y = z^2$, where $\sqrt{b+1}$ is an integer.

Proof. Let y and z be non negative integers such that $1+b^y=z^2$. There is no solution for the equation when y=0 and y>1(By theorem(2.1). Suppose y=1, then we get z=7 and hence the solution for the Diophantine equation is $(1,\sqrt{b+1})$.

5.1 For the Diophantine equation $19.21^{z} + 19^{y} = z^{2}$

The Diophantine equation $19.21^{z} + 19^{y} = z^{2}$ is solved here using the theory and Python programming.

Theorem 5.1. (x, y, z) = (1, 0, 20) is the unique solution to the Diophantine equation $19.21^x + 19^y = z^2$ where x, y, z are non-negative integers.

Proof. Let x, y, z be non-negative integers such that $19.21^{v} + 19^{v} = z^{2}$. We consider the following cases.

Case 1: For x = y = 0, we have $z^2 = 20$ which is impossible.

Case 2: For x = 0 and y > 0, we have 19(1 + 19^{y-1}) = z². When y = 1, it has no solution. If y > 1, then 19|z². There is some positive integer k such that z = 19k and it becomes 19(k² - 19^{y-2}) = 1. This is not possible.

Case 3: For x > 0 and y = 0, we obtain $19.21^x + 1 = z^2$. By lemma (5.1), the only solution is (x, y, z) = (1, 0, 20).

Case 4: When x > 0 and y > 0, the equation $19.21^x + 19^y = z^2$ implies 19|z. Therefore z = 19k and it becomes

$$21^x + 19^{y-1} = 19k^2 (4)$$

. When y = 1, we get k² ≡ 2 (mod 4) (which impossible). When y > 1, from equation(4), 21^x ≡ 0 (mod 19) which is not possible.

Here, the python programming is provided for the existence of the solution of the exponential Diophantine equation $19.21^x + 19^y = z^2$ as shown:

```
# #For the squation 19*21**x*19**y*z**2

# import math
# def diophantine();
# print('x\ty\tz')
# for x in range(0,n+1):
# for y in range (0,n+1):
# for z in range (0,n+1):
# 19*21**x*19**y*=z**2:
# print(x,'\t',y,'\t',z,'\t')
# n *int(input(*Enter the maximum range:"))
# fin in the maximum range
# diophantine()
```

Coding 3: Calculating the solution for $19.21^x + 19^y == z^2$

```
Enter the maximum range:200 x y z 1 0 20
```

Figure 3: Output: Coding 3

6 Conclusion

Finally, we solved and established the existence of the positive integer solutions to the miscellaneous Diophantine equations with the Python programming. One can try to solve for any alternative forms of the Diophantine equation.

References

- Abdelkader Hamtat, An exponential diophantine equation on triangular numbers, Mathematica Applicanda, 51, 1, 2023, 99–107.
- [2] Kannan. J. Manju Somanath, and Raja. K. On a class of solutions for the hyperbolic diophantine equation, International Journal of Applied Mathematics. 32, 3, 2019, 443-449.
- [3] Kaleeswari K, Kannan J, and Narasimman, G, Exponential diophantine equations involving isolated primes, Advances and Applications in Mathematical Sciences. 22, 1, 2022, 169-177.
- [4] Manju Somanath, Kannan. J, and Raja. K, Exponential diophantine equation in two or three variables, Global Journal of Pure and Applied Mathematics. 13, 5, 2017, 128-132.
- [5] Manju Somanath, Raja. K, Kannan. J, and Mahalakshmi. M, On a class of solution for a quadratic diophantine equation, Advances and Applications in Mathematical Sciences. 19, 11, 2022, 1097-1103.

- [6] Manju Somanath, Raja. K, Kannan. J, and Nivetha. S, Exponential diophantine equation in three unknowns, Advances and Applications in Mathematical Sciences, 19, 11, 2020, 1113-1118.
- [7] Mahalakshmi. M, Kannan. J, Deepshika. A, and Kaleeswari, K, (2023). Existence and non existence of exponential diophantine triangles over triangular numbers, Indian Journal of Science and Technology. 16, 41, 2023, 3599–3604.
- [8] Kannan. J, and Manju Somanath, Fundamental perceptions in contemporary number theory, Nova Science Publisher, New York, 2023.
- [9] Manju Somanath, Kannan. J, and Raja, K, Exponential diophantine equation in three variables 7^x + 7^{2y} = z², International Journal of Engineering Research-Online, 5, 4, 2017, 91-93.
- [10] Rosen. K.H., Elementary number theory and its applications, Addison-Wesley Publishing Company, Boston, 1987.
- [11] Telang, S.G., Number theory, Tata McGraw Hill Publishing Company Limited, New York, 1996.
- [12] Titu Andreescu, Dorin Andrica, and Ion Cucurezeanu, An introduction to diophantine equations: a problem - based approach, Birkhauser Boston, 2010.
- [13] William Sobredo Gayo, Jr., and Jerico Bravo Bacani, On the diophantine equation M_p^x + (M_q + 1)^y = z², European Journal of Pure and Applied Mathematics. 14, 2, 2021, 396-403.

^{1,3} Department of Mathematics, Ayya Nadar Janaki Ammal College (Autonomous, affiliated to Madurai Kamaraj University, Madurai), Sivakasi - 626124, India. Email: deepshi20mar@ymail.com

Email: jayram.kannan@gmail.com

School of Advanced Sciences, Kalanatingam Academy of Research and Education, Krishnankoil - 626 126, Tamil Nadu, India.

Email: vimalkathir 15@gmail.com

(Received, February 25, 2025)

Swati Chaudhari'. Archana Thakur¹,

ANOMALY DETRECTION FOR WEB ATTACK PREVENTION: ANALYZING WEB ACCESS Alpana Rajan' LOGS FOR THREAT MITIGATION

ISSN: 0970-5120

Abstract: With the increasing sophistication of cyber threats, web applications are prime targets for attackers seeking to exploit vulnerabilities. Traditional signature-based security solutions struggle to detect novel and evolving attack patterns. This paper presents an anomaly detection approach for web attack detection and mitigation by analyzing web access logs. Using machine learning techniques, we identify deviations from normal traffic patterns that may indicate potential threats such as SQL injection, cross-site scripting (XSS), and Local File Inclusion (LFI) and Directory Traversal attacks.

We conducted a study on a real-world dataset comprising 50 million HTTP requests collected over three months from a real world web application platform. By leveraging an unsupervised machine learning model, we detected 5% anomalous requests, of which 85% were confirmed as actual attacks through manual verification and cross-referencing with intrusion detection system (IDS) logs. Notably, our model identified previously undetected zero-day threats, including 400+ directory traversal attacks, 156 stealthy SQL injection attempts and 150 botdriven credential stuffing incidents. The proposed system enhances real-time threat detection and response, improving web security by proactively identifying and mitigating attacks before they cause significant damage. Experimental results demonstrate 87% precision, 92% recall and 93.94% accuracy in detecting anomalies, offering a scalable and adaptive solution for modern web security challenges.

Keywords: Web Attack, Machine Learning, Anomaly detection, web log

Mathematic Subject Classification (2020) No.: 68M25, 68M11, 68M10.

1. Introduction

The rapid expansion of web applications and online services has made them prime targets for cyber-attacks, ranging from SQL injection (SQLi), cross-site scripting (XSS), Local File Inclusion (LFI), Directory Traversal and credential stuffing attacks. Traditional security measures, such as signature-based intrusion detection systems (IDS) and firewalls, often struggle to detect evolving and zero-day threats, as they rely on predefined rules and known attack patterns. Consequently, there is a growing need for more adaptive and intelligent security mechanisms that can proactively detect malicious activities before they compromise web systems.

Anomaly detection has emerged as a powerful technique for identifying suspicious behaviour in network traffic and web access logs. Instead of relying on predefined attack signatures, anomaly detection models learn normal usage patterns and flag deviations that may indicate potential threats. This paper presents a machine learning-based approach to web attack detection and mitigation using anomaly detection techniques on web server access logs. By analyzing request parameters, response codes, traffic patterns, and other features, our system can effectively distinguish between normal and malicious activity.

We conducted a real-world case study on a web application platform, analyzing 50 million HTTP requests over a three-month period. Our proposed anomaly detection model successfully identified 5% anomalous requests, of which 85% were confirmed as actual attacks through cross-verification with traditional IDS logs. The system detected over 400+ directory traversal attacks, 156 stealthy SQL injection attempts and 150 credential stuffing attacks that were previously unnoticed, demonstrating its effectiveness in identifying novel threats.

The contributions of this paper are as follows:

- Unsupervised Anomaly Detection for Web Security We develop a machine learning model Isolation Forest (IF) algorithm that detects web-based attacks without relying on labelled attack data.
- Real-Time Detection and Adaptive Security The system provides real-time threat detection capabilities, adapting to new and evolving attack patterns.
- Experimental Validation on Large-Scale Data We validate our approach using realworld web traffic data and measure its effectiveness with precision, recall, and F1score.

The rest of this paper is organized as follows: Section 2 provides an overview of related work in web attack detection. Section 3 describes problem statement, Section 4 explains mathematical model of the system, and Section 5 describes our proposed anomaly detection methodology. Section 6 discusses results and comparative analysis and Section 7 concludes the paper with future research directions.

2. Related Work

Web attack detection has been an active area of research, with various approaches proposed to enhance cyber security. Traditional methods rely on signature-based intrusion detection systems (IDS) and rule-based firewalls, but these techniques struggle with zero-day attacks and evolving attack patterns. Recent advancements in machine learning and anomaly detection have provided more adaptive and intelligent solutions for web security.

Traditional Signature-Based and Rule-Based Intrusion web security mechanisms such as Snort [1] and Suricata [2] rely on predefined attack signatures to detect malicious traffic. While these systems are effective against known attacks, they require continuous updates and cannot detect new, unknown threats. Studies have shown that signature-based IDS have low detection rates for emerging threats due to their reliance on static rules [3]. Recent studies on Machine Learning based web attack detection have explored the use of supervised machine learning for web attack detection. Canali et al. [4] proposed a model using Random Forest and Support Vector Machines (SVM) to classify HTTP requests as benign or malicious, Similarly, Pan et al. [5] developed a deep learning-based web attack detection system using Convolutional Neural Networks (CNNs), achieving high accuracy but requiring extensive labelled datasets. However, supervised learning approaches suffer from the challenge of label scarcity and require frequent retraining as new attack patterns emerge. Unsupervised learning methods for anomaly detection for web security have gained attention for detecting web attacks without labelled data. Shams et al. [6] implemented an Isolation Forest-based anomaly detection model, achieving 82% accuracy in detecting anomalous HTTP requests. Krügel et al. [7] applied clustering techniques to identify abnormal traffic patterns, improving the detection of SQL injection and XSS attacks. More recently, deep autoencoders have been used to learn the distribution of normal web traffic and flag deviations as potential threats [8]. Several real-world studies highlight the effectiveness of anomaly detection in detecting cyber threats. A case study on a large-scale e-commerce platform by Ma et al. [9] analyzed 100 million HTTP requests, identifying previously undetected bot-driven attacks. While anomaly detection techniques improve detection rates, challenges such as high false positives and computational overhead remain key concerns [10]. A study published by D. Y. Demirel et al., introduced a novel Zero-Shot Learning method employing a Convolutional Neural Network (CNN) for web-based anomaly detection [11]. This approach addresses the challenge of unbalanced data in web applications, where malicious requests are significantly fewer than benign ones. The proposed method enhances the detection of previously unseen attacks by leveraging the CNN's ability to generalize from limited data. Limitations of this work is it requires labelled data for initial training and careful tuning to prevent over fitting and handling of imbalanced data is explicitly requires to be addressed, Rahul Kale et al. [12] proposed an enhancement to an existing fewshot weakly-supervised deep learning anomaly detection framework. This framework incorporates data augmentation, representation learning, and ordinal regression to improve detection performance. The study evaluated the framework on benchmark datasets such as NSL-KDD, CIC-IDS2018, and TON IoT, demonstrating its effectiveness in scenarios with limited labelled data. Apparently it has deployment complexities in real world environment as it requires model training & fine-tuning. A comprehensive literature review published by S. M. Rayavarapu et al. [13], examined the application of Generative Adversarial Networks (GANs) in cyber security, including their use in anomaly detection. The study highlighted how GANs are utilized in areas like intrusion monitoring, steganography, cryptography, and password cracking. The review provided an in-depth examination of the most popular GAN-based methods and their effectiveness in detecting anomalies within eyber security contexts, GANbased anomaly detection approach is complex to deploy, computational power intensive, requires large datasets and difficult to interpret results. A study carried out by Elion Harlicai [14] focused on anomaly detection of web-based attacks in micro services architectures. The proposed solution achieved a 91% detection rate with only a 0.11% false positive rate by carefully selecting parameters. This approach underscores the importance of parameter tuning in enhancing detection performance in complex micro services environments. A study published by A. D. Katurde et al. [15], discussed the development of Al/ML-based anomaly detection tools, emphasizing the principles underpinning behaviour-based anomaly detection systems (BBADS) and their application in real-world scenarios. The research delved into model selection nuances, highlighting critical factors influencing the effectiveness of anomaly detection in cyber security. A systematic review carried out by Sureda et al. [17] examines various anomaly detection techniques employed to prevent and detect web attacks, providing a comprehensive analysis of existing methodologies.

The study revealed that signature-based IDS have low detection rates for emerging threats due to their reliance on static rules. The existing research demonstrates the effectiveness of machine learning-based web attack detection. However, most methods either rely on labelled data (supervised learning) or suffer from high false positives (unsupervised learning) and initial training and careful tuning to prevent over fitting and handling of imbalanced data is explicitly requires to be addressed. Some approaches are complex to deploy, computational power intensive, requires large datasets and difficult to interpret results. If anomalies are rare and accuracy is 92%, it may just be predicting most requests as normal. The Precision (87%) and Recall (92%) values are more meaningful, as they directly evaluate how well anomalies are detected. The model with 87% precision and 92% recall is preferable over just using accuracy, especially for anomaly detection tasks. Our work builds on these studies by implementing an unsupervised anomaly detection model on real-world web logs, addressing key challenges in accuracy, scalability, and real-time detection.

3. Problem Statement

With the increasing complexity and frequency of cyber threats, web applications face constant risks from attackers exploiting vulnerabilities. Traditional signature-based security mechanisms struggle to detect novel and evolving attack patterns, leaving systems vulnerable to zero-day exploits. Existing security solutions often generate high false positive rates or fail to adapt to sophisticated attack techniques. There is a critical need for an intelligent, adaptive, and scalable anomaly detection system that can proactively identify and mitigate malicious activities in real time. This research addresses the challenge by leveraging machine learning-based anomaly detection on web access logs to detect and respond to web-based attacks, including SQL injection, cross-site scripting (XSS), Local File Inclusion (LFI), and credential stuffing, thereby enhancing web security and reducing attack impact.

4. Mathematical Model for Anomaly Detection in Web Attack Detection and Mitigation

The anomaly detection approach can be formalized using a mathematical model based on statistical and machine learning techniques. Below is a step-by-step formulation of the model:

4.1 Input Representation

Let X be the set of web access log entries, where each request is represented as a feature vector:

$$X = \{x_1, x_2, ..., x_n\}$$

where x_i is a feature vector representing an HTTP request, such as:

- Source IP (h_i)
- Timestamp (t_i)
- HTTP request type (r_i)
- Status code (s_i)
- Response size (b_i)
- Referer (ref.)
- User-Agent (ua_i)

Thus, each request can be represented as:

$$x_i = [h_i, t_i, r_i, s_i, b_i, ref_i, ua_i]$$

The dataset can be written as a matrix:

$$X = \begin{bmatrix} x_1 \\ x_2 \\ \vdots \\ x_n \end{bmatrix} \in \mathbb{R}^{n \times d}$$

where d is the number of features.

4.2 Feature Transformation and Anomaly Score Computation

To detect anomalies, we map the feature space into a lower-dimensional representation or define an anomaly scoring function. Possible techniques include:

4.2.1 Statistical Anomaly Detection (Z-score)

For each feature x_i , compute the mean μ_i and standard deviation σ_i :

$$Z_{ij} = \frac{x_{ij} - \mu_j}{\sigma_i}$$

If $Z_{ij} \ge \tau$ (where τ is a predefined threshold), the request is considered anomalous.

4.2.2 Unsupervised Learning (Autoencoder Reconstruction Error)

Using an autoencoder neural network, the model learns the mapping and detects anomalies based on reconstruction error. Low reconstruction error indicates normal request, high reconstruction error means anomalous request:

$$f: X \to H \to X'$$

where H is a latent representation. The reconstruction error is given by:

$$E_{\ell} = ||x_{\ell} - x_{\ell}||_{12}$$

A request is flagged as anomalous if:

$$E_i > \theta$$

where θ is a threshold derived from training.

4.2.3 Isolation Forest Anomaly Score

The Isolation Forest algorithm assigns an anomaly score:

$$S(x) = 2^{-\frac{E(b(x))}{E(b)}}$$

where E(h(x)) is the average path length of x in the tree, and c(n) is the average path length of a random search tree.

4.3 Decision Function and Classification

Define the final anomaly decision function:

$$A(x_i) = \begin{cases} 1, & \text{if } S(x_i) > \delta \text{ (Anomalous request)} \\ 0, & \text{otherwise (Normal request)} \end{cases}$$

where δ is a threshold derived from training.

4.4 Evaluation Metrics

To assess the performance of the model, we use precision, recall, and F1-score:

$$Precision = \frac{TP}{TP + FP}$$

$$Recall = \frac{TP}{TP + FN}$$

$$F1 - score = 2 \times \frac{Precision \times Recall}{Precision + Recall}$$

where:

- TP (True Positives) are correctly identified attacks.
- FP (False Positives) are incorrectly classified normal requests.
- FN (False Negatives) are undetected attacks.

5. Methodology for Web Attack Detection Using Anomaly Detection

The methodology for this work is structured into six key phases, ensuring a systematic approach to detecting and mitigating web attacks using anomaly detection techniques.

5.1 Data Collection

Data: Real-world apache/ nginx web access logs are gathered for analysis. Additionally some of publically available datasets e.g. CIC-IDS2018, CSIC 2010, DARPA are used. Synthetic data is also collected through simulated attacks in controlled environment for testing.

Log Format Example (Apache Log Format)

```
192.168.1.10 - - [12/Feb/2025:10:15:30 +0000] "GET /index.php?id=1 HTTP/1.1" 200 512 "-" "Mozilla/5.0"
```

Features Engineering: Row data is transformed into meaningful features to improve the performance of machine learning model. Following are features which we have used in our work:

- Size: Helps to identify suspicious patterns hidden in payload
- IP Address: Source of the request
- . Timestamp: Time of the request
- Request Type: Helps to identify unusual behaviour
- URL Length: Helps to identify unusual behaviour
- Is numeric URL: Helps to identify suspicious URL
- special chars URL: Helps to identify suspicious URL
- · Status Code: Can indicate errors or forbidden access attempts
- Bytes Transferred: Abnormal request sizes may indicate attacks
- · User-Agent: Identifies browser, bots, or scripts

5.2 Data Pre-processing

Data pre-processing is an essential step in the machine learning (ML) pipeline. It involves preparing and cleaning data to ensure that it is suitable for training a machine learning model. It involved following steps:

- Log Parsing: Convert unstructured text logs into structured tabular format.
- . Handling Missing Values: Replace or remove incomplete log entries.
- Feature Engineering: Convert categorical data (e.g., User-Agent) into numerical values using encoding techniques.
- Normalization: Standardize numerical values to ensure consistency in ML models.
- Removing Noise: Filter out normal bot traffic (e.g., search engine crawlers).

5.3 Anomaly Detection Model

The model identify the data points, events, or observations that deviate significantly from the rest of the data and are considered unusual, abnormal, or outliers using isolation forest algorithm of unsupervised machine learning. The Isolation Forest constructs multiple decision trees and isolates anomalies based on tree depth. It is efficient for detecting rare attack patterns and fast, scalable, and effective in high dimensional data. The Isolation Score is calculated as:

Anomaly Score =
$$2^{-E(h(x))/c(n)}$$

Where:

- E(h(x)) is the average path length of the instance in the isolation trees.
- c(n) is the normalization factor.

5.4 Attack Classification & Thresholding

The objective of the attack classification is to distinguish between normal data (non-attacks) and anomalous or attack data. It works as a binary classifier in the context of anomaly detection because it classifies data points into two categories: normal and anomalous. The algorithm works by building an ensemble of random trees where each tree isolates a data point by randomly selecting a feature and then randomly selecting a split value within that feature's range. The anomaly score is calculated based on the path length required to isolate a data point: the shorter the path, the more anomalous the point is considered, and the longer the path, the more likely it is normal.

5.5 Threat Response & Mitigation

Threat response and mitigation are critical components of any anomaly detection system. It focuses on detecting, analyzing, and neutralizing threats to prevent or minimize damage to an organization's systems and data. It react to detected attacks in real-time. Alerts are generated for the detected attacks and sent to the security administrators for quick actions against the threat. Malicious IPs involved in attacks are checked against AbuseIPDB [16]. The IPs having IP reputation score above 41 is blocked in perimeter firewalls by updating firewall rules to prevent further attacks. The attack data is stored for forensic analysis.

5.6. Continuous Model Optimization & Adaptive Learning

Periodically the model is updated with fresh web logs which is an ongoing process of refining and improving the model through real-time learning. Anomaly threshold is adjusted based on false positives to support adaptive learning. Feedback looping is carried out by human analyst to review flagged anomalies to refine model accuracy.

Figure 1 illustrates work flow of our web attack detection system using anomaly detection technique.

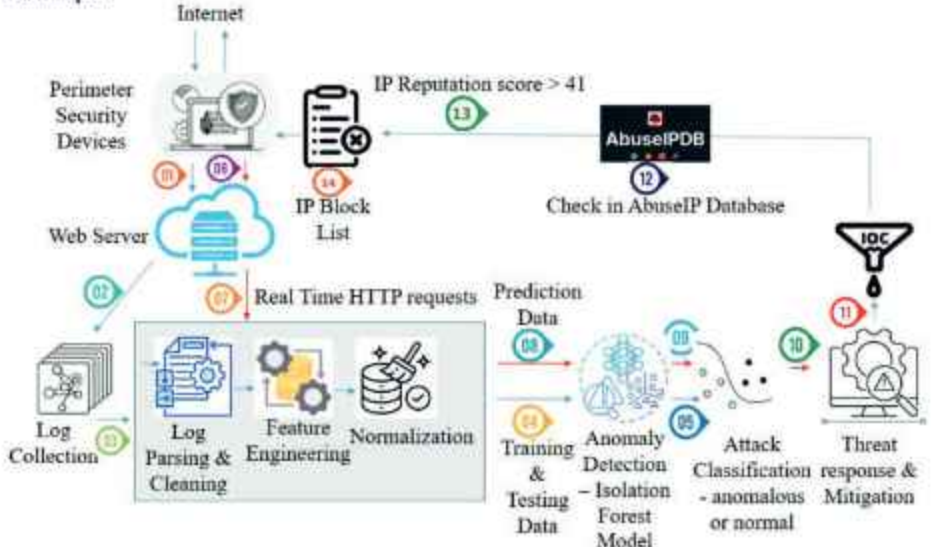


Fig. 1: Workflow of our web attack detection using system anomaly detection technique.

6. Results and Comparative Analysis

The Table 1 provides a comparison of our web attack detection system with recent related studies, focusing on methodology, performance, and applicability.

Reference	Methodology	Strengths	Limitations	Novelty, Significance and Impact of Our Work
Sureda et al. [17]	Systematic review of anomaly detection techniques for web attack prevention.	Provides a broad review of existing techniques.	No practical implementation or model evaluation.	Implements and evaluates a specific anomaly detection approach, while this study only reviews prior methods.

R. Kumar et al. [18]	Empirical methods for anomaly detection in web attacks.	Focuses on real- world attack scenarios.	Does not explore deep learning techniques.	Incorporates autoencoders and Isolation Forest, offering better anomaly detection accuracy.
Giovanni Vigna et al. [19]	Reducing false positives in anomaly detection.	Highlights error reduction techniques.	Based on older, rule-based methods.	Incorporates machine learning, which is more adaptive than static rule- based approaches.
Christopher Kruegel et al. [20]	Early study on anomaly detection for web attacks.	Foundational work in web attack detection.	Outdated methods with no modern ML techniques.	Leverages deep learning and adaptive learning, making it more relevant to current threats.
S. Zhang et al. [21]	Novel transformation model for anomaly detection.	Introduces a new feature extraction technique.	Lacks comparison with ML-based models.	It is machine learning-based, allowing it to detect evolving attack patterns more effectively.
Almourish et al. [22]	Machine learning for web attack detection.	Uses feature selection techniques to improve accuracy.	Requires large labelled datasets.	It is unsupervised, making it more scalable to real- world attack detection.
Udi Aharon et al. [23]	GAN-inspired learning to detect API attacks.	Handles data scarcity well using few-shot learning.	High computational cost.	It is faster and more scalable for real-time detection compared to GAN-based techniques.
D. Y. Demirel wt al. [11]	CNN-based zero-shot learning for web anomaly detection.	Effective for new/unseen attacks.	Computationally expensive.	It is lighter and more efficient, making it better suited for real- time scenarios.
Tikam Alma et al. [24]	Uses deep learning (autoencoders)	High detection accuracy.	Requires a large training dataset.	It combines deep learning with statistical methods,

	to detect web threats.			making it more adaptive.
Mohammed Abo Sen et al. [25]	Uses Attention- GAN to detect anomalies.	Strong performance for complex attack scenarios.	Computationally heavy, not real- time.	It is faster and deployable in real-time environments.

Table 1: Comparison of our web attack detection system with recent related studies.

Figure 2 shows URL length vs. response time plots classify unusual patterns in how users (or bots) interact with a web server, specifically focusing on the relationship between the length of the requested URL and the time it takes for the server to respond. Malicious requests (like SQL injection, directory traversal, or buffer overflow attacks) often use abnormally long URLs. Very long URLs causing short or extremely long response times. Normal-length URLs causing abnormal delays (indicating deeper issues).

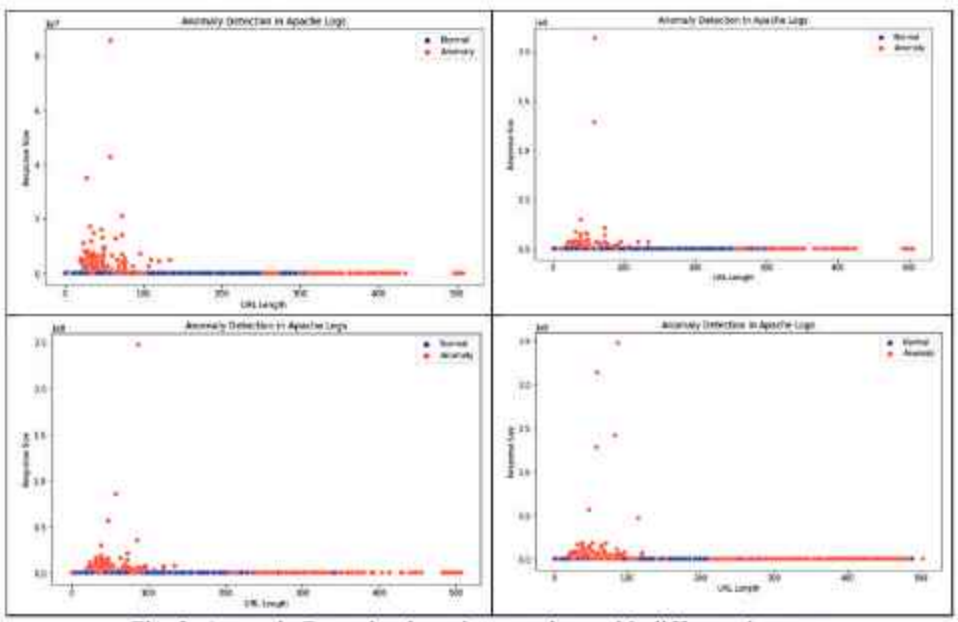


Fig. 2: Anomaly Detection in web server logs with different datasets.

Figure 3 illustrates comparison of the performance of the web attack detection model against existing approaches.

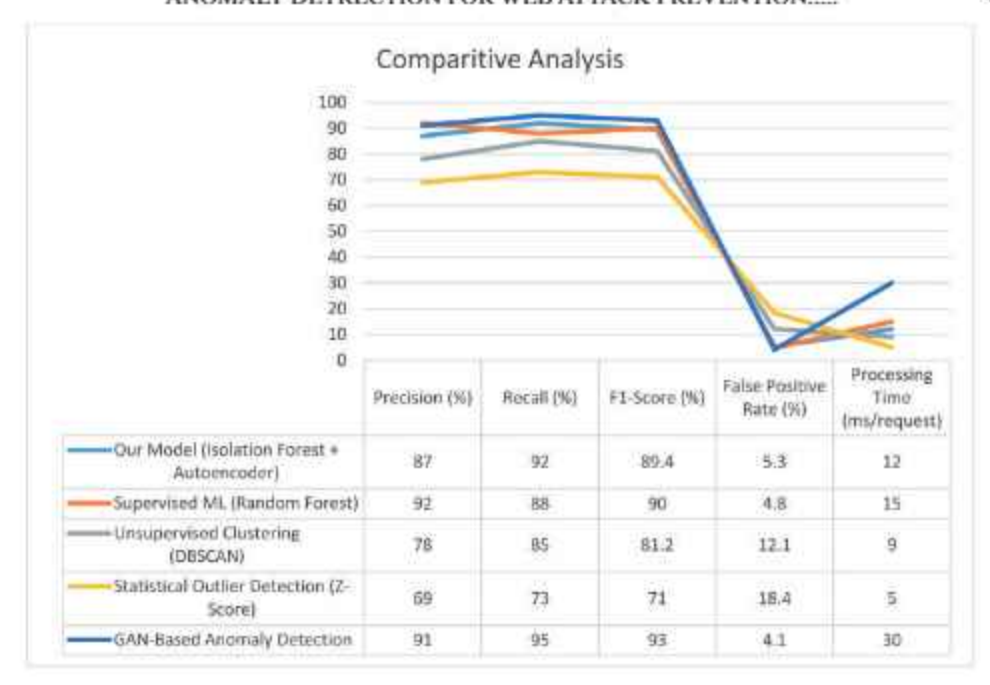


Fig.3: Comparative analysis with different approaches with our model

7. Conclusions and Future work

Web-based attacks, such as SQL injection (SQLi), cross-site scripting (XSS), Local File Inclusion (LFI), Directory Traversal and credential stuffing are increasing due to the widespread use of web applications. Traditional rule-based security systems struggle to detect zero-day attacks and evolving threats, making anomaly detection a critical defense mechanism. The research work demonstrates the effectiveness of machine learning-based web attack detection. However, most methods either rely on labelled data using supervised learning or suffer from high false positives using unsupervised learning. The presented mathematical model provides a structured approach to anomaly detection by defining; feature extraction from web logs, statistical and machine learning-based anomaly scoring, classification using a decision function, evaluation using precision, recall, and F1-score. The results demonstrate 87% precision, 92% recall and 93.94% accuracy in detecting anomalies offering a scalable and adaptive solution for modern web security challenges. This model enables real-time detection and mitigation of web attacks capable of adapting to evolving threats. Our work contributes a practical, scalable, and real-world tested anomaly detection framework, Organizations can deploy this model as part of a Web Application Firewall (WAF) or integrate it with Security Information and Event Management (SIEM) systems for continuous monitoring and proactive threat detection. It balances computational efficiency with strong detection capabilities, making it a viable solution for real-time web security monitoring. Future enhancements may integrate deep learning-based Zero-Shot Learning or hybrid methods to further improve accuracy and adaptability. Our work's usefulness extends to industries, cyber security professionals, and researchers looking to improve web security through machine learning-based anomaly detection.

References

- Roesch, M. (1999): Snort: Lightweight Intrusion Detection for Networks, In Proceedings of LISA '99.
- [2] Open Information Security Foundation (2010): Suricata: The Next Generation IDS/IPS.
- [3] Sommer, R., & Paxson, V. (2010): Outside the Closed World: On Using Machine Learning for Network Intrusion Detection, IEEE Symposium on Security and Privacy.
- [4] Canali, D., Cova, M., & Vigna, G. (2011): Detecting Web-Based Attacks Through Machine Learning, Proceedings of RAID.
- [5] Pan, L., He, J., & Wei, L. (2020): Deep Learning for Web Attack Detection: A Convolutional Neural Network Approach, IEEE Transactions on Information Forensics and Security.
- [6] Shams, R., & Rizaner, A. (2018): Anomaly-Based Web Attack Detection Using Isolation Forest, Journal of Cyber Security and Mobility.
- [7] Krügel, C., Vigna, G. (2005) & Robertson, W. (2005): Anomaly Detection for Web-Based Attacks, ACM Transactions on Information and System Security.
- [8] Mirsky, Y., Doitshman, T., & Shabtai, A. (2021): Autoencoder-Based Anomaly Detection for Web Security, IEEE Transactions on Cybersecurity.
- [9] Ma, Z., Li, X., & Wang, P. (2022): Large-Scale Anomaly Detection in Web Traffic: A Case Study on E-commerce Security, Proceedings of Annual Computer Security Applications Conference (ACSAC), Association for Computing Machinery.
- [10] Chandola, V., Banerjee, A., & Kumar, V. (2009): Anomaly Detection: A Survey, ACM Computing Surveys.
- [11]D. Y. Demirel and M. T. Sandikkaya (2023): Web Based Anomaly Detection Using Zero-Shot Learning With CNN, IEEE Access, vol. 11, pp. 91511-91525, 2023, doi: 10.1109/ACCESS.2023.3303845.
- [12] Rahul Kale & Vrizlynn L. L. Thing (2023): Few-shot Weakly-supervised Cybersecurity Anomaly Detection, Computers and Security, Vol. 130, No. C, doi.org/10.1016/j.cosc.2023.103194.
- [13] S. M. Rayavarapu, T. S. Prasanthi, G. S. Rao & G. S. Kumar (2023): Generative Adversarial Networks for Anomaly Detection in Cyber Security: A Review, 4th International Conference on Electronics and Sustainable Communication Systems (ICESC), Coimbatore, India, 2023, pp. 662-666, doi: 10.1109/ICESC57686.2023.10193331.
- [14] Eljon Harlicaj (2021): Anomaly Detection of Web-Based Attacks in Microservices, Master's thesis, Aalto University - School of Science, EURECOM.
- [15] A. D. Katurde (2024): SecureSense: AI/ML Based Anomaly Detection Tool, International Conference on Intelligent Systems for Cybersecurity (ISCS), Gurugram, India, pp. 1-6, doi: 10.1109/ISCS61804.2024.10581060.
- [16] AbuseIPDB: A project dedicated to helping combat the spread of hackers, spammers, and abusive activity on the internet, https://www.abuseipdb.com/account/api
- [17] Tomas Sureda, Juan-Ramón Bermejo Higuera, Juan-Ramón Bermejo Higuera, José-Javier Martinez Herraiz & Juan-Antonio Sicilia Montalvo (2020): Prevention and Fighting against Web Attacks through Anomaly Detection Technology: A Systematic Review, Sustainability, 12(12), 4945, https://doi.org/10.3390/su12124945.
- [18]R. Kumar, N. Arora, T. Gera, A. Jain & D. Thakur (2022): Empirical Methods, Anomaly Detection and Preventive Measures of Web Attacks, 10th International Conference on Reliability, Infocom Technologies and Optimization (Trends and Future Directions) (ICRITO), Noida, India, pp. 1-5, doi: 10.1109/ICRITO56286.2022.9964908.

- [19] Giovanni Vigna, Fredrik Valeur, Davide Balzarotti, William Robertson, Christopher Kruegel & Engin Kirda (2009): Reducing errors in the anomaly-based detection of webbased attacks through the combined analysis of web requests and SQL queries, Journal of Computer Security 17 305–329 305, DOI 10.3233/JCS-2009-0321.
- [20] Christopher Kruegel, Giovanni Vigna (2003): Anomaly Detection of Web-Based Attacks, Proceedings of the 10th ACM Conference on Computer and Communications Security.
- [21] S. Zhang, B. Li, J. Li, M. Zhang & Y. Chen (2015): A Novel Anomaly Detection Approach for Mitigating Web-Based Attacks Against Clouds, IEEE 2nd International Conference on Cyber Security and Cloud Computing, New York, NY, USA, pp. 289-294, doi: 10.1109/CSCloud.2015.46.
- [22] Almourish, M.H., Abduljalil, O.A.I. & Alawi, A.E.B. (2022): Anomaly-Based Web Attacks Detection Using Machine Learning. Proceedings of 2nd International Conference on Smart Computing and Cyber Security. SMARTCYBER 2021. Lecture Notes in Networks and Systems, vol 395. Springer, Singapore. https://doi.org/10.1007/978-981-16-9480-6 29
- [23] Udi Aharon, Revital Marbel, Ran Dubin, Amit Dvir & Chen Hajaj (2024): Few-Shot API Attack Detection: Overcoming Data Scarcity with GAN-Inspired Learning, https://arxiv.org/abs/2405.11258.
- [24] Tikam Alma, Manik Lal Das (2020): Web Application Attack Detection using Deep Learning, https://arxiv.org/abs/2011.03181.
- [25] Mohammed Abo Sen (2024): Attention-GAN for Anomaly Detection: A Cutting-Edge Approach to Cybersecurity Threat Management, https://arxiv.org/abs/2402.15945.

Raja Ramanna Centre for Advanced Technology, Department of Atomic Energy, Govt. of India, Indore, M.P. India E-mail: swatil@rrcat.gov.in (Received, April 21, 2025)

School of Computer Science & Information Technology, Devi Ahilya Vishwavidyalaya, Indore, M.P., India E-mail: archana227/@gmail.com

Raja Ramunna Centre for Advanced Technology, Department of Atomic Energy, Govt. of India, Indore, M.P. India I alpana@recut.gov.in Debadatta Adak", Shekhar Das², Bindu Ranjan Chakma'

CONTROLLING INSURGENCY IN NORTHEAST INDIA BY GENERATION OF EMPLOYMENT AND AWARENESS: A SOCIO – MATHEMATICAL STUDY

ISSN: 0970-5120

Abstract

Insurgency is a persistent issue in Northeast India. This region of India is a habitat of different tribes with distinct ethnicity and cultural diversity. However, due to the mountainous and hilly territory Northeast India not well connected with the mainland. Therefore, it has been deprived of various socioeconomic development opportunities like the rest part of India. This deprivation fused with social, political and religious prosecutions has many times resulted in outburst of extremism and insurgency in different parts of Northeast India. It has caused unnecessary waste of lives and a major concern for law & order. Foreign powers also instigate such radical ideologies for their own vested interest. Therefore, eradication of this problem of insurgency from Northeast India is essentially required not only for this region but also for whole India. In this article we propose a deterministic mathematical model using the nonlinear differential equations to establish the hypothesis that the issue of insurgency in Northeast India can be resolved by adequate socioeconomic developments. We consider generation of employments and awareness against insurgency through proper education as the vital indicators of socioeconomic development. The boundedness and positivity of solutions have been studied. The existence and stability of the equilibrium solutions have been analyzed analytically as well as numerically. It has been shown that even in a society where unemployed youth are more prone to get involved in extremism due to their socioeconomic frustrations, insurgency can be eradicated by creating new jobs in a sufficiently higher rate and generating awareness against insurgency through appropriate education. Therefore, our results can be applied while framing various governmental policies for Northeast India to resolve the persistent issue of insurgency in this region.

Keywords: Insurgency, Employment, Northeast India, Mathematical model, Stability analysis, Numerical analysis, Critical values, Control mechanisms.

Mathematics Subject Classification 2020: 91D10, 97M10.

*Corresponding author.

1 Introduction

Insurgency has been one of the major problems that India had to encounter in the Northeast India since the time of India's independence. The Nagas were the first to raise their voice for a free Naga homeland and against forceful imposition of India's rule in the Naga hills. The Naga National Council (NNC) was formed under the leadership of A. Z. Phizo in 1946. The NNC under the leadership of Phizo declared Naga independence on 14 August 1947 and led an armed insurrection movement from early 1950s when their demand for a sovereign Naga state was turned down. The problem did not come down even after the formation of Nagaland in December 1963 due to refusal of NNC to recognize the new state. A peace accord was signed in 1975 in Shillong but the stalemate continued because Issac Swu and Thuingleng Muivah denounced the accord and they along with S S Kaphlang formed the Nationalist Socialist Council of Nagaland (NSCN) on January 31, 1980. The situation has improved considerably since the time of singing the "Indo-Naga" ceasefire between NSCN (I-M) and the Government of India on July 1, 1997 (Kotwal, 2000). However, the problem still remains unresolved (Karmakar, 2022). Following the footsteps of the Naga insurgency, the Mizo National Front (MNF) under the leadership of Phu Laldenga declared independence in Mizo hills and began a secessionist movement. With the formation of Mizoram state in 1987, the problem of Mizo insurgency had been resolved (Saikia, 2022). Tripura merged with the Union of India on September 9, 1949. But, disgruntlement among the tribal communities continued. The problem of insurgency turned into a serious law and order problem in Tripura in the 1980s with formation of Tripura National Volunteer (TNV) in 1981, National Liberation Front of Tripura (NLFT) in 1989 and All Tripura Tiger Force (ATTF) in 1990 demanding for political sovereignty of Tripura (Ghosh, 2003). Similarly, Manipur also merged with the Union of India on October 15, 1949. However, a section of the Meiteis was unhappy with the post-merger political development in Manipur fuelling secessionist tendencies. A number of separatist groups such as United National Liberation Front (UNLF), People's Liberation Army (PLA), People's Revolutionary Party of Kangleipak (PREPAK) were formed in 1960s and 1970s to achieve independence through armed struggle (Singh, 2015; Sundari & Sasikala, 2020) Assam has also been inflicted by insurgency problem. The insurgent groups like United Liberation Front of Assam (ULFA), National Democratic Front of Bodoland (NDFB), Bodo Territorial Tiger Force (BTLF) carried on their subversive activities against India's security establishment (Bhuyan, 2019).

1.1 Causes for the growth of insurgency in the Northeast India

There are different reasons that caused to the growth of insurgency and reasons which factored to sustain insurgency in the Northeast India. All these factors did not have similar effect in all the states and but incited the growth of ethnic nationalism in the entire Northeast.

1.1.1 Ethnicity in the Northeast India

Northeast India is home of different ethnic groups. Majority of these ethnic groups belong to the Sino-Tibetan and Tibeto-Burman groups of people. Therefore, in term of ethnic affiliation, they have closer proximity with the people of South East Asia than the people of mainland India (Hazarika, 2013). The British colonial administration, albeit, exploited the resources of Northeast India, yet it provided protection to the many Northeast hill tribes from the exploitation of the plain businessmen by promulgating the Bengal Eastern Frontier Regulations of 1887. The regulations restricted the entry of outsiders without permit obtaining from designated officers and provided internal autonomy to the hill tribes (Bengal Eastern Frontier Regulations, 2020). Naturally, following British decision to withdraw from India and India's attainment of independence, when there was jubilation and celebration, many hill tribes looked dejected thinking about their future political future. There was confusion whether they would get similar political protection following their integration with India or they would face cultural assimilation in the process of Indianization (Nag., 1998). Ethnicity, which De Vos defined as subjective, symbolic or emblematic use to differentiate themselves from other groups (Brass, 1991) was employed by many ethnic groups in the Northeast to reiterate their distinctive cultural identities and need for a homeland to protect and preserve their distinctiveness. Their apprehension has been addressed by the Government of India. New states such as Arunachal Pradesh, Nagaland, Mizoram, Meghalaya were created. Autonomous District Council under Sixth Schedule of the Indian Constitution were created in Mizoram, Tripura, Assam and Meghalaya were formed to address the ethnic demands of the small minority ethnic groups. The Government of India retained the Inner Line Regulations of the Bengal Eastern Regulations of 1887 in states like Arunachal Pradesh, Nagaland, Mizoram and Manipur. The constitution of India accepted cultural pluralism as symbol of national identity giving importance to the cultural values of every community in the country (Mohammed, 2016).

1.1.2 Illegal migration and demographic changes in the Northeast India

Following partition of the Indian sub-continent and formation of India and Pakistan, there had been an influx of refugees from East Pakistan (now Bangladesh) in Assam, Tripura and Meghalaya. The situation of minorities did not improve even after emergence of Bangladesh as an

independent nation state in 1971. Northeast Indian states sharing international border with Bangladesh in the western side continued to experience influx of illegal migration from Bangladesh. The influx of refugee and illegal migration from Bangladesh brought a dramatic change in demographic landscape in the Northeast India particularly in Tripura and Assam with the indigenous peoples converting into minority in Tripura. Anti-foreigner agitation in Assam, Tripura and Meghalaya turned violent threatening law and order situation in the Northeast India. Naturally, the Government of India decided to insert Section 6A in the Citizenship Act defining March 25, 1971 as the prescribed cut-off date for detection and deportation of foreigners in Assam. The Government of India promulgated several acts such as the Passport (Entry into India) Act, 1920 restricting and regulating the entry of the foreigners into India, the Foreigners (Tribunals) Order of 1964 empowering the district magistrates in all States and Union Territories to set up tribunals to decide on whether a person staying illegally is a foreigner or not. The illegal Migrants (Determination by Tribunals) Act, 1983 was enacted for detection and deportation of all illegal migrants who entered into India after March 25, 1971 (Singh, 2019).

1.1.3 Lack of economic development and sense of deprivation & exploitation

Geographically Northeast India is connected with the mainland India only through the Jalpaiguri corridor. The region did not witness much economic development due to its geographical isolation, road and connectivity problem and lack of attention of Government of India in economic development policies caused resentment and insecurity amongst the people in the Northeast India. The economic underdevelopment exacerbated the employment problem luring many youths to join various insurgent groups. The Mizo nationalism which culminated into a secessionist movement under the umbrella of MNF was a ramification of economic deprivation from the Government of Assam during the outbreak of rat famine in the Mizo hills in 1959 (Benjamin, 2022). The Government of India converted the Look East Policy into Act East Asia Policy in 2014. Northeast India has been projected as India's gateway to South East Asia. Since then, Government of India has been developing the road and connectivity in the Northeast to accelerate the process of economic development in the region. The development of tourism sector is given top priority. The Government of India is encouraging in entrepreneurship proving training to the youths. The Tribal Welfare Department, the nodal department for tribal development, in every state in the Northeast India provides short terms loans to become entrepreneurs.

The intensity of the insurgency movement has substantially declined in the Northeast India not only due to some proactive political measures but also largely it is because of economic growth and development that Northeast India has been experiencing in the last two decades. G Kishan Reddy, the Union Minister of Development of Northeast Region said in 2022 in the Parliament that the notable decline in insurgency in the region was due to Government of India's agenda of transforming Northeast India with a new phase of peace and prosperity (Singh, 2022). Therefore, if the pace of economic development can be accelerated, the problem of ethnic insurgency can be contained.

2 Mathematical models to contain the insurgency problem

A thorough understanding of the insurgency problem, namely, the causation, propagation, prevention etc. is essentially required to develop the effective and viable intervention strategies to mitigate the issues and challenges of insurgency and associated violence. In this regard mathematical models can provide an important insight in this direction. Applications of differential equations and related mathematical techniques to study various socio-economic problems was first pioneered by Lewis F. Richardson (Richardson, 1960). He studied the causes of war, its propagation, impacts of arms race between countries and the eruption of war using mathematical models (Richardson, 1935). In recent times various mathematical models have been studied by various researchers to analyze the dynamics of political party growth, the spread of crime etc. (see for instance Crisosto et al., 2010; Hayward, 1999; Jeffs et al., 2016; McMillon, Simon & Morenoff, 2014; Mohammad & Roslan, 1870; Perc, Donnay & Helbing, 2013; Romero et al., 2011; Sooknanan, Bhatt & Comissiong, 2013, 2016 and the references therein). A comprehensive review of the mathematical models to study the dynamics of crimes can be found in (D'Orsogna & Perc, 2015; Sooknanan & Comissiong, 2018). Use of compartmental models to study various socioeconomic issues such as insurgency, terrorism, fanatic behavior, violence, radicalization etc. can be found in Camacho (2013), Castillo-Chavez (2003), Galam (2016), Helbing et al. (2015), McCluskey (2018), Nathan (2018), Santoprete (2018) and the references therein. Chuang (2018) studied an age-structured model of radicalization and a bistable model of terrorism (Chuang, 2017). A game theoretic terrorism model was proposed and analyzed by Short (2017). A mathematical study involving terrorist and fanatic was proposed by Camacho (2013). In this study the population has been divided into core and non-core groups. In the first model two core populations have been considered with no interactions between the subpopulations and both of the core-groups are taken from the same general designated population. They have shown that, with increasing implementation of efforts to recruit and retain, terrorist groups will be able to influence vulnerable individuals. They have however, did not consider the impacts of governmental interventions to combat the terrorism. A deterministic model of incorporating the allocation of optimal human resources to implement counter-terrorism operations was proposed by Udoh (2019). They studied possible strategies to allocate counter-terrorism resources towards providing a long-term mitigation

of the terrorism problem. In this article coupled differential equations have been used with system variables representing the internal and external dynamics of the insurgent organization. In their model, they have not considered the effect of detention/rehabilitation facility. The model proposed by Castillo-Chavez (2003) was extended by Cherif, et al. (2010) where the authors developed a mathematical model of insurgency process. They have considered the spread of radical ideologies, recruitment of new terrorists, impacts of fanatisms etc. including control of terrorism and radicalization process. A deterministic model to study the radicalization process in Kenya is proposed by Ngari (2016). Authors proposed control of the insurgency problem through rehabilitation centres but did not consider implementation of detention facility. A compartmental model to analyse the impacts of de-radicalization programs is studied by Sandler (2014). The authors have divided the general population in the following four compartments, namely, Susceptible (S), Extremists (E), Recruiters (R), and Under Treatment or deradicalization programs (T). They however, did not incorporate the possibility of force recruitment of the susceptible or already treated individuals. A five compartmental model including the vaccinated compartment that incorporates the individuals who have already gone through Countering Violent Extremism (CVE) programs before being radicals is studied by Santoprete (2019). In this study the authors analysed the impacts of CVE programs to counter terrorism. Chuang (2019) proposed a mathematical model with two cross sections to analyse the propagation of insurgency among different sub populations. The first model exhibits the possibility of an individual to progress from susceptible to moderate group before becoming a terrorist. Whereas, in the second model authors have considered two radical groups, which emerge from the susceptible before becoming fully radical without any possibility of control strategies. An optimal control model to implement counter-terrorism was studied by Bayon et al. (2019). The authors proposed "fire" and "water" control strategies but did not consider surveillance, detention/rehabilitation, facilities, force recruitment etc. Applications of optimal control strategies using Differential Transformation Method (DTM) is proposed by Akande (2017). Interestingly their result shows that implementation of the best control strategy does not always imply optimality but accuracy in result compared to other possible control mechanisms. Udwadia (2006) developed a dynamical model of terrorism incorporating the impacts of direct governmental interventions through military and police to control the terrorist population. Their study concluded that that using military and police actions may reduce the threat of insurgency, A dynamic model considering suicide bombers and political influence is studied by Geller (2015). Their study provided the emphasized and de-emphasized impacts of the forces in controlling the insurgency problem.

3 Mathematical models of unemployment

Adequate generation of employment is a vital indicator of economic development. Unemployment is an increasing global concern and according to Global Employment Trends 2012 out of a global labor force of 3.3 billion people all over the world almost 200 million people are unemployed. In a pioneering work to understand the dynamics of the problem of unemployment Nikolopoulos (2003) proposed a mathematical model and provided few measures to control unemployment. Some notable studies in this field have been performed by Misra (2011, 2013). Misra (2013) assumed a constant rate of increase of the unemployed individuals. Whereas, their number decreases due to death and emigration, at fixed constant rate proportional to the number of unemployed individuals They have also considered that the unemployed people acquire jobs at a rate proportional to the number of present unemployed persons and the number of available vacancies. A delay mathematical model incorporating the job creation delay has been studied by Misra (2013). According to their analysis if the rate of getting employment increases or the number of newly created vacancies increases then number of unemployed people decreases. Their study also suggests that creation of new job opportunities can be a solution of unemployment problem. Hence, they suggested that government must create new jobs parity with the present number of unemployed individuals to overcome the unemployment crisis.

In this article we propose a deterministic mathematical model with an aim to control the issues and challenges of the insurgency problem in Northeast India by generation of adequate employment opportunity which is considered as one of the important indicators of socioeconomic development. We also incorporate the awareness against the insurgency and violence among the people of Northeast India. In fact, proper awareness can be generated only with appropriate education which can only be sustained with adequate socioeconomic development.

4 Model Formulation

Let, us denote U(t), R(t), T(t), J(t) and E(t) respectively be the densities of unemployed individuals, recruiters of insurgency groups, insurgents, available jobs and employed individuals at any time t in any designated area. Let Δ be the constant input of unemployed people, especially youth, who can be exploited by the insurgent groups. β be the rate at which recruiters interact with those unemployed people. However, α fraction of the unemployed people who get convinced by the recruiters to participate in insurgency groups become recruiters and $(1 - \alpha)$ portion becomes insurgents themselves. Recruiters can become insurgents at a rate σ_1 and the insurgents can become recruiters at a rate σ_2 . New jobs are created at a rate ϕ depending on the density of present unemployed people. Unemployed people get jobs at a rate γ . The parameter γ also provides a measurement of the available skills and training of the unemployed individuals to obtain the new

job opportunities. Various job opportunities are shut down or lapsed at a rate m. The employed people lose their jobs and again become unemployed at a rate θ . The removal rate of unemployed and employed people due to migration, retirement or natural death is considered to be μ . However, the recruiters and insurgents experience some additional death rate due to be killed by police/army, incarcerated in jail etc. Their extra death rate is represented by δ . It is important to mention that, even employed individuals may get influenced by insurgency ideologies. However, in our work we do not consider that case, as one of the objectives of our study is to understand the impacts of generation of new employments on controlling the insurgency. We propose the following schema diagram to provide a pictorial demonstration of the interactions between different system classes:

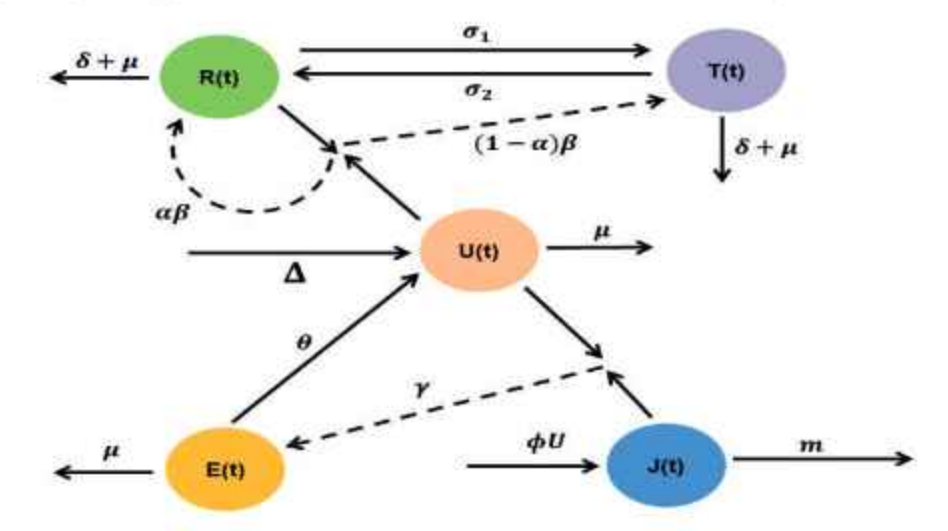


Figure 1. Schema diagram of the interactions between system populations.

We propose the following deterministic mathematical model using nonlinear ordinary differential equations based on the interactions described in the schema diagram given in Fig. 1:

$$\begin{split} \frac{dU}{dt} &= \Delta - \beta U R - \gamma U J + \theta E - \mu U, \\ \frac{dR}{dt} &= \alpha \beta U R - \sigma_3 R + \sigma_2 T - (\delta + \mu) R, \\ \frac{dT}{dt} &= (1 - \alpha) \beta U R + \sigma_1 R - \sigma_2 T - (\delta + \mu) T, \\ \frac{dJ}{dt} &= \phi U - m J, \\ \frac{dE}{dt} &= \gamma U J - \theta E - \mu E. \end{split}$$
 (1)

If the rate of awareness against insurgency increases then insurgency should decrease. Moreover, if adequate job opportunities are generated for people of Northeast India, then their quality of life will increase through proper socio-economic development. Let, c be the rate of awareness against the insurgency among the people. $c \in [0,1]$, where c=1 implies 100% awareness and c=0 signifies absence of awareness. We therefore, modify Model System (1) to the following model incorporating the effect of awareness against insurgency:

$$\frac{dU}{dt} = \Delta - \frac{(1-c)\beta UR}{a+J} - \gamma UJ + \theta E - \mu U,$$

$$\frac{dR}{dt} = \frac{(1-c)\alpha\beta UR}{a+J} - \sigma_1 R + \sigma_2 T - (\delta + \mu) R,$$

$$\frac{dT}{dt} = \frac{(1-c)(1-\alpha)\beta UR}{a+J} + \sigma_1 R - \sigma_2 T - (\delta + \mu) T,$$

$$\frac{dJ}{dt} = \phi U - mJ,$$

$$\frac{dE}{dt} = \gamma UJ - \theta E - \mu E.$$
(2)

Here a is a constant. We will study this Model System (2) under the initial conditions given by:

$$U(0) > 0, R(0) \ge 0, T(0) \ge 0, I(0) > 0, T(0) > 0.$$
 (3)

5 Analytical results

In this section we derive different analytical results such as positivity and boundedness of the solutions of the Model System (2), existence and stability of the equilibrium points etc.

5.1 Positivity and boundedness

Proposition 5.1 All solutions of System (2) are positively invariant and uniformly bounded in Γ for all large t where,

$$\Gamma = \left\{ (U,R,T,J,E) \in \mathbb{R}^5_+ \mid 0 < U(t) + R(t) + T(t) + E(t) \leq \frac{\Delta}{\mu} , 0 \leq J(t) \leq \frac{\Delta \phi}{\mu m} \right\}$$

Proof. First, we show that all the solutions of the System (2) starting with initial conditions (2) are positive, using a lemma proposed by Nagumo (1952).

Lemma 5.1 Consider a system $\dot{X} = F(X)$ where $F(X) = [F_1(X), F_2(X), ..., F_n(X)], X \in \mathbb{R}^n$ with initial condition $X(0) = X_0 \in \mathbb{R}^n$. If for $X_i = 0, i = 1, 2, ..., n$ we get $F_i(X)|_{X_i = 0} \ge 0$, then any solution of $\dot{X} = F(X)$ with given initial condition, say, $X(t) = X(t; X_0)$ will be positive i.e., $X(t) \in \mathbb{R}^n_+$.

It can be easily seen from (2) that $\frac{dU}{dt}|_{U=R=T=J=E=0}=\Delta>0$ and when U=R=T=J=E=0 then $\frac{dR}{dt}=\frac{dT}{dt}=\frac{dJ}{dt}=\frac{dR}{dt}=0$. Hence following Lemma 3.1 all solutions of (2) starting with initial conditions (3) are positive.

Next, we establish the boundedness of the solutions of (1) for all large t. Let, W(t) = U(t) + R(t) + T(t) + J(t) + E(t). Differentiating W(t) along the solutions of (2), we find

$$\dot{W}(t) = \dot{U}(t) + \dot{R}(t) + \dot{T}(t) + \dot{E}(t) \Rightarrow \dot{W}(t) \leq \Delta - \mu W \Rightarrow \lim_{t \to \infty} W(t) \leq \frac{\Delta}{\mu}.$$

Therefore, the solutions U(t), R(t), T(t), E(t) of (2) are all bounded above by $\frac{\Delta}{\mu}$. Again, from the 4^{th} equation of (2) one can calculate that

$$\frac{dJ}{dt} = \phi U - mJ \Rightarrow \frac{dJ}{dt} + mJ \leq \frac{\phi \delta}{\mu} \Rightarrow \lim_{t \to \infty} J(t) \leq \frac{\Delta \phi}{\mu m}.$$

Therefore, for all large t, solutions of System (2) are positively invariant and uniformly bounded in the region Γ . Hence the proposition is proved.

5.2 Equilibrium points and their existence conditions

Model System (2) has two equilibrium points. Namely insurgency free equilibrium point $P_0(U_0,0,0,J_0,E_0)$ and insurgency equilibrium $P^*(U^*,R^*,T^*,J^*,E^*)$. The population densities at the equilibrium P_0 are given by $J_0 = \frac{\phi U_0}{m}$, $E_0 = \frac{\Delta}{\mu} - U_0$ and U_0 is given by the positive roots of the following quadratic equation:

$$A_1 U^2 + A_2 U + A_3 = 0,$$

where $A_1 = \frac{r\phi}{m} > 0$, $A_2 = \theta + \mu > 0$, $A_3 = -\frac{\Delta(\theta + \mu)}{\mu} < 0$. Clearly, this equation has exactly one positive root given by: $U_0 = \frac{-A_2 + \sqrt{A_2^2 - 4A_1A_2}}{2A_1}$.

The equilibrium
$$P_0$$
 will be feasible if $0 < U_0 < \frac{\Delta}{\mu}$. (4)

Again, at $P^*(U^*, R^*, T^*, J^*, E^*)$ we have

$$\begin{split} E^* &= \lambda (U^*)^2 \,, \\ J^* &= \frac{\phi U^*}{m}, \\ R^* &= \frac{B_1 (U^*)^3 + B_2 (U^*)^2 + B_3 (U^*) + B_4}{B_5 U^*}, \\ T^* &= \frac{B_6 (U^*)^3 + B_7 (U^*)^2 + B_8 (U^*) + B_9}{B_{10} U^*}, \end{split}$$

where $\lambda = \frac{\gamma\phi}{m(\theta+\mu)} > 0$, $B_1 = \phi\left(\theta\lambda - \frac{\gamma\phi}{m}\right)$, $B_2 = \left(\theta\lambda - \frac{\gamma\phi}{m}\right)am - \mu\phi$, $B_3 = \phi\Delta - \mu am$, $B_4 = \Delta am$, $B_5 = \beta m(1-c)$, $B_6 = -\mu B_5\lambda - (\delta+\mu)B_1$, $B_7 = -\mu B_5 - B_2(\delta+\mu)$, $B_8 = B_5\Delta - B_3(\delta+\mu)$, $B_9 = -B_4(\delta+\mu)$, $B_{10} = B_5(\delta+\mu)$. The equilibrium density U^* is found to be the positive roots of the following equation:

$$D_1(U^*)^4 + D_2(U^*)^3 + D_3(U^*)^2 + D_4(U^*) + D_5 = 0,$$

where,

$$\begin{split} D_1 &= B_{10}\bar{C}_1B_1 + B_5\bar{C}_3B_6, \\ D_2 &= B_{10}(\bar{C}_1B_2 + B_1\bar{C}_2) + B_5(\bar{C}_3B_6\bar{C}_4 + \bar{C}_3B_8), \\ D_3 &= B_{10}(B_3\bar{C}_1 + B_2\bar{C}_2) + B_5(\bar{C}_3B_7\bar{C}_4 + \bar{C}_3B_8), \\ D_4 &= B_{10}(B_4\bar{C}_1 + B_3\bar{C}_2) + B_5(\bar{C}_3B_8\bar{C}_4 + B_4\bar{C}_3), \\ D_5 &= B_{10}B_4\bar{C}_2 + B_5\bar{C}_3B_9\bar{C}_4, \\ \bar{C}_1 &= (1 - c)\alpha\beta - \frac{\phi}{m}(\delta + \mu + \sigma_1), \\ \bar{C}_2 &= -a(\delta + \mu + \sigma_1), \bar{C}_3 = \frac{\sigma_2\phi}{m}, \bar{C}_4 = \frac{am}{\phi}. \end{split}$$

However, due to the high parametric complexity of the equilibrium population densities at P^* we will verify its existence numerically.

5.3 Local stability analysis of the equilibrium points

First, we discuss the local stability of the equilibrium point P_0 using linearization method. The Jacobian matrix evaluated at P_0 is given by

$$W_1(U_0, 0, 0, J_0, E_0) = \begin{pmatrix} m_{11} & m_{12} & 0 & m_{14} & m_{15} \\ 0 & m_{22} & m_{23} & 0 & 0 \\ 0 & m_{32} & m_{33} & 0 & 0 \\ m_{41} & 0 & 0 & m_{44} & 0 \\ m_{51} & 0 & 0 & m_{54} & m_{55} \end{pmatrix},$$

where,

$$\begin{split} m_{11} &= \gamma J_0 - \mu, \\ m_{12} &= -\frac{(1-c)\beta U_0}{a+J_0}, \\ m_{24} &= -\gamma U_0, \\ m_{15} &= \theta, \\ m_{22} &= \frac{(1-c)\alpha\beta U_0}{a+J_0} - \sigma_1 - (\delta+\mu), \\ m_{23} &= \sigma_2, \\ m_{32} &= \frac{(1-c)(1-\alpha)\beta U_0}{a+J_0} + \sigma_1, \\ m_{33} &= -\sigma_1 - (\delta+U_0), \\ m_{41} &= \phi, \\ m_{44} &= -m, \\ m_{51} &= \gamma J_0, \\ m_{54} &= \gamma U_0, \\ m_{55} &= -\theta - \mu. \end{split}$$

The characteristic equation of the Jacobian matrix W_1 is given by

$$\lambda^{5} + V_{1}\lambda^{4} + V_{2}\lambda^{3} + V_{3}\lambda^{2} + V_{4}\lambda + V_{5} = 0$$

where,

$$\begin{split} V_1 &= \frac{X_2}{X_1}, & V_2 &= \frac{X_3}{X_1}, & V_3 &= \frac{X_4}{X_1}, & V_4 &= \frac{X_5}{X_1}, & V_5 &= \frac{X_6}{X_1}, & X_1 &= R_6, \\ X_2 &= R_5, & X_3 &= O_4 + R_4 + T_4, & X_4 &= O_3 + R_3 + T_3, \\ X_5 &= O_2 + R_2 + T_2, & X_6 &= O_1 + R_1 + T_1, & O_1 &= N_1 N_2 + N_5 N_2, \\ O_2 &= N_1 N_3 + N_5 N_3 + N_6 N_2, & O_3 &= N_1 N_4 + N_5 N_4 + N_6 N_3, \\ O_4 &= N_6 N_4, & N_1 &= m_{15} m_{41} m_{54}, & N_2 &= m_{33} m_{22} - m_{32} m_{23}, \\ N_3 &= -(m_{33} + m_{22}), & N_4 &= 1, & N_5 &= -m_{15} m_{51} m_{44}, \\ N_6 &= m_{15} m_{51}, & R_1 &= Q_1 Q_4, & R_2 &= Q_1 Q_5 + Q_2 Q_4, \\ R_3 &= Q_1 + Q_2 Q_5 + Q_3 Q_4, & R_4 &= Q_2 + Q_3 Q_5 + Q_4, \\ R_5 &= Q_3 + Q_5, & R_6 &= Q_6, & Q_1 &= P_1 P_3, & Q_2 &= P_1 P_4 + P_2 P_3, \\ Q_3 &= P_2 P_4 + P_3, & Q_4 &= P_5, & Q_5 &= P_6, & Q_6 &= 1, \\ P_1 &= m_{55} m_{11}, & P_2 &= -(m_{55} + m_{11}), & P_3 &= m_{44}, & P_4 &= -1, \\ P_5 &= m_{22} m_{33} - m_{32} m_{23}, & P_6 &= -(m_{22} + m_{33}), & T_1 &= S_1 S_3, \\ T_2 &= S_2 S_3 + S_1 S_4, & T_3 &= S_1 + S_2 S_4, & T_4 &= S_2, \\ S_1 &= -m_{14} m_{41} m_{55}, & S_2 &= m_{41} m_{14}, & S_3 &= m_{22} m_{33} - m_{23} m_{32}, \\ S_4 &= -(m_{22} + m_{33}), & T_1 &= S_1 S_3, \\ \end{array}$$

Hence, we obtain the following proposition:

Proposition 5.2 If the insurgency-free equilibrium P_0 exists following (4) then it will be is locally asymptotically stable if and only if:

$$V_1 > 0, V_5 > 0, V_1V_2 > V_3, V_1(V_2V_3 + V_5) > V_3^2 + V_1^2V_4,$$

 $V_1V_2V_3V_4 + 2V_1V_4V_5 + V_2V_3V_5 > V_1V_2^2V_5 + V_1^2V_4^2 + V_4V_4^2 + V_5^2$

where the expressions of V_t , t = 1, 2, 3, 4, 5 are given in (4).

The Jacobian matrix evaluated at the insurgency equilibrium P^* is given by,

$$W_2(U^*,R^*,T^*,J^*,E^*) = \begin{pmatrix} a_{11} & a_{12} & 0 & a_{14} & a_{15} \\ a_{21} & a_{22} & a_{23} & a_{24} & 0 \\ a_{31} & a_{32} & a_{33} & a_{34} & 0 \\ a_{41} & 0 & 0 & a_{44} & 0 \\ a_{51} & 0 & 0 & a_{54} & a_{55} \end{pmatrix}$$

where,

$$\begin{split} a_{11} &= -\frac{(1-c)\beta R^*}{a+J^*} - \gamma J^* - \mu, a_{12} = -\frac{(1-c)\beta U^*}{a+J^*}, \ a_{14} = \frac{(1-c)\beta U^*R^*}{(a+J^*)^2} - \gamma U^*, \ a_{15} = \theta, \\ a_{21} &= \frac{(1-c)\alpha\beta R^*}{\alpha+J^*}, a_{22} = \frac{(1-c)\alpha\beta U^*}{a+J^*} - \sigma_1 - (\delta+\mu), a_{23} = \sigma_2, \qquad a_{24} = \frac{(1-c)\alpha\beta U^*R^*}{(a+J^*)^2}, \\ a_{31} &= \frac{(1-c)(1-\alpha)\beta R^*}{a+J^*}, a_{32} = \frac{(1-c)(1-\alpha)\beta U^*}{a+J^*} + \sigma_1, \qquad a_{33} = -\sigma_1 - (\delta+U^*), \\ a_{34} &= -\frac{(1-c)(1-\alpha)\beta U^*R^*}{(a+J^*)^2}, \qquad a_{41} = \phi, \qquad a_{44}(U^*,R^*,T^*,J^*,E^*) = -m, \qquad a_{51} = \gamma J^*, \end{split}$$

$$a_{54} = \gamma U^*$$
, $a_{55} = -\theta - \mu$.

The characteristic equation of W_2 is given by:

$$\lambda^{5} + U_{1}\lambda^{4} + U_{2}\lambda^{3} + U_{3}\lambda^{2} + U_{4}\lambda + U_{6} = 0$$

where,

$$\begin{array}{llll} U_1 = \frac{M_2}{M_1}, & U_2 = \frac{M_3}{M_1}, & U_3 = \frac{M_4}{M_1}, & U_4 = \frac{M_5}{M_1}, & U_5 = \frac{M_6}{M_1}, & M_1 = L_6, & M_2 = L_5, \\ M_3 = G_4 + I_4 + L_4, & M_4 = G_3 + I_3 + L_3, & M_5 = G_2 + I_2 + L_2, \\ M_6 = G_1 + I_1 + L_1, & G_1 = F_1F_3 + F_5F_3, & G_2 = -F_1F_4 + F_2F_3 - F_5F_4, \\ G_3 = F_1 - F_2F_4 - F_5, & G_4 = F_2, & F_1 = -a_{15}a_{51}a_{44}, & F_2 = a_{15}a_{51}, \\ F_3 = a_{22}a_{33} - a_{23}a_{32}, & F_4 = a_{22} + a_{33}, & F_5 = a_{54}a_{15}a_{41}, \\ I_1 = H_5H_7 + H_1H_3, & I_2 = -H_1H_4 + H_2H_3 - H_5H_8 + H_6H_7, \\ I_3 = -H_2H_4 + H_5 - H_6H_8, & I_4 = H_6, & H_1 = -a_{41}a_{12}a_{55}, & H_2 = a_{41}a_{12}, \\ H_3 = a_{23}a_{34} - a_{24}a_{33}, & H_4 = -a_{24}, & H_5 = -a_{41}a_{14}a_{55}, & H_6 = a_{41}a_{14}, \\ L_1 = K_7 + K_1K_5, & L_2 = K_1K_6 + K_2K_5 + K_6, & L_3 = K_1 + K_2K_6 + K_9, \\ L_4 = K_2 + K_3K_6 + K_4K_5 + K_{10}, & L_5 = K_3 + K_4K_6, & L_6 = K_4, & K_1 = J_1J_3, \\ K_2 = -J_1 - J_2J_3, & K_3 = J_2J_3 + J_3, & K_4 = -1, & K_5 = J_4, K_6 = J_5, \\ K_7 = J_6J_9, & K_8 = J_6J_{10} + J_7J_9, & K_9 = J_7J_{10} + J_8J_9, K_{10} = J_9J_{10}, \\ J_1 = a_{55}a_{44}, J_2 = a_{55} + a_{44}, & J_3 = a_{11}, & J_4 = a_{22}a_{33} - a_{23}a_{32}, \\ J_4 = -(a_{22} + a_{33}), & J_6 = -a_{55}a_{44}a_{12}, & J_7 = a_{12}(a_{55} + a_{44}), \\ J_8 = -a_{12}, & J_9 = a_{21}a_{33} - a_{23}a_{31}, & J_{10} = -a_{21}, \end{array}$$

Hence, we obtain the following proposition:

Proposition 5.3 If the insurgency equilibrium P* exists then it will be is locally asymptotically stable if and only if:

$$\begin{split} &U_1>0, U_5>0, U_1U_2>U_3, U_1(U_2U_3+U_5)>U_3^2+U_1^2U_4,\\ &U_1U_2U_3U_4+2U_1U_4U_5+U_2U_3U_5>U_1U_2^2U_5+U_1^2U_4^2+U_4U_3^2+U_5^2 \end{split}$$

where the expressions of U_i , i = 1, 2, 3, 4, 5 are given in (6).

6 Numerical simulations

In this section we perform numerical simulations of model System (2) using MATLAB 2015a. First, we consider a society that is highly prone to insurgency activities with the following characteristics and denote it by Society – X.

CH1. Low rate of awareness against insurgency practices. This basically implies low rate of the parameter c that measures the mass awareness against insurgency, terrorism and violence.

- CH2. High rate of interactions between recruiters of insurgent groups and unemployed persons. Namely value of the parameter β, that represents the rate of interaction between unemployed individuals and recruiters is considerably high.
- CH3. Low employment rate. In this case the rate y at which unemployed individuals get employed is low.
- CH4. Low creation rate of new employment opportunities, which implies the rate of creation of new jobs (φ) is low.

Based on the above discussion we consider the following parameter set to numerically simulate the characteristics CH1 to CH4 of Society – X.

$$\Delta = 5, \beta = 0.056, \alpha = 0.5, c = 0.3, \mu = 0.007, \theta = 0.15, m = 0.2, \gamma = 0.005,$$

 $\sigma_1 = 0.08, \sigma_2 = 0.06, \delta = 0.003, \phi = 0.1, \alpha = 50.$
(7)

For these parameter values one can calculate that $U_1 = 0.2232 > 0$, $U_5 = 11.43 > 0$, $U_1U_2 - U_3 = 0.6653 > 0$, $U_1(U_2U_3 + U_5) - (U_3^2 + U_1^2U_4) = 3.8772 > 0$, $U_1U_2U_3U_4 + 2U_1U_4U_5 + U_2U_3U_5 - (U_1U_2^2U_5 + U_1^2U_4^2 + U_4U_3^2 + U_5^2) = 0.00532 > 0$. Hence following Proposition 5.3 we obtain that the insurgency equilibrium P^* is locally asymptotically stable. It signifies that insurgency persists in a stable condition in the Society – X. The time evolutions of system trajectories have been depicted in Fig. 2. It shows that with lower level of awareness, rate of being employed, rate of new job creation and higher level of interactions between unemployed people and insurgent recruiters, insurgency prevails in the Society – X that has the aforementioned characteristics given in CH1 – CH4.

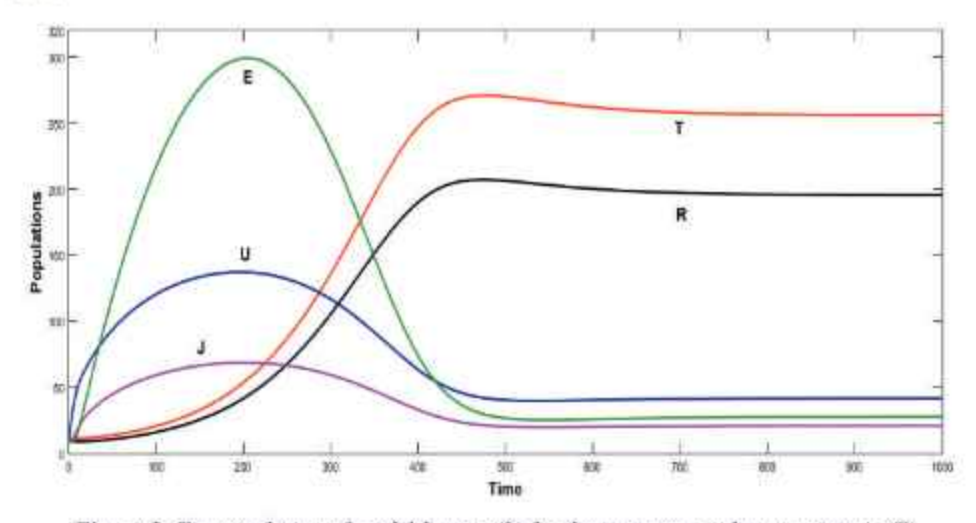


Figure 2. Time evolution of model System (2) for the parameter values as given in (7).

Next, we perform PRCC (Partial Rank Correlation Analysis) with p-value < 0.0001 to identify the most sensitive parameters of System (2). The PRCC analysis diagram is shown in Fig. 3. It clearly shows that the parameters c, β , γ and ϕ are the most sensitive parameters and act as the major regulators of the system dynamics and controlling the insurgency. Our objective is to check the impacts of the aforementioned four most sensitive parameters to control and if possible, eradicate insurgency from the Society – X.

6.1 Joint effect of c and β

First, we study the joint effect of the parameter c that measures the awareness against insurgency and β , the rate of interaction between unemployed individuals with recruiters of the insurgency organizations. It should be noted that c and β are interconnected. The basic hypothesis behind it is that if awareness against extremism increases then interactions between recruiters of insurgency groups and unemployed individuals will decrease and vice versa. This will provide an effective strategy to control insurgency through generation of awareness. The stability regions of the equilibrium points P_0 and P^* for joint variation of c and β are depicted in Fig. 4a.

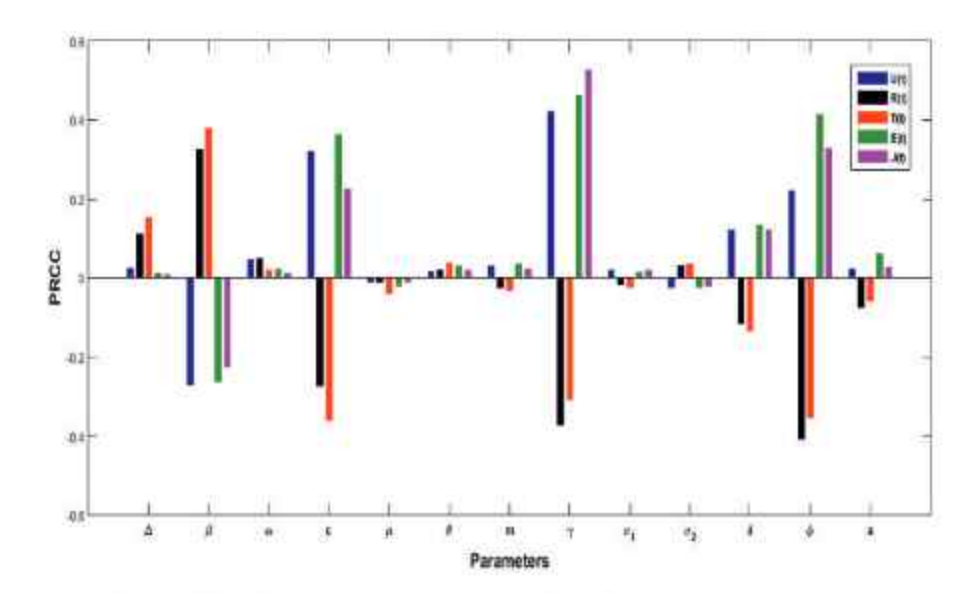


Figure 3. PRCC analysis with p -value < 0.0001 of the parameters of System (2).

It clearly conforms to our hypothesis that, by increasing awareness against insurgency practices, the rate of interactions between unemployed people and insurgency group recruiters can be decreased and thereby, insurgency can be contained. Now our objective is to free the Society – X from the

insurgency practices. We have considered $\beta = 0.056$ and c = 0.3 to simulate Society – X. Now from Fig. 4a one can see that for these values of β and c Society – X will not be free of insurgency (see Fig. 2). Now, we increase c from c = 0.3 to c = 0.55. From Fig. 4a we can assert that insurgency will not be eradicated, but the population density of insurgents and recruiters in Society – X will decrease. This case is depicted in Fig. 4b. The decrease in number of insurgents and recruiters can easily be seen by comparing Fig. 4b with Fig. 2.

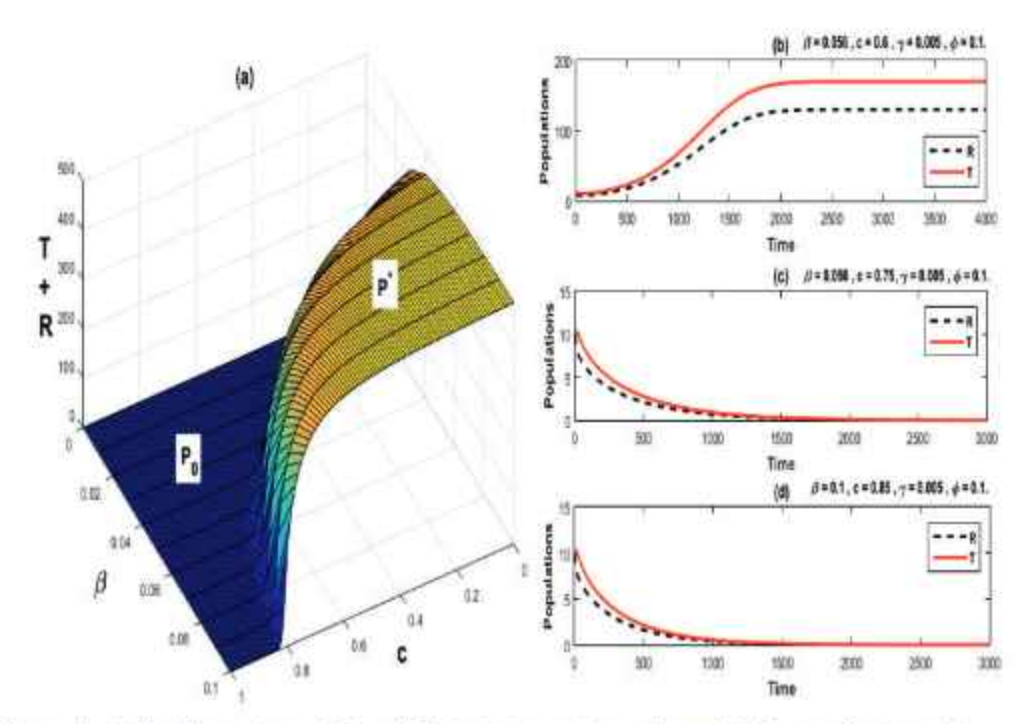


Figure 4. (a) Stability regions of P_0 and P^* for joint variation of c and β . Time evolutions of the System (2) for different values of c and β (b) $\beta = 0.056$, c = 0.55, (c) $\beta = 0.056$, c = 0.75 and (d) $\beta = 0.1$, c = 0.85. Other parameters are as in (7).

However, following Fig. 4a if c is increased to c = 0.75 then insurgent and recruiter population dies out. This case is shown in Fig. 4c. It shows, if we wish to free Society – X from insurgency, the awareness (c) has to be at least 0.75. In this case it is calculated that $U_0 = 182.376 < \frac{\delta}{\mu} = 714.2857$. Hence, P_0 exists following (4) and as $V_1 = 21.781 > 0$, $V_5 = 2.398 > 0$, $V_1V_2 - V_3 = 0.0098 > 0$, $V_1(V_2V_3 + V_5) - (V_3^2 + V_1^2V_4) = 0.0734 > 0$, $V_1V_2V_3V_4 + 2V_1V_4V_5 + V_2V_3V_5 - (V_1V_2^2V_5 + V_1^2V_4^2 + V_4V_3^2 + V_5^2) = 11.2541 > 0$, following Proposition 5.2 we obtain that P_0 is

locally asymptotically stable. Therefore, all system trajectories converge to insurgency-free equilibrium P_0 and insurgency is removed from the Society – X. Interestingly, if we can increase the awareness against insurgency and extremism to a level higher than $c^* = 0.85$ (approximately, following Fig. 4a) which is basically the critical level of awareness to be generated, then from Fig. 4a one can easily see that even with high rate of interactions between unemployed individuals and recruiters of insurgency groups, the society can be made free of insurgency (Fig. 4d). Hence, utilizing Fig. 4a we can determine the level of awareness against insurgency practices is necessarily required to free Society – X of insurgency practices, if the rate of interactions between unemployed individuals and recruiters of insurgency groups is known.

6.2 Joint effect of y and ϕ

The combined effect of γ and ϕ is an important aspect of our study. The parameter γ measures the rate of new employment of the unemployed individuals. Whereas, the parameter ϕ signifies the rate at which new employments are created. Evidently effects of these two parameters are interlinked. We consider the hypothesis that if ϕ increases, then more new jobs will be created and as a result unemployed individuals will be employed at a higher rate i.e., y will increase. And as the unemployed individuals get employed, their economic condition will develop and they will stay away from insurgency. It is also important to under stand that mere creation of new jobs does not always imply less unemployment, as without proper training and skills required for the new jobs, unemployed will remain unemployed. Therefore, once new job opportunities are created, it is essential to provide the necessary skill development trainings to the unemployed individuals to increase the rate of employment among them. The stability regions of P_0 and P^* for varying ϕ and y have been drawn in Fig. 5a. This figure provides an important estimate about the level of skill development and training to be given to the unemployed individuals, if the rate of new jobs creation is known. Now as mentioned before we wish to make the Society - X free of insurgency. So, keeping all other parameters fixed at (7), if we increase y from y = 0.005 to y = 0.05, we can see by comparing Fig. 5b and Fig. 2, that insurgency is not cradicated, but surely decreased. Observing Fig. 5a, if we further increase γ to $\gamma = 0.135$, then Society – X can be made free of insurgency (Fig. 5c). Therefore, if the rate of new job creation is known, then we can determine the required rate of employment necessarily required to eradicate insurgency using Fig. 5a. Another interesting observation that can be derived from Fig. 5a, that if the rate of new job creation ϕ is higher than an upper critical level, in this case it is approximately $\phi^* = 0.35$, then even with low rate of employment Society – X can be made free of insurgency (Fig. 5d). However, if ϕ is below a lower critical lower level, which is in this case approximately $\phi_* = 0.55$, then even with quite high rate of employment, say $\gamma = 0.2$, insurgency will prevail in the Society – X (Fig. 5e). Therefore, to free Society – X from insurgency, the rate of generation of new jobs must be higher than a critical value ϕ_{i} .

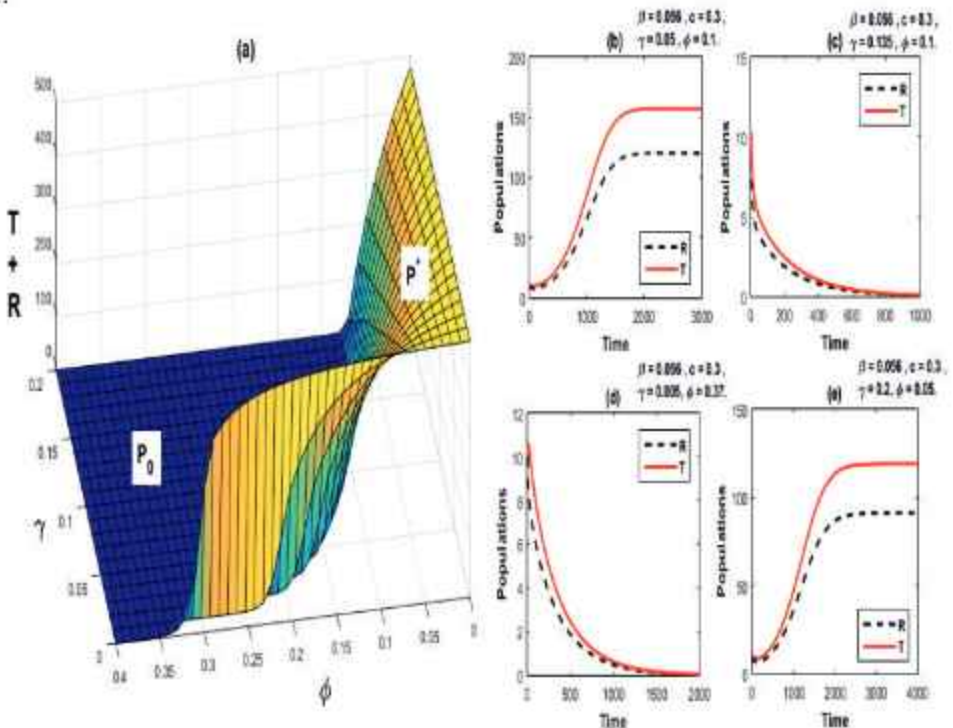


Figure 5. (a) Stability regions of P_0 and P^* for joint variation of γ and ϕ . Time evolutions of the System (2) for different values of γ and ϕ (b) $\gamma = 0.05$, $\phi = 0.1$, (c) $\gamma = 0.135$, $\phi = 0.1$, (d) $\gamma = 0.005$, $\phi = 0.37$ and (e) $\gamma = 0.2$, $\phi = 0.05$. Other parameters are as in (7).

6.3 Joint effect of c and ϕ

We now study the combined effect of awareness against insurgency (c) and the rate of generation of new jobs (ϕ) to mitigate the issue of insurgency in Society – X. It is evident that creation of new jobs will encourage the unemployed youth not to choose violence over socioeconomic development. Moreover, this mechanism to control insurgency is directly related to governmental policies & schemes. It is important to understand that the creation of new jobs is actually interlinked with the awareness against insurgency practices. If more new jobs are created unemployed youth will be more hopeful towards socioeconomic developments by being employed. For being employed they will require skill development training and proper educational qualifications. To acquire that they will go to educational institutes & participate in various

governmental skill development initiatives like Make in India, Digital India, Self-Reliant India, Skill India Programs etc. In this way they will get proper education and eventually become aware against the ways of extremism. Hence their possibility of being brainwashed by the recruiters of insurgency groups will be low. As a result, insurgency will decrease due to lack of new recruits.

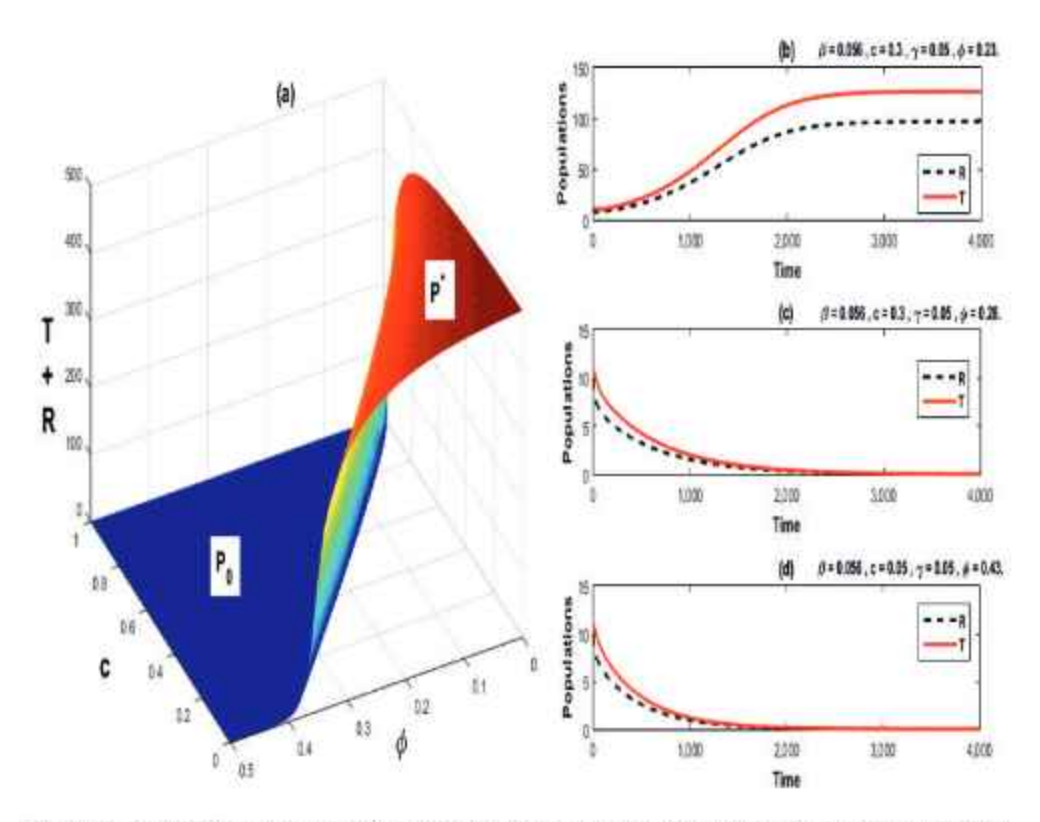


Figure 6. (a) Stability regions of P_0 and P^* for joint variation of c and ϕ . Time evolutions of the System (2) for different values of c and ϕ (b) c = 0.3, $\phi = 0.23$, (c) c = 0.3, $\phi = 0.28$, (d) c = 0.05, $\phi = 0.43$. Other parameters are as in (7).

The stability regions of the equilibrium points P_0 and P^* for varying c and ϕ have been drawn in Fig. 6a. It shows a reverse relation between c and ϕ , i.e., the level of awareness required to free Society – X from the menace of insurgency will be high if the rate of generation of new jobs is low and vice versa. The rate of new employments to be generated to make Society – X free of extremism for a known level of awareness against insurgency, can be decided using Fig. 6a. For, example we consider the case of Society – X where c = 0.3. The density of recruiters of insurgency groups and insurgents decrease in Society – X if ϕ is increased from 0.1 to 0.23. This claim can

easily be verified by comparing Fig. 2 and Fig. 6b. Moreover, if ϕ is increased further to 0.28, we can see from Fig. 6c that Society – X becomes free of insurgency. Another important observation can directly be obtained from Fig. 6a, that if the rate of generation of new jobs is higher that a critical level, say ϕ_c , then even with low awareness against insurgency, Society – X can be made free of insurgency. From Fig. 6a we assert that $\phi_c \approx 0.41$. The time evolution of System (2) with c = 0.05 and $\phi = 0.43 > \phi_c$ has been drawn in Fig. 6d. It shows when ϕ is more than the critical value ϕ_c , even with low level of c = 0.05, insurgency is eradicated.

7 Summary and discussion

In this article we have proposed and analyzed a deterministic mathematical model using nonlinear differential equations to establish the hypothesis that the issue of insurgency can be contained by adequate socioeconomic developments. The problem of insurgency is a persistent issue in Northeast India and socioeconomic developments can be a feasible way to mitigate this problem. For that purpose, we have considered generation of new employment opportunities and proper awareness against the radical ideologies through proper education, as the important indicators of socioeconomic developments. Through our analysis we have shown that a society, termed as Society - X with high rate of interaction between unemployed individuals & recruiters of insurgent groups (β) , low rate of awareness against insurgency (c), low rate of new job creation (φ) & low rate of employment (γ) is prone to persistent insurgency activities. Sensitivity analysis using PRCC method shows that these four parameters are the major regulators to control and if possible, eradicate insurgency from the Society - X. These four parameters can individually regulate the insurgent population. But their combined effect is much more effective from real time application point of view. In light of this, we have explored three control mechanisms of insurgency depending on the combined effects of the parameters that are interconnected from realistic point of view. The first one is the joint effect of c and β . We have shown that when ϕ and γ are fixed, then c and β are negatively correlated in view of controlling insurgency. If fact if c is increased, then with low level of β , insurgency can be controlled in Society – X. On the other, to overcome the adverse effect of high rate of β , the level of c has to be increased. And if we can increase c more than a critical value c^* then even with high rate of β Society – X can be made free of insurgency. Another important mechanism to control insurgency in Society - X is to regulate the combined effect of γ and ϕ by considering fixed c and β . It has been shown that if ϕ increases, then γ will increase. As the unemployed individuals becomes employed, their economic condition will develop and eventually they will stay away from insurgency. It is also proven that if ϕ is higher than an upper critical level ϕ^* , then even with low γ Society – X can be made free of insurgency. However,

if ϕ is below a lower critical lower level ϕ_c , then even with quite high rate of γ , insurgency will prevail in the Society – X. Therefore, to free Society – X from insurgency, the rate of generation of new jobs must be higher than a critical value ϕ_c . Finally, we analyze the combined effect of the interlinked parameters c and ϕ . It is obtained that the required rate of c to free Society – X from insurgency has to be high if the rate of ϕ is low and vice versa. It has been further derived that if ϕ is higher that a critical level, say ϕ_c , then even with low rate of c, Society – X can be made free of insurgency. Therefore, our study shows that apart from generation of awareness, sufficiently higher creation rate of new employments can also be a useful tactic to control insurgency. If unemployed youths get jobs at a higher rate and their quality-of-life increases, they will not opt for insurgency practices and eventually the effect of insurgency will decrease due to lack of new recruits. Moreover, the critical values associated with the awareness against insurgency ideologies and the rate of generation of new employments determined by our study can be applied while framing various governmental policies for Northeast India to contain and even cradicate the persistent issue of insurgency in this region.

8 References

- Akande, K. B., Mohammed I., Application of Differential Transformation
 Method in solving Optimal Control of Terrorism Model. *Journal of the Mathematical Association of Nigeria* 44, 1, 2017, 127-133.
- Bayon, L; Fortuny, P. A., Garcia-Nieto, P.J., Grau, J.M., Ruiz, M. M., Optimal Control of Counter-Terrorism Tactics, Journal of Applied Mathematics and Computation, 347, 2019, 477-491.
- Bengal Eastern Frontier Regulations, Retrieved: January 20, 2020, https://journalsofindia.com/bengal.
- Bhuyan, B., State and Insurgency: Study on Counter Terrorism Strategy in Assam. International Journal of Humanities and Social Sciences Invention 8(6), 1, 2019, 56 – 61.
- Brass, P. R., Ethnicity and Nationalism: Theory and Comparison. New Delhi: Sage Publications, 1991.
- Camacho, E., The Development and Interaction of Terrorist and Fanatic Groups, Communications in Nonlinear Science and Numerical Simulation 18,11, 2013, 3086-3097.
- Castillo-Chavez, C., Song, B., Models for the transmission dynamics of fanatic behaviors, in: Bioterrorism-Mathematical Modeling Applications in Homeland Security. SIAM, Philadelphia, 2003, 155–172.
- Cherif, A., Yoshioka, H., Ni, W., Bose, P., Terrorism Mechanism of Radicalization Process, Control of Contagion and Counter-Terrorist Measures, arXiv, 0910.5272, 2010, 1-14.
- Chuang, Y. L., D'Orsogna, M. R., Chou, T., A bistable belief dynamics model for radicalization within sectarian conflict. Q. Appl. Math. LXXV, 1, 2017, 17–37.

- Chuang, Y. L., Chou, T., D'Orsogna, M. R., Age-structured social interactions enhance radicalization. J. Math. Sociol. 42, 3, 2018, 1–24.
- Chuang, Y. L., D'Orsogna, M. R., Mathematical Model of Radicalization and Terrorism. Physics and Society 1903, 0848, 2019, 1-56.
- Crisosto, N., Kribs-Zaleta, C. M., Castillo-Chávez, C., Wirkus, S.,
 Community resilience in collaborative learning. Discrete Contin. Dyn. Syst. Ser. B 14, 1, 2010, 17–40.
- D'Orsogna, M. R., Perc, M., Statistical physics of crime: a review. Phys. Life Rev. 12, 2015, 1-21.
- Galam, S., Javarone, M. A., Modeling radicalization phenomena in heterogeneous populations. PloS One 11, 5, 2016, e0155407.
- Geller, D. S., Saperstein, A. M., A dynamic model of suicide terrorism and political mobilization. *International Political Science Review* 36, 5, 2015, 562-577.
- Ghosh, B., Ethnicity and Insurgency in Tripura. Sociological Bulletin, 52, 2, 2003, 221 243.
- Global Employment Trends, International Labor Office, Geneva. Retrieved on 5 Oct 2012.
 www.ilo.org/ publis, 2012.
- Hayward, J., Mathematical modeling of church growth, J. Math. Sociol. 23, 4, 1999, 255-292.
- Holt, B., Building the state and conceiving the nation: the origins of separatist insurgency in the Mizo Hills, 1945-61, Contemporary South Asia 30, 3, 2022, 313 – 330.
- Hazarika, M., Prehistoric Cultural Affinities between Southeast Asia, East Asia and Northeast India: An Exploration, Unearthing Southeast Asia's Past, 1, 2013, 16 – 25.
- Helbing, D., Brockmann, D., Chadefaux, T., Donnay, K., Blanke, U., Woolley-Meza, O., Moussaid, M., Johansson, A., Krause, J., Schutte, S, Perc, M., Saving human lives: What complexity science and information systems can contribute, J. Stat. Phys. 158, 3, 2015, 735–781.
- Jeffs, R., Hayward, J., Roach, P. A., Wyburn, J., Activist model of political party growth, Phys. A Stat. Mech. Appl. 442, 2016, 359–372.
- Karmakar, S., 25 years of 'Indo-Naga' ceasefire but a solution remains elusive, Deccan Herald, Guwahati 03 August: 2022.
- Kotwal, D., The Naga Insurgency: The Past and the Future. Strategic Analysis 24, 4, 2000, 751-772.
- Mccluskey, C., Santoprete, M., A bare-bones mathematical model of radicalization. J. Dyn. Games 5, 2018, 243.
- McMillon, D., Simon, C. P., Morenoff, J., Modeling the underlying dynamics of the spread of crime. PloS One 9, 4, 2014, e88923.
- Misra, A, Singh, A., A mathematical model for unemployment, Nonlinear Anal. RWA 12, 2011, 128–136.
- Misra, A., Singh, A., A Delay Mathematical Model for the Control of Unemployment, Differ. Equ. Dyn. Syst. 21, 3, 2013, 291–307.

- Mohammad, F., Roslan, U. M., Analysis on the crime model using dynamical Approach, In: Proceedings of the AIP Conference. AIP Publishing, 2017, 040067.
- Mohammed, K., Cultural Pluralism in India: Protecting a Symbol of National Identity, Revamping Indian Society in the Era of Modernization: Issues and Dilemmas. Patiala: Twenty First Century Publications, 2016.
- Nag, S., India and Northeast India: Minds, Politics and the Process of Integration 1946-1950. New Delhi: Regency Publications, 1998.
- Nagumo, M., Über die Lage der Integralkurven gewöhnlicher Differentialgleichungen. Proc. Phys. Math. Soc. Jpn. 24, 1942, 551.
- Nathan, O., Lawi, G., Nthiiri, J., Modelling the dynamics of radicalization with government intervention, Neural Parallel Scient. Comput. 26, 2018, 211–224.
- Ngari, C. G., Modelling Kenya Domestic Radicalization like a Disease Incorporating Rehabilitation Centers. Academic Journal of Applied Mathematical Sciences 2, 4, 2016, 27-39.
- Nikolopoulos, C. V., Tzanetis, D. E., A model for housing allocation of a homeless population due to a natural disaster. Nonlinear Anal. RWA 4, 2003, 561–579.
- Perc, M., Donnay, K., Helbing, D., Understanding recurrent crime as system-immanent collective behavior, PloS One 8 (10), 2013, e76063.
- Richardson, L. F., Mathematical psychology of war. Nature 136, 3452, 1935, 1025.
- Richardson, L. F. Arms and Insecurity: Mathematical Study of the Causes and Origins of War. Boxwood Press, 1960.
- Romero, D., Kribs-Zaleta, C., Mubayi, A., Orbe, C., An epidemiological approach to the spread of political third parties. *Discrete Cont. Dyn. Syst.* Ser. B (DCDS-B) 15, 3, 2011, 707– 738.
- Saikia, J., 36 years of Mizoram Accord: A historic Move that ended two decades of Mizo Insurgency, Firstpost 01 July: 2022.
- Sandler, T., The analytical study of terrorism: Taking stock. Journal of Peace Research 51, 2, 2014, 257-271.
- Santoprete, M., Xu, F., Global stability in a mathematical model of deradicalization. Phys. A Stat. Mech. Appl. 509, 2018, 151-161.
- Santoprete, M., Countering violent extremism: A mathematical model. Applied Mathematics and Computation 358, 2019, 314–329.
- Short, M. B, McCalla, S. G., D'Orsogna, M. R., Modelling radicalization: how small violent fringe sects develop into large indoctrinated societies. R. Soc. Open Sci. 4, 8, 2017, 170678.
- Singh, B., Notable decline in insurgency related incidents in Northeast India, The Economic Times, Retrieved: March 23, 2022.
- Singh, R., Problems of Insurgency: A Holistic Understanding from Manipur, India, Journal of Northeast India Studies 5, 1, 2015, 30 - 38.

- Singh, S. R., What are the laws in place to tackle illegal non-citizens. The Hindu 24 November, 2019.
- Sooknanan, J., Bhatt, B., Comissiong, D., Catching a gang—a mathematical model of the spread of gangs in a population treated as an infectious disease, *Int. J. Pure Appl. Math.* 83, 1, 2013, 25–43.
- Sooknanan, J., Bhatt, B., Comissiong, D., A modified predator-prey model for the interaction of police and gangs. R. Soc. Open Sci. 3, 9, 2016, 160083.
- Sooknanan, J., Comissiong, D., A mathematical model for the treatment of delinquent behaviour, Socio-Econ. Plann. Sci. 63, 2018, 60–69.
- Sundari, M. S., Sasikala, K., History of Insurgency in Manipur. The International Journal of Analytical and Experimental Modal Analysis 11, 12, 2020, 2888-2891.
- Udoh, I., Oladejo, M. O., Optimal Human Resources Allocation in Counter Terrorism Operation, A Mathematical Deterministic Model. *International Journal of Advances in Scientific Research and Engineering* 5, 1, 2019, 96-115.
- Udwadia, F., Leitmann, G., Lambertini, L., A Dynamical Model of Terrorism. Discrete Dynamics in Nature and Society. Vol. 2006; https://doi.org/10.1155/DDNS/2006/85653, 2006.

¹, Department of Mathematics, Maharaja Bir Bikram University, Agartala, Tripura Email Id: devadak.math93325@gmail.com (Received, May 16, 2025)

Email Id: shekhar2018agt@gmail.com

*Department of Political Science, Maharaja Bir Bikram University, Agastala, Tripura Email Id: br-chakma@rediffmail.com Pramod Shinde¹, Aditi S. Phadke², Samina Boxwala¹

STUDY OF FRAME STEWART NUMBERS OF THE MULTI-PEG TOWER OF HANOI PROBLEM

ISSN: 0970-5120

ABSTRACT. In this paper we have studied the set of best known solutions (called Frame Stewart Numbers) obtained so far, for the multipeg Tower of Hanoi problem for r rings, $r \ge 1$ and p pegs, $p \ge 3$. These solutions obtained using the Frame Stewart algorithm are denoted by T(r,p). Some interesting observations of the set $T = \{T(r,p)|r \ge 1, p \ge 3\}$ have been made. In this study we have proved that the set of all odd natural numbers and the set T are equal. For a fixed p, we define $T_p = \{T(r,p) | r \ge 1\}$. We have proved that $T_p \nsubseteq T_{p+1}$. A combinatorial identity for a specific value of r depending on p has been proved. Three conjectures about the set T_p have been made.

Mathematical Subject Classification (2020) No.: 05A10, 05A19

Key words: Multi-peg Tower of Hanoi Problem; Frame Stewart Algorithm; Frame Stewart Numbers.

1. Introduction

The Tower of Hanoi problem was proposed over a hundred years ago by Lucas [1], in which, a player is given 3 pegs and a certain number r of rings of distinct sizes. The player is required to transfer the rings from one peg to another. Initially all rings are stacked (composing a tower) on the first peg (the source) ordered monotonically by size, with the smallest at the top and the largest at the bottom. The goal is to transfer them to the third peg (the destination), while observing the following rules:

- at each step only one ring can be moved;
- (2) the moved ring must be the topmost one;
- (3) at any moment, a ring cannot reside on a smaller one.

The well-known recursive algorithm that accomplishes this task requires $2^r - 1$ steps, and is the unique optimal algorithm for the Tower of Hanoi problem [6]. One natural generalization is the multi-peg case with $(p \ge 4)$ pegs, P_1, P_2, \ldots, P_p . This generalization was first proposed by Lucas in 1889. Later, it was revived by Stewart [2]. It has been shown that seven different approaches, including those by Frame and Stewart, to the p peg tower of Hanoi problem are all equivalent i.e. achieve the same number of moves, though their optimality has not yet been proved [9]. Thus the optimality of the solution stands as an interesting and challenging open problem [4]. Let T(r, p) denote the minimum number of (legal) moves required to solve the Tower of Hanoi problem with $r \ge 1$ rings and $p \ge 3$ pegs using the Frame Stewart algorithm. The minimal solution obtained using Frame Stewart Algorithm for different values of r and p are called as Frame Stewart numbers in literature [5][8].

Section 2 describes the Frame Stewart algorithm. In section 3, Table 1, we have obtained the values of T(r,p) for $3,4,\ldots,10$ pegs for $1 \le r \le 30$. Observing table 1, we have denoted the size of a block for $p \ge 3$ pegs by $B_p(k)$ for $k \ge 0$, with the condition that the consecutive entries of T(r,p) in the k^{th} block for p-pegs differ by 2^k . Table 2 gives the sizes of different blocks for different values of r and p. In Table 3, we have calculated the Frame Stewart numbers when the block described above is of full size.

In section 4, some interesting observations of the set $T = \{T(r,p)|r \ge 1, p \ge 3\}$ have been made. In this study we have proved that the set of all odd natural numbers and the set T are equal. For a fixed p, we define $T_p = \{T(r,p)|r \ge 1\}$. We have proved that $T_p \not\subseteq T_{p+1}$. A combinatorial identity for specific value of rdepending on p has been proved. Three conjectures about the set T_p have been made.

2. The Frame Stewart Algorithm

The Frame Stewart algorithm is described as follows:

For $p \ge 4$, the transfer of rings from P_1 to P_p may be carried out using the following steps:

- Move optimally the topmost t (smallest) rings from P₁ to some intermediate peg, using all the pegs, in T(t, p) number of moves.
- (2) Transfer the remaining (r − t) largest rings from P₁ to P_p, using the (p − 1) pegs available (the intermediate peg cannot be used by the condition of the problem) in an optimal way in T(r − t, p − 1) number of moves.
- (3) Shift optimally the t rings from the intermediate peg to P_p, using all the p pegs, again in T(t, p) number of moves.

Then, t is to be determined so as to minimize the total number of minimum moves in the above three steps.

For the 3-peg Tower of Hanoi problem, Wood [6] has shown that the policy leading to the recurrence relation is indeed optimum. The recursive solution describing the above steps is given by the following equation:

$$\begin{split} T(r,p) &= \min_{0 \leq t \leq (r-1)} \{2T(t,p) + T(r-t,p-1)\}; r \geq 1, p \geq 4, \\ T(0,p) &= 0, T(1,p) = 1, \ \forall p \geq 3. \end{split}$$

For $r \ge 1, p \ge 4$,

$$\begin{split} T(r,p) &= \min_{0 \leq t \leq (r-1)} \{2T(t,p) + T(r-t,p-1)\}; \\ T(0,p) &= 0, T(1,p) = 1, \ \forall \ p \geq 3. \end{split}$$

The values of T(r, p) for $r \ge 1$ rings and $p \ge 3$ pegs obtained using the above recursive algorithm are called Frame Stewart numbers.

3. Tables using Frame Stewart Algorithm

The values tabulated below have been obtained using the Frame Stewart Algorithm. Some of the values for T(r,p) have been obtained in [3]. In this section, using the Frame Stewart Algorithm we find the number of moves required to move r rings for $3, 4, \ldots, 10$ pegs where $1 \le r \le 30$.

p.\r	554.5	.2	-3-	4	- 5	6.	7	. 5	9	10	- 11	12	13	24	15	16
3	1	3.	- 7	15	31	.63	127	255	511	1023	2047	4095	8191	44	- 64	1447
- 4	-1	-a	- 75	9.0	1.0	17	25.1	33	41	49	65	81	97	113	129	161
- 5	- 1	< 8	-6	7.	1.1	15	3.9	23	27	31	(20)	4.E.:	55	63	71	-79
- 6	1	a.	-6	-7	.0	13.	175	2-1	25	26	100	77	43	-40	- A17	117
7	1.2	· a.	- 5	7.1	.0	11	1.5	10	23	127	31	1904	39	43	476	-:54
-8	1123	3	- 5	7	9	.11	435	No.	21	255	20	353	37.1	41	45	49
- 9	-21	3	- 5	7	. 9	4.1	13	2.5	19	23	27	33	225	39	4.3	47
10	1	18	- 6	7.	- 9	11	121	15	17	-21	125	29	202	87	41	145

TABLE 1: T(r, p)

110	17	18	19	20	21	22	23	24	25	26	24	2.4	26	30
3	- 100	146	-	- 11	10.744	44	1.45	0.00	.0.	- 11	ald l	36	++	125
4	100	225	267	289	221	385	449	513	677	641	705	769	897	1020
6	87	95	103	111	127	143	150	170	191	207	223	239	255	271
6	605	73	-81	89	97	105	1.13	121	129	187	1:45	153	161	160
7	65	89	63	67	TA	79	87	95	103	111	119	127	135	1.635
B	53	-02	61.	65	69	441	783	81	184	89	93	197	105	113
9	51	56	59	-63	67	7.1	15	75	83	87	91	95	99	103
10	49	1933	157	62	16.0	60	73	77	9440	85	38/1	90	97	101

Let us denote the size of a block for $p \geq 3$ pegs by $B_p(k)$ for $k \geq 0$, with the condition that the consecutive entries of T(r,p) in the k^{th} block for p-pegs differ by 2^k . Note that $B_p(0) = 1$, $\forall p \geq 3$. For a fixed p these are precisely the cells with the same colour as shown in TABLE 1.

Using Frame Stewart algorithm, we get

$$B_p(k) = \binom{p+k-3}{k}$$
.

Note that $B_p(k)$ is the coefficient of x^k in the expansion of $\frac{1}{(1-x)^{p-2}}$.

This gives the following generating function for $B_p(k)$.

$$\frac{1}{(1-x)^{p-2}} = B_p(0) + B_p(1)x + B_p(2)x^2 + ... + B_p(l-1)x^{l-1} + B_p(l)x^l +$$

We enumerate the values of the blocks $B_p(k)$ in the table given below for $3 \le p \le 10$ and $0 \le k \le 12$.

TABLE 2: $B_n(k)$

$p \setminus k$	0	1	2	3	4	5	6	7	8	9	10	11	12
3	1	1	1	1	1	1	1	1	1	1	1	1	1
4	1	2	3	4	5	6	7	8	9	10	11	12	13
5	1	3	6	10	15	21	28	36	45	55	66	78	91
6	1	4	10	20	35	56	84	120	165	220	286	364	455
7	1	5.	15	35	70	126	210	330	495	715	1001	1365	1820
8	1	6	21	56	126	252	462	792	1287	2002	3003	4368	6188
9	1	7	28	84	210	462	924	1716	3003	5005	8008	12376	1856
10	1	8	36	120	330	762	1716	3432	6435	11440	19448	31824	50388

Using a standard combinatorial identity we get,

$$B_{p+1}(l) = B_p(0) + B_p(1) + B_p(2) + ... + B_p(l)$$

This can also be observed in the above table.

TABLE 2 gives the sizes of blocks for different values of r and p. The table below shows the Frame Stewart numbers for various block-ends or when the block is of full size. The Frame Stewart number for the case when r = 6435 and p = 9 is $T(B_{9+1}(8), 9) = T(6435, 9) = 1066495$.

							Scott State Co.		
$p \setminus k$	0	1	2	3	4	5	6	7	8
3	1	3	7	15	31	63	127	255	511
4	1	5	17	49	129	321	769	1793	4097
5	1	7	31	111	351	1023	2815	7423	18943
6	1	9	49	209	769	2561	7137	23297	65537
7	1	11	71	351	1471	5503	18943	61183	187903
8	1	13	97	545	2561	10625	40193	141569	471041
9	1	15	127	799	4159	18943	78079	297727	1066495
10	1	17	161	1121	6401	31745	141569	580965	2228225

TABLE 3: $T(B_{p+1}(k), p)$

The results and notation of this section can be found in [10]

4. Observations About the Frame Stewart numbers

Observing TABLE 1, TABLE 2 and TABLE 3, we arrive at few observations related to the Frame Stewart numbers of the multi-peg Tower of Hanoi problem.

Proposition 4.1. a) T(r+1,p) - T(r,p) is some non-negative integral power of 2.

b) For
$$r$$
 satisfying $\binom{p+l-3}{l-1} \le r < \binom{p+l-2}{l}$
 $T(r,p) = \sum_{k=0}^{l-1} B_p(k) 2^k + \left\{r - \sum_{k=0}^{l-1} B_p(k)\right\} 2^l$.

For a proof of the above theorem refer to [7].

Lemma 4.2. T(r, p) is always odd for $r \ge 1$ and $p \ge 3$.

$$\begin{split} & \textit{Proof. For } r \text{ satisfying } \binom{p+l-3}{l-1} \leq r < \binom{p+l-2}{l}, \\ & T(r,p) = \sum_{k=0}^{l-1} B_p(k) 2^k + \left\{r - \sum_{k=0}^{l-1} B_p(k)\right\} 2^l. \end{split}$$

Since $B_p(0) = 1$, the first term on the right is 1 and the remaining terms are all multiples of 2. Thus the right hand side is odd.

Theorem 4.3. The set $T = \{T(r, p)|r \ge 1, p \ge 3\}$ and the set of all odd positive integers are equal.

Proof. Using Lemma 4.2, it is clear that T is the subset of odd positive integers. Conversely, let n be an odd positive integer. Clearly $n=1\in T$. Let n>1 where n=2q+1 for some $q\geq 1$. Take p=q+2. Thus $p\geq 3$. Consider $T(B_{p+1}(1),p)=T(B_p(0)+B_p(1)2,p)=1+\binom{p+1-3}{1}2=1+2(p-2)=2p-3=2(q+2)-3=2q+1=n$. Therefore for all odd $n\in \mathbb{N},\ n\in T$.

Thus the set T and the set of all odd positive integers are equal.

For a fixed p, let $T_p = \{T(r, p)|r \ge 1\}$, the set of Frame Stewart numbers of the multi-peg Tower of Hanoi problem for p-pegs.

Theorem 4.4. $T_p \not\subseteq T_{p+1}$ for any $p \ge 3$.

Proof. For any $p \ge 3$, take $n = 1 + 2B_p(1) + 4$. Clearly $n \in T_p$. Note that $n - 2 = 1 + 2B_{p+1}(1) \in T_{p+1}$ and is the last number in the block of size 1. Therefore $n - 2 + 2 = n \notin T_{p+1}$.

From the TABLES 1, 3 and using Mathematica we have computed values of Frame Stewart numbers for the end of the block for $3 \le p \le 150$ and observed that:

(1)
$$T(B_{p+3}(p-2), p+2) = T(B_{p+1}(p-1), p).$$

(2)
$$T(B_{p+3}(2p-4), p+2) = T(B_{p+1}(2p-2), p).$$

We prove the first observation using the identity $B_{p+3}(p-2) = B_{p+2}(0) + B_{p+2}(1) + B_{p+2}(2) + \ldots + B_{p+2}(p-2) = \sum_{i=0}^{p-2} B_{p+2}(i)$ followed by a combinatorial argument.

Theorem 4.5.
$$T(B_{p+3}(p-2), p+2) = T(B_{p+1}(p-1), p), p \ge 3.$$

Proof. We begin with the LHS,

$$T(B_{p+3}(p-2), p+2)$$

$$= 2^{0}B_{p+2}(0) + 2^{1}B_{p+2}(1) + 2^{2}B_{p+2}(2) + \dots + 2^{p-2}B_{p+2}(p-2)$$

$$= 2^{0}\binom{p-1}{0} + 2^{1}\binom{p}{1} + 2^{2}\binom{p+1}{2} + \dots + 2^{p-2}\binom{2p-3}{p-2}.$$

Now RHS =
$$T(B_{p+1}(p-1), p)$$

= $2^0B_p(0) + 2^1B_p(1) + 2^2B_p(2) + ... + 2^{\mu-1}B_p(p-1)$

$$=2^0\binom{p-3}{0}+2^1\binom{p-2}{1}+2^2\binom{p-1}{2}+\ldots+2^{p-1}\binom{2p-4}{p-1}.$$

We thus need to prove

$$\binom{p}{1} + 2^1 \binom{p+1}{2} + \ldots + 2^{p-3} \binom{2p-3}{p-2} = \binom{p-2}{1} + 2^1 \binom{p-1}{2} + \ldots + 2^{p-2} \binom{2p-4}{p-1}.$$

By using Pascal's identity and simplifying, the problem reduces to proving

$$1 + \left[\binom{p-1}{0} + 2 \binom{p-1}{1} \right] + 2^1 \left[\binom{p}{1} + 2 \binom{p}{2} \right] + \ldots + 2^{p-4} \left[\binom{2p-5}{p-4} + 2 \binom{2p-5}{p-3} \right] = 2^{p-3} \binom{2p-4}{p-1}.$$

Right hand side is the number of sequences of length 2p-4 with exactly p-1 a's and either b or c in the remaining p-3 places.

We shall now characterize all these sequences with the occurrence of the rightmost a or c and followed by all b's.

For the first sequence, place a in the first p-1 places and b in all the remaining p-3 places. This can be done in 1 way.

The second type of sequence can be formed by placing a in the first p-1 places, c in the pth place and b in the remaining p-4 places. This can be done in $\binom{p-1}{0}$ ways.

Next we fix a in the pth position followed by all b's and in one position out of the first p-1 places we place either b or c. This can be done in $2\binom{p-1}{1}$ ways.

Next we count the number of sequences with rightmost c in the (p+1)th position followed by all b's. Among the first p positions, we choose to fill exactly one place with either b or c and the remaining with a's. This can be done in 2 $\binom{p}{1}$ ways. We place b in the remaining p-5 places. We then count the number of sequences with the rightmost a in the (p+1)th position. Out of the first p places, we have to place

a's in p-2 places and two places need to be filled with either b or c. This can be done in $2^2 \binom{p}{2}$ ways. We continue this process.

Now the last place is filled with either a or c. If it is filled with c then out the first 2p-5 places we need to fill (p-1) places with a's and remaining p-4 places with b or c. This can be done in $2^{p-4}\binom{2p-5}{p-4}$ ways. If the last place is filled with a then among the first 2p-5 places we have to place (p-2) a's and p-3 places have to be filled with either b or c. This can be done in $2^{p-3}\binom{2p-5}{p-3}$ ways.

Thus all the strings are completely characterized by the occurrence of the rightmost a or c which are followed by b at all remaining places, if any. This proves the identity.

Observation 2:

$$T(B_{p+3}(2p-4), p+2) = T(B_{p+1}(2p-2), p).$$

Observing the values of T(r, p) in TABLES 1, 2 and 3; we propose the following three conjectures.

Conjecture 4.6. $T_p \subseteq T_{p+2}$ for any $p \ge 3$.

Conjecture 4.7. $T(B_p(2), p-1) + 4 \notin \bigcup_{i=3}^p T_i$ for any $p \ge 4$.

Conjecture 4.8. There does not exist an $n \in \mathbb{N}$ such that $\bigcup_{p=3}^{n} T_p$ is equal to the set of all odd natural numbers.

The proof of the first conjecture will lead to many combinatorial identities related to the Frame Stewart numbers of the multi-peg Tower of Hanoi problem.

Acknowlegement: We thank Prof. S. A. Katre, Bhaskaracharya Pratishthana, Pune for meaningful discussions during this research work.

REFERENCES

- Lucas. E, Recreations Mathematiques, Vol. III, Gauthier-Villars, Paris.
- B. M. Stewart, Problem 3918, American Mathematical Monthly, 46 (1939), 363.
- [3] Houston, Ben, and Hassan Masum, comps., Explorations in 4-Peg Tower of Hanoi. 29 Nov. 2004. Carleton University, School of Computer Science. http://www.scs.carleton.ca/research/tech-eports/2004/TR - 04 - 10.pdf
- [4] Hinz, A. M., Pascal's Triangle and the Tower of Hanoi, American Mathematical Monthly,99 (1992), 538-544.
- [5] Hinz, A. M., An iterative algorithm for the Tower of Hanoi with four pegs, Computing, 42 (1989), 133-180.
- [6] Wood, D., The Towers of Brahma and Hanoi Revisited, J. Recreat, Math., 14 (1981), 17-24.
- [7] J.S. Frame, Solution to AMM Problem 3918, American Mathematical Monthly, 48 (1941), 216-219.
- [8] Sandi Klávzar and Uros Milutinovic, Simple Explicit Formulas for the Frame-Stewart Numbers, Annals of Combinatorics, 6(2002), 157-167.
- [9] Sandi Klavzar, Uros Milutinovic, Ciril Petr, On the Frame-Stewart algorithm for the multi-peg Tower of Hanoi problem, Discrete Applied Mathematics, 120, (2002) 141-157.
- [10] Shinde P. N. and Phadke A. S., Explorations of the Multi-peg Tower of Hanoi Problem, Proceedings of the International Conference on Perspectives of Computer Confluence with Sciences 2012, (2012), 122-126.

^{1.2.} Department of Mathematics, Novensjee Wadia College, Pune Email: pramohinde@gmail.com, Email: phadke udit@gmail.com Email: samboxwala@gmail.com

Titli Maiti', ON PREY-PREDATOR DYNAMICS WITH Avijit Sarkar² CERTAIN INTRINSIC BEHAVIOURS

ISSN: 0970-5120

Abstract. The present article investigates prey-predator interactions by incorporating not only the classical predation dynamics but also infighting among preys and retaliation against predators framed within the context of herd behaviour in prey populations. The study presents a thorough analysis that includes both stability and bifurcation assessments supported by detailed numerical simulations. The existence of transcritical and Hopf bifurcations is established and analyzed.

Keywords: Prey-predator interactions, stability, Hopf bifurcation, herd behavior.

Mathematics Subject Classification 2020: Primary: 92B05, 93E15, Secondery: 60H10, 34E10.

1. Introduction

The study of population dynamics, nowadays, has become a prime topic in the arena of applied mathematics. The seed of the topic was planted by Lotka [9] and Volterra [14] by improving the theory of Malthus [12]. In the recent decades the theory has been further developed by several authors in several perspectives. For instance, we refer the works in [3, 4, 8, 13, 15] among many others. Very recently, in [10], the present authors with Mondal have studied prey-predator model in the light of Smith growth dynamics and established several significant results of population biology.

The number of preys attacked by a predator in certain time is known as functional response. C. S. Holling [5] introduced three kind of functional responses which have become a lucrative field of non-linear analysis in view of their ecological significance.

A fundamental feature of the behaviour of the forest dwelling animals such as buffaloes, sheep, deer is that they roam in groups in forests. Such behaviours are also exhibited by birds and fishes. When the animals move in herd the attack by predators are possible only from a boundary of the herd. In Savana region movement of preys and predators in groups are well known and established fact. Considering upon this phenomenon Ajraldi et al [1] proposed the herd behaviour model in population system. In order to develop the analytical aspects of such situations, they introduced square root functional response. But a lacuna of the square root model is that it needs critical analysis near the origin since a square root function is not differentiable at the origin and due to this fact it prevents the linearization of the model. Some minute aspects of this model was critically analyzed by Braza [2] considering square root and Holling type II functional responses in a common framework. In spite of this limitation square root models are being considered by several authors [4] due to its realistic nature. Square root models with combination of other functional responses are prime topics of study in the field of mathematical ecology. Retaliation towards predators by preys is a common fact in Savana region wild lives. In [11], the present authors studied retaliation behaviours but they did not consider the infighting of preys.

The intra or infighting among populations is a common phenomenon. In [6], Kooi studied the dynamics of a predator-prey system where predators fight for captured prey besides searching and handling of preys. In real situation, it is seen that not only the predators exhibit infighting behaviours. Sometimes the preys also involve with infighting due to their intrinsic behaviour. For example, wild buffaloes show infighting behaviour. In addition wild buffaloes also defend in groups if they are attacked by wild animals like tiger. They take revenge or retaliation. In this paper we would like to analyze such situations i.e., we consider prey-predator model where preys move in groups, show infighting and also take revenge or retaliation towards to the predators.

The present article is organized as follows: After the introduction, the model is formulated in Section 2. Section 3 and Section 4 contain the analysis of stability and bifurcation respectively. The final section provides numerical simulations with graphical representations.

2. Derivation of predator-prey model with herd and infighting behaviour in preys and retaliation towards predators

It is known that the predator-prey model with logistic growth in the prey and Holling type II functional response [5] is given by

$$\frac{dX}{dt} = rX(1 - \frac{X}{N}) - \frac{\alpha XY}{1 + t_h \alpha X},$$
(2.1)

$$\frac{dY}{dt} = -sY + \frac{c\alpha XY}{1 + t_b\alpha X}.$$
(2.2)

Here X(t) and Y(t) denote the prey population and predator population respectively. r is the growth rate of the prey population and N is its carrying capacity. In absence of prey population the death rate of the predator is s. The search coefficient of Y for X is α , c being biomass conversion or consumption rate. The average handling time of Y for X is t_h . Suppose T indicate the total time that each Y takes to collect food from X, T_s is the time taken by each Y looking for X and the time t_h that each Y takes handling X. Modifying the above model, Braza [2], developed prey-predator models as follows that have the interaction term as the square root of the prey population.

$$\frac{dX}{dt} = rX(1 - \frac{X}{N}) - \frac{\alpha\sqrt{X}Y}{1 + t_h\alpha\sqrt{X}},$$
(2.3)

$$\frac{dY}{dt} = -sY + \frac{c\alpha\sqrt{X}Y}{1 + t_b\alpha\sqrt{X}}.$$
(2.4)

Now, here we develop a model where the preys are involved with intra species fighting due to their intrinsic behaviour. Assume β is the rate of death of preys due to the infighting and the death rate for the predator is γ due to retaliation of the preys towards the predators. In that case the above model reduces to

$$\frac{dX}{dt} = rX(1 - \frac{X}{N}) - \frac{\alpha\sqrt{X}Y}{1 + t_{\nu}\alpha\sqrt{X}} - \beta X^{2}, \quad (2.5)$$

$$\frac{dY}{dt} = -sY + \frac{c\alpha\sqrt{X}Y}{1 + t_h\alpha\sqrt{X}} - \gamma Y. \qquad (2.6)$$

Here X(0) > 0 and $Y(0) \ge 0$.

- 3. STABILITY ANALYSIS OF PREDATOR-PREY MODEL WITH HERD AND INFIGHTING BEHAVIOUR IN PREYS AND RETALIATION TOWARDS PREDATORS
- 3.1. Positivity and boundedness of the model: Let us investigate the positivity and boundedness of the system of equations (2.5) and (2.6). The right hand sides of (2.5) and (2.3) are continuous functions of the dependent variables X and Y. Integrating both sides of the equations of the system, we have

$$\begin{split} X(t) &= X(0) exp \left[\int_{0}^{t} \left(r \left(1 - \frac{X}{N} \right) - \frac{\alpha Y}{1 + t_{h} \alpha X} - \beta X \right) dx \right] \\ Y(t) &= Y(0) exp \left[\int_{0}^{t} \left(-s + \frac{c \alpha \sqrt{X}}{1 + t_{h} \alpha \sqrt{X}} - \gamma \right) dx \right] \end{split}$$

In view of the above expressions of X(t) and Y(t) it can be inferred that X(t) and Y(t) remain non-negative for the infinite time, if they starts from an interior point of

$$R_+^2=\{(X(t),Y(t))\in R^2: X(t)>0, Y(t)\geq 0\}.$$

Thus R_+^2 is positively invariant for the system considered. Regarding the uniform boundedness, let us prove the following

Theorem 3.1. The solutions of the system of equations (2.5) and (2.6) consisting the model with non-negative initial conditions (X(0), Y(0)) starting from the interior of R^2_+ are uniformly bounded.

Proof. Let

$$W(t) = X(t) + \frac{1}{c}Y(t).$$
 (3.1)

Hence, along the solution trajectories of the model

$$\frac{dW}{dt} = rX(1 - \frac{X}{N}) - (\beta + \gamma + \frac{s}{c})Y. \tag{3.2}$$

By virtue of (3.1) and (3.2)

$$\frac{dW}{dt} + \theta W = (r + \theta)X - \frac{r}{N}X^2 - (\beta + \gamma + \frac{s - \theta}{c})Y.$$

Choosing θ such that $0 < \theta < s$, we have from above

$$\begin{array}{rcl} \frac{dW}{dt} + \theta W & \leq & (r+\theta)X - \frac{r}{N}X^2 \\ & = & \frac{r}{N}\left(\frac{N^2(r+\theta)^2}{4r^2} - \left(\frac{N(r+\theta)}{2r} - X\right)^2\right) \\ & \leq & \frac{N(r+\theta)^2}{4r}. \end{array}$$

Thus from above

$$\frac{dW}{dt} + \theta W \le P,$$
 (3.3)

where $P = \frac{N(r+\theta)^2}{4\tau}$. In view of differential inequality from (3.3), one obtains

$$0 \le W(t) \le \frac{P}{\theta}(1 - e^{-\theta t}) + W(0)e^{-\theta t}$$
.

As $t \to \infty$, we infer $0 \le W(t) \le \frac{P}{\theta} + \epsilon$ for $0 < \epsilon < W(0)$. Hence, in view of positivity of X(t) and Y(t), we conclude that all solutions initiating in R_+^2 are restricted in the region $D = \{(X(t), Y(t)) \in R^2 : X(t) + \frac{1}{\epsilon}Y(t) \le \frac{P}{\theta} + \epsilon, \epsilon > 0\}$. Thus the solutions of the system are uniformly bounded. Hence the model is biologically well posed.

3.2. Equlibrium points and their stability: Using, MAPLE we find the equilibrium points of the above model are

(i)
$$X = 0, Y = 0$$

(ii)
$$X = \frac{Nr}{N\beta + r}$$
, $Y = 0$.

(iii)
$$X = \frac{(s+\gamma)^2}{\alpha^2(c-t_h(s+\gamma))^2}$$
, $Y = \frac{c(s+\gamma)}{\alpha^2(c-t_h(s+\gamma))^2} \left(\frac{r-\beta}{\alpha^2} - \frac{r}{N} \frac{(s+\gamma)^2}{(c-t_h(s+\gamma))^2}\right)$.

The Jacobian of the system is

$$\begin{bmatrix} r - \frac{2rX}{N} - \frac{\alpha Y}{2\sqrt{X}(1 + t_h\alpha\sqrt{X})^2} - + \frac{\alpha^2 Y t_h}{2(1 + t_h\alpha\sqrt{X})^2} - 2\beta X & -\frac{\alpha\sqrt{X}}{1 + t_h\alpha\sqrt{X}} \\ \frac{\alpha Y}{2\sqrt{X}(1 + t_h\alpha X)} - \frac{\epsilon\alpha^2\sqrt{X}Y t_h}{(1 + t_h\alpha X)^2} & -s + \frac{\epsilon\alpha\sqrt{X}}{1 + t_h\alpha X} - \gamma \end{bmatrix}.$$

3.3. Local stability for case (i). In this subsection, we discuss the nature of stability for X=0 and Y=0. Since $\frac{1}{\sqrt{X}}$ is indeterminate for X=0 and the square root function is not differentiable at X=0, the stability of this case cannot be determined by simply evaluating the Jacobian matrix at X=0 and Y=0. So let us consider a deleted neighbourhood of (0,0), say $(\epsilon,0)$, where ϵ is arbitrarily small and tends to zero. At that point the Jacobian matrix is of the form

$$\left[\begin{array}{cc} a_{11} & a_{12} \\ 0 & a_{22} \end{array}\right],$$

where $a_{11}=r-\frac{2r\epsilon}{N}-2\beta\epsilon$. $a_{12}=-\frac{\alpha\sqrt{\epsilon}}{1+t_h\alpha\sqrt{\epsilon}}$. $a_{22}=-s+\frac{\alpha\sqrt{\epsilon}}{1+t_h\alpha\epsilon}-\gamma$. Thus the eigenvalues are $r-\frac{2r\epsilon}{N}-2\beta\epsilon$ and $-s+\frac{c\alpha\sqrt{\epsilon}}{1+t_h\alpha\epsilon}-\gamma$. It is seen that in such a case the values of r,s and γ are very crucial to determine the stability. The above discussion leads us to state the following:

Theorem 3.2. A deleted neighbourhood $(0, \epsilon)$ of the trivial equilibrium point is locally stable if $r < \frac{2r\epsilon}{N} + 2\beta\epsilon$ and $s + \gamma > \frac{\cos\sqrt{\epsilon}}{1+b_0\alpha\epsilon}$.

3.4. Local stability for case (ii). In this subsection, we investigate the nature of stability for X = Nr / NS+r, Y = 0. and prove the following:

Theorem 3.3. The equilibrium point $X = \frac{Nr}{N\beta + \tau}$, Y = 0 is locally stable $1 > \frac{r}{N\beta + \tau}$ and $s + \gamma > \frac{c\alpha \sqrt{\frac{Nr}{N\beta + \tau}}}{1 + \frac{r_1Nr\alpha}{N\beta + \tau}}$.

Proof. The Jacobian matrix for case (i) is of the form

$$\begin{bmatrix} a_{11} & a_{12} \\ a_{21} & a_{22} \end{bmatrix}$$
,

where

$$\begin{split} a_{11} &= -r (1 - \frac{r}{N\beta + r}) - \frac{r^2}{N\beta + r} - \frac{2\beta Nr}{N\beta + r} \\ a_{12} &= -\frac{\alpha \sqrt{\frac{Nr}{N\beta + r}}}{1 + t_h \alpha \sqrt{\frac{Nr}{N\beta + r}}}, \\ a_{21} &= 0, \\ a_{22} &= -s - \gamma + \frac{c\alpha \sqrt{\frac{Nr}{N\beta + r}}}{1 + \frac{t_h Nr\alpha}{N\beta + r}}, \end{split}$$

The eigenvalues are $-r(1-\frac{r}{N\beta+r})-\frac{r^2}{N\beta+r}-\frac{2\beta Nr}{N\beta+r}$ and $-s-\gamma+\frac{c\alpha\sqrt{\frac{Nr}{N\beta+r}}}{1+\frac{t_NNr\alpha}{N\beta+r}}$. Both the eigenvalues will be negative if $1>\frac{r}{N\beta+r}$ and $s+\gamma>\frac{c\alpha\sqrt{\frac{Nr}{N\beta+r}}}{1+\frac{t_NNc\alpha}{N\beta+r}}$.

3.5. Local stability for case (iii). In this subsection, we investigate the nature of stability for $X = \frac{(s+\gamma)^2}{\alpha^2(c-t_h(s+\gamma))^2}$, $Y = \frac{c(s+\gamma)}{\alpha^2(c-t_h(s+\gamma))^2} \left(\frac{r-\beta}{\alpha^2} - \frac{r}{N}\frac{(s+\gamma)^2}{(c-t_h(s+\gamma))^2}\right)$ and establish the following:

Theorem 3.4. The equilibrium point

$$X = \frac{(s+\gamma)^2}{\alpha^2(c-t_h(s+\gamma))^2} \text{ and } Y = \frac{c(s+\gamma)}{\alpha^2(c-t_h(s+\gamma))^2} \left(\frac{r-\beta}{\alpha^2} - \frac{r}{N}\frac{(s+\gamma)^2}{(c-t_h(s+\gamma))^2}\right)$$

is locally asymptotically stable if

$$\frac{r\alpha^2}{N} \cdot \frac{(s+\gamma)^2}{(c-t_h(s+\gamma))^2} < r-\beta$$

$$< \frac{r\alpha(s+\gamma)^2 \left(4rc - \alpha(c-t_h(s+\gamma))\right) + (r-\beta)N(c-t_h(s+\gamma))^3}{2N\alpha^3 rc(c-t_h(s+\gamma))^2}.$$

Proof. The Jacobian matrix for case (ii) is of the form

$$\begin{bmatrix} a_{11} & a_{12} \\ a_{21} & a_{22} \end{bmatrix}$$
,

where

$$a_{11} = (r - \beta) - \frac{r\alpha(s + \gamma)^2 (4rc - \alpha(c - t_h(s + \gamma))) + (r - \beta)N(c - t_h(s + \gamma))^3}{2N\alpha^3 rc(c - t_h(s + \gamma))^2},$$

$$a_{12} = -\frac{s + \gamma}{c},$$

$$a_{21} = \frac{1}{2} \left(\frac{r - \beta}{\alpha^2} - \frac{r}{N} \frac{(s + \gamma)^2}{(c - t_h(s + \gamma))^2} \right),$$

$$a_{22} = 0.$$

The eigenvalues λ of the above Jacobian is given by

$$\lambda^2 - B_1\lambda + B_2 = 0,$$

where $B_1 = a_{11} + a_{12}$ and $B_2 = a_{11}a_{22} - a_{12}a_{21}$. Assume

$$r - \beta > \frac{r\alpha^2}{N} \cdot \frac{(s + \gamma)^2}{(c - t_b(s + \gamma))^2}$$
 (3.4)

Then $a_{22} = 0$, $a_{12} < 0$ and $a_{21} > 0$. So the determinant of the Jacobian for this case is positive. Consequently, $B_2 > 0$. Hence, by Routh Hurwitz criterion theorem [15], the solution will be asymptotically stable if $a_{11} + a_{22} < 0$. Now, $a_{22} = 0$. Hence, the solution will be asymptotically stable if $a_{11} < 0$., i.e.,

$$r - \beta < \frac{r\alpha(s + \gamma)^2(4rc - \alpha(c - t_h(s + \gamma))) + (r - \beta)N(c - t_h(s + \gamma))^3}{2N\alpha^3rc(c - t_h(s + \gamma))^2}$$
. (3.5)

Combining (3.4) and (3.5), we get the result.

4. Bifurcation Analysis:

In the present section, we shall analyze some aspects of local bifurcation analysis
of the model. The nature of solutions depend upon some changes of the associated
parameters. The value of a parameter for which the nature of the solution structurally changes is known as critical value and the changing phenomenon is known
as bifurcation. In the following we exhibit the presence of transcritical and Hopf
bifurcation in the system.

In the previous section, we have seen that the point $(0,\epsilon)$ is asymptotically stable if $r < \frac{2r\epsilon}{N} + 2\beta\epsilon$ and $s + \gamma > \frac{c\alpha\sqrt{\epsilon}}{1+t_h\alpha\epsilon}$. Now if we change r such that $r > \frac{2r\epsilon}{N} + 2\beta\epsilon$ without changing the other parameters, then the point becomes unstable and axial equilibrium arises. If $1 > \frac{r}{N\beta+r}$, then the axial equilibrium point is stable. Hence the point $(0,\epsilon)$ exchanges its stability with the axial equilibrium. If we change r again such that $1 < \frac{r}{N\beta+r}$, the axial equilibrium point becomes unstable. Now, we are in a position to state the following:

Theorem 4.1. The equilibrium point $(0, \epsilon)$ undergoes through transcritical bifurcation for $r = \frac{2r\epsilon}{N} + 2\beta\epsilon$, and the axial equilibrium point undergoes transcritical bifurcation for r satisfying $\frac{r}{N\beta+r} = 1$ with certain specific conditions.

Now we prove the following result related to Hopf bifurcation.

Theorem 4.2. At the equilibrium point

$$X = \frac{(s+\gamma)^2}{\alpha^2(c - t_h(s+\gamma))^2}, \ Y = \frac{c(s+\gamma)}{\alpha^2(c - t_h(s+\gamma))^2} \left(\frac{r-\beta}{\alpha^2} - \frac{r}{N} \frac{(s+\gamma)^2}{(c - t_h(s+\gamma))^2} \right)$$

for $r - \beta > \frac{r\alpha^2}{N} \cdot \frac{(s+\gamma)^2}{(c-t_h(s+\gamma))^2}$, the system undergoes Hopf bifurcation with respect to the parameter β for the critical value $\beta_0 = r \left(1 - \frac{\alpha(s+\gamma)^2 \left(4rc - \alpha(c-t_h(s+\gamma))\right)}{1 - N(c-t_h(s+\gamma))^3}\right)$.

Proof. Consider the Jacobian matrix

$$\begin{bmatrix} a_{11} & {}_{12} \\ a_{21} & a_{22} \end{bmatrix}$$
,

of the system for $X=\frac{(s+\gamma)^2}{\alpha^2(c-t_h(s+\gamma))^2}, \ Y=\frac{c(s+\gamma)}{\alpha^2(c-t_h(s+\gamma))^2}\left(\frac{r-\beta}{\alpha^2}-\frac{r}{N}\frac{(s+\gamma)^2}{(c-t_h(s+\gamma))^2}\right)$. For $r-\beta>\frac{r\alpha^2}{N}\cdot\frac{(s+\gamma)^2}{(c-t_h(s+\gamma))^2}$ and $\beta=r\left(1-\frac{\alpha(s+\gamma)^2\left(4rc-\alpha(c-t_h(s+\gamma))\right)}{1-N(c-t_h(s+\gamma))^3}\right),\ a_{12}<0$ and $a_{21}>0$. Again $a_{22}=0$. In this case the characteristic equation of the Jacobian matrix is $\lambda^2=a_{12}a_{21}<0$. Thus the eigenvalues are purely imaginary. Verifying the transversality condition, one can conclude that the model undergoes Hopf bifurcation at the considered point for $\beta=r\left(1-\frac{\alpha(s+\gamma)^2\left(4rc-\alpha(c-t_h(s+\gamma))\right)}{1-N(c-t_h(s+\gamma))^3}\right)$. \square

5. Numerical simulations

Theoretical results are better understood whenever they are supplemented by graphical representations as graphs are nice mathematical tools that provide quick concept of any theory. This is why we represent the stability, phase portrait and the aspects of bifurcation graphically in the subsequent part of the article.

5.1. Nullclines and solution curves. Let us now exhibit the graphs for the nullclines and solution curves for different numerical values of the parameters. Figures 1 and 2 show the existence of locally stable interior equilibrium that verifies Theorem 3.4. Figure 3 ensures the stability of the point (0, ε) in the tune of Theorem 3.2. Figure 4 verifies the existence of axial equilibrium point and its stability associated with Theorem 3.3.

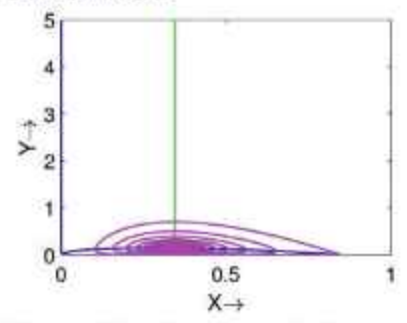


Fig. 1:Nullclines and solution curve for $c=5, s=5, r=1, N=200, \alpha=$ $2, \gamma=0.8, \beta=0.15, t_h=1$. The Figure shows the existence of stable interior equilibrium.

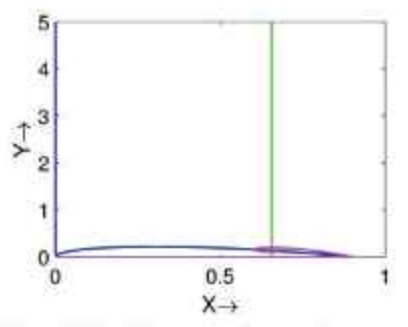


Fig. 2:Nullclines and solution curve for $c=5, s=5, r=0.1, N=200, \alpha=1.5, \gamma=1, \beta=0.1, t_h=1$. The Figure shows the existence of stable interior equilibrium.

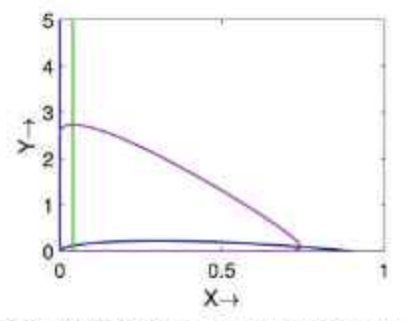


Fig. 3:Nullclines and solution curve for c = 5, s = 0.5, r = 1, N = 200, α = 1.5, γ = 1, β = 0.1, t_h = 1. The figure shows existence of stable trivial equilibrium.

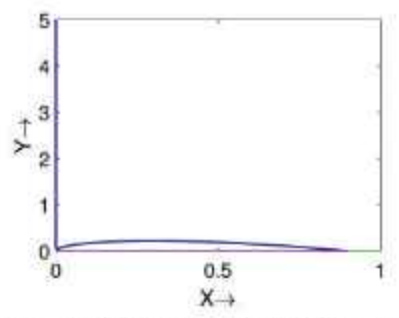


Fig. 4:Nullclines and solution curve for $c=1, s=0.5, r=1, N=200, \alpha=1.5, \gamma=1, \beta=0.1, t_h=1$. The figure shows existence of stable axial equilibrium

5.2. Phase portrait and time series. In the following, we plot phase portrait and time series of the model by using MATLAB for different numerical values of the associated parameters and verify existence of bifurcation. From Figures 7 and 8, it is seen that for change of s the asymptotically stable interior equilibrium point becomes unstable or vice versa which verifies the existence of Hopf bifurcation at interior equilibrium point. Since in the assumed condition of Theorem 4.2, β and s are related, so for change of β we must have Hopf bifurcation at the interior equilibrium. Thus the numerical representation agrees with Theorem 4.2.

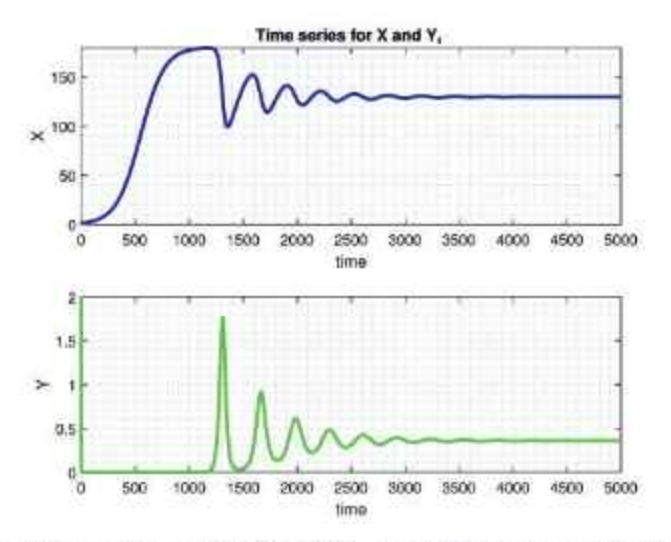


Fig. 5: $s = 3.2, c = 4, r = .01, N = 200, \alpha = 0.9t_h = 1, \gamma = 0.444, \beta = 0.001.$ The figure establishes Hopf bifurcation.

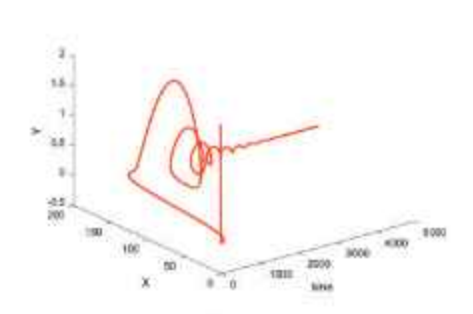


Fig. 6: $s=3.2, c=4, r=.01, N=200, \alpha=0.9t_h=1, \gamma=0.444, \beta=0.001.$ The figure establishes Hopf bifurcation.

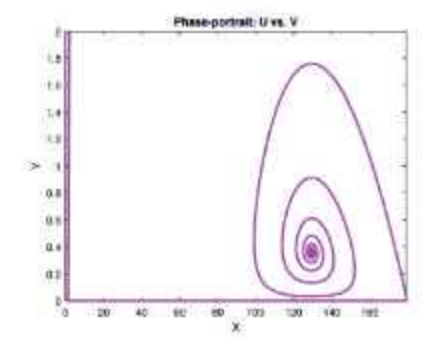


Fig. 7: $s=3.2, c=4, r=.01, N=200, \alpha=0.9t_h=1, \gamma=0.444, \beta=0.001$ The figure establishes Hopf bifurcation.

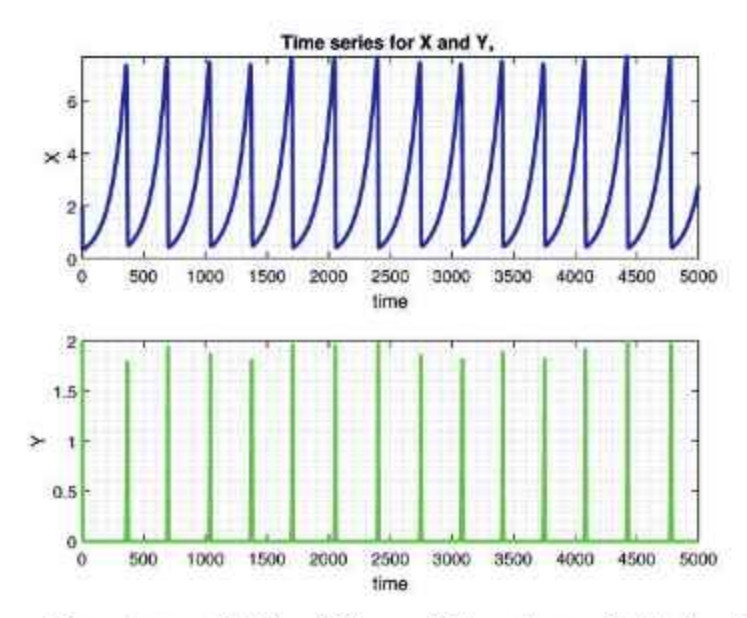


Fig. 8: $s = 2, c = 4, r = .01, N = 200, \alpha = 0.9t_h = 1, \gamma = 0.444, \beta = 0.001$ The figure establishes existence of limit cycle.

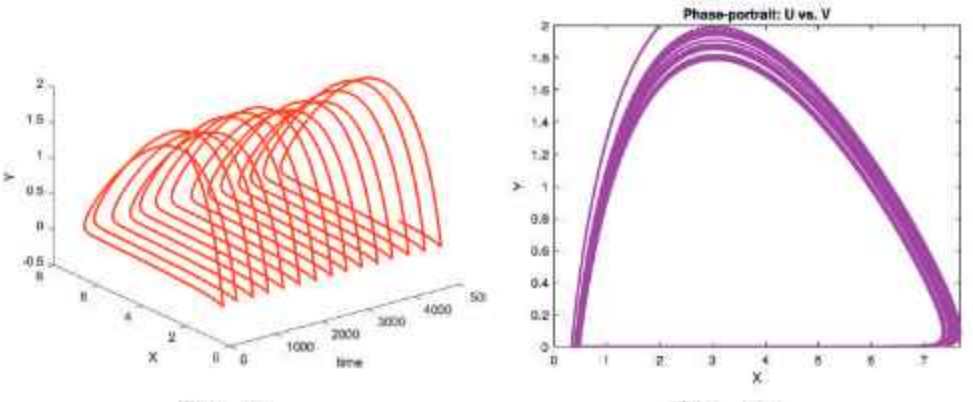


Fig. 9: $s=2, c=4, r=.01, N=200, \alpha=0.9t_h=1, \gamma=0.444, \beta=0.001 \text{ The figure establishes existence of limit cycle.}$

Fig. 10: $s=2, c=4, r=.01, N=200, \alpha=0.9t_h=1, \gamma=0.444, \beta=0.001.$ The figure establishes existence of limit cycle.

5.3. Bifurcation diagrams. In this sub-section, using MATLAB, we plot two bifurcation diagrams for different numerical values of the parameters exhibited against each figure.

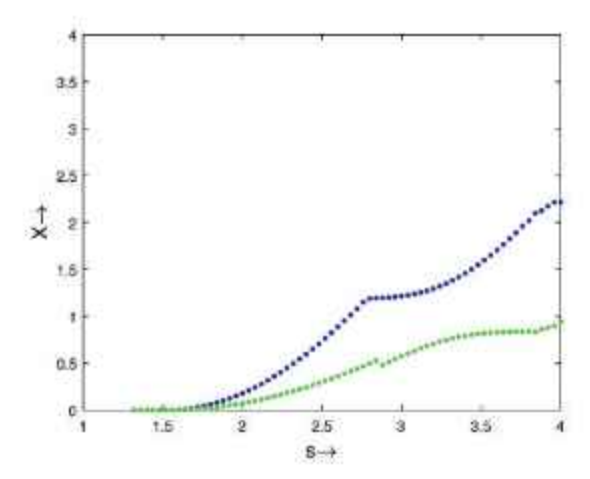


Fig. 11: Hopf Bifurcation diagram for $c = 4, r = 0.01, N = 200, \alpha = 0.9, t_h = 1, \gamma = 0.444, \beta = 0.001.$

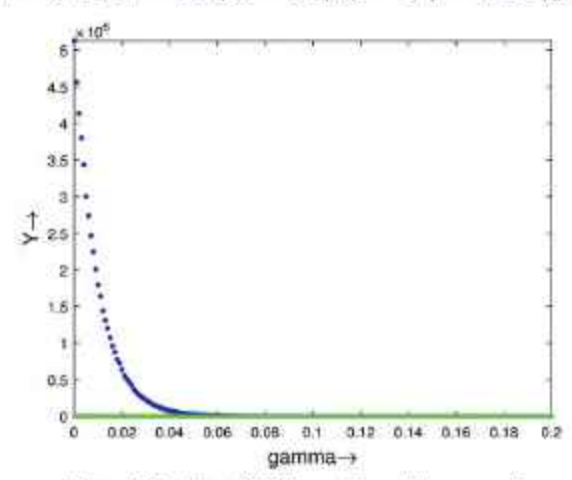


Fig. 12: Hopf Bifurcation diagram for $c = 5.5, t_h = 1, r = 0.01, \alpha = 4.7, s = 1, \beta = 0.001.$

Conclusion. The stability and local bifurcations are analyzed for prey predator system with infighting and herd behaviour in preys and the preys showing retaliation behaviour towards the predators. Theoretically the existence of Hopf bifurcations are shown and graphical representations are done for different numeric values of the associated parameters from where the aspects of stability and bifurcations are easily understood.

Future scope of study. It will be an interesting study if one considers Allee effect in preys and Hunting cooperation among predators in the perspective of present model.

Acknowledgement. The authors are thankful to the referees for his/her suggestions towards the improvement of the paper.

REFERENCES

- Ajraldi, V., Pittarino, M. Venturino, E., Modelling Herd behavior in population system, Nonlinear Analysis, RWA, 12(2011), 2319-2338.
- [2] Braza, P. A., Predator-prey dynamics with square root functional response, Nonlinear Analysis: real world Applications, 13(2012), 1837-1843.
- [3] Cosner, C., De Angelis, D. L., Effects of spatial grouping on functional response of predator, Theoretical population Biology, 56(1999), 65-75.
- [4] Debnath, S., Majumdar, P., Sarkar, S. and Ghosh, U., Complex dynamical behaviour of a delayed prey-predator model with square root functional response in presence of fear in the prey, Int J Modelling and simulation, 43(2023), 612-637.
- [5] Holling, C. S., The components of predation as revealed by a study of small mamal predation of the European pine sawfly. Can. Entomol. 91(1959), 293-320.
- [6] Kooi, B. W., Modelling the dynamic traits involved in fighting predator-prey system, J. Math. Biol. 71(2015), 1575-1605.
- [7] Kaushik, R. and Banerjee, S., Predator-prey system: Prey's counter-attack on juvenile predators shows opposite side of the same ecological coin, Applied Mathematics and Computation, 388(2021), 125330.
- [8] Kuang, Y., Beretta, E., Global qualitative analysis of a ratio dependent predator-prey system, J. Math. Biol., 36(1998), 389-406.
- [9] Lotka, A. J., Elements of physical biology, Williams and Wilkins Co., Inc., Baltimore.
- [10] Maiti, T., Mondal, B. and Sarkar, A., Dynamic Interplay: Cooperative hunting strategies in a predator-prey model with Smith growth dynamics, Brazilian J. Physics, 54(2024):82, 11pp.
- [11] Maiti, and Sarkar, A., On prey-predator model with herd and retaliation behaviours in preys, Appl. Math. E Notes, (To appear in 2025).
- [12] Malthus, T., An essay on the principle of population, J. Joston, St. Paul's Church-Yard, London, 1978.
- [13] Mondal, B., Roy S., Ghosh, U. and Tiwari, P. K., A systematic study of autonomous and non-autonomous predator prey models for the combined effects of fear, refuge, cooperation and harvesting, Eur. Phys J. Plus, 2022, 137: 724.
- [14] Volterra, V., Variazionj e fluttauazionidel numero d' individui in specie animals conviventi, Mem. Acad. Lincei, 2(1926), 31-33.
- [15] Wiggins, S., Stephen, W. and Martin, G., Introduction to applied nonlinear dynamical systems and chaos, Vol 2, No 3, New York, Springer, 2003.

DEPARTMENT OF MATHEMATICS
UNIVERSITY OF KALYANI, KALYANI 741235
NADIA, WEST BENGAL, INDIA
Email: titli96.raharafaymail.com

(Received, March 20, 2025), (Revised, May 06, 2025) Deepak Rout¹, Tanmoy Som², Jayanta Sarkar³ RESULTS ON FIXED POINTS UTILIZING TWO OR MORE GENERALIZED METRICS IN G-METRIC SPACE

ISSN: 0970-5120

Abstract

The primary objective of this study is to develop the fixed point conclusions for contractions of Banach, Chatterjea, and Kannan types within a complete G-metric space that utilizes two generalized metrics, G and H. Additionally, we provide all the sufficient conditions under which fixed point exists when considering three generalized metrics, G, H, and I, for the corresponding contractions in the conclusion section. To reinforce the findings, we include illustrative examples and numerical calculations, which also serve to extend certain theorems found in recent literature.

Keywords: G-metric space; fixed point theory; generalized metric space; complete metric space.

Mathematics Subject Classification (2020): 54H25; 47H10.

1 Introduction

In 1922, Banach [1] established both the conditions for existence and uniqueness of fixed points for a class of certain types of maps in metric space. This result was a remarkable contribution due to its wide theoretical and numerical applications. The conceptualization of spaces or, in particular generalization of metric spaces and studying properties on them has consistently been an engressing area of maths. Moreover, studying fixed point theory on such spaces has always been an interesting area of work for mathematicians due to its applications not only in other areas of mathematics but also in a few other disciplines.

Results related to fixed points in G-metric spaces involving two or more generalized metrics are a fascinating area of research within the broader field of fixed point theory and generalized metric spaces. These types of results generally extend classical fixed point theorems to spaces that are more generalized than traditional metric spaces, and they have applications in various fields, including analysis, optimization, and even differential equations.

Mustafa and Sims [2] in 2006 have proposed the framework of G-metric space. Later, several generalized fixed point conclusions in G-metric space were obtained by [4--11,17,21]. Recently, many authors have generalized several fixed point results with two or more generalized metrics in complete G-metric space. See, [3,12,13] for related results and extensions. The G-metric generalizes the classical metric by considering the distance between three points at once rather than two, which allows for more nuanced distance calculations and fixed-point theorems.

The introduction of two or more generalized metrics in the G-metric space extends the G-metric concept further, providing an even broader framework. In this context, instead of a single metric governing the space, multiple metrics are used. Each of these metrics could capture different distance properties or topological structures of the space.

Let us recall some of the preliminary results on the metric space for different types of contractions namely Banach, Chatterjea and Kannan contractions.

Theorem 1.1. [1] Suppose T is a self-map defined on a complete metric space (X, ρ) for which there exists a constant $k \in [0, 1)$ with

$$\rho(Tu, Tv) \le k\rho(u, v) \forall u, v \in X.$$

Then, there exists a single fixed point of T.

Theorem 1.2. [15] Suppose T is a self-mapping on complete metric space (X, ρ) for which $\exists k \in [0, \frac{1}{2})$ with

$$\rho(Tu, Tv) \le k[\rho(u, Tu) + \rho(v, Tv)] \forall u, v \in X.$$

Then, T admits a unique fixed point.

Theorem 1.3. [16] Suppose T be a self-mapping on complete metric space (\mathcal{X}, ρ) for which $\exists k \in [0, \frac{1}{2})$ with

$$\rho(Tu, Tv) \le k[\rho(u, Tv) + \rho(v, Tu)] \forall u, v \in X.$$

Then, there exists a single fixed point of T

In the present work, we have generalized Banach, Chatterjea, and Kannan type contractions in space equipped with two generalized metrics G and H. For complementary and related results, see, [17–19]. Here, we discuss some of the necessary lemmas and definitions in G-metric space, which are required to prove our results. However, for complementary and related information, see [2, 20, 21].

Definition 1.1. Suppose $X \neq \emptyset$ and $G : X^3 \rightarrow [0, \infty)$ is a map. Then G is called a generalized metric on X if it satisfies the following conditions:

- (i) G(u, v, w) = 0, if u = v = w
- (ii) $0 \le G(u, v, w)$, with $u \ne v$
- (iii) $G(u, u, v) \le G(u, v, w)$, with $v \ne w$
- (iv) G(u, v, w) = G(u, w, v) = G(v, u, w) = G(v, w, u) = G(w, u, v) = G(w, v, u)
- $(v) G(u, u, v) \le G(u, u, w) + G(w, w, v)$
- (vi) $G(u, v, w) \le G(u, \xi, \xi) + G(\xi, v, w)$ for any point $\xi \in X$

Then, (X, G) is called a G-metric space.

Definition 1.2. Suppose $\{u_n\}$ is a sequence in G-metric space (X, G) and $\{u_n\}$ converges to $u \in X$ if $\lim_{n,m\to\infty} G(u, u_n, u_m) = 0$, i.e, $\forall \epsilon > 0$, $\exists N_0 \in \mathbb{N}$ such that $G(u, u_n, u_m) < \epsilon$, $\forall n, m \ge N_0$.

Definition 1.3. A sequence $\{u_n\}$ in (X, \mathcal{G}) is called a \mathcal{G} -Cauchy sequence on X, if for every $\epsilon > 0$ $\exists N_0 \in \mathbb{N}$ such that $\mathcal{G}(u_n, u_m, u_l) < \epsilon$, $\forall l, m, n \geq N_0$. If every \mathcal{G} -Cauchy sequence is convergent then (X, \mathcal{G}) is complete.

Lemma 1.4. Suppose (X, G) is a G-metric space then $G(u, u, v) \leq 2G(u, v, v)$, $\forall u, v \in X$.

Proof. We know that by properties of G-metric space $G(u, v, w) \le G(u, \xi, \xi) + G(\xi, v, w)$ for any $\xi \in X$. Now $G(u, u, v) \le G(u, v, v) + G(v, u, v)$ for any $v \in X$. Therefore $G(u, u, v) \le 2G(u, v, v), \forall u, v \in X$. \square

Lemma 1.5. Consider (X, G) is a G-metric space and $\{u_t\}$ is a sequence in X, then each of the following statements implies others:

- (i) {u_t} converges to u ∈ X with respect to G-metric.
- (ii) $G(u_l, u_m, u) < \epsilon, \forall \epsilon > 0$, as $l, m \ge n_0$, for some $n_0 \in \mathbb{N}$.
- (iii) $G(u_l, u_l, u) < \epsilon, \forall \epsilon > 0$, as $l \ge n_0$, for some $n_0 \in \mathbb{N}$.
- (iv) $G(u_l, u, u) < \epsilon, \forall \epsilon > 0$, as $l \ge n_0$, for some $n_0 \in \mathbb{N}$.

2 Main Results

Theorem 2.1. (Banach type contraction with two generalized metrics) Suppose $X \neq 0$ and H, G: $X^3 \to [0, \infty)$ are two maps such that X is complete with respect to both H and G generalized metrics. Suppose $T : X \to X$ is a map such that $G(u, Tv, Tv) \le H(u, v, v)$ or $H(u, Tv, Tv) \le G(u, v, v)$ implies

(i)
$$G(Tu, Tv, Tv) \le \alpha (H(u, v, v))H(u, v, v)$$

(ii)
$$H(Tu, Tv, Tv) \le \alpha (G(u, v, v))G(u, v, v)$$
,

where $\alpha:[0,\infty)\to[0,\frac{1}{2})$ such that $\limsup_{s\to r+}\alpha(s)\leq \frac{1}{2}$. Then \exists a fixed point for T which is unique.

Proof. Let $u_1 \in X$. Let us construct the sequence $u_{l+1} = Tu_l$, $\forall l \in \mathbb{N}$

Now,
$$H(u_l, Tu_{l-1}, Tu_{l-1}) = H(u_l, u_l, u_l) = 0 \le G(u_l, u_{l+1}, u_{l+1})$$

$$\implies H(Tu_l, Tu_{l-1}, Tu_{l-1}) = H(u_{l+1}, u_l, u_l) \le \alpha \Big(G(u_l, u_{l+1}, u_{l+1})\Big)G(u_l, u_{l+1}, u_{l+1})$$
 (2.1)

and
$$G(Tu_{l+1}, Tu_l, Tu_l) \le \alpha (H(u_{l+1}, u_l, u_l)) H(u_{l+1}, u_l, u_l)$$
. (2.2)

Then from (2.1) and (2.2) we get,

$$G(u_{l+2}, u_{l+1}, u_{l+1}) \le \alpha \Big(H(u_{l+1}, u_l, u_l)\Big) \alpha \Big(G(u_l, u_{l+1}, u_{l+1})\Big) G(u_l, u_{l+1}, u_{l+1})$$

 $\le 2\alpha \Big(H(u_{l+1}, u_l, u_l)\Big) \alpha \Big(G(u_l, u_{l+1}, u_{l+1})\Big) G(u_{l+1}, u_l, u_l),$ [by Lemma 1.4]
 $\le rG(u_{l+1}, u_l, u_l),$ where $r \in [0, 1)$ as $\alpha : [0, \infty) \to [0, \frac{1}{\alpha}]$

Similarly, $H(u_{l+2}, u_{l+1}, u_{l+1}) \le rH(u_{l+1}, u_l, u_l)$.

Then $\lim_{l\to\infty} \mathcal{G}(u_l, u_l, u_{l+1}) = 0$ and $\lim_{l\to\infty} H(u_l, u_l, u_{l+1}) = 0$. Now we prove that $\{u_l\}$ is \mathcal{G} -Cauchy sequence with respect to both \mathcal{G} and H. Suppose m > l.

$$G(u_l, u_l, u_m) \le G(u_l, u_l, u_{l+1}) + G(u_{l+1}, u_{l+1}, u_m)$$

 $\le G(u_l, u_l, u_{l+1}) + G(u_{l+1}, u_{l+1}, u_{l+2}) + G(u_{l+2}, u_{l+2}, u_m)$
 $\le G(u_l, u_l, u_{l+1}) + G(u_{l+1}, u_{l+1}, u_{l+2}) + \cdots + G(u_{m-1}, u_{m-1}, u_m).$

Now, taking $\lim_{m,l\to\infty}$ on both sides, we obtain

$$\lim_{m,l\to\infty} G(u_l,u_l,v_m) = 0.$$

Therefore $\{u_i\}$ is a \mathcal{G} -Cauchy sequence with respect to \mathcal{G} . Similarly $\{u_i\}$ is a \mathcal{G} -Cauchy sequence with respect to H. Since X is complete with respect to both G and H so $\exists u, v \in X$ such that

$$\lim_{l\to\infty} G(u_l, u_l, u) = \lim_{l\to\infty} H(u_l, u_l, v) = 0.$$

Now, we claim that u = v. Suppose that $u \neq v$. Then we get $G(u, u, v) \neq 0$, $G(v, v, u) \neq 0$ and $H(u, u, v) \neq 0$, $H(v, v, u) \neq 0$. From Lemma 1.4 and Lemma 1.5, we can conclude that,

$$0 = \lim_{t \to \infty} G(u, Tu_t, Tu_t) \le H(u, v, v) = \lim_{t \to \infty} H(u, u_t, u_t).$$

 $0 = \lim_{l \to \infty} \mathcal{G}(u, Tu_l, Tu_l) \leq H(u, v, v) = \lim_{l \to \infty} H(u, u_l, u_l),$ For a large integer value of l, we have, $\mathcal{G}(u, Tu_l, Tu_l) \leq H(u, u_l, u_l)$ therefore from the hypothesis of the Theorem 2.1 we have,

$$G(Tu, u_{l+1}, u_{l+1}) = G(Tu, Tu_l, Tu_l) \le \alpha (H(u, u_l, u_l)) H(u, u_l, u_l)$$
 (2.3)

$$H(Tu, u_{l+1}, u_{l+1}) = H(Tu, Tu_l, Tu_l) \le \alpha (G(u, u_l, u_l))G(u, u_l, u_l).$$
 (2.4)

Taking $\lim_{l\to\infty}$ on both sides of (2.4) we get $\lim_{l\to\infty} H(Tu, u_{l+1}, u_{l+1}) = 0$. This implies $\{u_l\}$ converges to Tu. Thus Tu = v. Similarly, Tv = u. Now, $G(u, u, v) = \lim_{l\to\infty} G(v, u_{l+1}, u_{l+1}) = G(Tu, u_{l+1}, u_{l+1}) = G(Tu, Tu_l, Tu_l) \le \alpha \Big(H(u, u_l, u_l)\Big)H(u, u_l, u_l) = \lim_{l\to\infty} \alpha \Big(H(u, u_l, u_l)\Big)H(u, v, v)$, then $\exists k_1 \in [0, \frac{1}{2})$ such that $G(u, u, v) \le k_1H(u, v, v)$.

Similarly, $\exists k_2 \in [0, \frac{1}{2})$ such that $H(u, u, v) \le k_2 G(v, u, u) \le 2k_2 G(v, v, u)$. [by Lemma 1.4]

Thus, $G(u, u, v) \le k_1 H(u, v, v) \le 2k_1 H(u, u, v) \le 2k_1 k_2 G(u, u, v)$. If $G(u, u, v) \ne 0$, then $k_1 k_2 \ge \frac{1}{2}$. This is contradiction. Therefore, G(u, u, v) = 0. Hence u = v and Tu = u.

For uniqueness, let u and v be two fixed points of T with $u \neq v$, then $G(u, v, v) \neq 0$ and $H(u, v, v) \neq 0$. So one of the following inequality holds:

$$G(u, v, v) < H(u, v, v)$$
 or $H(u, v, v) < G(u, v, v)$.

Suppose $G(u, Tv, Tv) = G(u, v, v) \le H(u, v, v)$, then by hypothesis of Theorem 2.1 we have $G(Tu, Tv, Tv) \le \alpha (H(u, v, v))H(u, v, v)$ and $H(Tu, Tv, Tv) \le \alpha (G(u, v, v))G(u, v, v)$ which implies

$$G(u, v, v) \le \alpha \Big(H(u, v, v)\Big)\alpha \Big(G(u, v, v)\Big)G(u, v, v).$$

Thus $\alpha(H(u, v, v))\alpha(G(u, v, v)) \ge 1$. This is a contradiction. So G(u, v, v) = 0 and u = v.

Example 2.2. Let X = [0, 1] and we define two metrics G and H on X as,

$$G(u, v, w) = \max\{|u - v|, |v - w|, |w - u|\}\ and\ H(u, v, w) = 2\max\{|u - v|, |v - w|, |w - u|\}.$$

Let $T: X \to X$ be the map define as,

$$T(u) = \frac{u^2}{16} + \frac{u}{16} + \frac{1}{16}$$
.

Now, $G(u, Tv, Tv) = |u - Tv| = |u - \frac{v^2}{16} - \frac{v}{16} - \frac{1}{16}|$ and H(u, v, v) = 2|u - v| and G(u, v, v) = |u - v|.

Therefore we have, $G(u, Tv, Tv) \le H(u, v, v)$ $\forall u, v \in X$.

(i) Now,
$$G(Tu, Tv, Tv) = |Tu - Tv| = \frac{1}{16}(1 + u + v)|u - v| \le \frac{3}{16}|u - v| = \frac{3}{32}H(u, v, v) \ \forall \ u, v \in [0, 1].$$

(ii) Again,
$$H(Tu, Tv, Tv) = 2|Tu - Tv| \le \frac{3}{2}|u - v| \le \frac{3}{2}G(u, v, v) \forall u, v \in [0, 1].$$

From these two if we choose a function $\alpha: [0, \infty) \to \left[\frac{3}{3}, \frac{1}{2}\right]$ then both of the conditions of Theorem 2.1 are justified. Hence, T admits a fixed point on X, which is unique.

Theorem 2.3. (Chatterjea type contraction with two generalized metrics) Suppose X is a non-empty set equipped with two generalized metrics G and H and $T: X \to X$ such that X is complete with respect to both H and G and $G(u, Tv, Tv) \le H(u, v, v)$ or $H(u, Tv, Tv) \le G(u, v, v)$ implies

(i)
$$G(Tu, Tv, Tv) \le \alpha (H(u, v, v))[G(v, v, Tu) + H(u, u, Tv)]$$

(ii)
$$H(Tu, Tv, Tv) \le \alpha (\mathcal{G}(u, v, v))[H(v, v, Tu) + \mathcal{G}(u, u, Tv)],$$

where $\alpha:[0,\infty)\to[0,\frac{1}{4})$ such that $\limsup_{t\to r+}\alpha(t)\leq \frac{1}{4}$. Then \exists is a fixed point for $\mathcal T$, which is unique.

Proof. Let $u_l \in \mathcal{X}$. Construct the sequence $u_{l+1} = \mathcal{T}(u_l), \forall l \in \mathbb{N}$.

Now,
$$G(u_{l+1}, Tu_l, Tu_l) = G(u_{l+1}, u_{l+1}, u_{l+1}) = 0 \le H(u_{l+1}, u_l, u_l)$$

$$\implies$$
 $G(Tu_{l+1}, Tu_l, Tu_l) \le \alpha \Big(H(u_{l+1}, u_l, u_l)\Big)[G(u_l, u_l, Tu_{l+1}) + H(u_{l+1}, u_{l+1}, Tu_l)]$

Therefore,
$$G(Tu_{l+1}, Tu_l, Tu_l) \le \alpha \Big(H(u_{l+1}, u_l, u_l)\Big)G(u_l, u_l, u_{l+2})$$

$$G(u_{l+2}, Tu_l, Tu_l) \le \alpha \Big(H(u_{l+1}, u_l, u_l)\Big) [G(u_{l+2}, u_{l+1}, u_{l+1}) + G(u_{l+1}, u_l, u_l)]$$

$$G(u_{l+2}, u_{l+1}, u_{l+1}) \le \frac{\alpha(H(u_{l+1}, u_l, u_l))}{1 - \alpha(H(u_{l+1}, u_l, u_l))}G(u_{l+1}, u_l, u_l)$$
 (2.5)

and
$$H(Tu_{l+1}, Tu_l, Tu_l) \le \alpha (G(u_{l+1}, u_l, u_l)) [H(u_l, u_l, Tu_{l+1}) + G(u_{l+1}, u_{l+1}, Tu_l)]$$

Therefore,
$$H(\mathcal{T}u_{l+1}, \mathcal{T}u_l, \mathcal{T}u_l) \le \alpha (\mathcal{G}(u_{l+1}, u_l, u_l)) H(u_l, u_l, u_{l+2})$$

$$H(Tu_{l+1}, Tu_l, Tu_l) \le \alpha (G(u_{l+1}, u_l, u_l))[H(u_{l+2}, u_{l+1}, u_{l+1}) + H(u_{l+1}, u_l, u_l)]$$

$$H(u_{l+2}, u_{l+1}, u_{l+1}) \le \frac{\alpha(\mathcal{G}(u_{l+1}, u_l, u_l))}{1 - \alpha(\mathcal{G}(u_{l+1}, u_l, u_l))} H(u_{l+1}, u_l, u_l)$$
 (2.6)

Now, $\limsup_{t\to r_+} \alpha(t) < \frac{1}{4}$, for all $t\in [0,\infty)$. It follows that, $\lim_{s\to t_+} \sup \frac{\alpha(s)}{1-\alpha(s)} \leq \frac{1}{3} < \frac{1}{2}$. Then $\exists \ r_1, r_2 \in \mathbb{R}$

$$[0,\frac{1}{4}) \text{ and } p_1,p_2 \in \mathbb{N} \text{ such that } \frac{\alpha\Big(H(u_{l+1},u_l,u_l)\Big)}{1-\alpha\Big(H(u_{l+1},u_l,u_l)\Big)} < r_1 \ \forall l > p_1, \text{ and } \frac{\alpha\Big(\mathcal{G}(u_{l+1},u_l,u_l)\Big)}{1-\alpha\Big(\mathcal{G}(u_{l+1},u_l,u_l)\Big)} < r_2 \ \forall l > p_2.$$
It follows that,

$$G(u_{l+2}, u_{l+1}, u_{l+1}) \le r_1 G(u_{l+1}, u_l, u_l)$$
 and $H(u_{l+2}, u_{l+1}, u_{l+1}) \le r_2 H(u_{l+1}, u_l, u_l)$.

If $\lim_{l\to\infty} \mathcal{G}(u_{l+1},u_l,u_l)\neq 0$, then $r_1\geq 1$, this is a contradiction. Therefore, $\lim_{l\to\infty} \mathcal{G}(u_{l+1},u_l,u_l)=0$, similarly $\lim_{l\to\infty} H(u_{l+1},u_l,u_l)=0$. By proceeding similarly as in the proof of 2.1, we can conclude that $\{u_l\}$ is a Cauchy sequence relative to both \mathcal{G} and H in \mathcal{X} . Since the given \mathcal{X} is complete with respect to both \mathcal{G} and H so $\exists u,v\in\mathcal{X}$ such that $\lim_{l\to\infty} \mathcal{G}(u_l,u_l,u)=0$. Similarly $\lim_{l\to\infty} H(u_l,u_l,v)=0$, then $\lim_{l\to\infty} H(u_l,u_l,u)=H(u,v,v)>0$ and $\lim_{l\to\infty} \mathcal{G}(u_l,u_l,u)=0 \leq \lim_{l\to\infty} H(u_l,u_l,u)=H(u,v,v)$. For some large value of l we have, $\mathcal{G}(u,\mathcal{T}u_l,\mathcal{T}u_l)\leq H(u,u_l,u_l)$. From the hypothesis of Theorem 2.3 we obtain

$$G(Tu, Tu_l, Tu_l) \le \alpha \Big(H(u, u_l, u_l)\Big)[G(u_l, u_l, Tu) + H(u, u, Tu_l)],$$
 (2.7)

$$H(Tu, Tu_l, Tu_l) \le \alpha (G(u, u_l, u_l))[H(Tu, u_l, u_l) + G(Tu_l, u, u)].$$
 (2.8)

Taking limit $l \to \infty$ in (2.8) we get,

$$\lim_{l\to\infty} H(Tu, Tu_l, Tu_l) \leq \lim_{l\to\infty} \alpha \Big(\mathcal{G}(u, u_l, u_l) \Big) \lim_{l\to\infty} [H(Tu, u_l, u_l) + \mathcal{G}(Tu_l, u, u)].$$

If $\lim_{l\to\infty} H(Tu, Tu_l, Tu_l) \neq 0$, then $\lim_{l\to\infty} \sup \alpha \left(\mathcal{G}(u, u_l, u_l)\right) \geq 1$. Therefore, Tu = v. Analogously, we can prove that Tv = u.

Taking limit $l \to \infty$ in (2.7) we obtain,

$$\lim_{l\to\infty} G(Tu, Tu_l, Tu_l) \le \lim_{l\to\infty} \alpha \Big(H(u, u_l, u_l) \Big) \lim_{l\to\infty} [G(u_l, u_l, Tu) + H(u, u, Tu_l)]$$

$$\Longrightarrow G(Tu, u, u) \le \lim_{l\to\infty} \alpha \Big(H(u, u_l, u_l) \Big) [G(u, u, v) + H(v, u, u)].$$

Since $\limsup_{t\to u+} \alpha(t) < \frac{1}{4}$, then $\exists k_1 \in [0, \frac{1}{4})$ such that $\mathcal{G}(v, u, u) \leq k_1 |\mathcal{G}(u, u, v) + H(v, u, u)|$.

Therefore, from Lemma 1.4,
$$G(v, u, u) \le \frac{k_1}{1 - k_1}H(v, u, u) \le 2\frac{k_1}{1 - k_1}H(v, v, u)$$
.

Similarly $\exists k_2 \in [0, \frac{1}{4})$ such that

$$H(u,v,v) \le \frac{k_2}{1-k_2}\mathcal{G}(u,v,v) \implies H(v,v,u) \le 2\frac{k_2}{1-k_2}\mathcal{G}(v,u,u)$$

which implies $G(v, u, u) \le \frac{k_1}{1-k_1} \frac{k_2}{1-k_2} 4G(u, v, v)$. If $G(v, u, u) \ne 0$, then we have $4 \frac{k_1}{1-k_1} \frac{k_2}{1-k_2} \ge 1$, which contradicts our assumption. Hence G(v, u, u) = 0 and u = v. So T admits a fixed point.

For uniqueness, let u and v be two fixed points of the map T with $u \neq v$. Then we have Tu = u, Tv = v and $G(u, u, v) \neq 0$, $G(u, v, v) \neq 0$, $G(u, v, v) \neq 0$, $G(u, u, v) \neq 0$. It follows that either $G(u, v, v) = G(u, v, v) \leq G(u, v, v) \leq G(u, v, v)$. Then from (2.5) and (2.6) we get,

$$G(u, u, v) \le \frac{\alpha(H(u, v, v))}{1 - \alpha(H(u, v, v))}H(u, u, v)$$
 and $H(u, v, v) \le \frac{\alpha(G(u, v, v))}{1 - \alpha(G(u, v, v))}G(u, u, v)$.

Now applying the lemma 1.4 we get,

$$G(u, v, v) \le \frac{\alpha(H(u, v, v))}{1 - \alpha(H(u, v, v))} \cdot \frac{\alpha(G(u, v, v))}{1 - \alpha(G(u, v, v))} 4G(u, v, v).$$

If $\mathcal{G}(u, v, v) \neq 0$, then $\frac{\alpha(H(u, v, v))}{1 - \alpha(H(u, v, v))} \cdot \frac{\alpha(\mathcal{G}(u, v, v))}{1 - \alpha(\mathcal{G}(u, v, v))} \geq \frac{1}{4}$, which is a contradiction. Hence $\mathcal{G}(u, v, v) = 0$ and u = v.

Example 2.4. Let $X = \{0, \frac{1}{2}, 1\}$, define two metrics G and H as,

$$\mathcal{G}(u,v,w) = \begin{cases} 0, & \text{if } u = v = w \\ \max\{u,v,w\} & \text{else} \end{cases}$$

and

$$H(u, v, w) = \max\{|u - v|, |v - w|, |w - u|\}.$$

Let $T(u) = \frac{u}{5}$ be a map on X. Since X is a finite set therefore, it is complete with respect to both G and H. Let u, v be two arbitrary elements of X. Therefore,

(i) if
$$u = 0$$
, $v = \frac{1}{2}$ then

$$G\left(u, T(v), T(v)\right) = \frac{1}{10} \le H(u, v, v) = \frac{1}{2} \text{ or } H\left(u, T(v), T(v)\right) = \frac{1}{10} \le G(u, v, v) = \frac{1}{2} \text{ implies}$$

$$G\left(T(u), T(v), T(v)\right) = \frac{1}{10} \le \alpha \left(H(u, v, v)\right) \left[\frac{1}{2} + \frac{1}{10}\right] \text{ and}$$

$$H\left(T(u), T(v), T(v)\right) = \frac{1}{10} \le \alpha \left(G(u, v, v)\right) \left[\frac{1}{2} + \frac{1}{10}\right],$$

(ii) if
$$u = 0, v = 1$$
 then

$$G\left(u, T(v), T(v)\right) = \frac{1}{5} \le H(u, v, v) = 1 \text{ or } H\left(u, T(v), T(v)\right) = \frac{1}{5} \le G(u, v, v) = 1 \text{ implies}$$

 $G\left(T(u), T(v), T(v)\right) = \frac{1}{5} \le \alpha \left(H(u, v, v)\right) \left[\frac{1}{2} + \frac{1}{16}\right] \text{ and}$
 $H\left(T(u), T(v), T(v)\right) = \frac{1}{5} \le \alpha \left(G(u, v, v)\right) \left[\frac{1}{2} + \frac{1}{16}\right],$

(iii) if
$$u = \frac{1}{2}$$
, $v = 0$ then

$$\begin{split} \mathcal{G}\Big(u, \mathcal{T}(v), \mathcal{T}(v)\Big) &= \tfrac{1}{2} \leq H(u, v, v) = \tfrac{1}{2} \text{ or } H\Big(u, \mathcal{T}(v), \mathcal{T}(v)\Big) = \tfrac{1}{2} \leq \mathcal{G}(u, v, v) = \tfrac{1}{2} \text{ implies} \\ \mathcal{G}\Big(\mathcal{T}(u), \mathcal{T}(v), \mathcal{T}(v)\Big) &= \tfrac{1}{10} \leq \alpha \Big(H(u, v, v)\Big) [\tfrac{1}{10} + \tfrac{1}{2}] \text{ and} \\ H\Big(\mathcal{T}(u), \mathcal{T}(v), \mathcal{T}(v)\Big) &= \tfrac{1}{10} \leq \alpha \Big(\mathcal{G}(u, v, v)\Big) [1 + \tfrac{1}{5}], \end{split}$$

(iv) if
$$u = \frac{1}{9}, v = 1$$
 then

$$\begin{split} \mathcal{G}\Big(u, \mathcal{T}(v), \mathcal{T}(v)\Big) &= \tfrac{1}{2} \leq H(u, v, v) = \tfrac{1}{2} \text{ or } H\Big(u, \mathcal{T}(v), \mathcal{T}(v)\Big) = \tfrac{3}{10} \leq \mathcal{G}(u, v, v) = 1 \text{ implies } \\ \mathcal{G}\Big(\mathcal{T}(u), \mathcal{T}(v), \mathcal{T}(v)\Big) &= \tfrac{1}{5} \leq \alpha \Big(H(u, v, v)\Big)[1 + \tfrac{3}{10}] \text{ and } \\ H\Big(\mathcal{T}(u), \mathcal{T}(v), \mathcal{T}(v)\Big) &= \tfrac{1}{10} \leq \alpha \Big(\mathcal{G}(u, v, v)\Big)[\tfrac{9}{10} + \tfrac{1}{2}], \end{split}$$

(v) if
$$u = 1, v = 0$$
 then

$$\begin{split} &\mathcal{G}\Big(u,\mathcal{T}(v),\mathcal{T}(v)\Big) = 1 \leq H(u,v,v) = 1 \text{ or } H\Big(u,\mathcal{T}(v),\mathcal{T}(v)\Big) = 1 \leq \mathcal{G}(u,v,v) = 1 \text{ implies} \\ &\mathcal{G}\Big(\mathcal{T}(u),\mathcal{T}(v),\mathcal{T}(v)\Big) = \frac{1}{5} \leq \alpha \Big(H(u,v,v)\Big)[\frac{1}{5}+1] \text{ and} \\ &H\Big(\mathcal{T}(u),\mathcal{T}(v),\mathcal{T}(v)\Big) = \frac{1}{5} \leq \alpha \Big(\mathcal{G}(u,v,v)\Big)[\frac{1}{5}+1], \end{split}$$

(vi) if
$$u = 1, v = \frac{1}{3}$$
 then

$$G(u, T(v), T(v)) = 1 \le H(u, v, v) = \frac{1}{2}$$
 (which is absurd case) but we have the another condition $H(u, T(v), T(v)) = \frac{9}{10} \le G(u, v, v) = 1$ which implies

$$\mathcal{G}\left(\mathcal{T}(u), \mathcal{T}(v), \mathcal{T}(v)\right) = \frac{1}{5} \le \alpha \left(H(u, v, v)\right) \left[\frac{1}{2} + \frac{9}{10}\right] \text{ and }$$

$$H\left(\mathcal{T}(u), \mathcal{T}(v), \mathcal{T}(v)\right) = \frac{1}{16} \le \alpha \left(\mathcal{G}(u, v, v)\right) \left[\frac{3}{16} + 1\right].$$

Now if we choose function $\alpha: [0, \infty) \to [\frac{1}{4}, \frac{1}{4})$ then all the conditions of Theorem 2.3 are satisfied. Hence, we can conclude that T admits a unique fixed point on X.

Theorem 2.5. (Kannan type contraction with two generalized metrics) Suppose X is a non-empty set equipped with two generalized metrics G and H and $T: X \to X$ mapping such that X is complete relative to both G and H and $G(u, Tv, Tv) \le H(u, v, v)$ or $H(u, Tv, Tv) \le G(u, v, v)$ implies

(i)
$$G(Tu, Tv, Tv) \le \alpha (H(u, v, v))[G(u, u, Tu) + H(v, v, Tv)]$$

(ii)
$$H(Tu, Tv, Tv) \le \alpha (G(u, v, v))[H(u, u, Tu) + G(v, v, Tv)],$$

where $\alpha:[0,\infty)\to[0,\frac{1}{4})$ such that $\limsup_{t\to\infty}\alpha(t)\leq\frac{1}{4}$. Then \exists a fixed point of T, which is unique.

Proof. Let $u_1 \in X$. Let us construct the sequence $u_{l+1} = T(u_l)$, $\forall l \in \mathbb{N}$. Now,

$$G(u_{l+1}, Tu_l, Tu_l) = 0 \le H(u_{l+1}, u_l, u_l)$$

 $\Longrightarrow G(Tu_{l+1}, Tu_l, Tu_l) \le \alpha (H(u_{l+1}, u_l, u_l)) [G(u_{l+1}, u_{l+1}, Tu_{l+1}) + H(u_l, u_l, Tu_l)],$

and
$$H(Tu_{l+1}, Tu_l, Tu_l) \le \alpha (\mathcal{G}(u_{l+1}, u_l, u_l))[H(u_{l+1}, u_{l+1}, Tu_{l+1}) + \mathcal{G}(u_l, u_l, Tu_l)]$$

then we get,

$$G(Tu_{l+1}, Tu_l, Tu_l) \le \alpha \Big(H(u_{l+1}, u_l, u_l)\Big)[G(u_{l+1}, u_{l+1}, Tu_{l+1}) + H(u_l, u_l, Tu_l)],$$

Therefore,
$$G(u_{l+1}, u_{l+1}, u_{l+1}) \le \frac{\alpha \left(H(u_{l+1}, u_l, u_l)\right)}{1 - \alpha \left(H(u_{l+1}, u_l, u_l)\right)} H(u_l, u_l, u_{l+1}),$$

$$H(u_{l+2}, u_{l+1}, u_{l+1}) \le \frac{\alpha(\mathcal{G}(u_{l+1}, u_l, u_l))}{1 - \alpha(\mathcal{G}(u_{l+1}, u_l, u_l))} \mathcal{G}(u_l, u_l, u_{l+1}).$$

$$\operatorname{Put} \, a(l) = \frac{\alpha \Big(H(u_{l+1}, u_l, u_l) \Big)}{1 - \alpha \Big(H(u_{l+1}, u_l, u_l) \Big)} \, \text{ and } \, b(l) = \frac{\alpha \Big(\mathcal{G}(u_{l+1}, u_l, u_l) \Big)}{1 - \alpha \Big(\mathcal{G}(u_{l+1}, u_l, u_l) \Big)},$$

Then we have, $\mathcal{G}(u_{l+2}, u_{l+1}, u_{l+1}) \le a(l)H(u_l, u_l, u_{l+1}) \le a(l)b(l-1)\mathcal{G}(u_l, u_{l-1}, u_{l-1})$.

If $\lim_{l\to\infty} \mathcal{G}(u_l,u_{l-1},u_{l-1})\neq 0$ then $\lim_{l\to\infty} a(l)b(l-1)\geq 1$, which leads to a contradiction. Therefore, $\lim_{l\to\infty} \mathcal{G}(u_{l+1},u_l,u_l)=0$. Similarly we can prove that $\lim_{l\to\infty} H(u_{l+1},u_l,u_l)=0$.

By proceeding similarly as in the proof of 2.1, we can conclude that $\{u_l\}$ is a Cauchy sequence relative to both \mathcal{G} and H in \mathcal{X} . By completeness of \mathcal{X} relative to \mathcal{G} and $H \ni u, v \in \mathcal{X}$ such that $\lim_{l \to \infty} \mathcal{G}(u_l, u_l, u) = 0 = \lim_{l \to \infty} H(u_l, u_l, v)$.

Therefore, $\lim_{l\to\infty} H(u_l,u_l,u) = H(u,v,v) > 0$ and $\lim_{l\to\infty} \mathcal{G}(u_l,u_l,u) = 0 < \lim_{l\to\infty} H(u_l,u_l,u) = H(u,v,v)$. Now, $\lim_{l\to\infty} \mathcal{G}(u_l,u,u) = 0 \le H(u,v,v) = \lim_{l\to\infty} H(u_l,u_l,u)$. For some large value of l we have, $\mathcal{G}(u,Tu_l,Tu_l) \le H(u,u_l,u_l)$. From hypothesis of Theorem 2.5 we get,

$$G(Tu, Tu_l, Tu_l) \le \alpha (H(u, u_l, u_l))[G(u, u, Tu) + H(Tu_l, Tu_l, Tu_{l+1})],$$
 (2.9)

$$H(Tu, Tu_l, Tu_l) \le \alpha (G(u, u_l, u_l))[H(u, u, Tu) + G(Tu_l, Tu_l, Tu_{l+1})].$$
 (2.10)

Taking limit as $t \to \infty$ on both sides in (2.9) we have, $\mathcal{G}(\mathcal{T}u, u, u) \le \lim_{t \to \infty} \alpha \Big(H(u_t, u_t, u)\Big) \mathcal{G}(u, u, \mathcal{T}u)$. If $\mathcal{G}(\mathcal{T}u, u, u) \ne 0$, then $\lim_{t \to \infty} \alpha \Big(H(u_t, u_t, u)\Big) \ge 1$. This is a contradiction. So, $\mathcal{G}(u, \mathcal{T}u, \mathcal{T}u) = 0$ and $\mathcal{T}u = u$. Hence \mathcal{T} has a fixed point on \mathcal{X} .

For the uniqueness part, let T have two fixed points u and v. Then T(u) = u and T(v) = v, $G(u, u, v) \neq 0$, $G(u, v, v) \neq 0$, $G(u, v, v) \neq 0$, $G(u, v, v) \neq 0$. It follows that either G(u, v, v) < G(u, v, v) < G(u, v, v) < G(u, v, v). Suppose G(u, v, v) < G(u, v, v), then it implies that G(u, Tv, Tv) < G(u, v, v). Then by hypothesis of Theorem 2.5 we get,

$$G(Tu, Tv, Tv) \le \alpha \Big(H(u, v, v)\Big)[G(u, u, Tu) + H(v, v, Tv)],$$

$$H(Tu, Tv, Tv) \le \alpha (G(u, v, v))[H(u, u, Tu) + G(v, v, Tv)].$$

Since, G(u, u, Tu) = H(v, v, Tv) = H(v, v, v) = 0. Therefore, $G(Tu, Tv, Tv) \le 0$, which implies G(Tu, Tv, Tv) = G(u, v, v) = 0. Hence u = v.

Example 2.6. Let X = [0, 1] and we define two metrics G and H on X as,

$$G(u, v, w) = \max\{|u - v|, |v - w|, |w - u|\}$$
 and $H(u, v, w) = 2\max\{|u - v|, |v - w|, |w - u|\}$.

Let $T: X \rightarrow X$ be the map defined as,

$$T(u) = \frac{u}{16}$$
.

Now, $G(u, Tv, Tv) = |u - Tv| = |u - \frac{v}{16}|$ and H(u, v, v) = 2|u - v|.

Therefore we have, $G(u, Tv, Tv) \le H(u, v, v)$ $\forall u, v \in X$.

(i) Now,
$$G(Tu, Tv, Tv) = \frac{1}{16}|u - v| \le \frac{1}{16} \ \forall \ u, v \in [0, 1] \ and$$

$$G(u, u, Tu) + H(v, v, Tv) = |u - Tu| + 2|v - Tv| = \frac{15u + 30v}{16} \le \frac{45}{16} \ \forall \ u, v \in [0, 1]$$
also, $G(Tu, Tv, Tv) \le \alpha \Big(H(u, v, v)\Big) [G(u, u, Tu) + H(v, v, Tv)] \ \forall \ u, v \in [0, 1].$

(ii) Again,
$$H(Tu, Tv, Tv) = \frac{2}{16}|u-v| \le \frac{2}{16} \ \forall \ u, v \in [0, 1] \ and$$

 $H(u, u, Tu) + \mathcal{G}(v, v, Tv) = 2|u - Tu| + |v - Tv| = \frac{36u + 15v}{16} \le \frac{45}{16} \ \forall \ u, v \in [0, 1]$
also, $H(Tu, Tv, Tv) \le \alpha (\mathcal{G}(u, v, v)) [H(u, u, Tu) + \mathcal{G}(v, v, Tv)] \ \forall \ u, v \in [0, 1].$

Now if we choose function $\alpha: [0, \infty) \rightarrow \left[\frac{2}{45}, \frac{1}{4}\right)$ then all the conditions of Theorem 2.5 are satisfied. Hence, we can conclude that T has exactly one fixed point in X.

3 Concluding remarks

The broadening of fixed-point theory in the setting of G-metric spaces with two or more generalized metrics provides a rich framework for exploring more general types of distance and convergence properties. These results not only generalize classical fixed-point theorems but also have important implications for theoretical and applied mathematics.

In this work, in Theorem 2.1, we have extended the Banach contraction principle in complete G-metric space with two generalized metrics G and H. In Theorem 2.3 and Theorem 2.5, we have generalized Chatterjea and Kannan type of contractions, respectively, in a complete G-metric space with two generalized metrics G and H. Further, we have given sufficient conditions for an existing unique fixed point of the self-map in the setting of a complete G-metric space for the case of three generalized metrics G, H, and I for the contractive classes Banach, Chatterjea, and Kannan contractions.

Let G, H, I be three generalized metrics on complete metric space X. Suppose $T : X \to X$ such that $G(u, Tu, Tv) \le H(u, v, v)$ or $H(u, Tv, Tv) \le I(u, v, v)$ or $I(u, Tv, Tv) \le G(u, v, v)$ implies,

- Bannch-type contraction with three generalized metrics:
 - (i) $G(Tu, Tv, Tv) \le \alpha (H(u, v, v))H(u, v, v)$
 - (ii) $H(Tu, Tv, Tv) \le \alpha (I(u, v, v))I(u, v, v)$
- (iii) $I(Tu, Tv, Tv) \le \alpha (G(u, v, v))G(u, v, v)$.

where $\alpha : [0, \infty) \to [0, \frac{1}{2})$ such that $\limsup_{s \to r+} \alpha(s) \le \frac{1}{2}$. Then, T has only one fixed point.

- (2) Chatterjea type contraction with three generalized metrics:
 - (i) $G(Tu, Tv, Tv) \le \alpha (H(u, v, v))[G(v, v, Tu) + H(u, u, Tv)]$
- (ii) $H(Tu, Tv, Tv) \le \alpha (I(u, v, v))[H(v, v, Tu) + I(u, u, Tv)]$

(iii)
$$I(Tu, Tv, Tv) \le \alpha (G(u, v, v))(I(v, v, Tu) + G(u, u, Tv)),$$

where $\alpha:[0,\infty)\to[0,\frac{1}{4}]$ such that $\limsup_{t\to r+}\alpha(t)\leq \frac{1}{4}$. Then, T has a unique fixed point.

(3) Kannan type contraction with three generalized metrics:

(i)
$$G(Tu, Tv, Tv) \le \alpha \left(H(u, v, v)\right) \left[G(u, u, Tu) + H(v, v, Tv)\right]$$

(ii)
$$H(Tu, Tv, Tv) \le \alpha (I(u, v, v))[H(u, u, Tu) + I(v, v, Tv)]$$

(iii)
$$I(Tu, Tv, Tv) \le \alpha (\mathcal{G}(u, v, v))[I(u, u, Tu) + \mathcal{G}(v, v, Tv)],$$

where $\alpha:[0,\infty)\to[0,\frac{1}{4})$ such that $\limsup_{t\to r+}\alpha(t)\leq\frac{1}{4}$. Then, the fixed point of $\mathcal T$ is exactly one.

Acknowledgements

The work of the third author is financially supported by the CSIR, India, with grant no: 09/1217(13093)/2022-EMR-I.

Conflict of Interest

The authors have no conflict of interest in this paper.

References

- Banach, S. Sur les opérations dans les ensembles abstraits et leur application aux équations intégrales, Fundamenta mathematicae, 3 (1922), no. 1,133-181.
- [2] Mustafa, Z., Sims, B. A new approach to generalized metric spaces, Journal of Nonlinear and Convex Analysis, 7 (2006), no. 2, 289.
- [3] M. Abbas., Khan, A. R., T. Nazir. Coupled common fixed point results in two generalized metric spaces, Applied Mathematics and Computation, Elsevier 217 (2011), no. 13, 6328-6336.
- [4] Chen, J. Zhu, C., Zhu, L. A note on some fixed point theorems on G-metric spaces, J. Appl. Anal. Comput., 11 (2021), no. 1, 101-112.
- [5] Gaba, Y. U. Fixed point theorems in G-metric spaces, Journal of Mathematical Analysis and Applications, Elsevier 455 (2017), no. 1, 528-537.
- [6] Gautam, P., Kumar, S., Verma, S., Gupta, G. Existence of common fixed point in Kannan F-contractive mappings in quasi-partial b-metric space with an application, Fixed Point Theory and Algorithms for Sciences and Engineering, SpringerOpen 2022 (2022), no. 1, 1-19.
- [7] Mustafa, Z., Obiedat, H., Awawdeh, F. Some fixed point theorem for mapping on complete G-metric spaces, Fixed Point Theory and Algorithms for Sciences and Engineering, Springer Nature BV, (2008). doi:10.1155/2008/189870.
- [8] Mustafa, Z., Shatanawi, W., Bataineh, M., Volodin, A. Existence of fixed point results in G-metric spaces, International Journal of Mathematics and Mathematical Sciences, 2009 (2009), no. 10, 10.
- Zheng, D. Fixed Point Theorems for Generalized θ-φ-Contractions in G-Metric Spaces, Journal of Function Spaces, Hindawi Limited, 2018 (2018), 1-8.
- [10] Luong, Van, W., Thuan, N. X. Coupled fixed point theorems in partially ordered G-metric spaces, Mathematical and Computer Modelling, Elsevier, 55 (2012), no. (3-4), 1601-1609.

- [11] Reddy, G, Sudhaamsh, Mohan., Chary, V, Srinivas., Chary, D, Srinivasa., Radenovic, Stejan., Mitrovic, Slobodanka. Coupled fixed point theorems of JS-G-contraction on G-Metric Spaces, Boletim da Sociedade Paranaense de Matemática, 41(2023), 1-10.
- [12] Maharani, E. M., Chaira, K. Fixed point theorems in a space with two metrics, Adv. Fixed Point Theory, 5 (2014), no. 1, 1-12.
- [13] Shatanawi, W., Abbas, M., Nazir, T. Common coupled coincidence and coupled fixed point results in two generalized metric spaces, Fixed Point Theory and Applications, Springer 2011 (2011), 1-13.
- [14] Edelstein, M. An extension of Banach's contraction principle, Proceedings of the American Mathematical Society, JSTOR, 12 (1961), no. 1, 7-10.
- [15] Kannan, R. Some results on fixed points, Bull. Cal. Math. Soc. 60 (1968), 71-76.
- [16] Chatterjea, S. Fixed-point theorems, Dokladi na Bolgarskata Akademiya na Naukite, 25(1972), no. 6, 727.
- [17] Al-Khaleel, M., Al-Sharif, S., AlAhmad, R. On Cyclic Contractive Mappings of Kauman and Chatterjea Type in Generalized Metric Spaces, Mathematics, MDPI 11 (2023), no. 4, 890.
- [18] Mohsenialhosseini, S. Approximate fixed points of operators on G-metric spaces, University Politehnica of Bucharest Scientific Bulletin Series A Applied Mathematics and Physics, 79 (2017), 85-96.
- [19] Phaneendra, T., Saravanan, S. On some misconceptions and Chatterjee-type G-contraction, Int. J. Pure Appl. Math., 109 (2016), no. 4, 789-797.
- [20] Mustafa, Z., Obiedat, H. A fixed point theorem of Reich in G-metric spaces, Cubo (Temuco) SciELO Chile 12(2010), no. 1, 83-93.
- [21] Asadi, M., Karapinar, Erdal., Salimi, P. A new approach to G-metric and related fixed point theorems, Journal of Inequalities and Applications, SpringerOpen (2013), no. 1, 1-14.

* DEPARTMENT OF MATHEMATICS JAI PRAKASH UNIVERSITY, CHHAPRA-841301, BIHAR, INDIA E-mail: deepak.gymmaster@gmail.com (Received, February 21, 2025)

** DEPARTMENT OF MATHEMATICAL SCIENCES, INDIAN INSTITUTE OF TECHNOLOGY (BHU), VARANASI-22100S, UTTAR PRADESH, INDIA E-muil: tsom.apm@iitbhu.ac.in

E-mail: jayantasarkar.rs.mat20/@ithhu.ac.in

FORM IV (See Rule 8)

Title of the Journal Journal of Indian Academy of Mathematics

Place of Publication
 I* floor, I. K. Girls School Campus,

14/1 Ushagani, Near G.P.O. Indore - 452 001 India

Periodicity of Publication Bi-Annual (Twice in a Year)

Language in which it is published English

Publisher's Name
 C. L. Parihar (Editor)

Nationality Indian

Address 5, 1st floor, I. K. Girls School Campus,

14/1 Ushaganj, Near G.P.O. Indore - 452 001 India

Printer's Name Hemant Khurana

Nationality Indian

Address 26 NX, Vishnupuri, A.B. Road, Indore

7. Editor's Name C. L. Parihar
Nationality Indian
Address Indore

Name of the Printing Press, Print Solutions

where the publication is printed 35/B-2/1, Laxmibai Nagar Industrial Estate, Kila

Maidan Road, Indore 452 006

Name and addresses of the individuals

who own the newspaper/journal and partners or shareholders holding more

than one per cent of the total capital

No Individual:

It is run by Indian Academy of Mathematics 5, 1st floor, I. K. Girls School Campus,

14/1 Ushagani, Near G.P.O. Indore - 452 001 India

I, C. L. Parihar, hereby declare that the particulars given above are true to the best of my knowledge and belief.

Sd. C. L. Parihar

Editor
Indian Academy of Mathematics

Dated: September 30, 2025

INDIAN ACADEMY OF MATHEMATICS

Regd. No. 9249

Office: 5, 1st floor, I. K. Girls School Campus, 14/1 Ushaganj, Near G.P.O. Indore 452 001, India

> Mobile No.: 07869410127 E-mail; indacadmath@hotmail.com profparihar@hotmail.com

Executive Committee (2022-2025)

President Narendra. S. Chaudhary: IIT, Indore. E-mail: nsc183@	@gmail.com
--	------------

Vice Presidents S. Ponnusamy: IITM, Chennai, E-mail: samy@iitm.ac,in

S. Sundar: IITM, Chennai, B-mail: slnt@iitm.ac.in

P.K. Benarji: Professor Emeritus, J.N.V. University. Jodhpur, S.K. Sahoo: IIT, Indore. E-mail: swadesh.sahoo@iiti.ec.in

B.C. Tripathy: Tripura University, Agartala, Tripura. E-mail: tripathybc@yahoo.com

V.P. Pande: Kumaun University, Almoda, Uttarakhand. E-mail: vijpande@gmail.com

S.B. Joshi: Walchand College of Engineering, Sangli, MS. E-mail: joshisb@hotmail.com

A.P. Khurana: Retd. Professor, DAVV, Indore. E-mail: apkhurana26@gmail.com

Secretary C.L. Parihar: Retd. Professor, Holkar Science (Auto) College, Indore,

E-mail: profparihar@hotmail.com

Joint-Secretary Natresh Berwal: Raja Bhoj Government College, Katangi, Balaghat (M.P.)

E-mail: nareshberwal.019@gmail.com

Treasurer Madhu Tiwari: Govt. New Science College, Indore, E-mail: madhu26938@gmail.com

Members Mahesh Dube: Retd. Profesoor, Holkar Science College, Indore.

S. Lakshmi: Govt. Arts & Science College, Peravurani. E-mail: lakshmi291082@yahoo.co.in R. K. Sharma: Holkar Science (Autonomous) College, Indore. E-mail: raj_rma@yahoo.co.in

H. S. P. Shrivastava: Retd. Professor. E-mail: hsp shrivastava@yahoo.com

Jitendra Binwal: Mody University of Science & Technology, Lakshamangarh, Rajisthan.

E-mail: r.iitendrabinwaldkm@gmail.com

Sushma Duraphe: M, V.M. Mahavidyalaya, Bhopal. E-mail: duraphe sus65@rediffmail.com

To Tanks

O. L. L. T. T.

Membership Subscription

Ordinary Membership (For calendar year)	Sibili III	US\$
Institutional Membership (For calendar year)	900/-	75
Processing Charges (a minimum of Rs 1500/-)	1500/-	100
Back Volumes priced at the current year price.	350/-	25

The subscription payable in advance should be sent to The Secretary, 500, Pushp Ratan Park, Devguradiya, Indore-452016, by a bank draft in favour of "Indian Academy of Mathematics" payable at Indore.

Published by: The Indian Academy of Mathematics, Indore-452 016, India, Mobile: 7869410127 Composed & Printed by: Print Solutions, Indore (M.P.) Mob: +91 98260 92006

INDEX

Massimiliano Ferrara	Multi-time Evolution Models in Deep Learning Dynamics	282
Ajoy Mukharjee1, Rebati Mohan Roy2	On M-Paracompactness and M-Localness on GT Spaces	295
Thalmi, B.1. Jayasri, C2	Generalized Totally Positive Functions and Generalized Totally Bounded Functions in a Particular Ect-space	302
Ranjan S. Khatu	Coefficient Estimates for a Certain Subclass of Analytic and BI Univalent Functions Defined using an Operator Associated with Generalized Mittag-Leffler Function	315
Dhiraj Kumar I, Manoranjan K. Singh2, Sanjeet Kumar 3	Number of Fuzzy Subgroups of $D_3 \times C_2$	322
Stvasankar S1, Babysuganya K2	Some Distance-based Topological Indices of Double Starbarbell Graph and Petersenbarbell Graph	329
Mohanapriya Rajagopal1, D. Shanmugasundaram2	Enhancing Scada Cybersecurity Through Neutrosophic Graph Topological Analysis	349
Swaroopa Rani N CI. B. Shanmukha2	Restrained Pendant Domination In Graphs	359
Christopher MI. Ramachandran V2	Modulo Two Square Mean Labeling of Hurdle Graphs, Comb Graphs and $F(P_{\star})$ Graphs and its Algorithms	368
Keerti Acharya1, Rinku Verma2, Pranjali Kekre3	A Novel Technic Using Complete Graph Labeling and Ascii Representation	381
Thomas Koshy	Sums Involving a Family of Gibonacci Polynomial Squares: Graph-theoretic Confirmations	392
P. Saha1, Samten Tamang2, M. Mallik3,Sanjib K. Datta4	Growth of The Solutions of N ^a Order Linear Shift Differential Equations with Uncertain Coefficient	397
Suman Sindhwani	Linear and Non-linear Study of Magneto-Diffusive Convection in Dufour-Soret Induced Nanofluid Layer	406
A. Deepshika I, J. Kannan*2, and P. Vimala Devi3	On The Miscellaneous Exponential Diophantine Equations	418
Swati Chaudhari I, Archana Thakur2, Alpana Rajan3	Anomaly Detrection for Web Attack Prevention: Analyzing Web Access Logs for Threat Mitigation	427
Dehadatta Adakl*, Shekhar Das2, Bindu Ranjan Chakma3	Controlling Insurgency in Northeast India by Generation of Employment and Awareness: A Socio-Mathematical Study	440
Pramod Shindel, Aditi S. Phadke2, Samina Boxwala3	Study of Frame Stewart Numbers of The Multi-peg Tower of Hanoi Problem	464
Titli Maiti1, Avijit Sarkar2	On Prey-Predator Dynamics with Certain Intrinsic Behaviours	470
Deepak Routl, Tanmoy Som2. Jayanta Sarkar3	Results on Fixed Points Utilizing Two or More Generalized Metrics in G-metric Space	483